

Analysing dopamine receptor interacting  
proteins using the biomedical model

*Dictyostelium discoideum*

Nicholl Kelly Pakes

Research thesis submitted for the degree of Doctor of Philosophy at Royal  
Holloway University of London in March 2012

## Declaration of Authorship

I, Nicholl Pakes, hereby declare that the work presented in this thesis is my own unless otherwise indicated, and that all published work has been acknowledged. Furthermore, I affirm that I have neither fabricated nor falsified the results reported herein.

Signed:

Date:

## Abstract

The dopamine signalling pathway has been implicated in the pathophysiology of neuropsychiatric conditions including bipolar disorder and schizophrenia. A detailed analysis of this pathway is essential for understanding these conditions. Previous work (Zhan *et al.*, 2008) has identified eleven novel human dopamine receptor interacting proteins (DRIPs), but their role in cell signalling remains unclear.

In this project we have employed a biomedical model, *Dictyostelium discoideum*, to help elucidate the cellular signalling of two DRIPs, the Zizimin GEF (DRIP2) and MARK (DRIP9) proteins. Bioinformatics analysis of these proteins shows conservation of the domain structure in the human and *Dictyostelium* gene products. To investigate the function of these proteins during development, two *Dictyostelium* homologues within each family (ZizA and ZizB; MrkA and MrkC) were ablated and changes in developmental for resulting null mutants were analysed. Development was unaltered following ablation of *zizA*, *mrkA* and *mrkC*, however, ablation of *zizB* gave rise to a clear change in developmental morphology. To further understand the developmental defect of *zizB*, directional cell movement (chemotaxis) was analysed in the *zizA* and *zizB* null mutants. Ablation of *zizA* caused no gross phenotypic change in chemotaxis, whereas *zizB* ablation gave rise to a reduction in cell speed, directionality and aspect (roundness). Furthermore, expression studies showed *zizA* and *zizB* were constantly expressed throughout development. Overexpression of each gene (labelled with the fluorescent tag, GFP) demonstrated a cytosolic localisation the gene products, with the ZizB-GFP fusion protein additionally exhibiting enrichment of the cortex, causing a large increase in filopodia formation and a partial inhibition of cytokinesis. Analysis of protein binding partners for ZizB indicates specific interaction with Rac1A and a range of actin-interacting proteins.

In conclusion this project provides the first insight into the molecular and cellular functions of Zizimin proteins, potential dopamine receptor interacting protein.

## Table of Contents

1	Introduction .....	1
	Schizophrenia.....	2
	Bipolar disorder .....	3
	Treatment of schizophrenia and bipolar disorder .....	4
	Dopamine .....	5
	Dopamine neurotransmission .....	6
	Dopamine Receptor Interacting Proteins (DRIPs).....	7
	<i>Dictyostelium discoideum</i> as a biomedical model .....	10
	<i>Dictyostelium</i> Development .....	12
	Chemotaxis .....	13
	Cytokinesis .....	15
	Small GTPase signalling.....	17
	Rho family of small GTPases .....	18
	Small GTPase signalling in <i>Dictyostelium</i> .....	19
	Guanine nucleotide Exchange Factor proteins.....	21
	PIM2 (DRIP 9) .....	25
	Microtubule Affinity Regulating Kinases (MARKs).....	25
	Aims of this work .....	27
2	Materials and Methods .....	28
	Materials.....	29
	General chemicals .....	29
	Methods.....	32
	Bioinformatic analysis .....	32
	<i>Dictyostelium discoideum</i> Methods .....	33
	Molecular Biology methods .....	34
	Image Acquisition and Microscopy .....	40
	Proteomics .....	41
	Software .....	43
	Websites.....	43
3	Bioinformatics .....	45
	Introduction.....	46
	BLAST Analysis.....	47
	Domain structure analysis.....	50
	Dedicator of Cytokinesis proteins .....	50
	Microtubule Affinity Regulating Kinase .....	53

Phylogenetic analysis .....	55
Dedicator of Cytokinesis proteins .....	55
Microtubule Affinity Regulating Kinases .....	60
Discussion .....	64
Summary .....	67
4 Gene ablation.....	68
Introduction.....	69
Creating Knock out mutants.....	70
PCR screening analysis .....	73
Loss of gene transcription .....	76
Effect of gene ablation on development .....	79
Discussion .....	83
Creating knockout cell lines.....	83
Effect of gene ablation on development .....	84
Summary .....	87
5 Zizimin cellular function .....	88
Introduction.....	89
Expression profile of <i>Dictyostelium</i> Zizimin proteins.....	90
Rescuing the developmental defects of <i>zizB</i> ablation .....	92
Chemotaxis .....	94
Cellular localisation of ZizA and ZizB .....	97
Cytokinesis .....	100
Growth.....	104
Stress .....	105
Discussion .....	108
Expression levels .....	108
Development and chemotaxis .....	108
Localisation .....	110
Cytokinesis and growth .....	113
Stress response .....	116
Summary .....	118
6 Zizimin binding partners .....	119
Introduction.....	120
Proteomics .....	121
Intracellular protein-protein interaction .....	121
Discussion .....	128
Summary .....	134

7 Conclusion .....	135
The cellular function of ZizA in <i>Dictyostelium</i> .....	136
The cellular function of ZizB in <i>Dictyostelium</i> .....	139
Summary .....	144
References.....	145
Appendix.....	164
Publications .....	164
Journal of Cell Science (2012) .....	164
Journal of the Royal Society Interface (2011).....	165

## List of Tables and Figures

Figure 1.1 - Synthesis of catecholamine neurotransmitters.....	6
Figure 1.2 - Dopamine receptor signal transduction targets.....	7
Figure 1.3 - DRIP regulation within the dopamine signalling pathway.....	8
Table 1.1 - Dopamine Receptor Interacting Proteins (DRIPs).....	9
Table 1.2 - <i>Dictyostelium</i> homologues of human disease related proteins.....	11
Figure 1.4 - Developmental life cycle of <i>Dictyostelium</i> .....	12
Figure 1.5 - Signalling Pathways in <i>Dictyostelium</i> Chemotaxis.....	15
Figure 1.6 - Stages of cytokinesis.....	16
Figure 1.7 - GTPase cycling mechanism.....	18
Figure 1.8 - Phylogenetic analysis of the Rho family of small GTPases.....	20
Figure 1.9 - Phylogenetic and domain structure analysis of the Dock protein family.....	22
Figure 1.10 - Model of Dock10-Cdc42 in amoeboid movement.....	24
Figure 2.1 - Schematic diagrams showing the knockout and screening procedure.....	37
Table 3.1 - BLAST analysis results of the potential <i>Dictyostelium</i> homologues.....	47
Table 3.2 - BLAST analysis results for all 5 potential <i>Dictyostelium</i> DRIP homologues.....	49
Figure 3.1 - Domain structure analysis of the <i>Homo sapien</i> Dock family.....	51
Figure 3.2 - Domain structure analysis of the <i>Dictyostelium</i> DOCK family proteins.....	52
Figure 3.3 - Domain structure analysis of the <i>Homo sapien</i> and <i>Dictyostelium</i> PIM/MARK family.....	54
Figure 3.4 - Phylogenetic analysis of <i>Homo sapien</i> DOCK family proteins.....	55
Figure 3.5 - Sequence alignments of the DHR2 domains of Dock10 in different species.....	57
Figure 3.6 - Phylogenetic analysis Dock proteins across different kingdoms.....	59
Figure 3.7 - Sequence alignment of the MARK and PIM ser/thr kinase domain.....	61
Figure 3.8 - Sequence alignment of the ser/thr kinase domain for MARK family proteins.....	62
Figure 3.9 - Phylogenetic analysis of MARK proteins and the related protein PIM2.....	63
Figure 4.1 - Restriction digest analysis of the <i>zizA</i> and <i>zizB</i> knockout vectors.....	71
Figure 4.2 - Restriction digest analysis of the <i>mrkA</i> and <i>mrkC</i> knockout vectors.....	72
Figure 4.3 - PCR screening analysis for <i>zizA</i> and <i>zizB</i> knockout cell lines.....	74
Figure 4.4 - PCR screening analysis for <i>mrkA</i> and <i>mrkC</i> knockout cell lines.....	75
Figure 4.5 - PCR analysis of Zizimin gene transcription, in wild type and putative null cells.....	77
Figure 4.6 - PCR analysis of MARK gene transcription in wild type and putative null mutants.....	78
Figure 4.7 - Development of <i>zizA</i> <sup>-</sup> and <i>zizB</i> <sup>-</sup> cell lines.....	80
Figure 4.8 - Development of <i>mrkA</i> <sup>-</sup> and <i>mrkC</i> <sup>-</sup> cell lines.....	81
Figure 4.9 - Early stages of development for wild type, <i>zizA</i> <sup>-</sup> and <i>zizB</i> <sup>-</sup> cell lines.....	82
Figure 5.1 - <i>Dictyostelium</i> Zizimin gene expression throughout 24 hr development.....	91
Figure 5.2 - RNA-Seq data for Zizimin A-D from DictyExpress.....	91
Figure 5.3 - Development of <i>zizA</i> <sup>+</sup> and <i>zizB</i> <sup>+</sup> cell lines.....	93
Figure 5.4 - Chemotactic effects of <i>zizA</i> ablation and overexpression.....	95
Figure 5.5 - Chemotactic effects of <i>zizB</i> ablation and overexpression.....	96
Table 5.1 - Summary of chemotaxis analysis.....	97

Figure 5.6 - Full length expressions of ZizA-GFP and ZizB-GFP.....	98
Figure 5.7 - Cellular localisation of ZizA-GFP and ZizB-GFP.....	98
Figure 5.8 - Quantification of filopodia in zizB <sup>+</sup> cells. ....	99
Figure 5.9 - Cytokinesis defect in cells overexpressing ZizB-GFP.....	101
Figure 5.10 - Variation in nuclei number in cells lacking Zizimin activity.....	102
Figure 5.11 - Analysis of nuclei in Zizimin overexpressor cells.....	103
Figure 5.12 - Growth curve of cell lines lacking or overexpressing ZizA or ZizB.....	104
Figure 5.13 - Expression of <i>Dictyostelium</i> stress related genes following osmotic, oxidative and heat stress.....	105
Figure 5.14 - Osmotic stress response of cells lacking or overexpressing ZizA or ZizB.....	107
Figure 6.1 - Co-immunoprecipitation of ZizA and ZizB proteins – Silver stain.....	122
Figure 6.2 - Co-immunoprecipitation of ZizA and ZizB proteins – Coomassie stain.....	123
Figure 6.3 - Zizimin protein interaction analyses.....	123
Table 6.1 - List of potential ZizA and ZizB binding partners.....	125
Figure 6.4 - Co-immunoprecipitation of ZizB with Rac-GST.....	127
Figure 7.1 - Zizimin A transduction mechanisms.....	139
Figure 7.2 - Rac1 GTPase transduction mechanisms.....	140
Figure 7.3 - Zizimin B transduction mechanisms.....	143



## Abbreviations

aa	Amino acid
AC	Adenylate cyclase
AIP1	ALG-2 Interacting Protein 1
APS	Ammonium Persulfate
Ax	Axenic
BLAST	Basic Local Alignment Search Tool
cAMP	cyclic Adenosine Monophosphate
CAR1	cAMP Receptor 1
CDD	Conserved Domain Database
cDNA	Complementary DNA
cGMP	cyclic Guanosine Monophosphate
CIAP	Calf Alkaline Phosphatase
CRAC	Cytosolic Regulator of Adenylate Cyclase
DA	Dopamine
DAG	Diacylglycerol
DAPI	4',6-Diamidino-2-phenylindole
DAR	Dopamine Receptor
ddH <sub>2</sub> O	Double distilled water
DH-PH	Dbl Homology–Pleckstrin Homology
DHR1	Dock Homology Region 1
DHR2	Dock Homology Region 2
DIF-1	Differentiation Inducing Factor – 1
DMSO	Dimethyl Sulfoxide

dNTPs	Deoxynucleotide Triphosphates
Dock	Dedicator of Cytokinesis
DRIP	Dopamine Receptor Interaction Protein
DTT	Dithiotreitol
EDTA	Ethylenediaminetetraacetic acid
EGTA	Ethylene Glycol Tetraacetic Acid
GAP	GTPase Activating Proteins
GDI	Guanosine diphosphate Dissociation Inhibitor
gDNA	Genomic DNA
GDP	Guanosine Diphosphate
GEF	Guanine nucleotide Exchange Factor
GFP	Green Fluorescent Protein
GlcS	Glycogen Synthase
GPCR	G-protein Coupled Receptors
GSK-3	Glycogen Synthase Kinase-3
GTP	Guanosine Triphosphate
Ig7	Immunoglobulin 7
IL-3	Interleukin-3
IP3	Inositol triphosphate
IPTG	$\beta$ -D-1-thiogalactopyranoside
IRdye 800	InfraRed dye 800
MAP	Microtubule Associated Proteins
MARK	Microtubule Affinity Regulating Kinases
MARKK	Microtubule Affinity Regulating Kinases Kinase

MOPs	3-(N-morpholino)propanesulfonic acid
MZ	Monozygotic
NCBI	National Centre for Biotechnology Information
NCS1	Neuronal Calcium Sensor-1
NP40	Nonidet P 40
PAK	p21-Activated Kinase
PAR-1	Protease Activated Receptor-1
PBS	Phosphate Buffered Saline
PCR	Polymerase Chain Reaction
PFA	Paraformaldehyde
PH	Plekstrin Homology
Phalloidin-TRITC	Phalloidin-tetramethylrhodamin isothiocyanate
PhdA	PH-domain containing protein
PI3K	Phosphoinositol-3-kinase
PIP2	Phosphatidylinositol (4, 5)-bisphosphate
PIP3	Phosphatidylinositol (3, 4, 5)-triphosphate
PkbA	PKB-related protein
PKBR1	Protein Kinase B-like Receptor 1
PKC	Protein Kinase C
PLA2	Phospholipase A2
PLC	Phospholipase C
PMSF	Phenylmethylsulfonyl fluoride
PTEN	Phosphatase and Tensin homologue
SDS	Sodium dodecyl sulphate

SDS-PAGE	Sodium dodecyl sulphate Polyacrylamide Gel Electrophoresis
Ser/Thr	Serine/Threonine Kinase
SH3	Src Homology domain 3
TEMED	N,N,N'N' – Tetramethyl-ethylene-1,2-diamine
TORC	Target of Rapaycin complex 2
WASP	Wiskott-Aldrich Syndrome Protein
Zir	Zizimin related family proteins
Ziz	Zizimin family proteins

## Acknowledgements

Firstly I would like to thank my supervisor at Royal Holloway, Dr Robin Williams, for all his guidance and support throughout the three years of my PhD. I would also like to thank my second supervisor at St Georges, Dr Jamal Nasir, since without his preliminary work in identifying the novel human DRIPs, my project would not have transpired. I am also appreciative to my advisor at Royal Holloway, Dr Philip Chen, for all his invaluable advice throughout the last three years. Also, I would like to thank all the member of the Williams lab for their countless help, support and discussions over the years, without you guys I may not have made it this far.

This project would not have been possible without funding from the South West London Academic Network (SWAN). I would also like to extend a big thank you to the Rob Insalls Lab with special mention to Douwe Veltman at the Beatson Institute for Cancer Research, for providing me with the ZizA-GFP and ZizB-GFP tagged constructs, analysing the protein interaction samples by Mass Spectrometry, allowing me to pick his brain from time to time and for sharing his vast knowledge and expertise. I would also like to acknowledge BRAIN for their generous support in funding my attendance at the annual International *Dictyostelium* conference 2010, which allowed me to make important collaborations and present my work.

I would also like to thank all my friends and family for ALL their constant encouragement, love and support throughout the last three years. To my family, you have all provided me with endless encouragement, advice and laughter that I have needed throughout the years, which has made me into the person I am today. To my 'UK family', Lauren, Steph, Rachel and Kate, you guys have been my strength when I needed you to be and have made the last three years doable. I value your friendships more than words can express and am so thankful to have such amazing friends. And finally special thank you to Nicolas for helping me de-stress throughout the last few months, you have helped me grow in so many ways.

So to all of you, I would not have made it through without your help, encouragement and support so THANK YOU, it is because of you guys that I have got this far.

## **1 Introduction**

## 1.1 Schizophrenia

Schizophrenia is a severe psychiatric disorder that affects about 1% of the population worldwide (Lewis and Lieberman, 2000; Seeman and Kapur, 2000; Tsuang, 2000). This is a debilitating psychiatric disorder with an onset in early adulthood (Seeman and Kapur, 2000). The clinical features of schizophrenia are divided into positive, negative and cognitive symptoms. The positive symptoms include delusions (often paranoia), hallucinations, thought disorder and abnormal behaviour such as aggressive behaviour. The negative symptoms include social withdrawal and flattening of emotional responses. The cognitive functions, such as attention and memory, are also often affected in this disorder. It is unclear what causes the illness and whether it can be classified as a single disease or a collection of disorders (Lewis and Lieberman, 2000).

Familial studies provide strong evidence that schizophrenia is a hereditary disease, although, specific genes have not yet been identified, genetic association studies have implicated some genetic loci associated with the onset of this disorder (Lewis and Lieberman, 2000; Tsuang, 2000). In monozygotic (MZ) twin studies, a 50% concordance for schizophrenia was observed between the twins. Since MZ twins have identical DNA, the incomplete concordance rate suggests that the onset of schizophrenia is not influenced solely by genetic factors, but the prevalence of the disorder is also influenced by environmental factors. Those could be prenatal, perinatal or postnatal (Gottesman and Erlenmeyer-Kimling, 2001; Tsuang, 2000).

The pathophysiology behind the disorder has mainly focused on the “dopamine hypothesis” which suggests that certain dopaminergic pathways are overactive in schizophrenia (Seeman, 1987). This theory is based on the evidence that drugs used to treat the symptoms of schizophrenia act by inhibiting Dopamine 2 (D2) receptors (Bonci and Hopf, 2005). The earliest evidence for this effect dates back to 1966 when van Rossum showed that potent neuroleptic drugs work by blocking the dopamine receptors, currently known to be specifically targeting the D2 receptor subtype (Seeman, 1987). Potent agonists for the dopamine receptor, such as amphetamine and d-

lysergic acid diethylamide (LSD), were shown to mimic symptoms seen in schizophrenia (Seeman et al., 2006), giving the pathological profile that further supports the “dopamine hypothesis”.

## 1.2 Bipolar disorder

Bipolar disorder (formerly known as manic depression) affects about 1.3 - 1.6% of the world population (Montezinho et al., 2007; Muller-Oerlinghausen et al., 2002). This is a severe psychiatric disorder, characterised by episodic pathological changes in mood (Muller-Oerlinghausen et al., 2002). There are two major forms of the illness, bipolar I and bipolar II. As a result, the clinical features between patients can vary. Bipolar I patients experience predominantly manic episodes with fewer depressive states, whereas bipolar II patients suffer more frequent depressive episodes with occasional mania (Craddock and Sklar, 2009). The symptoms of episodic depression and mania are often accompanied by psychotic features such as delusions and hallucinations (Muller-Oerlinghausen et al., 2002).

Similar to schizophrenia, the familial and twin studies conducted in bipolar disorder patients, point to genetics as the basis of the disease. The study showed a lifetime prevalence of 40 - 70% for MZ twins and 5 - 10% for other 1<sup>st</sup> degree relatives (Craddock and Jones, 2001; Muller-Oerlinghausen et al., 2002). The pathophysiology of bipolar disorder remains unclear, although, there is increasing clinical evidence of elevated levels of catecholamine neurotransmitters during the manic episodes (Newberg et al., 2008). The catecholamine, dopamine, has been suggested to be one of these neurotransmitters (Montezinho et al., 2007; Newberg et al., 2008).



### 1.3 Treatment of schizophrenia and bipolar disorder

Antipsychotics currently used to treat bipolar disorder and schizophrenia act mainly via antagonism of the D2 dopamine receptor (Bonci and Hopf, 2005). Those drugs can be divided into two subclasses: typical (e.g. haloperidol) and atypical (e.g. clozapine). Since there is often an overlap in many symptoms in bipolar disorder and schizophrenia, the treatments also overlap. Antipsychotics are used singularly or in conjunction with other neuroleptic drugs, like those which were originally used in the treatment of epilepsy (valproic acid or VPA and carbamazepine), as well as mood stabilisers such as lithium (Citrome et al., 2000). In 1994 lithium and VPA were the most commonly prescribed mood stabiliser treatments for bipolar disorder and schizophrenia (Citrome et al., 2000).

In schizophrenia, however, antipsychotic drugs treat mainly the positive symptoms of the disorder, with some newer atypical antipsychotics, having effects on the negative symptoms (Strange, 2001). Furthermore, in bipolar disorder, dopamine is one of the main neurotransmitters implicated in the hypermania (Newberg et al., 2008), however, the varying symptoms and complexity of these disorders makes them difficult to treat. Thus, pharmacotherapy often has to be tailored to the individual symptoms of the patient.

The limitations with typical antipsychotics are the dramatic extrapyramidal adverse effects. These effects are due to the non-specific binding of the typical antipsychotics to the different dopamine receptor subtypes. Antagonism of the D2 receptor in the striatum is thought to be the main cause of the extrapyramidal adverse effects (Strange, 2001). Therefore, the identification of potential new downstream targets for novel compounds could reduce the adverse effects.

## 1.4 Dopamine

Dopamine, along with adrenaline and noradrenaline, belong to the catecholamine family of neurotransmitters. These neurotransmitters have very distinct structural features consisting of an amine group, a catechol nucleus and an ethylamine derivative (Vallone et al., 2000). Dopamine is synthesised from the aromatic amino acid tyrosine in a two step reaction via the enzymes: tyrosine hydroxylase and aromatic L-amino acid decarboxylase (Vallone et al., 2000) (**Figure 1.1**). In the first step of the reaction L-3,4-dihydroxyphenylalanine (L-DOPA), a precursor for dopamine, is produced. Dopamine is then converted into adrenaline which is further modified into noradrenaline. Aberrant dopamine signalling has been linked to a range of psychiatric disorders, including bipolar disorder and schizophrenia. Thus, understanding the normal functioning of dopamine neurotransmission is essential for elucidating its pathophysiological role in many neurological (e.g. Parkinson's disease) and psychiatric (e.g. bipolar and schizophrenia) disorders. Dopamine has a wide variety of functions in the brain; therefore, disorders that are affected by the disruption of the dopaminergic pathways give rise to a range of symptoms. The dopaminergic functions include: behaviour, cognition, motor activity, motivation and reward, inhibition of prolactin release, sleep, mood, attention and learning (Jaber et al., 1997; Missale et al., 1998).

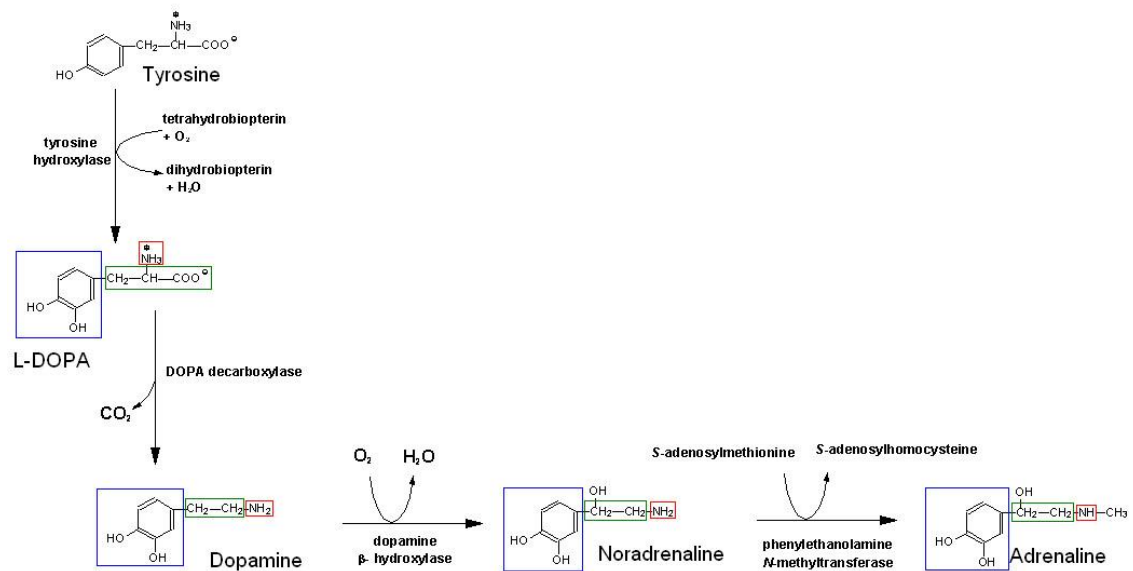


**Figure 1.1 Synthesis of catecholamine neurotransmitters.**

Flow diagram illustrating the steps involved in the production of dopamine, adrenaline and noradrenaline. The red, blue and green boxes show the amine group, a catechol nucleus and the ethylamine derivative, respectively.

## 1.5 Dopamine neurotransmission

Dopamine binds to one of the five G-protein coupled receptors (GPCR) which are grouped into two sub-classes, the D1-like (D1 and D5) and D2-like (D2, D3 and D4) receptors. This classification is based on their downstream effects, where D1-like receptors stimulate adenylate cyclase (AC) and D2-like receptors inhibit the AC system (Sunahara et al., 1991; Vallone et al., 2000; Van Tol et al., 1992). Activation of AC (in the case of D1-like receptors) leads to the stimulation of the cAMP pathway and the modulation of calcium signalling (**Figure 1.2**). Other downstream effects of the receptors include arachidonic acid modulation, sodium/potassium ATPase stimulation, phospholipase C activation, potassium channel activation and sodium/proton exchanger inhibition (Missale et al., 1998).

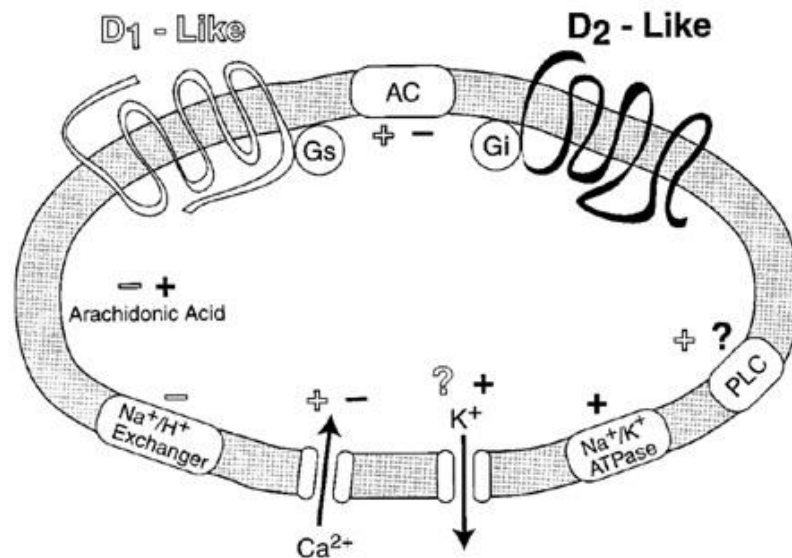


**Figure 1.2 Dopamine receptor signal transduction targets**

Schematic diagram illustrating the downstream signalling effects of the D1-like (white filled) and D2-like (black filled) dopamine receptors (Missale *et al.*, 1998). D1-like receptors are stimulatory G-protein coupled receptors, activation of which is thought to result in an increase in adenylate cyclase (AC) activity, phospholipase C (PLC) activation, L-type calcium channel activation, inhibition of Na<sup>+</sup>/H<sup>+</sup> exchanger and an inhibition in arachidonic acid release. D2-like receptors however are inhibitory G-protein coupled receptors which inhibit AC. Other downstream processes affected by D2-like receptors are: Na<sup>+</sup>/K<sup>+</sup> ATPases, K<sup>+</sup> channels activation, Ca<sup>2+</sup> inhibition and potentiation of arachidonic acid release.

## 1.6 Dopamine Receptor Interacting Proteins (DRIPs)

Dopamine Receptor Interacting Proteins (DRIPs) have become a focus of the research to further the understanding of dopamine signalling at a molecular level. Several DRIPs, such as Spinophilin (Smith *et al.*, 1999) and ALG-2 Interacting Protein 1 (AIP1), a protein involved in neuronal cell death and intracellular trafficking (Zhan *et al.*, 2008; Zhan *et al.*, 2010a), have been identified using a yeast two-hybrid screen. DRIPs have been implicated in the regulation of many aspects of the dopamine receptor life cycle, from biosynthesis to desensitisation (**Table 1.1**) (Bergson *et al.*, 2003). Identification of these proteins and their potential binding targets gives a more detailed picture of how dopamine functions within its diverse signalling pathways in the human brain. This, in turn, provides a better understanding of the aetiology of dopamine related disorders.

Many DRIPs have been shown to be elevated in psychiatric disorders. Calcyon and Neuronal Calcium Sensor-1 (NCS1) were reported to be increased by ~100% and ~50% in post-mortem brains of schizophrenic and bipolar disorder patients, respectively (Kho *et al*, 2003a; Kho *et al.*, 2003b). These studies suggest that DRIPs contribute to the pathophysiology of dopamine related psychiatric disorders. Therefore, the search for other potential DRIPs is at the leading edge of research into these diseases (**Figure 1.3**).

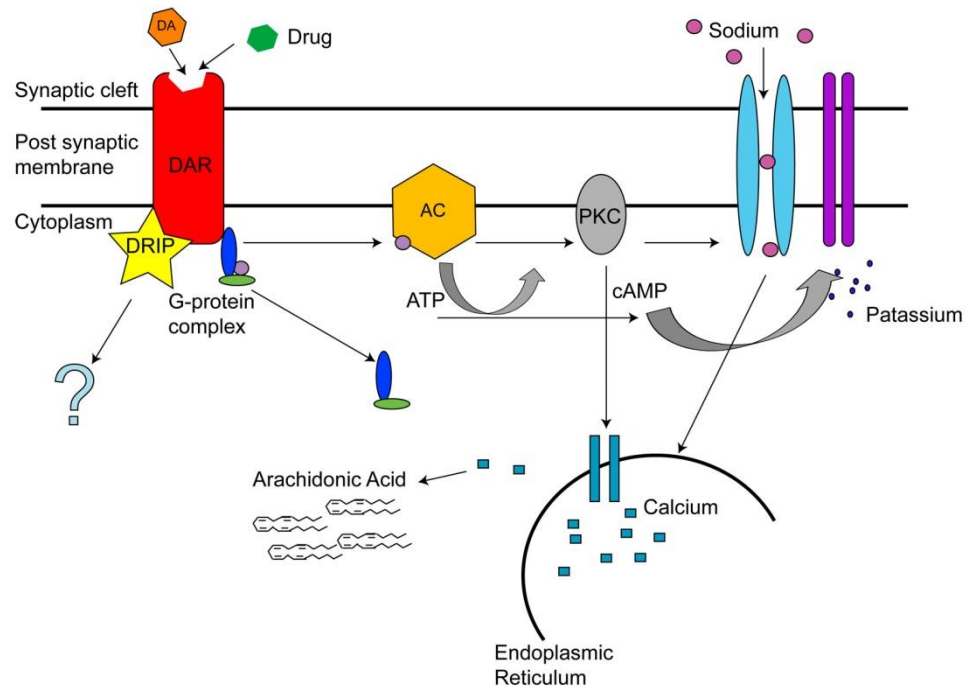


**Figure 1.3 DRIP regulation within the dopamine signalling pathway**

Schematic representation of the intracellular transduction mechanisms within the dopamine signalling pathway shows the unknown action of DRIPs. The binding of dopamine (DA) to the dopamine receptor (DAR) activates (or inhibits) adenylyl cyclase (AC) via the heterotrimeric G-protein complex. Stimulation of adenylyl cyclase activates protein kinase C (PKC), increasing cAMP, which regulates sodium and potassium channels. Sodium influx initiates release of internal calcium stores, which has been shown to cause an increase in arachidonic acid release. DRIP interaction and signalling with the DAR remains unclear.

**Table 1.1 Dopamine Receptor Interacting Proteins (DRIPs)**

	D1	D2	D3	D4	D5
<b>Receptors and channels</b>					
Dopamine D2 receptor	-	Yes	Yes	-	-
Dopamine D3 receptor	-	Yes	Yes	-	-
NMDA receptor NR1-1a subunit	Yes	-	-	-	-
NMDA receptor NR2A subunit	Yes	-	-	-	-
Somatostatin sst <sub>5</sub> receptor	-	Yes	-	-	-
Adenosine A <sub>1</sub> receptor	Yes	-	-	-	
Adenosine A <sub>2A</sub> receptor	-	Yes	-	-	-
GABA <sub>A</sub> receptor	-	-	-	-	Yes
Kir3 K <sup>+</sup> channel	-	Yes	-	-	-
<b>Cytoskeletal proteins</b>					
Neurofilament M	Yes	-	-	-	-
4.1N	-	Yes	Yes	-	-
4.1B	-	Yes	Yes	-	-
4.1G	-	Yes	Yes	-	-
Filamin A	-	Yes	Yes	-	-
Gamma COP	Yes	-	-	-	-
Spinophilin	-	Yes	-	-	-
<b>Signalling proteins</b>					
NCS-1	-	Yes	-	-	-
Valcyon	Yes	-	-	-	-
<b>Kinases</b>					
GRK2	-	Yes	-	-	-
<b>Adaptors or chaperones</b>					
DRIP78	Yes	-	-	-	-
Nck	-	-	-	Yes	-
Grb2	-	-	Yes	Yes	-

Table listing DRIPs which has been divided into 5 classes based on function and shown which dopamine receptor (D1-5) they interact with. This list was compiled using the PubMed database (<http://www.ncbi.nlm.nih.gov>) and the Database of Interacting Proteins (<http://dip.doe-mbi.ucla.edu/>) (Bergson *et al.*, 2003).

Previous work by Dr Nasir and colleagues identified eleven human DRIPs by a yeast two-hybrid screen. Different domains of the 5 dopamine receptors were used as the bait proteins and a cDNA library for the prey proteins (Zhan et al., 2008; Zhan et al., 2010a). Currently, little is known on how these proteins interact with the dopamine receptor, their cellular functioning, or their implication in schizophrenia and bipolar disorder. Hence, further investigation within this research field is needed.

### **1.7 *Dictyostelium discoideum* as a biomedical model**

*Dictyostelium discoideum* is a simple model organism that is used in biomedical research to investigate the roles of human proteins and their signalling pathways. Its genome has been fully sequenced; it is about 34MB in size and consists of 12500 genes (Eichinger *et al.*, 2005), out of which, at least 33 have been identified and confirmed as orthologues of disease-related genes (Boeckeler et al., 2006; Eichinger et al., 2005; Williams et al., 2006). The list of *Dictyostelium* homologues showing sequence similarity to human genes implicated in disease are presented in **Table 1.2** (Boeckeler *et al.*, 2006).

Cre-Lox is a technology applied in genetics to create multiple knockouts in a single cell line using homologous recombination techniques (Faix *et al.*, 2004). Adaptation of the Cre-Lox technology for *Dictyostelium* and the unique lifecycle of this model organism allows for quick and efficient knockout mutants to be produced to explore the cellular functioning of different signalling pathways. Therefore, *Dictyostelium* provides a simple means for investigating the cellular functioning of these disease-related orthologues, thus, gaining a more detailed understanding of their pathological roles.

**Table 1.2 *Dictyostelium* homologues of human disease related proteins**

Disease Category <sup>a</sup>	SwissProt <sup>b</sup>	H (AA)	dictyBase ID <sup>c</sup>	D (AA)	E-value
<i>Cancer</i>					
Colon cancer ( <i>MSH2</i> )	<i>MSH2</i>	934	DDB0229897	937	0
Colon cancer ( <i>MLH1</i> )	<i>MLH1</i>	756	DDB0232418	884	1E-170
Colon cancer ( <i>PMS2</i> )	<i>PMS2</i>	862	DDB0232417	1022	1E-130
Xeroderma pigmentosum ( <i>ERCC3</i> )	<i>XPB</i>	782	DDB0214830	800	0
Xeroderma pigmentosum ( <i>XPB</i> )	<i>XPB</i>	760	DDB0191272	776	0
Oncogene ( <i>AKT2</i> )	<i>AKT2</i>	441	DDB0191195	444	4E-97
Oncogene ( <i>RAS</i> )	<i>RAS</i>	189	DDB0201663	189	6E-63
Cyclin-dependent kinase 4 ( <i>CDK4</i> )	<i>CDK4</i>	303	DDB0191155	292	2E-114
<i>Neurological</i>					
Lowe oculocerebrorenal ( <i>OCRL</i> )	<i>OCRL</i>	968	DDB0191151	787	1E-144
Miller–Dieker lissencephaly ( <i>PAF</i> )	<i>LIS1</i>	409	DDB0219930	408	1E-135
Adrenoleukodystrophy ( <i>ABCD1</i> )	<i>ALD</i> (P)	745	DDB0214891	741	2E-99
Angelman ( <i>UBE3A</i> )	<i>UBE3A</i>	852	DDB0188760	720	2E-99
Ceroid lipofuscinosis ( <i>CLN2</i> )	<i>TPP1</i> (C, P)	563	DDB0234303	600	5E-85
Tay–Sachs ( <i>HEXA</i> )	<i>HEXA</i> (C, P)	529	DDB0191256	532	7E-81
Ceroid lipofuscinosis ( <i>PPT</i> )	<i>PPT1</i> (C)	306	DDB0233890	303	5E-77
Thomsen myotonia congenita ( <i>CLCN1</i> )	<i>CLC1</i>	988	DDB0233307	809	3E-69
Choroideremia ( <i>CHM</i> )	<i>RAE1</i>	653	DDB0232224	661	1E-58
Amyotrophic lateral sclerosis ( <i>SOD1</i> )	<i>SODC</i>	154	DDB0188850	152	2E-50
Parkinson ( <i>UCHL1</i> )	<i>UBL1</i> (C, P)	208	DDB0205083	255	2E-44
<i>Cardiovascular</i>					
Hypertrophic cardiomyopathy	<i>MYH7</i>	1935	DDB0191444	2116	0
<i>Renal</i>					
Renal tubular acidosis ( <i>ATP6B1</i> )	<i>VAB1</i>	426	DDB0185207	493	0
Hyperoxaluria ( <i>AGXT</i> )	<i>SPYA</i> (C, P)	392	DDB0188646	407	3E-77
<i>Metabolic/endocrine</i>					
Niemann–Pick type C ( <i>NPC1</i> )	<i>NPC1</i> (P)	1278	DDB0191127	1342	1E-163
Hyperinsulinism ( <i>ABCC8</i> )	<i>ACC8</i>	1580	DDB0216251	1412	1E-171
McCune–Albright ( <i>GNAS1</i> )	<i>GBAS</i>	394	DDB0191255	356	5E-65
Pendred ( <i>PDS</i> )	<i>PEND</i> (C)	780	DDB0202939	944	2E-55
<i>Haematological/immune</i>					
G6PD deficiency ( <i>G6PD</i> )	<i>G6PD</i>	515	DDB0231285	497	1E-145
Chronic granulomatous ( <i>CYBB</i> )	<i>C24B</i> (C, P)	468	DDB0191274	517	2E-79
<i>Malformation</i>					
Diastrophic dysplasia ( <i>SLC26A2</i> )	<i>DTD</i> (C)	739	DDB0202939	944	8E-63
<i>Other</i>					
Cystic fibrosis ( <i>ABCC7</i> )	<i>CFTR</i>	1480	DDB0191225	1593	1E-165
Darier–White ( <i>SERCA</i> )	<i>ATA2</i>	1042	DDB0185106	1232	2E-96
Congenital chloride diarrhea ( <i>DRA</i> )	<i>DRA</i> (C)	764	DDB0202939	944	4E-61

From a list of 287 confirmed human disease protein sequences with human (H) and *Dictyostelium* (D) protein size given in amino acids (AA). Those listed share a high sequence similarity, are similar in length (+/225% in comparison to the *Dictyostelium* protein) and both proteins align over more than 70% of their respective lengths. <sup>b</sup>SwissProt identifiers for the human proteins (H). Human proteins which are absent in *S. cerevisiae* (C) or *S. pombe* (P) (defined as BLASTP probability of E\_1.0\_10230). <sup>c</sup>The best match to the human gene is listed by its dictybase ID number (Boeckeler and Williams 2007).



## 1.8 *Dictyostelium* Development

*Dictyostelium* is a unicellular social amoeba that inhabits the forest soil, feeding on yeast and bacteria (Eichinger *et al.*, 2005). When adverse conditions are enforced on *Dictyostelium*, the surrounding cells communicate with each other via pulses of extracellular cyclic Adenosine Monophosphate (cAMP). These signals act as a chemoattractant initiating aggregation by chemotaxis. Cells aggregate together forming mounds which differentiate into multi-cellular spore producing fruiting bodies within 24hr (**Figure 1.4**). When the conditions become favourable again the spores germinate and continue living as single celled organisms (Eichinger *et al.*, 2005; van et al., 2002). This process can be mimicked in a laboratory by pulsing cells with cAMP, creating a simple eukaryote biomedical model system which can be used to study cell and developmental biology (Williams *et al.*, 2006).

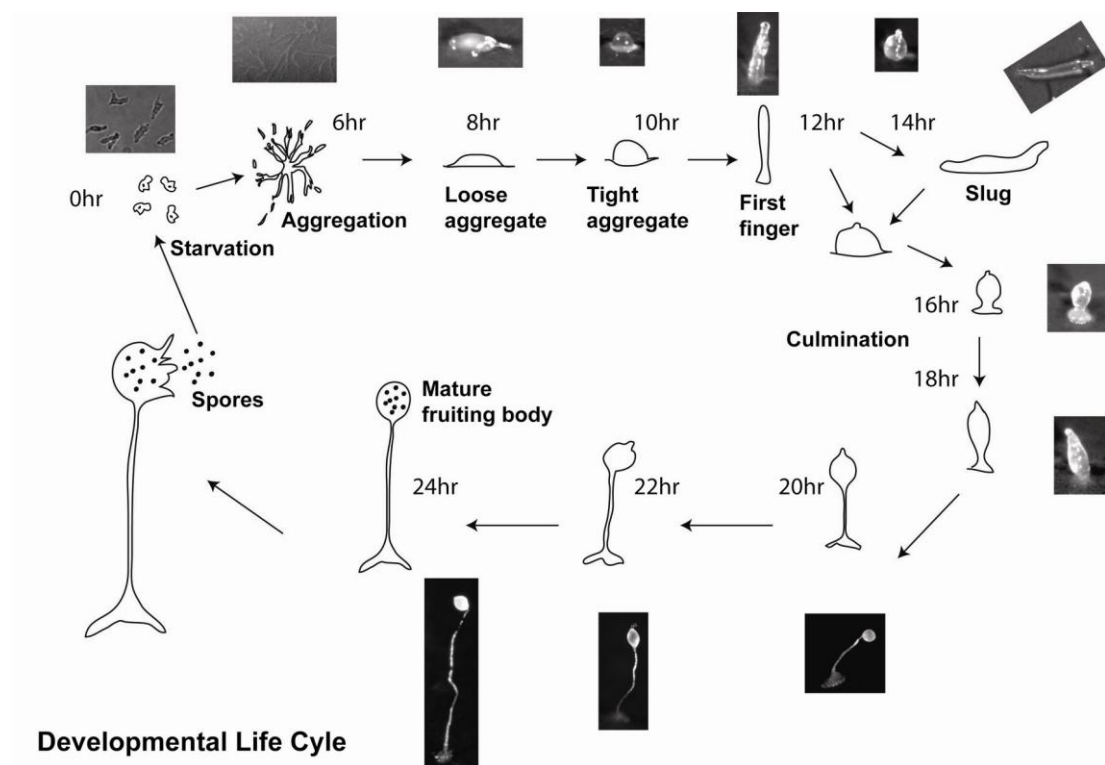


**Figure 1.4** Developmental life cycle of *Dictyostelium*

Schematic of the developmental life cycle of a single celled *Dictyostelium* which aggregates together producing a multi-cellular eukaryote organism within 24hr. Real images representing each stage can be seen next to the schematic image.

The developmental cycle is initiated by starvation when *Dictyostelium* cells secrete cAMP; the surrounding cells detect the extracellular cAMP and migrate towards the central location. During the aggregation process, cells interact with each other forming streams which migrate towards an aggregation centre producing mounds after 8-10hr. The cells that make up the mounds ( $\sim 10^5$  cells) begin to differentiate into prestalk ( $\sim 25\%$  of cells) and prespore cells ( $\sim 75\%$  of cells) causing the mound to elongate (forming a tipped mound). Continued elongation of the tip produces a structure called the first finger which is visible after 12-13hr. During this time, cell populations sort themselves along the anterior-posterior axis, consisting of anterior prestalk and posterior prespore cells which enable the formation of multi-cellular slugs. These motile slugs further differentiate into an early culminant and then the terminal structure (Chisholm and Firtel, 2004).

The differentiation into prestalk and prespore cells occurs through a number of signals, including cAMP and Differentiation Inducing Factor-1 (DIF-1). Prestalk cells are initially stimulated by cAMP during early stages of differentiation and inhibited in later stages, prespore cells, however, require a constant cAMP signal (Kay et al., 1978; Oyama and Blumberg, 1986; Schaap et al., 1986). DIF-1, however, specifically induces prestalk cell differentiation (Kay et al., 1983).

## 1.9 Chemotaxis

Chemotaxis is an essential part of early development whereby cells which have detected nutrient depletion release cAMP and stimulate surrounding cells to migrate towards this chemical signal. Detection of the cAMP signal occurs through activation of the CAR1 G-protein coupled receptor (GPCR), which, subsequently, activates intracellular signals via heterotrimeric G-protein coupling (Chung and Firtel, 2002), initiating forward movement. CAR1 activation, in turn, triggers a number of signal transduction pathways through G-protein signalling, including; the phosphoinositol-3-kinase (PI3K), Target of Rapamycin complex 2 (TORC) and the phospholipase A2 (PLA2) Pathway (Figure 1.5).

PI3K activation leads to the phosphorylation of phosphatidylinositol (4, 5)-bisphosphate (PIP2) into phosphatidylinositol (3, 4, 5)-triphosphate (PIP3), whereas phosphatase and tensin homologue (PTEN) converts PIP3 back into PIP2 through dephosphorylation of the 3' phosphate of the inositol ring. PTEN is located at the rear of the cell, thus, increasing posterior PIP2 concentrations, creating a PIP3 gradient (Huang *et al.*, 2003). PIP3 accumulation at the leading edge of migrating cells initiates a rapid translocation of PH domain proteins (Cote *et al.*, 2005). PIP3 has three known effectors: PhdA (PH-domain containing protein) (Funamoto *et al.*, 2001), cytosolic regulator of adenylate cyclase (CRAC) (Huang *et al.*, 2003) and PkbA (a PKB-related protein) (Meili *et al.*, 1999). All these effectors play an important role in chemotaxis. PhdA initiates increased F-actin polymerisation (Huang *et al.*, 2003) whereas CRAC and PkbA increases the production and release of intracellular cAMP through activation of adenylate cyclase (AC) (Insall *et al.*, 1994; Lilly and Devreotes, 1995). PkbA is also involved in regulating cell polarity through activation of p21 activated kinase A (PAKa) (Chung and Firtel, 2002).

The TORC2 complex was shown to play a role in F-actin polymerisation at the leading edge of the cell during PKB/Akt and RasG signalling (Charest *et al.*, 2010; Kamimura *et al.*, 2008; King and Insall, 2008). Furthermore, TORC2 plays a key role in regulating AC through PKB-like receptor 1 (PKBR1) (Kamimura *et al.*, 2008; King and Insall, 2008).

The PLA2 signalling pathway has been shown to be PI3K independent (Chen *et al.*, 2007). PLA2 converts cell membrane phospholipids to lysophospholipids and arachidonic acid, which is thought to lead to increases in intracellular calcium levels and thus, chemotaxis (King and Insall, 2009; Van Haastert *et al.*, 2007)

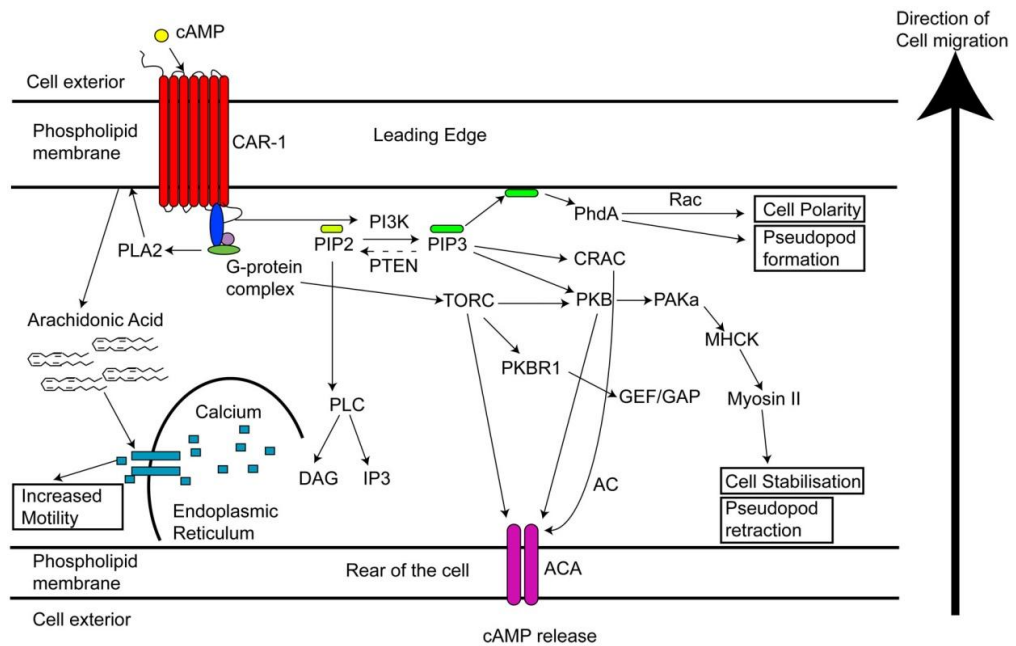


**Figure 1.5 Signalling Pathways in *Dictyostelium* Chemotaxis.**

Activation of CAR receptors by cAMP activates PI3K, TORC and PLA2 pathways. PI3K phosphorylates PIP2 to PIP3, initiating the localisation of PH domain containing proteins to the leading edge of a cell, through PhdA, CRAC and PKB. CRAC and PKB/Akt are both involved in the RasC activation of adenylate cyclase A (ACA) in the cell membrane which releases cAMP from the cell. PKB is also involved in the maintenance of cell polarity as well as activation of MCHKs, which in turn activate myosin II, a protein that assists cell stabilisation (rigidity) and pseudopod retraction from the rear of the cell. PTEN converts PIP3 back into PIP2, which is degraded by phospholipase C into DAG and IP3. TorC activates F-actin polymerisation at the leading edge through PKB (and RasG) signalling. Activation of PLA2 pathway converts phospholipids located on the cell membrane into arachidonic acid and leading to an increase in the intracellular calcium levels. This in turn drives cellular motility.

## 1.10 Cytokinesis

Cell division is a crucial cellular function that involves a dynamic interaction between the actin/myosin cytoskeleton and the microtubule network. The process of cytokinesis occurs through a series of stages (**Figure 1.6**). Microtubules initiate the first steps in cytokinesis, where the spindle fibres determine the cleavage furrow position. The next stage involves the accumulation of myosin II in the furrow, initiating the constriction of the actin contractile ring and causing furrow ingression. During the final stages of cytokinesis, the equatorial region constricts, producing a midbody (cytoplasmic bridge) which is finally severed, leading to the production of two daughter cells.

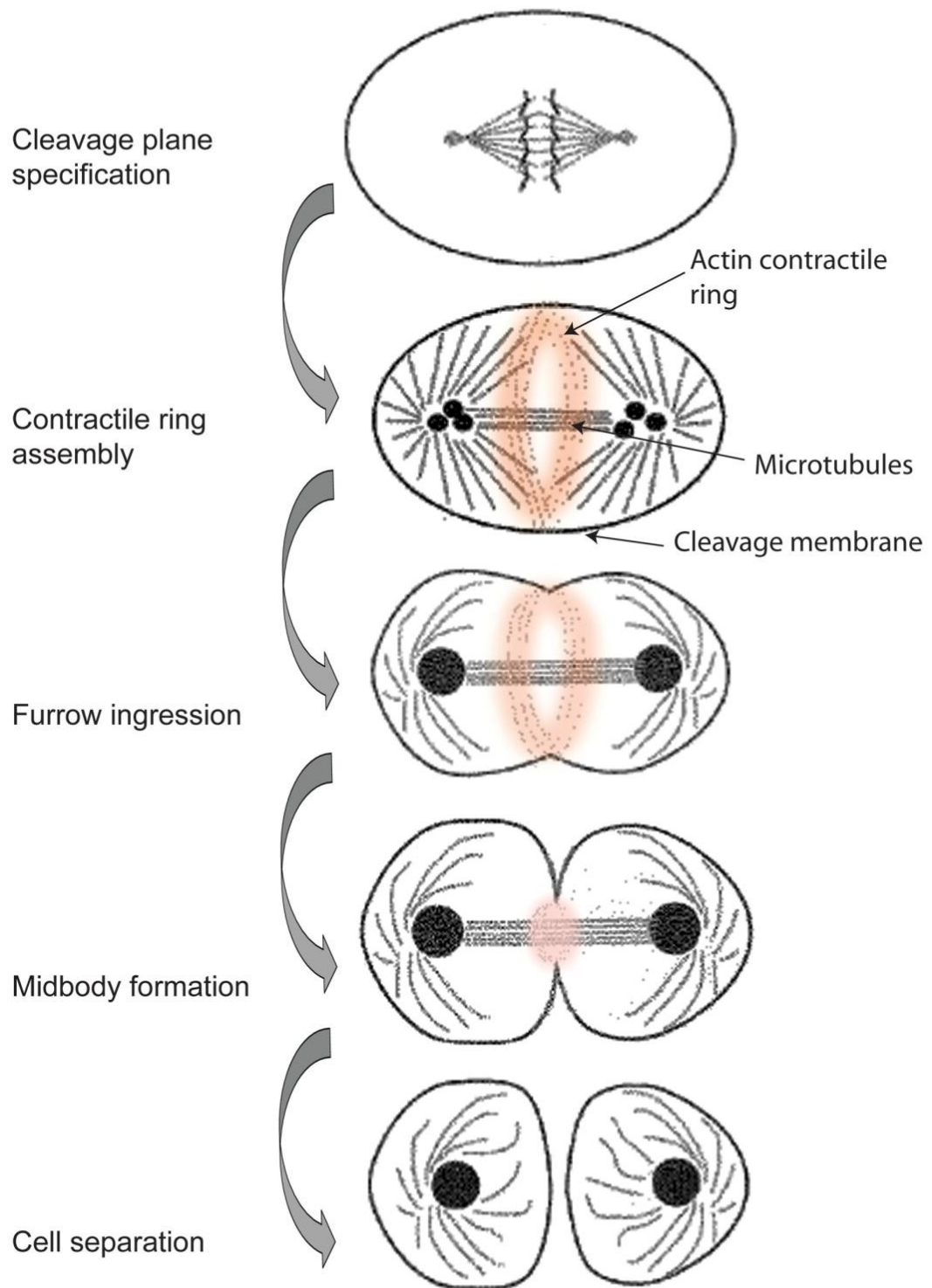


**Figure 1.6 Stages of cytokinesis**

Cytokinesis involves the interplay between microtubules, actin filaments (red) and the cell membrane, which occur through a series of steps: cleavage plane specification, contractile ring assembly, furrow ingression, midbody formation and finally daughter cell separation. Images adapted from Glotzer (, 1997).

The dynamic roles between microtubules, actin and myosin are not completely understood. The mechanism of how microtubules establish the plane of division is unclear, however, it is thought that they either provide a localised source of a signal that is delivered by a motor protein, or they make mechanical contacts with the cell cortex (Neujahr et al., 1998).

During cytokinesis, myosin accumulates in the cleavage furrow, initiating constriction of the actin contractile ring. In myosin II null cells, cytokinesis was completely inhibited in suspension, however, the cells were still able to undergo normal cytokinesis on a substrate (Neujahr et al., 1997b). This suggests that, on a substrate, there is another mechanism which acts through a myosin II independent pathway (De and Spudich, 1987; Knecht and Loomis, 1987; Neujahr et al., 1998). Together with myosin, the actin contractile ring is required to deliver the force needed to deform the cortex and separate the daughter cells. The disruption of either actin or myosin components severely impairs cytokinesis.

### **1.11 Small GTPase signalling**

G-proteins are small molecular switches within a cell that regulate a diverse range of intracellular signalling pathways. One common G-protein is the heterotrimeric G-protein that consists of 3 subunits ( $\alpha$ ,  $\beta$  and  $\gamma$ ) and is often activated by cell surface receptors such as G-protein coupled receptors (GPCRs). The Ras superfamily are small GTPase G-proteins which are structurally similar to the  $\alpha$ -subunit of the heterotrimeric G-protein, however, the Ras family of small GTPases function as a monomeric proteins (Biou and Cherfils, 2004; Wennerberg et al., 2005). This family can be subdivided into five subclasses: Ras, Ran, Rho, Arf and Rab.

When small GTPases are bound to guanosine triphosphate (GTP) they remain active. Inactivation occurs by the hydrolysis of GTP to guanosine diphosphate (GDP). Guanine nucleotide Exchange Factor (GEF) proteins facilitate the dissociation of GDP, allowing GTP to bind and re-activate the GTPase (Cerione and Zheng, 1996; Nishikimi et al., 2005). GTPase Activating Proteins (GAPs), on the other hand, are known to inactivate G-proteins by

binding to the active form stimulating the hydrolysis of GTP to GDP (Boguski and McCormick, 1993). GEFs and GAPs positively regulate the cycling of G-proteins between the active and inactive state, however, GDP Dissociation Inhibitors (GDIs) act as negative regulators of G-proteins by blocking the dissociation of GDP and thus inhibit its activation (Cherfils and Chardin, 1999; Siderovski and Willard, 2005) (**Figure 1.7**).

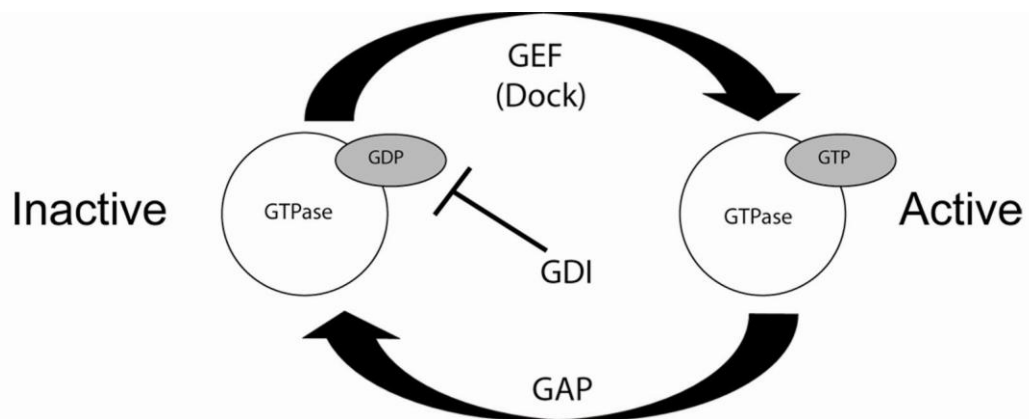


**Figure 1.7 GTPase cycling mechanism**

Schematic illustrating the regulatory GTPase cycling molecules. Guanine nucleotide Exchange Factor (GEF) facilitates guanine diphosphate (GDP) dissociation, allowing guanine triphosphate (GTP) to bind cycling the GTPase into its active state. GTPase Activating Protein (GAP) increases the hydrolysis of GTP to GDP, cycling the GTPase into its inactive state. GDP Dissociation Inhibitors (GDI) inhibits the dissociation of GDP thus acting as a negative regulator of GTPases, prolonging the inactive state of the GTPase.

### 1.11.1 Rho family of small GTPases

In humans, the Rho family of small GTPases consists of 22 proteins, the majority of which fall into the Rho, Rac and Cdc42 subclasses (Jaffe and Hall, 2005; Nishikimi et al., 2005). Rho family proteins are key regulators of the actin/myosin cytoskeleton during cellular movement (Raftopoulou and Hall, 2004). When in their active state, these GTPases regulate a wide diversity of cellular processes, such as cell adhesion, cytokinesis, cell-cycle progression, macropinocytosis, endocytosis, membrane trafficking, and signal transduction (Ridley, 2001).

RhoA, Rac1 and Cdc42 are the most studied Rho family proteins. RhoA has been shown to promote actin stress fibre formation and focal adhesion assembly (Ridley and Hall, 1992). Rac1 promotes lamellipodium formation and membrane ruffling (Ridley et al., 1992). Cdc42 promotes actin microspikes and

filopodia formation as well as cell adhesion, motility, polarity, cytokinesis and growth (Etienne-Manneville and Hall, 2002; Sinha and Yang, 2008). Rho, Rac and Cdc42 regulate three separate signal transduction pathways linking plasma membrane receptors to the assembly of F- actin. Apart from the regulation of the actin cytoskeleton, Rho family GTPase play other key roles within the cell, for example, Cdc42 is required to establish cell polarity through microtubule dynamic regulation (Etienne-Manneville, 2004; Etienne-Manneville and Hall, 2001).

### 1.11.2 Small GTPase signalling in *Dictyostelium*

In *Dictyostelium*, nineteen Rac homologues have been identified, although, homologues for Rho or Cdc42 have yet to be discovered (Rivero et al., 2001; Vlahou and Rivero, 2006; Wilkins and Insall, 2001). Phylogenetic analysis of these Rho-related genes illustrates the genetic evolution of the *Dictyostelium* proteins in comparison to their homologues in other organisms (Vlahou and Rivero, 2006). This analysis shows Rho-proteins which group in close evolutionary distance to both Rho and Cdc42 proteins (**Figure 1.8**). Sequence comparison data shows that Rac1a, Rac1b, Rac1c, RacF1, RacF2, RacB and the GTPase domain of RacA groups in the Rac sub-family, however, all the other *Dictyostelium* Rac proteins do not have clear affiliations and group amongst different GTPase families.





**Figure 1.8 Phylogenetic analysis of the Rho family of small GTPases.**

*Dictyostelium* Rho GTPases are highlighted in black. \* indicates a significant cluster of *Dictyostelium* Rho GTPases, suggesting that they might also function in the same processes (Vlahou and Rivero, 2006).

The overexpression, gain-of-function and knockout mutant studies have largely shown that the function of *Dictyostelium* Rho family GTPase is to regulate the actin cytoskeleton. These studies have demonstrated clear roles for these GTPases in morphology, chemotaxis, endocytosis and vesicle trafficking, cytokinesis and development (Dumontier et al., 2000; Park et al., 2004; Rivero et al., 1999a; Somesh et al., 2006).

Rac1 has been extensively studied in *Dictyostelium*. There are three isoforms of Rac1a-c, all of which behave in the same manner and have been shown to function in development, chemotaxis, filopodia formation, cytokinesis,

endocytosis, phagocytosis and growth (Dumontier et al., 2000; Faix, 2002; Palmieri et al., 2000). Rac1 has been shown to regulate F-actin polymerisation, since overexpression of Rac1a led to significant increases in polymerised F-actin. In contrast, constitutively active and dominant negative forms of Rac1 displayed inefficient F-actin polymerisation (Dumontier et al., 2000; Palmieri et al., 2000). This suggests that Rac1-dependent F-actin polymerisation requires the cycling of this GTPase between its active and inactive state.

Overlapping functions have been demonstrated in a number of other Rac GTPases in development, chemotaxis, filopodia formation, cytokinesis, endocytosis, phagocytosis and growth, which suggests that multiple Racs regulate these cellular functions. For example, RacE was the first *Dictyostelium* Rac shown to be essential in cytokinesis, since absence of this protein severely impaired this cellular process (Larochelle *et al.*, 1997), however, the lack of Rac1, RacC and RacB were also shown to cause defects in cytokinesis (Dumontier et al., 2000; Park et al., 2004; Seastone et al., 1998).

## 1.12 Guanine nucleotide Exchange Factor proteins

Guanine nucleotide Exchange Factor (GEF) proteins function to activate small GTPases, by facilitating dissociation of GDP and allowing GTP to bind. There are approximately 83 GEFs in the human genome which are divided into two major subfamilies (Gadea et al., 2008; Yelo et al., 2008). The largest subfamily consists of the classical Dbl Homology–Pleckstrin homology (DH-PH) containing proteins which mediate the GEF activity through the DH domain whereas the PH has an auto inhibitory role and controls membrane recruitment (Cerione and Zheng, 1996). The second major GEF subfamily is the Dock proteins. There are 11 human Dock proteins which are divided into four main subclasses: consisting of the Zizimin family (Ziz), Zizimin-related family (Zir), Dock4-related family and the Dock180-related family, based on their domain structure, sequence similarity and phylogenetic analysis (Meller *et al.*, 2005) (**Figure 1.9**).

The Dock family have two characteristic domains that make them distinct from the classical Dbl-Homology Plekstrin Homology (DH-PH) family GEFs,

which carry out their GEF activity through the DH domain. The characteristic domains for the Dock family are the Dock Homology Region 1 (DHR1) and Dock Homology Region 2 (DHR2) domains (also known as the CZH1 and CZH2 domains, respectively) (Cote *et al.*, 2005; Cote and Vuori, 2006). Little is known about the exact role of the DHR1, although, it is thought to be functionally linked to the DHR2 domain (Meller *et al.*, 2005). Other studies have shown that this DHR1 domain acts as a lipid binding domain and has shown specificity for PIP3 (Cote *et al.*, 2005; Kobayashi *et al.*, 2001). The Plekstrin Homology (PH) domain is a domain specific to the Zizimin subfamily and is involved in membrane localisation (Zheng *et al.*, 1996).

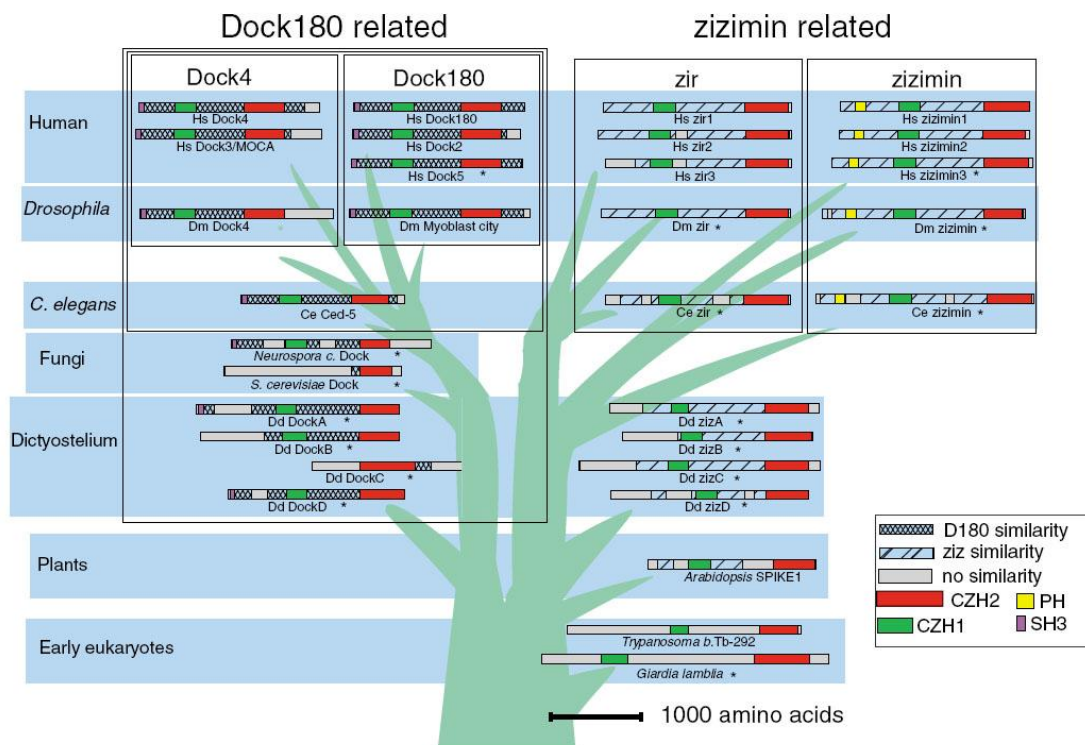


**Figure 1.9 Phylogenetic and domain structure analysis of the Dock protein family.**

Schematic diagram of the Dock (CZH) proteins, illustrating the hypothetical evolution of these proteins based on sequence similarity (Meller *et al.*, 2005). The SH3 (Src Homology domain 3) and PH domains have been shown as well as the DHR1 (CZH1) and DHR2 (CZH2) domains. Proteins that have Zizimin1 similarity Dock180 similarity are crossed or hatched.

The cellular role of the Dock family of GEF proteins has been shown to specifically activate the Rho family of small GTPases (Rac, Cdc42 and Rho) (Meller *et al.*, 2002; Nishikimi *et al.*, 2005). Dock180 was originally identified as one of two major proteins bound to the Crk complex, and has become the standard for studying Dock protein function (Hasegawa *et al.*, 1996; Kiyokawa

et al., 1998a; Kiyokawa et al., 1998b). Dock180 specifically binds Rac and forms a complex with Engulfment and Cell Motility (ELMO) protein and has been shown to be involved in cell migration and phagocytosis in mammalian systems (Cheresh et al., 1999; Hasegawa et al., 1996; Kiyokawa et al., 1998b).

The Zizimin and Zizimin-related subclass of Dock proteins have not been as extensively studied. The Zizimins (Dock 9, 10 and 11) subclass has been shown to specifically regulate Cdc42 (Kuramoto et al., 2009; Nishikimi et al., 2005), however, the Zizimin-related proteins (Dock6, 7 and 8) can activate both Rac and Cdc42 (Ruusala and Aspenstrom, 2004). Although, these proteins have been shown to specifically regulate Cdc42 and Rac, the signalling pathway and binding targets remains poorly characterised. In A375m2 melanoma cells Dock10 was identified to have key roles in amoeboid migration (Gadea et al., 2008). From those investigations it was proposed that Dock10 is a Cdc42 GTPase which also interacts with the effector proteins N-WASP and Pak2 to control actomyosin contractility in amoeboid motility in A375m2 melanoma cells (**Figure 1.8**). Although, this provides some insight into the functioning of this protein, the exact mechanism behind the cellular role remains poorly defined.

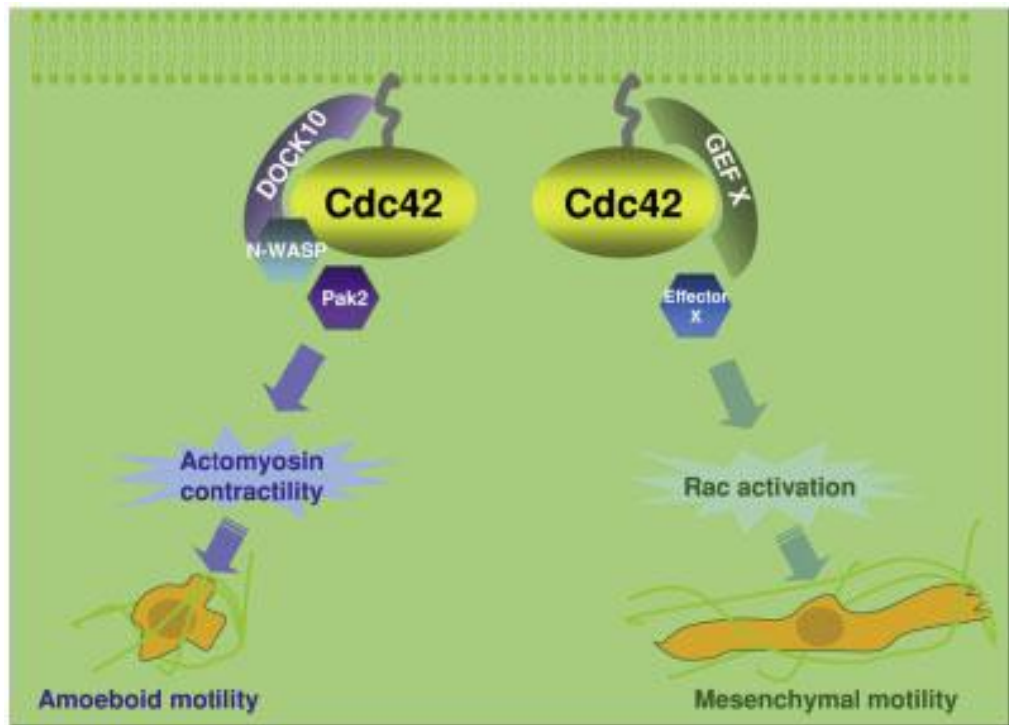


**Figure 1.10 Model of Dock10-Cdc42 in amoeboid movement.**

This model illustrates how Dock10-Cdc42-N-WASP complex contributes to actin assembly and Dock10-Cdc42-Pak2 leads to actomyosin contractility in amoeboid motility; as well as showing a different Cdc42-dependent axis involving other GEFs and effectors that leads to Rac1 activation and elongated-mesenchymal-type motility (Gadea *et al.*, 2008).

In *Dictyostelium*, there are eight known Dock related proteins, which can be grouped into the Zizimin-related (ZizA-D) and the Dock180-related (DocA-D) proteins. The four Dock180-related proteins have been studied, where they were found to be involved in chemotaxis as well as development. Interaction studies also showed that DocD interacts with ELMO, however, the exact cellular mechanisms remain poorly understood (Para *et al.*, 2009). The Zizimin-related subfamily have not previously been analysed in *Dictyostelium*, therefore, little is known about the cellular role or the target substrates of these proteins.

### 1.13 PIM2 (DRIP 9)

Human DRIP 9 or PIM2 protein has a documented role in oncogenesis. This protein is a serine/threonine (ser/thr) kinase which has been shown to be involved in cell survival pathways via resisting apoptotic signals (White, 2003). Fox *et al.* (2003) used oligonucleotide microarray analysis to illustrate the role of PIM2 in growth-factor mediated apoptotic resistance in hematopoietic cells. PIM2 contains 2 other members within its serine/threonine kinase family, PIM1 and PIM3. Fox *et al.* (2003) used FL5.12 cells, a murine, nontransformed, pro-B cell line dependent on IL-3 for survival, growth, and proliferation, to illustrate that PIM protein kinases are regulated by cytokines. They did this by depriving FL5.12 cells of interleukin-3 (IL-3) for 6 hrs, causing downregulation of PIM2 mRNA levels. However, normal levels were recovered upon IL-3 restoration. Moreover, the exact mechanism by which PIM2 resists apoptotic signal, and the mechanism as to how it is regulated remain unclear.

### 1.14 Microtubule Affinity Regulating Kinases (MARKs)

There are four known MARK proteins in human, MARK 1-4. These proteins are a group of serine/threonine kinases that regulate Microtubule Associated Proteins (MAPs). The regulation of the MAPs occurs by phosphorylation of a serine or threonine residue which triggers microtubule disassembly (Chen *et al.*, 2006; Schaar *et al.*, 2004). MARK proteins are related to Protease Activated Receptor-1 (PAR-1) and Kin-1, the MARK protein orthologues in *Caenorhabditis elegans*, *Drosophila melanogaster* and *Schizosaccharomyces pombe*, and have been shown to be involved in establishing cell polarity (Drewes *et al.*, 1997; Sun *et al.*, 2001; Trinczek *et al.*, 2004). The functional mechanisms of PAR-1, has been shown to involve the Wnt pathway, where it activates *dishevelled* as has been demonstrated in *Drosophila melanogaster* (Sun *et al.*, 2001). MARKs are potent regulators of MAPs and are highly regulated themselves through phosphorylation by Microtubule Affinity Regulating Kinase Kinase (MARKK) protein, a member of the Ste20 kinase family (Drewes *et al.*, 1997; Timm *et al.*, 2003). MARKK activates MARK by phosphorylation of a single residue, T208. A non-phosphorylated serine residue (S212) has been shown to be a prerequisite

for a MARKK phosphorylation of MARK. However, the phosphorylation of the S212 residue leads to an inhibition of the MARK protein (Timm *et al.*, 2003).

### 1.15 Aims of this work

Eleven novel human dopamine receptor interaction proteins (DRIPs) were identified using a yeast II hybrid screen (Zhan et al., 2008; Zhan et al., 2010b). Little is known about why these DRIPs interact with the dopamine receptor or their implications in schizophrenia and bipolar disorder. Furthermore, the cellular roles of these DRIPs as signalling molecules is poorly characterised. The aims of this thesis were to investigate the cellular functions of these novel DRIPs using the biomedical model *Dictyostelium discoideum*. To address this question I used the following strategies:

- Identify potential *Dictyostelium* homologues of the eleven novel human DRIPs.
- Analyse the structural characteristics of these potential *Dictyostelium* homologues and establish the evolutionary conservation of the protein families.
- Investigate the characteristics and cellular functions of a DRIP protein family in *Dictyostelium* using molecular biology and proteomic techniques:
  - Gene ablation
  - Cellular function assays
  - Microscopy
  - Protein interaction studies



## **2 Materials and Methods**

## 2.1 Materials

### 2.1.1 General chemicals

#### ***2.1.1.1 Reagents purchased from Sigma-Aldrich Co. Ltd. (Poole, Dorset, England)***

2-Propanol, 4',6-diamidino-2-phenylindole (DAPI), acrylamide (30% solution) ammonium persulfate (APS), bacteriological agar, beta-mercaptoethanol, caffeine, cyclic adenosine monophosphate (cAMP), dithiotreitol (DTT), ethylenediaminetetraacetic acid (EDTA) ethylene glycol tetraacetic acid (EGTA), horse serum, sodium dodecyl sulfate (SDS), Luria-Burtani (LB) broth tablets, magnesium chloride, nonidet p-40 (NP40), TWEEN20, phenylmethylsulfonyl fluoride (PMSF), phalloidin-tetramethylrhodamin isothiocyanate (phalloidin-TRITC), potassium chloride, sucrose, sodium chloride, sodium dihydrogen phosphate ( $\text{NaH}_2\text{PO}_4$ ), sodium fluoride, sodium orthovanadate, sodium phosphate dibasic ( $\text{Na}_2\text{HPO}_4$ ), N,N,N',N'-tetramethylethylene-1,2-diamine (TEMED), trisma base, tritonX-100.

#### ***2.1.1.2 Reagents purchased from other suppliers***

Agarose, deoxynucleotide triphosphates (dNTPs), (Bioline, London England)

6x Loading dye (MBI Fermentas, Sunderland, Tyne & Wear, England)

Ethanol, di-potassium hydrogen phosphate ( $\text{K}_2\text{HPO}_4$ ), glycerol, acetic acid, acetone, bromophenol blue, chloroform, dimethyl sulfoxide (DMSO), glucose (D-), hydrochloric acid, Isopropyl  $\beta$ -D-1-thiogalactopyranoside (IPTG), methanol, paraformaldehyde (PFA), phenol: chloroform: iso-Amyl alcohol, potassium dihydrogen phosphate ( $\text{KH}_2\text{PO}_4$ ), sodium hydroxide, (VWR International Ltd., Lutterworth, Leicestershire, England).

Tris-borate-EDTA (TBE) 10x, glycine, Coomassie Brilliant Blue G250 (Fisher Scientific, Loughborough, Leicestershire, England)

NuPage MOPS buffer, NuPage transfer buffer, NuPage SDS-polyacrylamide gel (Invitrogen Groningen, the Netherlands).

Ethidium bromide (Bio-Rad Laboratories, Hemel Hempstead, Hertfordshire England)

Axenic (Ax) medium, SM medium (ForMedium, Hunstanton, Norfolk, England)

Complete Mini Protease inhibitor cocktail (Roche, West Sussex, UK)

### **2.1.1.3 Antibiotics**

Ampicillin, (Sigma-Aldrich Co. Ltd. Poole, Dorset, England)

Blasticidin, penicillin/streptomycin (Pen/Strep) solution 100x (PAA Laboratories Ltd. Yeovil, Somerset, England)

Hygromycin, Geneticin (Invitrogen Groningen, the Netherlands)

### **2.1.1.4 Molecular weight standards**

GeneRuler 100bp plus and 1 kb DNA Ladder ( $0.1\mu\text{g}\cdot\mu\text{l}^{-1}$ ), PageRuler Plus Prestained protein ladder (MBI Fermentas, Sunderland, Tyne & Wear, England).

### **2.1.1.5 Restriction Enzymes**

All restriction enzymes and the corresponding buffers (MBI Fermentas, Sunderland, Tyne & Wear, England)

### **2.1.1.6 Other Enzymes**

RNase A, DNase (Sigma-Aldrich, Poole, Dorset, England)

BIOTaq polymerase (Bioline, London England)

Proteinase K, T4 DNA ligase (MBI Fermentas, Sunderland, Tyne & Wear, England)

Calf Alkaline Phosphatase (CIAP) (Promega UK Southampton, England)

### **2.1.1.7 Antibodies**

GFP rat monoclonal antibody, GFP Trap agarose beads (ChromoTek GmbH, Germany)

Anti-GST agarose beads (Sigma Aldrich, Poole, Dorset, UK)

Anti-Glutathione S-Transferase mouse monoclonal antibody (Millipore UK)

IRDye 800 Goat Anti-Rat, IRDye 800 Goat Anti-Mouse (Licor bioscience Ltd, Nebraska, USA)

#### **2.1.1.8 Kits**

QIAfilter Plasmid Maxi Kit and MinElute PCR Purification Kit (QIAGEN Ltd, Crawley, West Sussex, UK)

The GenElute HP Plasmid Midiprep and Maxiprep kit (Sigma-Aldrich, Poole, Dorset, UK)

GENOME DNA Kit (MP Biomedicals, Illkirch France)

High Pure RNA Isolation Kit (Roche, West Sussex, UK)

Illustra MicroSpin S-400 HR Columns (GE Healthcare, Buckinghamshire, UK)

DNase treated with DNA-free Kit (Ambion)

First Strand cDNA Synthesis Kit (Fermentas, Sunderland, Tyne & Wear, England)

#### **2.1.1.9 *Escherichia coli* (*E.coli*) strains**

TOP10 chemically competent *E.coli*, chemically competent *JM107 E.coli*

(Invitrogen, Groningen, the Netherlands)

10-beta Competent *E. coli* (New England Biolabs)

#### **2.1.1.10 Primers**

Primers were all purchased from VWR International Ltd. (Lutterworth, Leicestershire, England)

#### **2.1.1.11 Equipment**

Bio-Rad gel casting system, Bio-Rad wide mini-sub cell electrophoresis system, Gel Doc XR system, PowerPac 300 power supply, GenePulser Xcell electroporator (Bio-Rad Laboratories, Hemel Hempstead, Hertfordshire England)

GeneFlash gel documentation system (Syngene Bio Imaging)

Centrifuge (Biofuge 13, Jencons)

PeqSTAR 2x thermocycler, PeqSTAR 96 Universal thermocycler (PEQLAB Ltd, Fareham, Portsmouth, England)

Odyssey Infrared Imaging System (Li-cor Biosciences, Nebraska, USA).

4mm EP cuvettes (PEQLAB Ltd, Fareham, Portsmouth, England)

Olympus IX71 microscope (U-RFL-T laser, 482nm emission, Olympus UPlanFL 60x oil immersion objective with NA 1.25) with an QImaging RetigaExi Fast1394 digital camera.

## 2.2 Methods

### 2.2.1 Bioinformatic analysis

In order to identify the *Dictyostelium* homologues of DRIP proteins and homologues within other species the Basic Local Alignment Search Tool (BLAST) search optimised for more dissimilar sequences (discontinuous megablast) was conducted using the engine from the National Centre for Biotechnology Information site (NCBI, <http://www.ncbi.nlm.nih.gov/BLAST/>). The search was performed within the protein collection of the 'nr' database (others) using the BLASTP suite (Zhang *et al.*, 2000). This database contains most of the nucleic acid sequences that have been reported. The 'nr' stands for 'non-redundant' and implies that any given sequence within the database appears only once to minimise the duplication. Discontinuous megablast ignores some bases allowing mismatches and is intended for cross-species comparisons. The search was conducted with the following parameters: program = BLASTP 2.2.25; matrix = blosum62; threshold = 0.01.

Phylogenetic analysis was used to investigate the evolutionary history of the Zizimin and MARK family of proteins. This method used the neighbour-joining method to construct a phylogenetic tree using *MEGA* version 5 (Tamura, Peterson, Stecher, Nei, and Kumar 2011). The bootstrap test was performed with 500 replicates. The SMART engine and the Conserved Domain Database (CDD) accessible at NCBI website were used to obtain the information

regarding the structure and conserved functional domains in human and *Dictyostelium* Zizimin and MARK family proteins.

## 2.2.2 *Dictyostelium discoideum* Methods

### 2.2.2.1 Cell culture

Cells were stored as spores in 1x sterilised phosphate buffer, KK2 (16.2mM  $\text{KH}_2\text{PO}_4$ , 4mM  $\text{K}_2\text{HPO}_4$ ) at  $-80^\circ\text{C}$ . Every 4 weeks the frozen *Dictyostelium* stock was added to a SM agar (Sigma) plate containing 300  $\mu\text{l}$  of *Raoultella planticola* and incubated at  $21^\circ\text{C}$  for 3-4 days. Liquid plates were then prepared, containing Ax medium (ForMedium), 100  $\mu\text{g/ml}$  Penicillin, 100 $\mu\text{g/ml}$  Streptomycin and about a 2.5cm scrapping of the *Dictyostelium* growth zone of the SM agar plate, which had been wash twice with KK2, and kept at  $21^\circ\text{C}$ . The cells were maintained shaking (120rpm) at  $21^\circ\text{C}$  and harvested in mid-log phase ( $4 \times 10^6$  cells/ml). The cell concentration was determined using a Neubauer improved haemocytometer.

For growth curve assays, cells were seeded at a density of  $10^5$  cells/ml in Ax medium. Cell densities at various time points were determined by counting using a Neubauer improved haemocytometer.

### 2.2.2.2 Development assays

Wild type Ax2 and mutant cell lines were grown at  $21^\circ\text{C}$  in a shaking culture (120rpm) of Ax medium for 48hr. In these experiments  $1 \times 10^7$  cells were harvested, washed and resuspended in KK2. The cells were evenly distributed on a 47mm black nitrocellulose filter (Millipore), soaked in KK2. The cells were incubated at  $21^\circ\text{C}$  for 24hr.

### 2.2.2.3 Expression profile

The expression of the four Zizimin genes (*zizA-D*) were analysed during *Dictyostelium* development. Cells were harvested at a density of  $1 \times 10^7$  cells per ml before being washed in KK2 and evenly distributed on a 47mm nitrocellulose filter (Millipore). The filter was incubated for 24hr at  $21^\circ\text{C}$  on an absorbent pad soaked in KK2. RNA was extracted from developing cells at 4hr intervals throughout the 24hr developmental cycle, using the High Pure RNA Isolation Kit

(Roche Applied Science). The RNA samples were DNase treated with DNA-free Kit (Ambion) and cDNA was synthesised with First Strand cDNA Synthesis Kit (Fermentas) according to manufacturer's instructions. cDNA was amplified with gene specific primers and run on a 1% (w/v) agarose gel. Data was processed using Quantity One 1-D software (version 4.6.3, Bio-Rad Laboratories, Inc.) software. The intensities of the DNA bands were quantified and adjusted by the variation found in the expression of the control gene (*Ig7*).

## **2.2.3 Molecular Biology methods**

### ***2.2.3.1 Polymerase chain reaction***

DNA was amplified by polymerase chain reaction (PCR) under the following conditions: 5 $\mu$ l of DNA, 2 $\mu$ l of 2mM dNTPs, 2 $\mu$ l NH<sub>4</sub> BIOTAQ reaction buffer, 1 $\mu$ l MgCl<sub>2</sub>, 0.5 $\mu$ l BIOTAQ DNA polymerase (5U  $\mu$ l<sup>-1</sup>) and 2 $\mu$ l of each primer (10pmol) were used in a 20 $\mu$ l reaction.

The PCR was carried out under the following cycling conditions: initial denaturing 10min at 95°C, 30 cycles of denaturation for 30sec at 95°C, annealing for 45sec (with the temperature depending on primer melting points) and extension for 4min at 68°C (or 1min at 72°C depending on the primer) were followed by a final extension of 10min at 68°C (or 72°C). Samples were then stored at 4°C. PCR with BIO-X-ACT (Bioline) polymerases was performed according to manufacturer protocol.

### ***2.2.3.2 Agarose gel electrophoresis***

Agarose gel electrophoresis was used to separate and visualise DNA using 1% agarose gels containing ethidium bromide and TBE Buffer. 5 $\mu$ l of DNA were prepared in 1x DNA Loading Buffer. 100bp plus or 1kb DNA ladders (Fermentas) were used as molecular marker on the agarose gels. The gel was run in an electrophoresis tank for 40min at 100V and visualised using a GeneFlash gel documentation system (Syngene Bio Imaging)

### ***2.2.3.3 Transformation of competent E.coli***

Agar plates were made from 330ml sterile Luria-Burtani (LB) agar media (according to Sigma's protocol), to which 1.0 $\mu$ l ampicillin (50 $\mu$ g  $\mu$ l<sup>-1</sup>) per ml of

media was added. 30ml media was poured into 90mm diameter petri dish. Chemically competent *JM107 E.coli* cells were used for the transformations and thawed on ice until needed. 10 $\mu$ l of ligation DNA was added to 100 $\mu$ l of competent *E.coli* cells. After the 30min incubation on ice, the cells were heated at 42°C in a heat block for 60sec and then rapidly transferred to ice for 2min. 250 $\mu$ l LB media was added to the cells and incubated in a shaking incubator at 37°C for 1hr. After incubation, cells were spun down in a centrifuge and the LB media was removed. The cells were resuspended in 100 $\mu$ l fresh LB media, plated onto the agar plates, and incubated in at 37°C overnight.

#### **2.2.3.4 Plasmid preparation**

Plasmids used for cloning and sequencing were prepared using the Sigma GenElute Plasmid Miniprep Kit or Qiagen QIAfilter Plasmid Midi Kit columns as described by the manufacturers.

To verify positive transformants from *E.coli* without using commercial kits, 1.5ml of an overnight culture was harvested for 60 seconds at 13000rpm. The pellet was resuspended in 200 $\mu$ l P1 buffer (50mM Tris-Cl pH8.0, 10mM EDTA, 100 $\mu$ g/ml RNase A) and added to 200 $\mu$ l P2 buffer (200mM NaOH, 1% SDS (W/V)). After 5min incubation at room temperature 200 $\mu$ l P3 buffer (3M potassium acetate pH 5.5) was added, mixed and further incubated on ice for 5min. Cell debris was removed by centrifugation at 12, 000xg for 10min. The DNA was precipitated by adding 0.7vol isopropanol to the supernatant before centrifugation at 12, 000xg for 20min. The pellet was washed with 600 $\mu$ l 70% ethanol and further centrifuged at 12, 000xg for 10min. The resultant pellet was air dried to remove any residual ethanol and resuspended in 20 $\mu$ l ddH<sub>2</sub>O.

#### **2.2.3.5 Restriction digests**

All restriction digests were prepared according to the following conditions: in a 20 $\mu$ l reaction, 10  $\mu$ l of DNA was combined with 0.2 $\mu$ l of restriction enzyme (10U  $\mu$ l<sup>-1</sup>) and 2 $\mu$ l of the appropriate buffer. Reactions were incubated at 37°C for 2hr.



### 2.2.3.6 Construction of the knockout (KO) vector

PCR was used to amplify two fragments inside the open reading frame of the gene to be knocked out, using Ax2 genomic DNA as a template, illustrated in figure 2.1. PCR products were purified using the GenElute PCR purification kit (Qiagen) protocol or the GE Healthcare s400 MicroSpin columns. The pLPBLP vector and gene fragments were double-digested with suitable restriction enzymes, before each fragment was separately cloned into the pLPBLP vector backbone. Prior to cloning each gene flanking region, the double-digested pLPBLP vector was incubated for 1hr with 1 $\mu$ l of Calf Alkaline Phosphatase (CIAP) (1U  $\mu$ l<sup>-1</sup>) and its appropriate buffer and then heat inactivated at 65°C for 15min. The double digested PCR products were ligated into the CIAP treated pLPBLP vector backbone using 1 $\mu$ l T4 DNA ligase (1U  $\mu$ l<sup>-1</sup>), and its appropriate buffer, at different ratios of insert:vector (10:1 and 100:1) and incubated at room temperature for 1hr. The constructs were transformed into *JM107* chemically competent *E.coli* cells and the resulting colonies were prepared using Sigma GenElute Kit according to the supplied protocol. To confirm both vector and insert were present the plasmid preparations were digested with the previous used restriction enzymes. The second fragment was inserted using the same methodology. After confirmation of the correct insertion of both gene fragments, the construct was prepared, using the QIAfilter Plasmid Maxi Kit, according to the supplied protocol and stored as stock. A schematic of the knockout procedure can be seen in **Figure 2.1**.

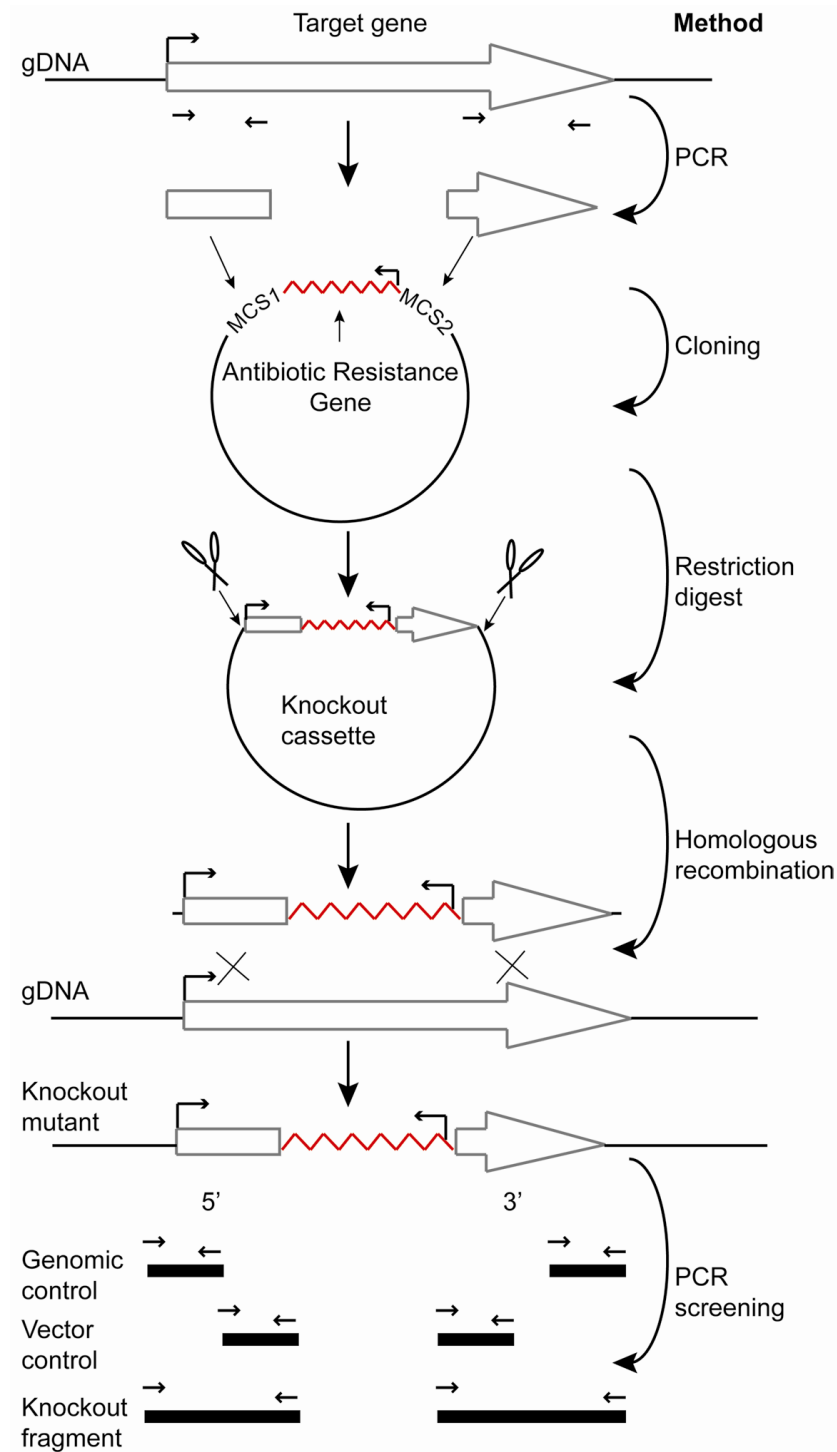


**Figure 2.1 Schematic diagrams showing the knockout and screening procedure.**

A schematic showing the method used for cloning and screening of the knockout cell lines. Gene fragments were amplified from gDNA (5' and 3') using PCR and cloned into the pLPBLP vector to create a knockout cassette. The 5' and 3' fragments cloned into the vector at the multiple cloning site (MCS) 1 and 2, respectively, flanking a blasticidin resistance cassette (~~~~~). The orientation of the promoter for the genes or the blasticidin resistance gene is also shown (↗). The knockout cassette was transformed into Ax2 *Dictyostelium* cells and correct transformants were identified using PCR screening. The arrows (←) show the primers used in the PCR screening, using a genomic (G) and a vector (V) control and a diagnostic knockout (KO) fragment (unique to homologously integrated transformants).

### **2.2.3.7 Transformation of *Dictyostelium* by electroporation**

The KO fragment containing the blasticidin resistance cassette was excised from the pLPBLP vector backbone using restriction enzymes BamH1 (10U  $\mu\text{l}^{-1}$ ) and Kpn1 (10U  $\mu\text{l}^{-1}$ ). The digested KO construct (10 $\mu\text{g}$ ) was purified using isopropanol precipitation.

For the electroporation,  $1 \times 10^7$  *Dictyostelium* cells/ml were incubated on ice for 10mins before centrifugation at 800xg for 5min at 4°C. The cells were then washed once with 10ml KK2 and then twice with 10ml sterile filtered EP-buffer (10mM sodium phosphate buffer pH 6.1, 50mM sucrose). The pellet was resuspended in 700 $\mu\text{l}$  EP-buffer added to a 0.4cm cuvette along with 10 $\mu\text{l}$  previously digest DNA (1 $\mu\text{g}/\mu\text{l}$ ) and incubated on ice for 10mins. The cells were electroporated with a BIO-RAD GenePulser Xcell electroporator using 1 pulse, 0.85kV and 25 $\mu\text{F}$ , 8 $\mu\text{l}$  of  $\text{CaCl}_2$  (100mM) and 8 $\mu\text{l}$  of  $\text{MgCl}_2$  (100mM) were added to each cuvette and further incubated for 15min at room temperature before being added to 10ml of Ax medium containing penicillin/streptomycin (100x). 100 $\mu\text{l}$  of this culture was transferred into each well of a 96 well plate. After 24hr, 100 $\mu\text{l}$  of double concentrated blasticidin (20 $\mu\text{g}/\text{ml}$ ) Ax media also containing penicillin/streptomycin (100x) was added to each well.

### **2.2.3.8 Overexpression of Fluorescently tagged protein**

Overexpression plasmids containing c-terminal GFP fused full length cDNA of either *zizA* and *zizB* were kindly provided by Douwe Veltman (Pakes et al., 2012; Veltman et al., 2009). The plasmids were transformed in to 10-beta Competent *E. coli* (New England Biolabs) and prepared using QIAfilter Plasmid Maxi Kit (Qiagen). 1ng of each plasmid was transformed via electroporation in wild type Ax2 or relevant mutant cell lines. After selection with 50 $\mu\text{g}/\text{ml}$  hygromycin (Invitrogen) for approximately 2 weeks, correct transformants were analysed using an Olympus IX81 microscope with FV1000 confocal laser (HeNe laser, 543nm emission, Olympus UPLSAPO 60x oil immersion objective with numerical aperture of 1.35).

### **2.2.3.9 Extraction of DNA from transformants**

When cells were grown to confluence, 200µl were removed and centrifuged at 2000xg for 3min. The pellet was resuspended in 48µl of lysis buffer (50mM KCl, 10mM Tris pH 8.3, 2.5M MgCl<sub>2</sub> 0.45% Nonidet P 40, 0.45% TWEEN 20) and 2µl of Proteinase K (822U/ml) and vortexed. After 5min of incubation at room temperature the samples were further incubated at 95°C for 1min. The extracted DNA was then used in a PCR reaction to screen for correctly transformed constructs.

### **2.2.3.10 Screening for correct mutants**

Screening primers were designed to detect whether the KO gene containing the blasticidin resistance cassette were inserted correctly into the *Dictyostelium* genomic DNA. PCR analysis was performed using these primers. Three primer sets were used to screen for the KO construct, a vector control, a genomic control and a diagnostic knockout primer set. The KO primer set used a primer outside the KO cassette in the genomic DNA and in the blasticidin resistance cassette. The vector control primer set amplified DNA from a primer based just within the KO DNA fragment and the blasticidin resistance cassette. Finally, the genomic control primer set consisted of the primer outside the KO cassette, within the genomic DNA to a primer within the KO DNA fragment as seen in figure 2.1. These primer sets were created from both the N and C terminal fragments of the KO gene.

### **2.2.3.11 Sub-cloning of correct transformants**

After confirmation of correct transformants using PCR, those colonies were selected for diluted in 200µl *Raoultella planticola* and spread onto a sterile SM agar plate. The plates were incubated at 21°C for 3-4 days, and the resulting sub-cloned colonies were again screened using the same screening primers previously used.

### **2.2.3.12 RNA Extraction**

Cells were harvested at  $2 \times 10^7$  cells/ml before being washed with KK2 buffer at 4°C. RNA was extracted using the High Pure RNA isolation kit (Roche) according to the manufacturer's instructions.

### **2.2.3.13 Reverse transcriptase PCR**

RNA was treated with the Ambion *DNAfree* kit to remove residual DNA contamination as described by the manufacturer. cDNA was synthesised from 1µg of RNA using the Fermentas First Strand cDNA synthesis kit and Oligo(dT)18 primers. The 2µl of the cDNA was used in a PCR reaction as previously described.

## **2.2.4 Image Acquisition and Microscopy**

### **2.2.4.1 Cell Movement**

For chemotaxis assays, cells were pulsed at a density of  $1.7 \times 10^6$  cells/ml with 30nM cAMP at 6min intervals for 5hr before being allowed to adhere to a coverslip. After cells had adhered, the coverslip was inverted onto a Dunn chamber containing 5µM cAMP in the outer well. The response of the cells was recorded using time-lapse imaging and ImagePro 6.3 software (one image every 6sec for 5min). Experiments were repeated in at least triplicate with an average of 20-30 cells. Computer-assisted analysis of cell movement and cell shape was performed using ImagePro 6.3, measuring the velocity (µm/s) and the aspect. The aspect parameter is a measure of roundness, where, perfectly round cells have a value of 1, compared to elongated cells which have a value of >1. For fluorescence chemotaxis, aggregation competent cells expressing either ZizA-GFP or ZizB-GFP were loaded into an Insall chemotaxis chamber (Muinonen-Martin *et al.*, 2010). The phosphate buffer in the outer well was replaced by 1µM cAMP and chemotaxing cells were visualized on a Nikon confocal microscope as above.

### **2.2.4.2 Fluorescence Microscopy**

For localisation, fluorescently tagged GFP fusion proteins were cultivated in nutrient media, washed with KK2 and allowed to adhere to a glass coverslip before being visualised with an Olympus IX71 microscope (U-RFL-T laser, 482nm emission, Olympus UPlanFL 60x oil immersion objective with NA 1.25) with an QImaging RetigaExi Fast1394 digital camera and ImagePro6.3 software.

To investigate cytokinesis defects, cells were cultured in a shaking suspension for 3 days and fixed with 100% methanol at -20°C for 15min before being fluorescently labeled with DAPI to visualise and count the number of nuclei per cell. All specimens were analysed using an Olympus IX71 microscope (U-RFL-T laser, 350nm and 543nm emission, respectively, Olympus UPlanFL 60x oil immersion objective with NA 1.25) with a QImaging RetigaExi Fast1394 digital camera.

To analyse the number of filopodia, time lapse images were taken every 5sec over a 10min period (Nikon Eclipse TE2000-E with a 1.4 NA Plan Apo 60x objective) using a Q Imaging RetigaEXi camera. To quantify the number of filopodia for wild type, *zizA*<sup>+</sup> and *zizB*<sup>+</sup> cells, an average of 27 individual cells were counted for three time points (0min, 5min and 10min) over the 10min period. A filopodia is identified as a thin projection that extends from a pseudopod. The time lapse movies were analysed and an average number of filopodia over the 3 time point was calculated for statistical analysis (Unpaired, two-tailed student t-test), a Kolmogorov-Smirnov test was performed as a pretest to ensure normal distribution of data.

## 2.2.5 Proteomics

### 2.2.5.1 Western blot analysis

Sodium dodecyl sulfate polyacrylamide gel electrophoresis SDS-PAGE (7%) were prepared (Resolving gel - 2.25ml 30% acrylamide solution, 1.9ml Tris pH8.8, 5.65ml ddH<sub>2</sub>O, 200µl 10% SDS, 100µl 10% APS in ddH<sub>2</sub>O; 10µl TEMED, stacking gel - 2.55ml 30% acrylamide solution, 0.94ml Tris pH6.8, 11.25ml ddH<sub>2</sub>O, 150µl 10% SDS, 150µl 10% APS in ddH<sub>2</sub>O; 15µl TEMED). Protein samples were analysed by gel electrophoresis where samples were prepared by boiling at 95°C for 10 minutes in 2x loading buffer (16ml 2M Tris pH 6.8, 6ml 80% glycerol, 10ml 10% SDS, β-mercaptoethanol, ddH<sub>2</sub>O, bromophenol blue). Protein samples and the molecular marker (Fermentas PageRuler Plus Prestained Protein Ladder) were loaded into the stacking gel. The gel was run at 200V in the running buffer for 1 – 1.5hr. The separated proteins were transferred to PDVF membrane (Immobilon-FL Transfer

Membrane) which was activated by saturation in methanol. Blotting paper (3mm), sponges and the activated membrane were soaked in a transfer buffer (1xETB made fresh with 100ml 10xETB (75g Tris base; 360g glycine; 25ml 10% SDS) with 10% methanol. The transfer block was prepared and placed into a tank that was located on ice and filled with the transfer buffer and run at 400mA for 1hr.

To visualise the proteins the western blot membrane was immunostained with appropriate antibodies. Here the membrane was blocked in milk buffer (5% milk in 1xPBS with 0.1% TWEEN20) for 1hr at room temperature. The primary antibody (Rat monoclonal GFP antibody; ChromoTek GmbH) was added in 1:1000 dilution in the milk buffer and incubated overnight at 4°C. Excess primary antibody was washed off with 3 x 10min washes in PBST (1xPBS with 1% TWEEN20) (for 10x PBS: 14.4g Na<sub>2</sub>HPO<sub>4</sub>, 80g NaCl, 2g KCl, 2.4g KH<sub>2</sub>PO<sub>4</sub>, made up to 1L with ddH<sub>2</sub>O, adjusted with HCl to pH7.4 ). The secondary antibody was added at a 1:2000 dilution in milk buffer (goat anti-rat IRDye 800 CW (Li-cor Biosciences)) and incubated at room temperature for 1hr. Excess secondary antibody was washed off with 3 x 10min washes in PBST. The image was taken with Odyssey Infrared Imaging System (Li-cor Biosciences).

### **2.2.5.2 Immunoprecipitation**

Aggregation competent cells were washed with potassium phosphate buffer (KK2), resuspended at a density of  $3 \times 10^8$  cells/ml in KK2, before being shaken for 20min at 250rpm with 2.5mM caffeine. Cells were lysed (0.5% NP40, 40mM Tris-HCl, 20mM NaCl, 5mM EGTA, 5mM EDTA, 10mM DTT, and 1mM PMSF, 2 x protease cocktail inhibitor (Roche)). The cell lysate was incubated with GFP-Trap agarose beads (ChromoTek GmbH) as per manufacturer's instructions. Briefly, the lysate was incubated with the GFP-Trap agarose beads at 4°C for 1hr before being collected and washed with the wash buffer (10mM Tris-HCl, 150mM NaCl, 0.5mM EDTA, 1mM PMSF, 2 x protease cocktail inhibitor (Roche)). Immunocomplexes were dissociated from the beads by incubating at 95°C for 10min before the beads were collected by centrifugation. The co-immunoprecipitated proteins were separated by SDS-PAGE and analysed by Coomassie staining and mass spectrometry (MS) analysis.

GST pulldown assays were performed as described previously by Mondal *et al.* (, 2007). Briefly, GST-Rac proteins were expressed in *E.coli* and bound to glutathione-sepharose beads (GE Healthcare). For the interaction of ZizA and ZizB with Rac proteins,  $4 \times 10^7$  *Dictyostelium* cells/ml expressing GFP tagged ZizA and ZizB were lysed in lysis buffer (25mM Tris, pH7.5, 150mM NaCl, 5mM EDTA, 0.5% Triton X-100, 1mM NaF, 0.5mM  $\text{Na}_3\text{VO}_4$ , 1mM DTT, 1mM PMSF, 2x protease cocktail inhibitor (Roche)) and incubated with equal amounts of GST-Rac bound beads for 3hr at 4°C. Beads were washed with the wash buffer (25mM Tris, pH 7.5, 150mM NaCl, 5mM EDTA). The eluate of the pull down was immunoblotted and the Zizimin protein was detected using the GFP specific monoclonal antibody (ChromoTek GmbH). Cells expressing only GST were used as a control. The immunoblot was visualised using the Odyssey Sa infrared imaging system.

## 2.3 Software

Phylogenetic analysis was performed using *MEGA* version 5 (Tamura *et al.*, 2007). Statistical analysis was conducted using Prism 5 (GraphPad Software, Inc). Microscopy images were captured using image Pro Plus version 6.3 (Media Cybernetics Inc.). Mass spectrometry data was analysed using Scaffold3.

## 2.4 Websites

### ***Dictyostelium* gene and proteins information**

<http://dictybase.org/>

### ***Dictyostelium* gene expression information**

<http://dictyexpress.biolab.si/>

### **Basic Local Alignment Search Tool (BLAST) analysis**

<http://dictybase.org/tools/blast>

<http://www.ebi.ac.uk/Tools/sss/psiblast/>

<http://www.ncbi.nlm.nih.gov/BLAST/>

### **Protein sequence alignment**



<http://www.ebi.ac.uk/Tools/msa/clustalw2/>

**Protein domain analysis**

<http://smart.embl-heidelberg.de/>

### **3 Bioinformatics**

### 3.1 Introduction

Eleven novel human Dopamine Receptor Interacting Proteins (DRIPs) were identified by Dr Jamal Nasir and colleagues, using a yeast two hybrid screen. Although, the identity of the proteins has been established their cellular roles remain unclear (Zhan et al., 2008; Zhan et al., 2010a). Positive clones were recognised by screening a human adult brain cDNA library using either the C-terminus or third cytoplasmic loop domains of the five dopamine receptors as 'bait' proteins. Sequence analysis of these positive clones (DRIP 1-11) allowed for the identification of a range of genes, some having well-established roles (G $\beta$  subunit) and others with a relatively poorly characterised cellular function (PIM2). Currently, little is known about how these proteins interact with the dopamine receptor, their cellular functioning, or their implication in schizophrenia and bipolar disorder. Further study is thus needed to advance the research in this field.

The cellular signalling of DRIPs has become a focal point in better understanding dopamine signalling at a molecular level. Several DRIPs, such as Spinophilin (Smith *et al.*, 1999) and AIP1, a protein involved in neuronal cell death and intracellular trafficking (Zhan *et al.*, 2008), have been identified using a yeast two-hybrid screen. DRIPs have been shown to regulate many aspects of the dopamine receptor life cycle (Bergson *et al.*, 2003). Identification of these proteins and their potential binding targets aids the understanding of the dopamine signalling pathway.

In this chapter, bioinformatic approaches are used to analyse the cellular function of these eleven human DRIPs in the model organism *Dictyostelium discoideum*. To gain a more detailed understanding of the structural characteristics of these proteins and their evolutionary conservation throughout different kingdoms, protein BLAST analysis, sequence alignment, phylogenetic and domain structure analysis were performed.

### 3.2 BLAST Analysis

The *Dictyostelium discoideum* biomedical model organism was used to investigate the cellular functions of these eleven novel DRIPs. Protein BLAST analysis of the eleven human DRIPs against the *Dictyostelium* genome revealed 5 potential homologues: DRIPs 2, 4, 7, 9 and 11. A protein was considered to be a potential homologue if it had an e-value around  $e^{-40}$  or below as suggested by Eichinger *et al.* (, 2005). DRIPs 4 and 7 had one potential homologue while DRIPs 2, 9 and 11 had a number of potential homologues with an e-value of around  $e^{-40}$  or below (**Table 3.1**).

**Table 3.1 BLAST analysis results of the potential *Dictyostelium* homologues**

DRIP	Name and Function	Dictybase ID	Gene Name	E-value
DRIP2	Dock 10	DDB0233623	ZizA	3e-78
	Small GTPase regulation	DDB0233621	ZizC	2e-63
		DDB0233622	ZizB	7e-60
		DDB0233624	ZizD	5e-55
DRIP4	AIP Apoptosis and cell death	DDB0185177	AlxA	5e-76
DRIP7	G $\beta$ subunit G-protein signalling	DDB0185122	GpbB	2e-99
DRIP9	PIM2	DDB0216323	MrkC	4e-39
	Cell death	DDB0216369	MrkA	3e-36
DRIP11	Kif1A	DDB0201559	Kif1	1e-151
	Molecular motor	DDB0216174	Kif3	2e-61
		DDB0185205	Kif5	6e-59

Putative *Dictyostelium* DRIP protein homologues for human DRIP 2, 4, 7, 9 and 11, showing the top protein blast hits with an e-value of around  $e^{-40}$  or below (Zhan *et al.*, 2010a).

BLAST analysis of a protein homologue with the smallest e-value present in the *Dictyostelium* genome (indicating the highest degree of homology), against the genomes of species across various biological kingdoms, revealed the conservation of each potential homologue. The homologues with the highest degree of homology coming from a range of species are presented in **Table 3.2**. A selection was made from the top results including species which had similar protein size to the *Dictyostelium* homologue. The table illustrates protein size, percentage identity and similarity as well as the e-value.

**Table 3.2 BLAST analysis results for all 5 potential *Dictyostelium* DRIP homologues.**

<b>Db ZizA (potential DRIP2 homologue)</b>	<b>Protein Length (aa)</b>	<b>Identity (%)</b>	<b>Similarity (%)</b>	<b>E-value</b>
<i>Dictyostelium discoideum</i>	2284	100	100	0
<i>Anopheles gambiae</i>	2077	28	47	1.00E-120
<i>Drosophila melanogaster</i>	2064	36	59	1.00E-112
<i>Xenopus laevis</i>	665	38	58	1.00E-107
<i>Tetraodon nigroviridis</i>	1950	35	55	1.00E-104
<i>Nematostella vectensis</i>	2151	36	58	1.00E-103
<i>Pongo abelli</i>	2093	32	53	3.00E-97
<i>Mus musculus</i>	2222	30	52	4.00E-94
<i>Homo sapien</i>	2186	30	51	1.00E-91
<b>Db AlxA (potential DRIP4 homologue)</b>	<b>Protein Length (aa)</b>	<b>Identity (%)</b>	<b>Similarity (%)</b>	<b>E-value</b>
<i>Dictyostelium discoideum</i>	794	100	100	0
<i>Nematostella vectensis</i>	851	32	51	1.00E-105
<i>Mus musculus</i>	869	30	50	2.00E-91
<i>Xenopus laevis</i>	867	29	50	7.00E-90
<i>Rattus norvegicus</i>	873	29	50	1.00E-89
<i>Homo sapien</i>	868	30	50	2.00E-89
<i>Nicotiana tabacum</i>	876	28	49	3.00E-89
<i>Gallus gallus</i>	882	29	49	1.00E-88
<b>Db Gβ subunit ( potential DRIP7 homologue)</b>	<b>Protein Length (aa)</b>	<b>Identity (%)</b>	<b>Similarity (%)</b>	<b>E-value</b>
<i>Dictyostelium discoideum</i>	329	100	100	0
<i>Drosophila Virillis</i>	318	58	73	1.00E-104
<i>Xenopus laevis</i>	317	60	75	1.00E-104
<i>Physcomitrella patens</i>	316	60	74	1.00E-103
<i>Meleagris gallopavo</i>	317	60	74	1.00E-103
<i>Gallus gallus</i>	317	60	74	1.00E-103
<i>Mus musculus</i>	317	60	74	1.00E-103
<i>Homo sapien</i>	317	60	74	1.00E-103
<b>Db MrkC ( potential DRIP9 homologue)</b>	<b>Protein Length (aa)</b>	<b>Identity (%)</b>	<b>Similarity (%)</b>	<b>E-value</b>
<i>Dictyostelium discoideum</i>	773	100	100	0
<i>Xenopus laevis</i>	780	29	49	1.00E-84
<i>Mus musculus</i>	776	28	49	3.00E-83
<i>Danio rerio</i>	754	28	50	6.00E-83
<i>Homo sapien</i>	788	29	49	1.00E-82
<i>Dictyostelium discoideum</i>	715	29	47	2.00E-82
<i>Rattus norvegicus</i>	797	28	48	1.00E-81
<i>Caenorhabditis elegans</i>	1096	39	59	1.00E-76
<b>Db Kif1A ( potential DRIP11 homologue)</b>	<b>Protein Length (aa)</b>	<b>Identity (%)</b>	<b>Similarity (%)</b>	<b>E-value</b>
<i>Dictyostelium discoideum</i>	2205	100	100	0
<i>Rattus norvegicus</i>	1687	39	54	0
<i>Anopheles gambiae</i>	1644	43	57	0
<i>Drosophila melanogaster</i>	1670	38	53	0
<i>Aedes aegypti</i>	1644	42	57	0
<i>Homo sapien</i>	1690	42	57	0
<i>Mus musculus</i>	1689	42	57	0
<i>Caenorhabditis ebriggsae</i>	1576	37	53	1.00E-166
<i>Pyrenophora tritici-repentis</i>	1580	50	67	1.00E-167

*Dictyostelium* protein with the smallest e-value was analysed in this BLAST search. The table shows the organism, protein length, % identity, % similarity and e-value. The Blast analysis used the *Dictyostelium* homologue protein sequence for comparison against all other genomes. A selection was then made from the top species results.

The results obtained from the BLAST analysis, combined with a scope for discovery, were used to decide which DRIP homologue to further characterise and analyse the cellular function. Detailed analysis of the *Dictyostelium* DRIP 2 and 9 homologues have not been previously carried out. In comparison, the other potential *Dictyostelium* DRIP homologues have been well described: DRIP4 has been identified as an ALG2 interaction protein (AIP), which is involved in apoptosis (Ohkouchi *et al.*, 2005); DRIP7 has been classed as the G $\beta$  subunit of the G-protein complex (Lilly *et al.*, 1993; Wu *et al.*, 1995); and DRIP11 has been demonstrated to be kinesin molecular motor, involved in movement of membrane cargos (Klopfenstein *et al.*, 2002). There have also been no studies published showing the ablation attempts of *Dictyostelium* DRIPs 2 and 9 potential homologues, whereas, DRIPs 4, 7 and 11 have been successfully knocked out by other research groups (Lilly *et al.*, 1993; Ohkouchi *et al.*, 2005; Pollock *et al.*, 1999). Thus, DRIPs 2 and 9 were chosen to investigate further. Sequence analysis of the potential *Dictyostelium* DRIP 2 and 9 homologues suggest they belong to the Dedicator of cytokinesis (Dock) and Microtubule Affinity Regulating Kinase (MARK) family of proteins, respectively.

### 3.3 Domain structure analysis

#### 3.3.1 Dedicator of Cytokinesis proteins

Since the potential *Dictyostelium* DRIP 2 homologue (ZizA) shows high sequence homology to the Dock family proteins, I have looked at different domain structures of all the human members of this protein family (Dock 1-11), in comparison to those in *Dictyostelium*. The domain structure analysis of the human Dock family shows conservation of the Docker Homology Region 1 (DHR1) and a Docker Homology Region 2 (DHR2) domain among all members of this family (Cote and Vuori, 2007). The Dock180 and Dock4 subclass, however, have a further Src Homology 3 (SH3) domain and proline rich (PxxP) motif, whereas, only Zizimin Docks have a Pleckstrin Homology (PH) domain (**Figure 3.1**).

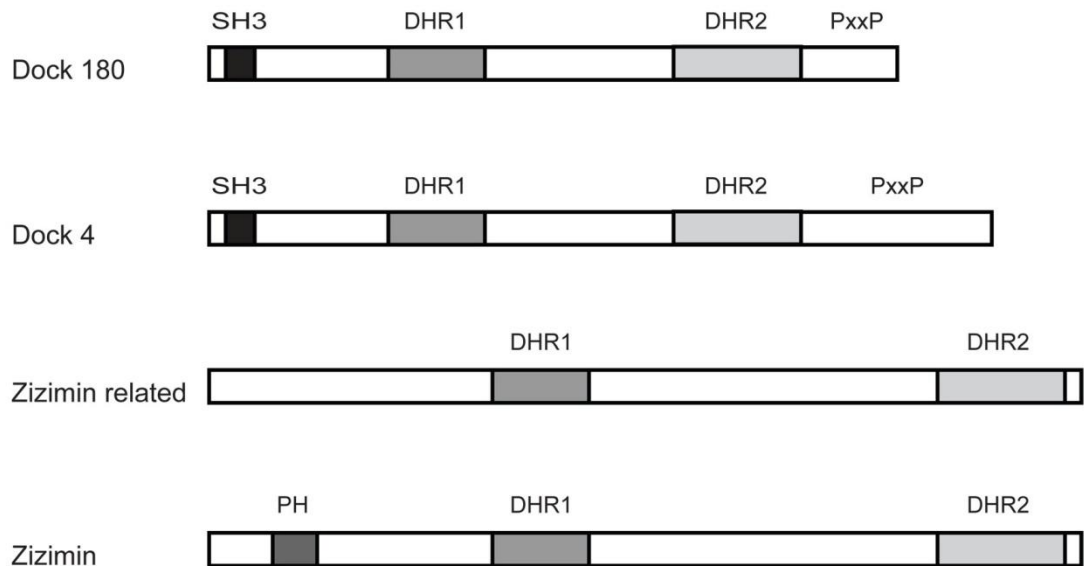


**Figure 3.1 Domain structure analysis of the *Homo sapiens* Dock family.**

Schematic representation of the domain structure human Dock proteins, Dock180, Dock4, Zizimin-related and Zizimin proteins. The different domains are SH3 domain, DHR1, DHR2 domain, PxxP and PH domain. Black boxes represent proteins with shaded areas indicating specific domains.

*Dictyostelium* has eight Dock family proteins that fall into two groups, four Dock180-related and four Zizimin-related proteins (Meller et al., 2005; Para et al., 2009). The detailed analysis of *Dictyostelium* Dock180-related homologues, shows DocA and DocD have the characteristic SH3 domain, although, none of these proteins contain the proline rich motif found in the human homologues.

The four zizimin proteins have not been extensively characterised in *Dictyostelium*. Domain structure analysis illustrates that the four Zizimin-related proteins have the evolutionary conserved DHR1 and DHR2 domains, although they do not have a characterised PH domain (**Figure 3.2**).



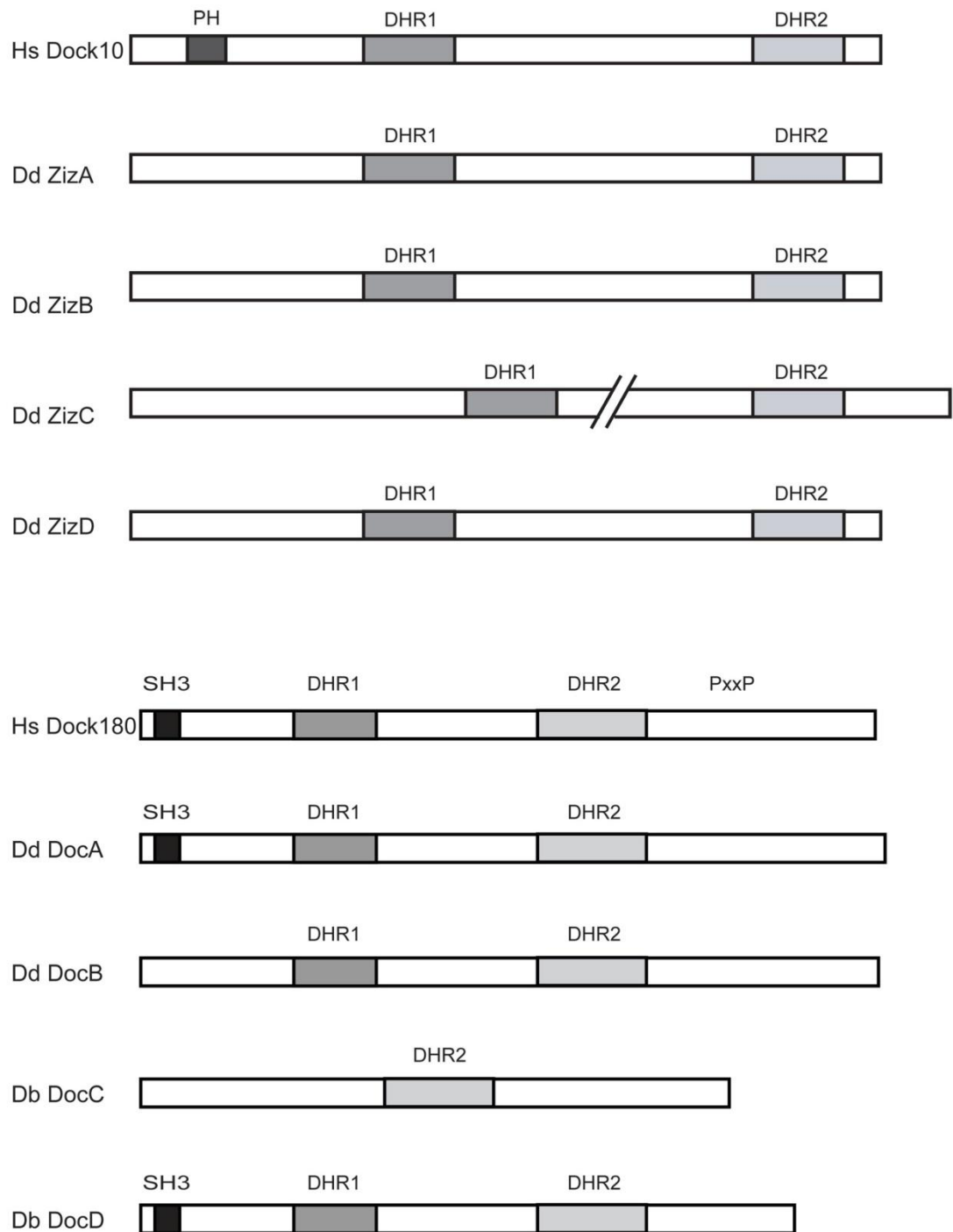


**Figure 3.2 Domain structure analysis of the *Dictyostelium* DOCK family proteins.**

Schematic representation of the *Dictyostelium* (Dd) Dock proteins domain structure compared to a *Homo sapien* (Hs) homologue. (A) Four Zizimin-related proteins compared to the human Dock10 (DRIP2). (B) Four Dock 180 related proteins compared to human Dock 180. The different domains are SH3 domain, DHR1, DHR2 domain, PxxP, PH domain.

### 3.3.2 Microtubule Affinity Regulating Kinase

The human DRIP 9 protein belongs to the PIM family of proteins. The top homologues for this protein in *Dictyostelium* were the MrkC (e-39) and MrkA (e-36) proteins. These proteins also show high sequence homology to human MARK family proteins. I have, therefore, analysed the different domain structures of all members of the human PIM and MARK family proteins, in comparison to those in *Dictyostelium*. Domain structure analysis of the human DRIP 9 (PIM2) and other members of the PIM family (1 and 3) as well as the human and *Dictyostelium* MARK family proteins show high conservation of the ser/thr kinase domain. The human and *Dictyostelium* MARK family proteins all have a further ubiquitin-associated domain (UBA). Furthermore, the *Dictyostelium* MrkA and MrkC proteins also have a C-terminal kinase associated domain (KA1) (**Figure 3.3**). MrkC however, does not contain a UBA domain.

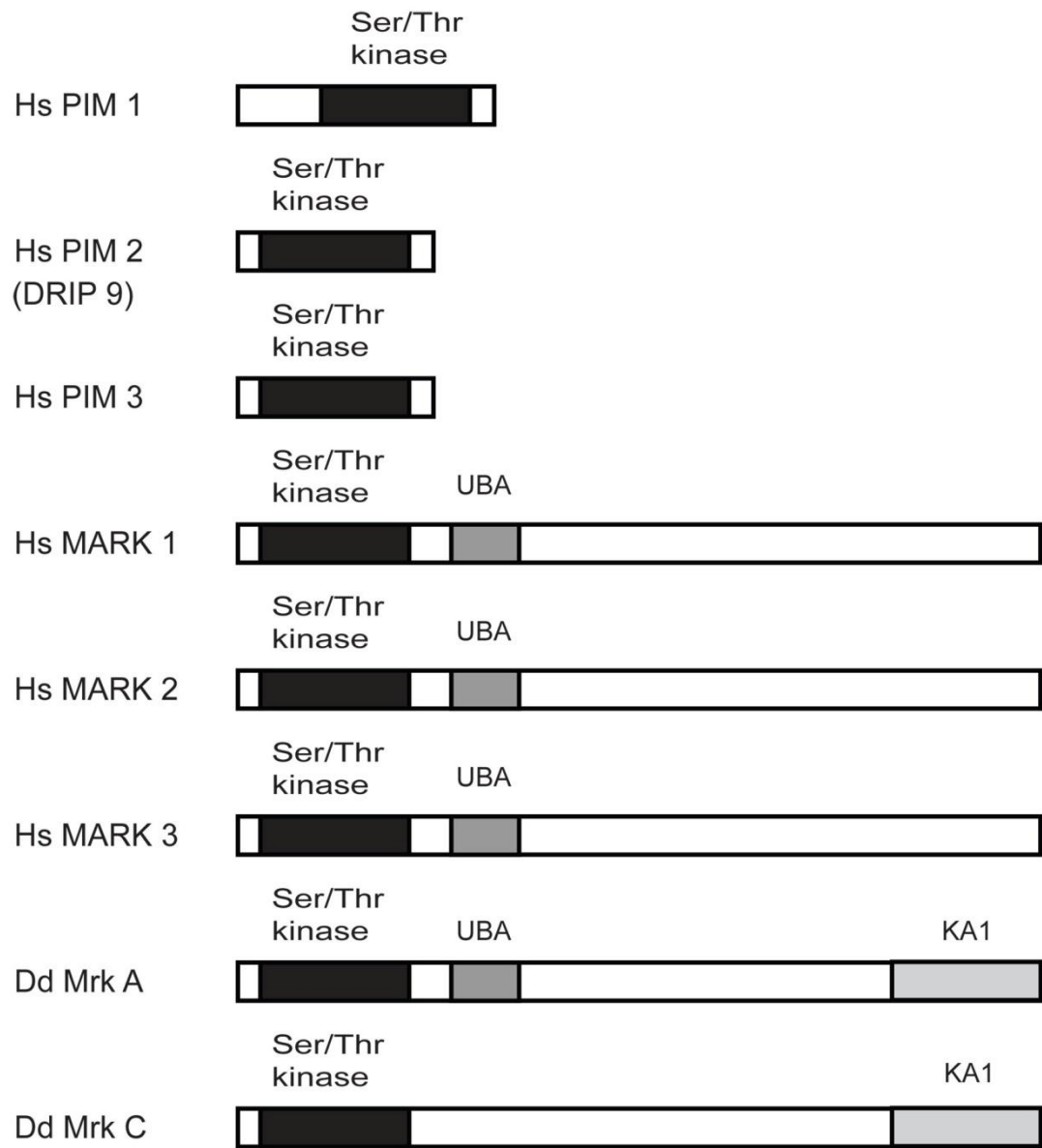


**Figure 3.3 Domain structure analysis of the *Homo sapien* and *Dictyostelium* PIM/MARK family.**

Schematic representation of the domain structure of the human PIM and MARK ser/thr kinase proteins compared to *Dictyostelium* homologues. Ser/thr (serine/threonine) kinase domain, UBA (ubiquitin associated) domain, KA1 (kinase associated) domain.

### 3.4 Phylogenetic analysis

#### 3.4.1 Deducator of Cytokinesis proteins

Phylogenetic analysis of the human Dock related proteins was carried out to better understand the evolutionary conservation of the different subclasses of proteins within this family. As previously shown in the domain structure analysis, the human Dock family proteins are categorised into 4 main subclasses: Zizimin, Zizimin-related, Dock180-related and Dock4-related (**Figure 3.4**). The bootstrap values in the phylogenetic tree show robust support for the sub-division of the human family of Dock proteins. Comparison of the entire protein sequence of this family shows there are two main clades that each separate further into two sub-classes (Zizimin/Zizimin-related and Dock4/Dock180-related).

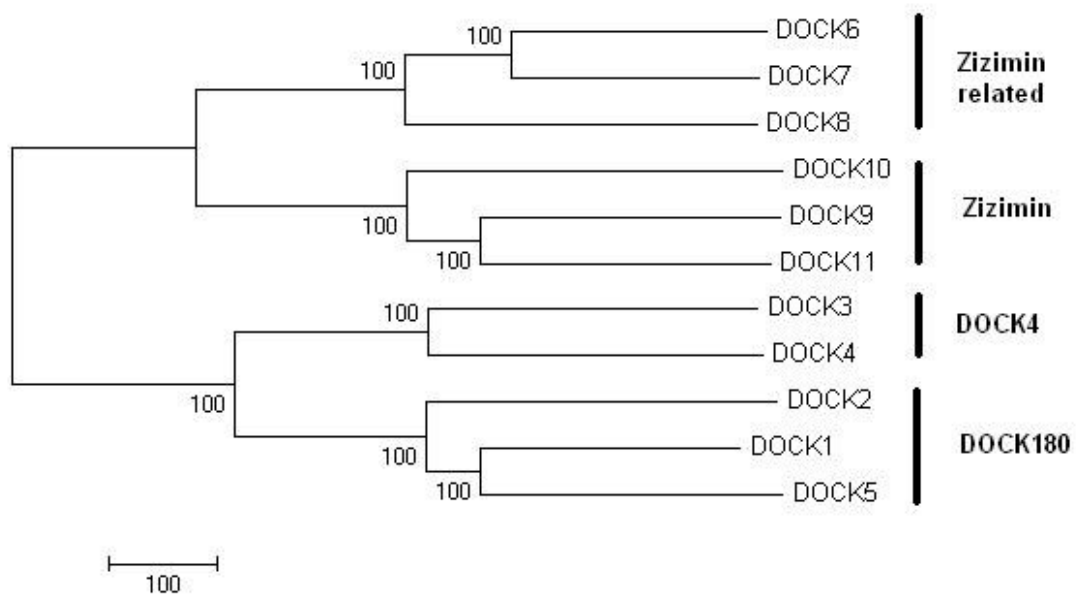


**Figure 3.4 Phylogenetic analysis of *Homo sapien* DOCK family proteins**

A phylogenetic tree showing the evolutionary conservation of the human Dock family proteins, that group into 4 sub-classes, Zizimin, Zizimin-related, Dock4-related and Dock180-related. Amino acid sequences were aligned using ClustalW with phylogenetic analysis using MEGA5 package. The tree was constructed using a neighbour-joining method. The percentage of replicate trees in which the associated taxa clustered together in the bootstrap test (500 replicates) is shown next to the branches.

Within the Zizimin/Zizimin-related clade of the Dock family phylogenetic tree, the Dock10 protein (DRIP2) has only been identified in higher organisms (e.g. human, mouse and chicken), however, other Zizimin (Dock9 and 11) and Zizimin-related (Dock6, 7 and 8) proteins have been shown in simpler organisms such as *C.elegans* and *D.Melanogaster* (Meller et al., 2002; Meller et al., 2005). Dock family of proteins all have a highly conserved Guanine nucleotide Exchange Factor (GEF) region which is responsible for the regulation of small GTPases. The alignment of the *Dictyostelium* putative Dock10 homologue against the Dock10 protein from other species showed conservation of amino acids throughout the protein sequence, where **Figure 3.5** illustrates the sequence alignment of the Dock10 DHR2 domain across different organisms. The high conservation in this domain indicates the structural and potential functional similarities between these proteins.

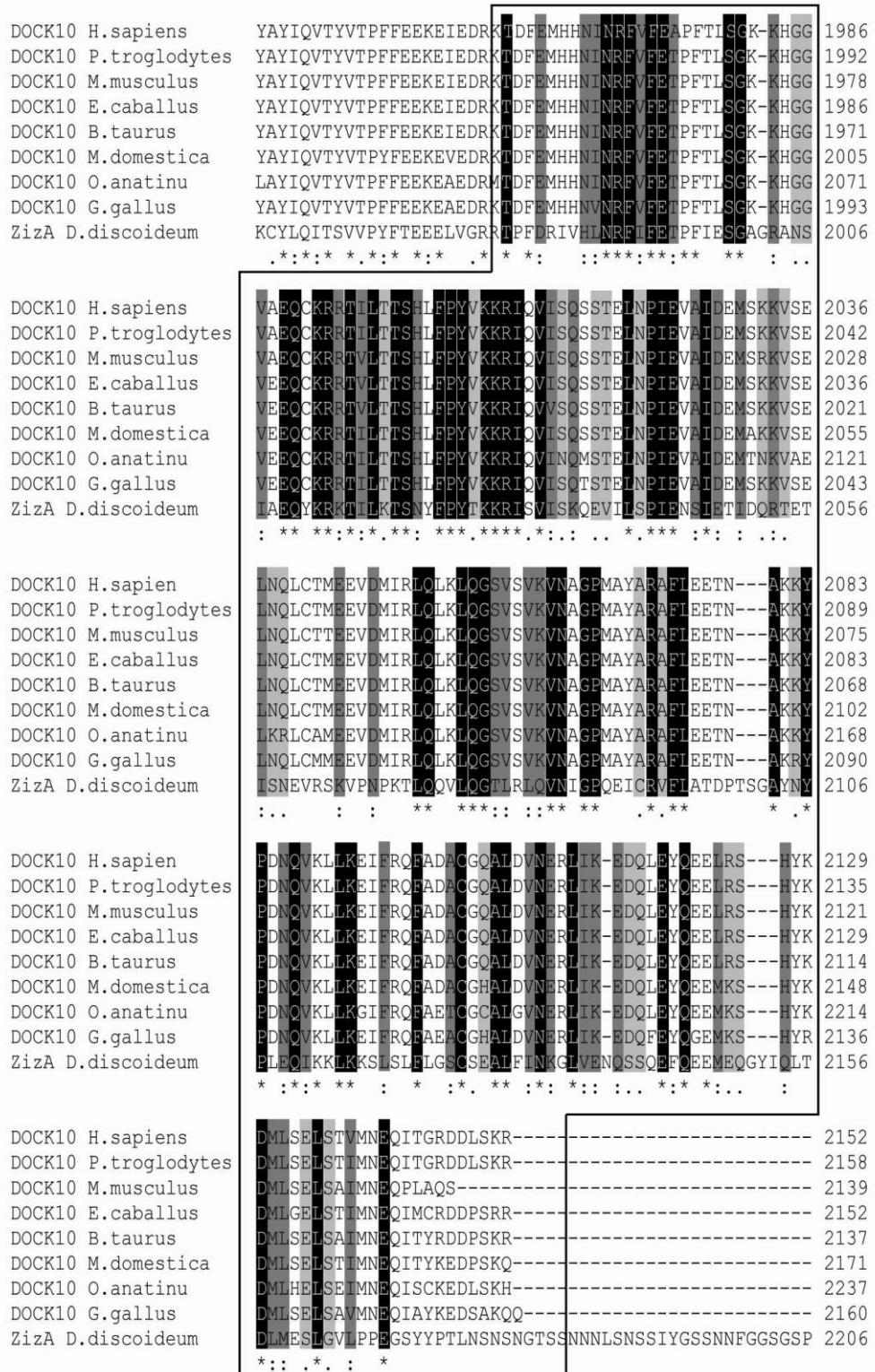


**Figure 3.5** Sequence alignments of the DHR2 domains of Dock10 in different species.

DHR2 domain of the Dock10 homologues from different species aligned against the *Dictyostelium* DRIP2 homologue (ZizA). The boxed area illustrates DHR2 domain of the Dock10 proteins. Stars (\*) and black highlighted region represent identical residues, colons (:) and dark grey highlighted region conserved substitutions and full stops (.) and light grey highlighted region semi-conserved substitutions. The alignment was performed using ClustalW online bioinformatics tool.

The reconstruction of the phylogenetic tree of the Dock family proteins, across different representative taxa, shows 2 distinct clades composed of the Zizimin and Zizimin-related proteins and the Dock4 and Dock180-related proteins (**Figure 3.6**). ZizA, the *Dictyostelium* homologue for Dock10, groups with the Zizimin/Zizimin-related clades. The inclusion of the *Dictyostelium* homologue in this clade gives robust support, as can be seen by the bootstrap values indicated in the tree.

The phylogenetic analysis together with the domain structure and alignment data suggest and support the assertion that ZizA can be analysed as a Zizimin homologue in *Dictyostelium*. The other *Dictyostelium* Zizimin proteins also group within this clade.

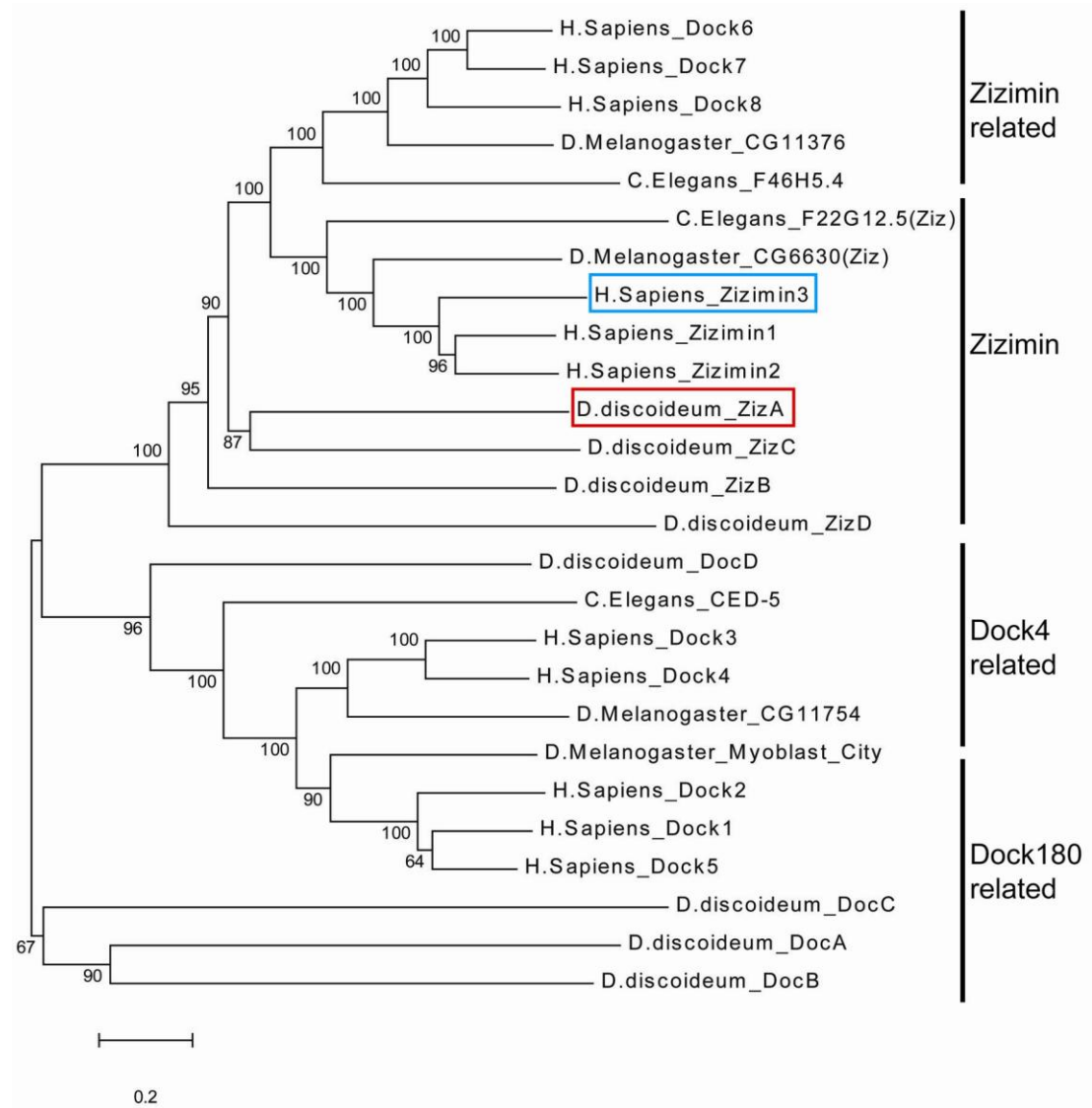


**Figure 3.6 Phylogenetic analysis Dock proteins across different kingdoms.**

The Phylogenetic tree shows the evolutionary distance of the Dock family from different taxa. The human DRIP2 protein, Dock10, is indicated by the blue box. The red box indicates the potential *Dictyostelium* DRIP2 homologue. The sub-classes (according to the human Dock family classification) are shown by the black bars on the right-hand side of the tree. Evolutionary history was inferred using the Neighbour-Joining method. Bootstrap test was performed with 500 replicates. Numbers represent percentage of replicate trees in which the associated taxa clustered together.



### 3.4.2 Microtubule Affinity Regulating Kinases

BLAST analysis showed MrkC and MrkA to be the top homologues for PIM2 in *Dictyostelium*, however, these proteins also show sequence homology to MARK family proteins. Phylogenetic analysis of the human DRIP9 (PIM2) and MARK2 proteins and the potential *Dictyostelium* DRIP9 homologue was carried out to better understand the evolutionary conservation of the ser/thr kinase domain within these families. The PIM2 protein only has a ser/thr kinase domain and not the UBA or KA1 domain. The *Dictyostelium* homologues MrkC and MrkA have both the ser/thr kinase and the KA1 domains; however the UBA domain is absent. The sequence alignment, of protein kinase domains, of the human MARK2 and PIM2 and the *Dictyostelium* MARK proteins (MrkA and MrkC), illustrates conservation of the essential amino acids in this domain (**Figure 3.7**).

Alignment of the *Dictyostelium* MARK proteins with other members of the MARK family of proteins from various organisms show high conservation of the ATP binding domain and the ser/thr kinase active site within the protein kinase domain (**Figure 3.8**)

MRKA	Dictyostelium	NITEELNKIPSSNNSSSSPNPLSISVSSSLGSASSIHLTPQGTIGNYLVIKTI	120
MARK2	Human	-----MIRGRNSATSADQPHIGNYRLKTI	31
MRKC	Dictyostelium	---MESNKSSSHGDVSTSPSFLNNHHQFNNGGDIIPKKNRIMHVGSY	57
PIM2	Human	-----MLTKPLQGPPAPPPTPTPPGGKDRFAEAEYRLGPI	43
		. . . : : * * *	
MRKA	Dictyostelium	GKVKLGYHKKIPNEKVAIKI INKGKLD-----PETLKMVQREVRIMKLLH---HPNI	172
MARK2	Human	AKVKLARHILTG-KEVAVKIIDKTQLN-----SSSLQKLFREVRMMKVLN---HPNIVK	82
MRKC	Dictyostelium	GKVKLGTNICTK-ENVAIKFIKNNKLS-----GKQKETCFREIDIMKLLD---HPNIVK	108
PIM2	Human	GTVFAGHRLTDR-LQVAIKVIIPNRVLGWSPLSDSVTCPLEVALLWKVGGGGHPGVIRL	102
		..* . . . : * * * . . . : . . . : * : * * : * * : * *	
MRKA	Dictyostelium	YEVIETSR---ALYLIMEYAGEGEVMDFMIAHGVLTESQARTFFFTQIVSAINYCHSKRAV	229
MARK2	Human	FEVIETEK---TLYLVMYASGGVEFDYLVAHGRMKEKEARAKFRQIVSAVQYCHQKFI	139
MRKC	Dictyostelium	LDVVDKREEEGTTYLIVEYVSGGELFDYIVAREYIKEKEARKFFRQIMISAIEYCHANLIV	168
PIM2	Human	LDWFETQEG--FMLVLERPLPAQDLFDYITEKGPLGEGPSRCFFGQVVAATIQHCHSRGV	160
		: . . . . : : . : * * * : : : * * * * * : * * * * * : *	
MRKA	Dictyostelium	HRDLKPENLLLDENR-QIKIIDFGLSNVFTPGSYLKTFCGSPPTYASPELILRKEYNGPSV	288
MARK2	Human	HRDLKAENLLLDADM-NIKIADFGLSNEFTFGNKLDTCGSPPIYAAPELFGKKYDGPV	198
MRKC	Dictyostelium	HRDLKPENLLLDNSG-DIKISDFGLSNNIQPGKLESFCGSPLYAAPEILKAEKYLGPV	227
PIM2	Human	HRDIKDENILIDLRGCAKLIDFGSG-ALLHDEPYTDFDGRVYSPPEWISRHQYHALPA	219
		***: * * * : * : * * * . : . . * * : * * : * * : * * : . : * . .	
MRKA	Dictyostelium	DVWSMGVVLVLTGYLPFDGDNYVELFQKILAGNYTIPSYLTHECKSLISRMLVDPDK	348
MARK2	Human	DVWSLGVILYTLVSGSLPFDGQNLKELRERVLRGKYRIPFYMSTDCENLLKFLILNPSK	258
MRKC	Dictyostelium	DIWSLGVIMYAVLCGNLPWEGDSQAEISFNSVHGNYEDPTHLSAEAVHILRRMIVPNPKD	287
PIM2	Human	TVWSLGIILLYDMVCGDIPFERD-----QEILEAELHFPAHVSPDCCALIRCLAPKPS	273
		: * * : * * : : : * * : : . . : : * : : : . . : : : . * . .	
MRKA	Dictyostelium	RATMEEIINHFWLSSSTKQIILSTMTDSLKNLNSCLEQQINVENLLNQLNNSNNNNINN	408
MARK2	Human	RGTLEQIMKDRWIN-----	272
MRKC	Dictyostelium	RATIQLKKNHPWIN-----	301
PIM2	Human	RPSLEEILLDPWVQ-----	287
		* : * * * : *	

**Figure 3.7** Sequence alignment of the MARK and PIM ser/thr kinase domain.

Protein sequence alignment analysing the ser/thr kinase domain of human MARK2 and PIM2 and *Dictyostelium* MrkA and MrkC homologues. Stars (\*) represent identical residues, colons (: ) conserved substitutions and full stops (.) semi-conserved substitutions. The black boxed area indicates the protein kinase domain. Within that domain the blue box shows the ATP binding. The red box shows the ser/thr kinase active site with the black bar indicating the proton donor. The alignment was performed using ClustalW program.

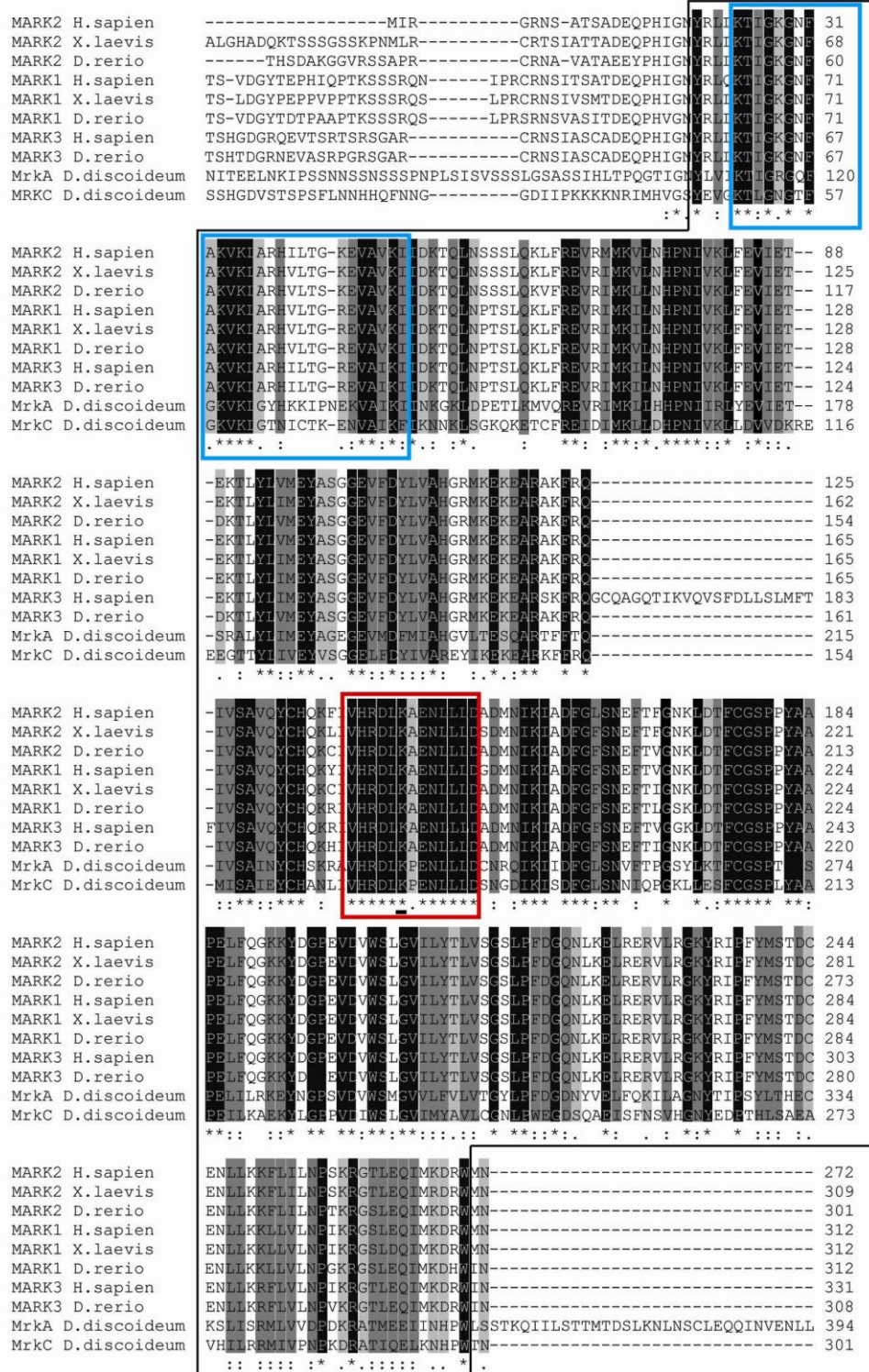


**Figure 3.8** Sequence alignment of the ser/thr kinase domain for MARK family proteins

Sequence alignment of the ser/thr kinase domain from different species showing a high level of conservation. Stars (\*) black highlighted region represent identical residues, colons (:) dark grey highlighted region conserved substitutions and full stops (.) light grey highlighted region semi-conserved substitutions. The black boxed area indicates the protein kinase domain, blue boxed area shows the ATP binding region and the red boxed area indicates the ser/thr kinase active site. The alignment was performed using ClustaW online bioinformatics tool.

The reconstruction of the phylogenetic tree for the ser/thr kinase proteins across different kingdoms, groups the DRIP9 *Dictyostelium* homologue, MrkC, amongst the various MARK proteins. PIM2 ser/thr kinase proteins also fall within these protein groups. The inclusion of the *Dictyostelium* homologue in this clade has robust support, as shown by the obtained bootstrap values in the tree (**Figure 3.9**).

The phylogenetic analysis, together with the domain structure and alignment data, suggests and supports the assertion that MrkC can be analysed as a MARK protein homologue in *Dictyostelium*. MrkC is the top homologue for the human PIM2 protein in *Dictyostelium*, showing high sequence homology to the ser/thr kinase domain. These data suggests shared functionality amongst these proteins. Thus, characterising the signalling role of the *Dictyostelium* MrkC protein can provide insight into the cellular roles and functioning of the human MARK and PIM ser/thr kinases.

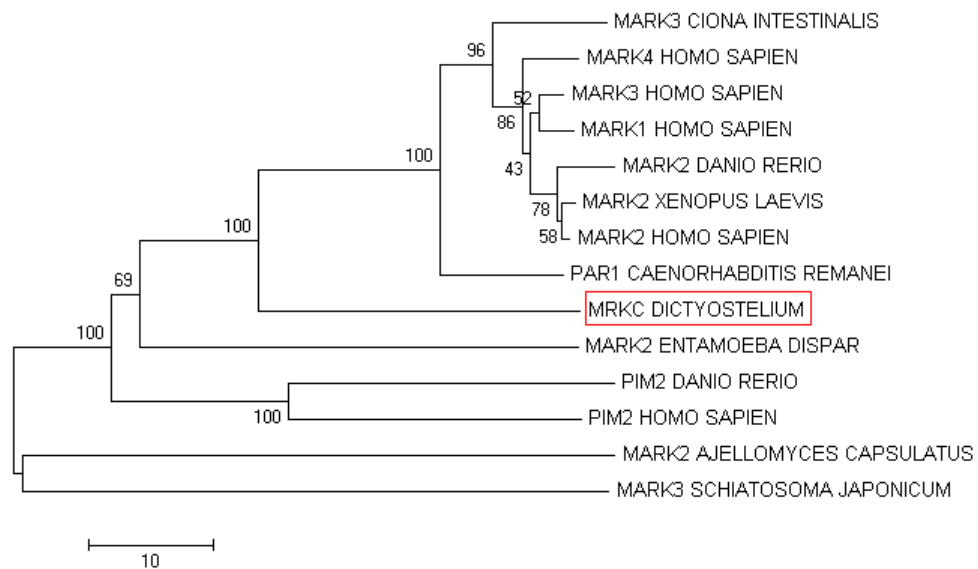


**Figure 3.9 Phylogenetic analysis of MARK proteins and the related protein PIM2.**

Phylogenetic tree showing the evolutionary history of MARK proteins and the related protein PIM2. The red box represents the potential *Dictyostelium* DRIP9 homologue (MrkC). Evolutionary history was inferred using the Neighbour-Joining method. Bootstrap test was performed with 500 replicates. Numbers represent percentage of replicate trees in which the associated taxa clustered together.

### 3.5 Discussion

Protein BLAST analysis of eleven human DRIPs revealed 5 potential homologues in the biomedical model *Dictyostelium discoideum*, DRIPs 2, 4, 7, 9 and 11. The *Dictyostelium* DRIP2 homologue which had the highest e-value was ZizA (3e-78). This protein shared a 50% identity and 29% similarity to the human DRIP2 protein. ZizA is likely to be one of four potential homologues in *Dictyostelium* since ZizC (2e-63), ZizB (7e-60) and ZizD (5e-55) also showed homology to the human DRIP2 protein but these potential homologues had a lower percentage identity and similarity. DRIP 4 and 7 had one potential homologue in *Dictyostelium* AlxA (5e-76) and Gbp $\beta$  (2e-99), respectively. DRIP9 had two potential homologues, MrkC (4e-39) and MrkA (3e-36). MrkC shares a 31% identity and 53% similarity with human DRIP9, whereas MrkA shares a 33% identity and 53% similarity. DRIP11 had 10 potential homologues with an e-value of e-40 or below, all belonging to the kinesin family; Kif1 (1e-151), Kif3 (2e-61) and Kif5 (6e-59) had the highest homology to the human DRIP11.

The top *Dictyostelium* potential homologues, with the highest e-value for each human DRIP were further analysed via protein BLAST analysis to see whether there was conservation of this protein family across different kingdoms. Each potential *Dictyostelium* homologue showed conservation throughout different taxa. The human DRIP 4, 7 and 11 have been extensively characterised in a number of organisms, including *Dictyostelium*.

The human DRIP4, along with the potential *Dictyostelium* homologue, were identified as Alix (ALG2 interacting protein X) proteins (Mattei et al., 2005; Mattei et al., 2006; Ohkouchi et al., 2004; Ohkouchi et al., 2005; Vito et al., 1999; Zhan et al., 2008; Zhan et al., 2010a). ALG-2 is a calcium-binding protein needed for cell death which has been shown to interact with Alix in a calcium dependent manner to facilitate apoptosis (Vito *et al.*, 1999). Characterisation the *Dictyostelium* homologue (*alx*) of the mammalian Alix protein showed that *alx* null cells have a severe developmental phenotype, which is stopped at the tight aggregate stage, failing to undergo morphogenesis and proper cell-type differentiation. However there were no measurable defects in the vegetative

phase (Mattei *et al.*, 2005). In mammals and yeast, Alix has been shown to be associated with the ESCRT (Endosomal Sorting Complex Required for Transport) machinery (Morita *et al.*, 2007; Odorizzi *et al.*, 2003). Since Alix has been characterised in *Dictyostelium* as well as other organisms by a number of research groups, this potential homologue was not chosen for further analysis.

Human DRIP7 is the *GNB2L1* gene which codes for a G $\beta$  subunit involved in G-protein coupling (Zhan *et al.*, 2010a). *Dictyostelium* contains one single G $\beta$  subunit. The deletion of this gene creates mutant cell lines which have no functional G-proteins (Lilly *et al.*, 1993; Peracino *et al.*, 1998; Wu *et al.*, 1995). G $\beta$  null cells showed impaired phagocytosis, although, with little effect on endocytosis, cytokinesis or random cell motility (Peracino *et al.*, 1998). As there is only one single G $\beta$  subunit in *Dictyostelium*, which has already been knocked out and characterised, this potential homologue was not chosen for further investigation.

Human DRIP11 is Kif1A, a kinesin molecular motor involved in organelle transport along microtubules (Goldstein, 2001; Klopfenstein *et al.*, 2002). The kinesin molecular motor (Unc104) has been extensively studied in *C.elegans* and has been shown to be exclusively expressed in neuronal cells (Klopfenstein and Vale, 2004; Zhou *et al.*, 2001). Kinesin molecular motors are involved in the plus end microtubule transport of organelles away from the nucleus. *Dictyostelium* Kif1A has been shown to be a homologue of the *C.elegans* Unc104/Kif1 family of proteins. *Dictyostelium kif1A* knockout mutants showed a loss microtubule plus-end-directed organelle movement (Pollock *et al.*, 1999). The molecular motor Kif1A has been broadly studied in a variety of organisms, including *Dictyostelium*, therefore, this potential DRIP homologue was not chosen for further cellular investigation.

Human DRIP2 (Dock10) and DRIP9 (PIM2) homologues still remain to be characterised in *Dictyostelium*, allowing more scope for discovery. Furthermore, the current understanding of the cellular signalling in *Dictyostelium*, but in all other organisms is also relatively limited, illustrating the need for further in depth analysis and characterisation of these individual proteins. Sequence homology shows that the *Dictyostelium* potential DRIP2 homologue is a member of the



Dock family of proteins, specifically of the Zizimin/Zizimin-related subclasses. The *Dictyostelium* DRIP9 homologue shows sequence homology to the PIM and MARK family proteins, all of which have a highly conserved ser/thr kinase domain.

Dock family proteins are Rho GEFs that regulate small GTPases within the cell. Bioinformatic analysis shows the Dock family can be divided into four sub-categories, Zizimin, Zizimin-related, Dock180 and Dock4-related. All members of the Dock family have two evolutionary conserved domains, the DHR1 and DHR2 domains. Dock180 and Dock4-related proteins also have a SH3 domain and a proline rich motif. The human Zizimin Dock proteins have been shown to all have a PH domain, however, the Zizimin-related proteins do not have a PH domain.

*Dictyostelium* has eight Dock family proteins that fall into two groups, the Dock180-related and the Zizimin-related proteins. The four Zizimin-related proteins have not been extensively characterised in this model organism. Recently, *Dictyostelium* DocA and DocD have been shown to be involved in cell migration (Para *et al.*, 2009) and DocC has been shown to have threefold overexpression in a *Dictyostelium* strain lacking the retinoblastoma-like gene *rbIA* (Doquang *et al.*, in preparation), suggesting that DocC has a role in cell cycle, possibly in cytokinesis. The domain structure analysis illustrates that the four Zizimin-related and Dock180-related proteins have the evolutionary conserved DHR1 and DHR2 domains. However, the Zizimin-related proteins do not have a PH domain which is present in the human Zizimin proteins.

The human DRIP9 (PIM2) is a protein that shows high sequence similarity to the MARK family proteins. Both families are ser/thr kinases that have highly conserved active sites and ATP binding domains, as seen in the domain structure analysis and sequence alignments. The phylogenetic analysis illustrates that the *Dictyostelium* DRIP9 homologue, MrkC, as well as the PIM2 protein, group within the MARK family of proteins.

MARK family proteins play a role in microtubule dynamics. Microtubules have key functions in cell division by establishing shape and polarity (Drewes *et al.*, 1997). The dynamic behaviour of microtubules has to be tightly regulated to allow the morphological changes to occur. This happens through a variety of

proteins such as the microtubule associated proteins (MAPs) that bind and stabilise microtubules (Drechsel et al., 1992; Drewes et al., 1995; Drewes et al., 1997; Illenberger et al., 1996; Trinczek et al., 2004). MARK family kinases regulate MAPs through phosphorylation of the C-terminal microtubule binding domain, causing dissociation from the microtubule (Ebner *et al.*, 1999). These proteins are important in regulating the microtubule dynamics, allowing the balance between plasticity and stability of the microtubule network.

### 3.6 Summary

In this chapter, BLAST analysis identified human DRIP2, 4, 7, 9, and 11 had potential homologues in *Dictyostelium*. Based on sequence alignment and scope for discovery, *Dictyostelium* DRIP2 (ZizA) and DRIP9 (MrkC) were chosen for further analysis. Bioinformatic approaches were used to assess the evolutionary conservation and structural characteristics of these DRIPs in *Dictyostelium*. Phylogenetic, domain structure and sequence alignment analysis suggested that DRIP2 belongs to the Dock family of proteins and groups amongst the Zizimin subfamily, whereas DRIP9 groups amongst the PIM/MARK family of kinases. These data supports the assertion that ZizA and MrkC can be analysed in *Dictyostelium* as Dock and MARK protein homologues, respectively. The bioinformatic data suggests shared functionality amongst the human proteins and the *Dictyostelium* homologues. Therefore, characterising the signalling role of the *Dictyostelium* ZizA and MrkC proteins may provide insight into the cellular roles and functioning of the human DRIP2 and DRIP9.



## **4 Gene ablation**

## 4.1 Introduction

Through protein BLAST analysis of the 11 DRIP proteins, 5 potential homologues were identified in *Dictyostelium*. Bioinformatic analysis including phylogenetics and sequence alignment was used to characterise the evolutionary conservation of these proteins within different taxa. From this data together with the scope for discovery, DRIP2 and DRIP9 were chosen for further analysis. The bioinformatic analysis showed that the DRIP2 shares homology with the Deducator of cytokinesis (Dock) family and the DRIP9 to the Microtubule Affinity Regulating Kinase (MARK) family.

The human DRIP2 protein was shown to group within the Zizimin/Zizimin-related clade of the Dock family phylogenetic tree and contains the characteristic functional DHR1 and DHR2 domains. Analysis of the potential *Dictyostelium* homologues shows there are four Zizimin-related proteins (ZizA-D) that share similar sequence homology to the human DRIP2 protein. ZizA and ZizB were chosen for further analysis since these proteins grouped within the Zizimin/Zizimin-related clade of the phylogenetic tree, have greatest homology to human Dock7 and Dock8 proteins, share a similar domain structure and have the highest expression levels of the four *Dictyostelium* Zizimins (dictyExpress).

The DRIP9 protein analysis revealed there are three MARK family proteins within the *Dictyostelium* genome (MrkA-C), all of which show high conservation of the serine/threonine (ser/thr) kinase domain, and the active residues shown in other MARK proteins. Furthermore phylogenetic analysis places these proteins amongst the MARK/Pim related proteins from other kingdoms. The *Dictyostelium* MrkA and MrkC proteins were chosen for further investigation as they had the greatest homology and share a similar domain structure to human MARK2 protein.

In this chapter, the role of the *Dictyostelium* Zizimin (ZizA and ZizB) and the MARK (MrkA and MrkC) proteins are investigated following gene ablation. Multiple isogenic cells lines were produced and confirmed by loss of gene expression and subsequent development assays assessed the role of each protein in *Dictyostelium* development.

## 4.2 Creating Knock out mutants

To investigate a potential role for the Zizimin and MARK family of proteins in *Dictyostelium*, the genes for *zizA* and *zizB* and, *mrkA* and *mrkC*, were ablated using homologous integration of a knockout cassette. Knockout cassettes were designed to delete the active residues or full domains, identified in chapter 3, thus ensuring only non-functional proteins could be produced following homologous integration of each cassette into the genome.

Knockout cassettes for each gene were created using PCR to amplify 5' (N-terminal) and 3' (C-terminal) regions from within each open reading frame. The 5' and 3' fragments for each gene were then cloned into the pLPBLP vector flanking the blasticidin resistance gene (Faix *et al.*, 2004). The *zizA* and *zizB* 5' fragments were cloned into the pLPBLP vector at the BamHI/PstI and the NotI/PstI restriction sites, respectively. Subsequently, the 3' fragments were cloned at the NcoI/KpnI and NcoI/HindIII restriction sites, respectively (**Figure 4.1**). To make the *mrkA* and *mrkC* knockout cassettes, 5' fragments were cloned into the pLPBLP vector at the BamHI/PstI restriction sites, this was followed by the cloning of the 3' fragments at the NcoI/KpnI and NcoI/AccI restriction sites, respectively (**Figure 4.2**).

The complete knockout plasmids for each gene were verified by restriction digest analysis. Here, the individual 5' and 3' fragments were digested with the restriction enzymes used for cloning (as detailed above). The whole gene including the resistance cassette was excised at the BamHI/KpnI (2806bp) and NotI/HindIII (3122bp) restriction sites for *zizA* and *zizB*, respectively (**Figure 4.1**). For *mrkA* and *mrkC* the whole gene was excised at the BamHI/KpnI (2839bp) and the BamHI/AccI (3380bp) restriction sites, respectively (**Figure 4.2**). The size of the gene fragments with the incorporated blasticidin resistance cassette was similar to that of the remaining vector backbone making it difficult to see the separate fragments. However, single digest of each restriction enzyme was used as an enzyme cutting control (**Figure 4.1 & 4.2**).

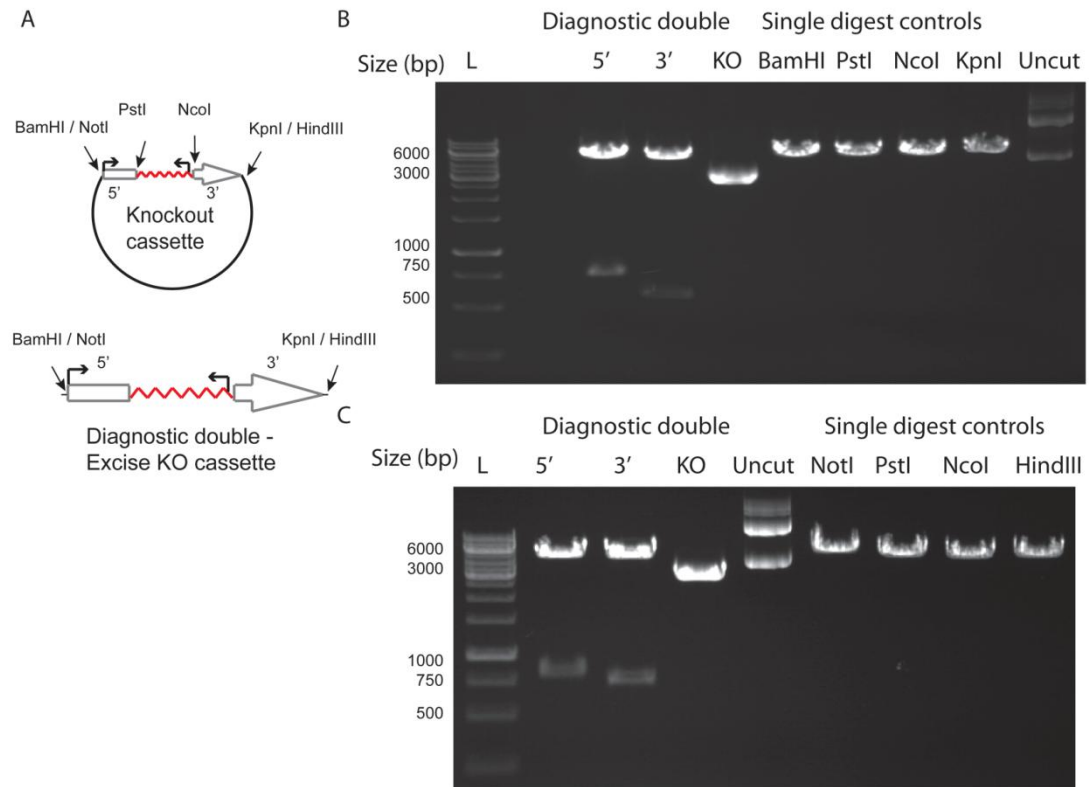


**Figure 4.1 Restriction digest analysis of the *zizA* and *zizB* knockout vectors.**

(A) Schematic showing the method used for cloning, indicating the 5' and 3' fragments and the corresponding restriction enzyme cut sites, flanking the blasticidin resistance cassette (~~~~~). The orientation of the promoter for the *ziz* gene or the blasticidin resistance gene is also shown (↗). (B) The *zizA* 5' and 3' fragments were cloned into the pLPBLP vector backbone using specific restriction enzymes BamHI/PstI (751bp) and NcoI/KpnI (623bp), respectively. The whole knockout cassette (KO) incorporating the blasticidin resistance cassette was excised with the BamHI and KpnI (2806bp) restriction enzymes. (C) The *zizB* 5' and 3' fragments were cloned into the pLPBLP vector backbone using specific restriction enzymes NotI/PstI (844bp) and NcoI/HindIII (778bp), respectively. The whole knockout cassette (KO) incorporating the blasticidin resistance cassette was excised with the NotI and HindIII (3122bp) restriction enzymes. The empty pLPBLP vector was used as a control to show undigested plasmid and the single digest for each different restriction enzyme to confirm the enzymes were cutting in a single place. The uncut lane indicates the undigested pLPBLP vector. L indicates a 1kb molecular weight marker with sizes indicated next to the lane.

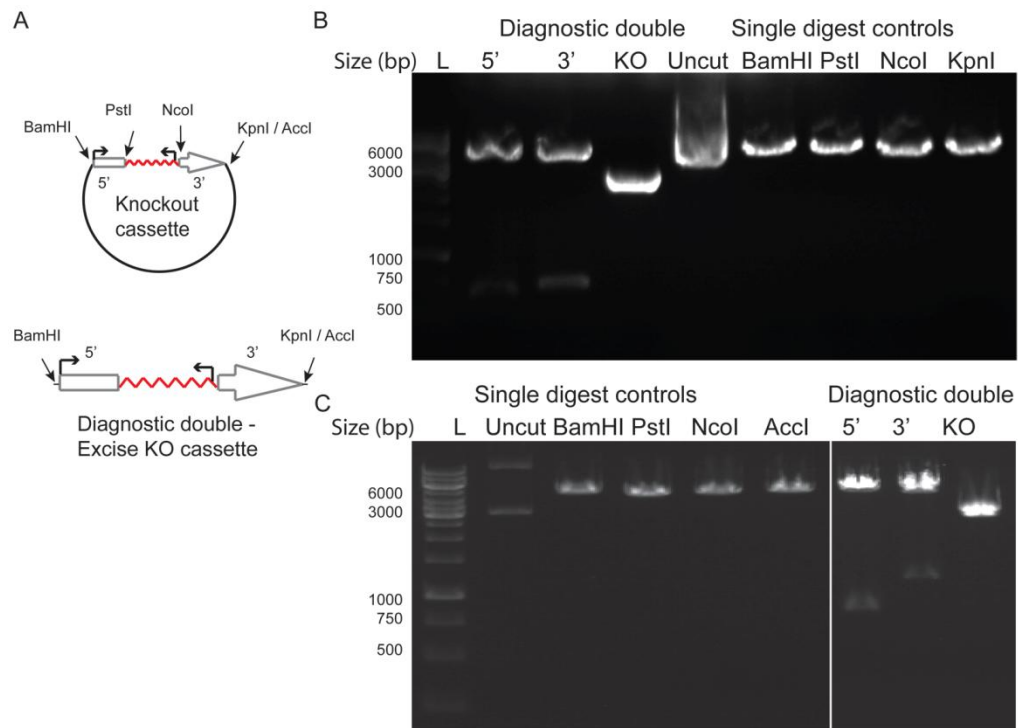


**Figure 4.2 Restriction digest analysis of the *mrkA* and *mrkC* knockout vectors.**

(A) Schematic showing the method used for cloning, indicating the 5' and 3' fragments and the corresponding restriction enzyme cut sites, flanking the blasticidin resistance cassette (~~~~~). The orientation of the promoter for the *ziz* gene or the blasticidin resistance gene is also shown (↗). B, The *mrkA* 5' and 3' fragments were cloned into the pLPBLP vector backbone using specific restriction enzymes BamHI/PstI (645bp) and NcoI/KpnI (694bp), respectively. The whole knockout construct (KO) incorporating the blasticidin resistance cassette was excised with the BamHI and KpnI (2839bp) restriction enzymes. (B) The *mrkC* 5' and 3' fragments were cloned into the pLPBLP vector backbone using specific restriction enzymes BamHI/PstI (766bp) and NcoI/AccI (1114bp), respectively. The whole knockout cassette (KO) incorporating the blasticidin resistance cassette was excised with the BamHI and AccI (3380bp) restriction enzymes. The empty pLPBLP vector was used as a control to show undigested plasmid and the single digest for each different restriction enzyme to confirm the enzymes were cutting in a single place. The uncut lane indicates the undigested pLPBLP vector. L indicates a 1Kb molecular weight marker with sizes indicated next to the lane.

The knockout cassettes (containing the blasticidin resistance gene flanked by the targeting gene-specific 5' and 3' regions) were excised with restriction enzymes (*zizA* & *zizB* - BamHI/KpnI & NotI/HindIII respectively, *mrkA* & *mrkC* - BamHI/KpnI & BamHI/AccI, respectively) and purified before transformation into wild type (Ax2) *Dictyostelium* cells. Colony plating (in 96 well dishes), and selection for cassette integration (by growth in the presence of blasticidin antibiotic) enabled the isolation of potential target gene knockout mutants. Surviving cells were then screened by PCR to identify homologous integrants (producing the null mutants - *zizA*<sup>-</sup>, *zizB*<sup>-</sup>, *mrkA*<sup>-</sup> & *mrkC*<sup>-</sup>).

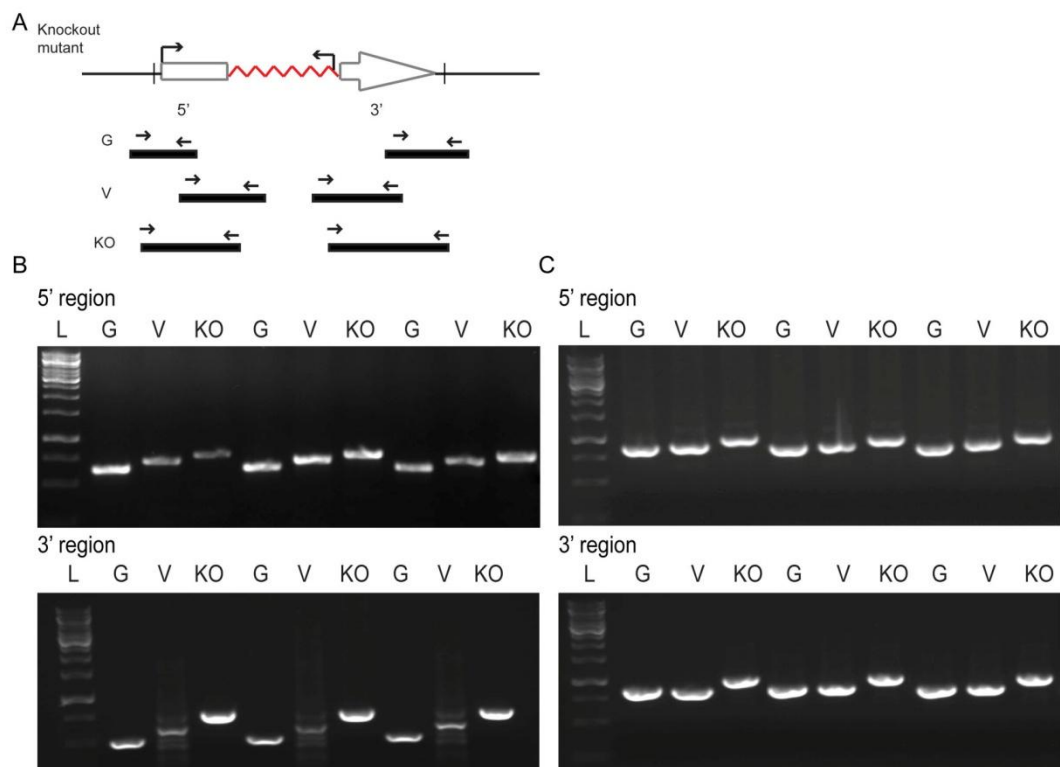
#### 4.2.1 PCR screening analysis

Colonies showing blasticidin resistance (derived from wild type cells transformed with Zizimin and MARK knockout cassettes) were screened by PCR analysis to identify cells showing homologous integration, as previously described (Adley *et al.*, 2006). Briefly, primer combinations were used in a PCR screen as genomic (G) and vector (V) controls and a unique diagnostic knockout fragment (KO). For the genomic controls, one primer was located in the gDNA outside the knockout cassette and the other within gDNA fragment used for the knockout cassette. The vector controls used primers within the gDNA fragment used for the knockout cassette and a primer within the blasticidin resistance cassette. A unique diagnostic knockout band confirmed homologous integration using a primer outside the gDNA fragment and within the blasticidin resistance cassette. These primer combinations were designed for (5' and 3'-regions) of each knockout cassette of the two Zizimin and two MARK family proteins (**Figure 4.3, Figure 4.4**).

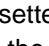
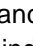

In the analysis of the potential Zizimin null cell lines 123 (*zizA*) and 48 (*zizB*) blasticidin resistant colonies were screened for homologous integration of the knockout cassettes. The *zizA*<sup>-</sup> transformed cells showed 9 positive integrants and *zizB*<sup>-</sup> transformed cells showed 15 positive integrants for the 5' region. These potential homologous integrants were then analysed by PCR over the 3' region where *zizA*<sup>-</sup> showed 4 homologously integrated transformants and *zizB*<sup>-</sup> showed 9 homologously integrated transformants for both 5' and 3' regions. Homologous integration events on both the 5' and 3' ends of the of the knockout cassette indicate successful ablation of the target gene. From these positive

colonies, three independent potential knockout mutants were chosen and further subcloned to derive isogenic cell lines.

In the analysis of the potential MARK null cell lines, 62 (*mrkA*) and 90 (*mrkC*) knockout cassette transformants were screened for homologous integration. The *mrkA*<sup>-</sup> mutants showed 12 homologously integrated transformants for the 5' region and *mrkC*<sup>-</sup> cells showed 9 homologously integrated transformants. These were then tested over the 3' region where *mrkA*<sup>-</sup> showed 8 homologously integrated transformants for both 5' and 3' regions and *mrkC*<sup>-</sup> showed all 4 homologously integrated transformants. Three independent colonies were chosen and subcloned to derive a cell line from a single cell colony.



**Figure 4.3 PCR screening analysis for *zizA* and *zizB* knockout cell lines.**

(A) Schematic of the PCR screening analysis. Here, the knockout mutant contains the blasticidin resistance cassette (  ) flanked by the 5' and 3' regions of the gene. The promoter (  ) indicates the orientation of the respective gene. The arrows (  ) show the primers used in the PCR screening. Blasticidin resistant colonies isolated following transformation with each knockout cassette were screened by PCR. B & C, PCR analysis was used to screen for homologous integration of *zizA* & *zizB* cells, respectively, at the 5' and 3' region using a genomic (G) and a vector (V) control and a diagnostic knockout (KO) fragment (unique to homologously integrated transformants). L indicates a 1kb molecular weight marker.

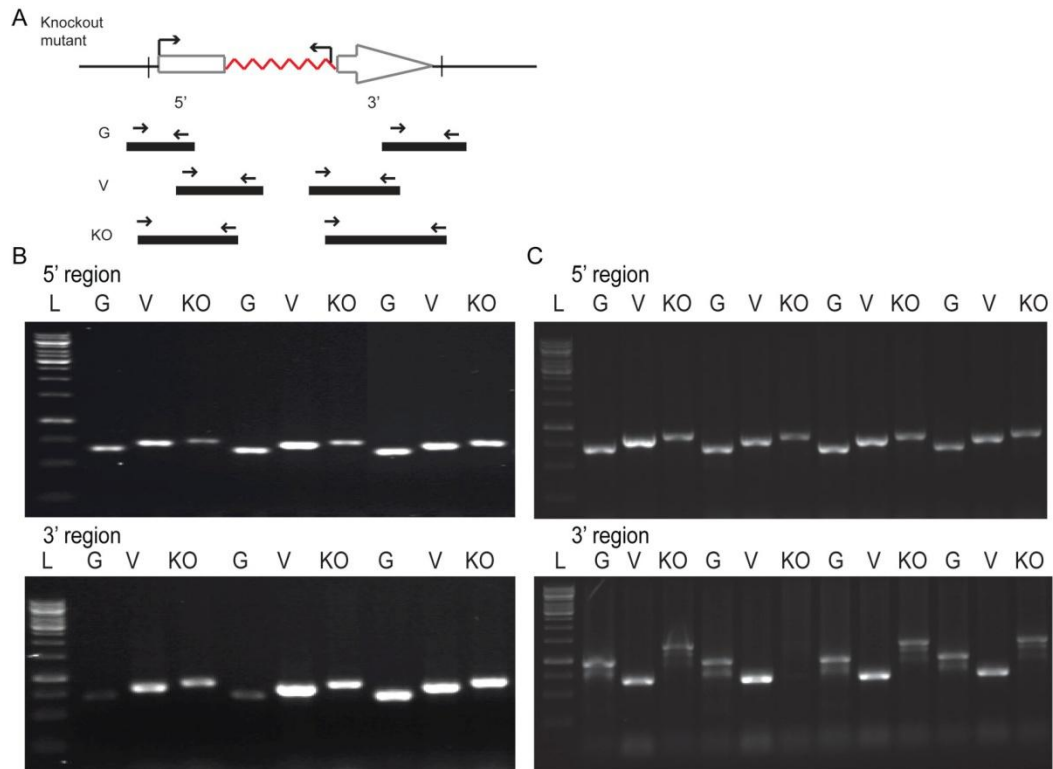


**Figure 4.4 PCR screening analysis for *mrkA* and *mrkC* knockout cell lines.**

(A) Schematic of the PCR screening analysis. Here the knockout mutant contains the blasticidin resistance cassette (~~~~~) flanked by the 5' and 3' regions of the gene. The promoter (  $\Gamma$  ) indicates the orientation of the respective gene. The arrows (  $\leftarrow$  ) show the primers used in the PCR screening. Blasticidin resistant colonies isolated following transformation with each knockout cassette was screened by PCR. (B & C) PCR analysis was used to screen for homologous integration of *mrkA* & *mrkC* cells, respectively, at the 5' and 3' region using a genomic (G) and a vector (V) control and a diagnostic knockout (KO) fragment (unique to homologously integrated transformants). L indicates a 1 kb molecular weight marker.



### 4.2.2 Loss of gene transcription

Subsequent to identifying knockout cell lines, reverse transcriptase PCR was used to confirm loss of gene transcription from the isogenic clones. cDNA derived from each clone was used to test for the presence or absence of the expressed target gene. Primers used to amplify diagnostic products from cDNA were located within the knocked out region of the gene. Successful amplification of a 308bp and a 541bp fragment from the wild type derived cDNA indicated expression of a functional gene for *zizA* and *zizB*, respectively (**Figure 4.5**). Also, the amplification of a 583bp PCR product and a 603bp PCR product in the wild type derived cDNA indicated the expression of a functional gene product for *mrkA* and *mrkC*, respectively (**Figure 4.6**). Glycogen synthase (*glcS*) PCR product was used as an expression control, which has been shown to be stably expressed throughout development (Williamson *et al.*, 1996). This control product gave rise to a 500bp fragment for cDNA and 600bp fragment for gDNA. This produced a second control for potential contaminating genomic DNA since the *glcS* primers were designed to flank an intron, such that, a different size PCR product is amplified from the cDNA compared to the gDNA.

Analysis of the three independent isogenic colonies for *zizA*, *zizB*, *mrkA* and *mrkC* null mutants identified through the flanking PCR screening, confirmed the loss of the encoded RNA in each isolate, thus, independently confirming gene ablation (**Figure 4.5 & 4.6**).

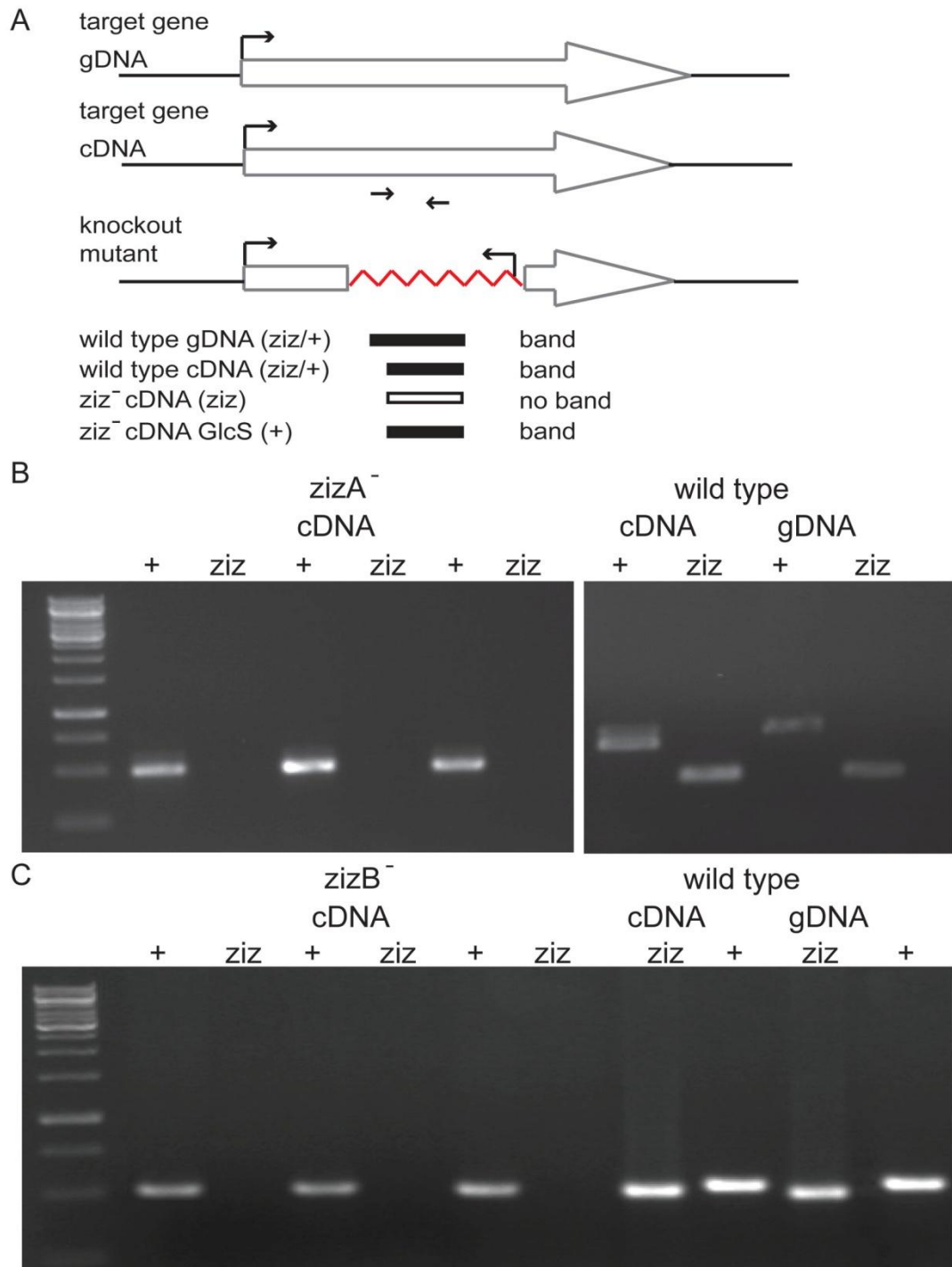


**Figure 4.5 PCR analysis of Zizimin gene transcription, in wild type and putative null cells.**

(A) Schematic showing the rationale of the primer design. Primers were designed within the excised region of each gene target (*ziz*) and used in PCR analysis with cDNA from the wild type, *zizA*<sup>-</sup> and *zizB*<sup>-</sup> cell lines. (B & C) RNA was extracted from wild type, *zizA*<sup>-</sup> and *zizB*<sup>-</sup> cell lines and converted to cDNA using reverse transcription PCR. Glycogen synthase (+) primers were used as a control, where primers were designed to flank an intron indicating a size difference between cDNA and gDNA.

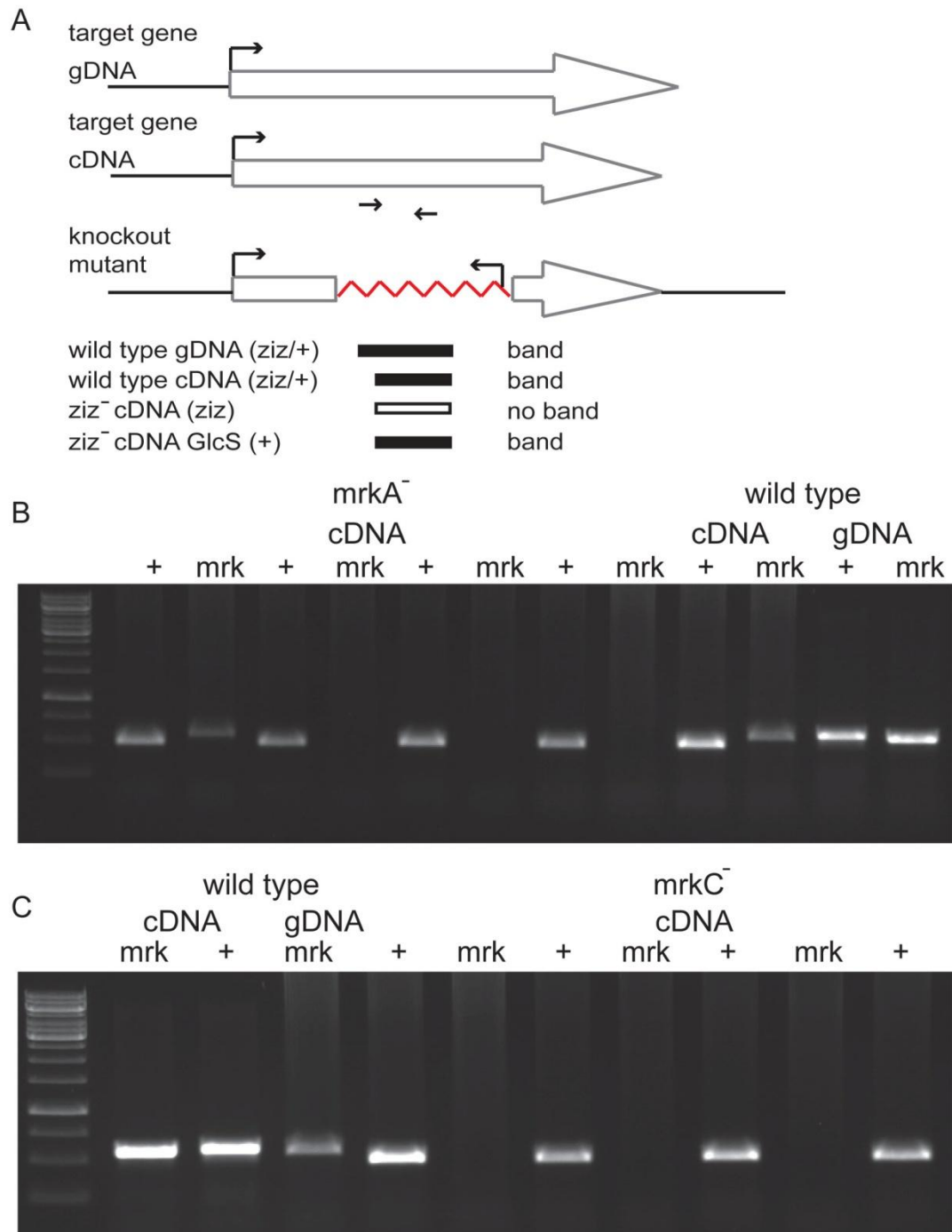


**Figure 4.6 PCR analysis of MARK gene transcription in wild type and putative null mutants.**

(A) Schematic showing the rationale of the primer design. Primers were designed within the excised region of each gene target (*mrk*) and used in PCR analysis with cDNA from the wild type, *mrkA*<sup>-</sup> and *mrkC*<sup>-</sup> cell lines. (B & C) RNA was extracted from wild type, *mrkA*<sup>-</sup> and *mrkC*<sup>-</sup> cell lines and converted to cDNA using reverse transcription PCR. Glycogen synthase (+) primers were used as a control, where primers were designed to flank an intron indicating a size difference between cDNA and gDNA.

### 4.3 Effect of gene ablation on development

During a 24hr development process, *Dictyostelium* cells aggregate and form a multi-cellular organism. To investigate the developmental effect of knocking out the *zizA* and *zizB* genes and the *mrkA* and *mrkC* genes, wild type and null mutants were starved on a nitrocellulose membrane over 24hr. Under these conditions, wild type cells form multi-cellular fruiting bodies containing a basal disc, stalk, and round spore head (Schaap and Wang, 1986).

Analysis of the cellular role of ZizA and ZizB proteins during the developmental process showed that cell lines lacking the ZizA protein did not exhibit altered developmental morphology when compared to wild type cells (**Figure 4.7**). In contrast, cells lacking the ZizB protein exhibited aberrant fruiting body morphology with thickened stalks and collapsed fruiting bodies in comparison to wild type (or *zizA*<sup>-</sup> cell lines) (**Figure 4.7**).

For cell lines lacking the MrkA and MrkC proteins, mature fruiting bodies showed wild type developmental morphology (**Figure 4.8**). The three independent isogenic cell lines obtained from ablation of *zizA*, *zizB*, *mrkA* and *mrkC* were tested over three experiments and the developmental morphology was consistent.

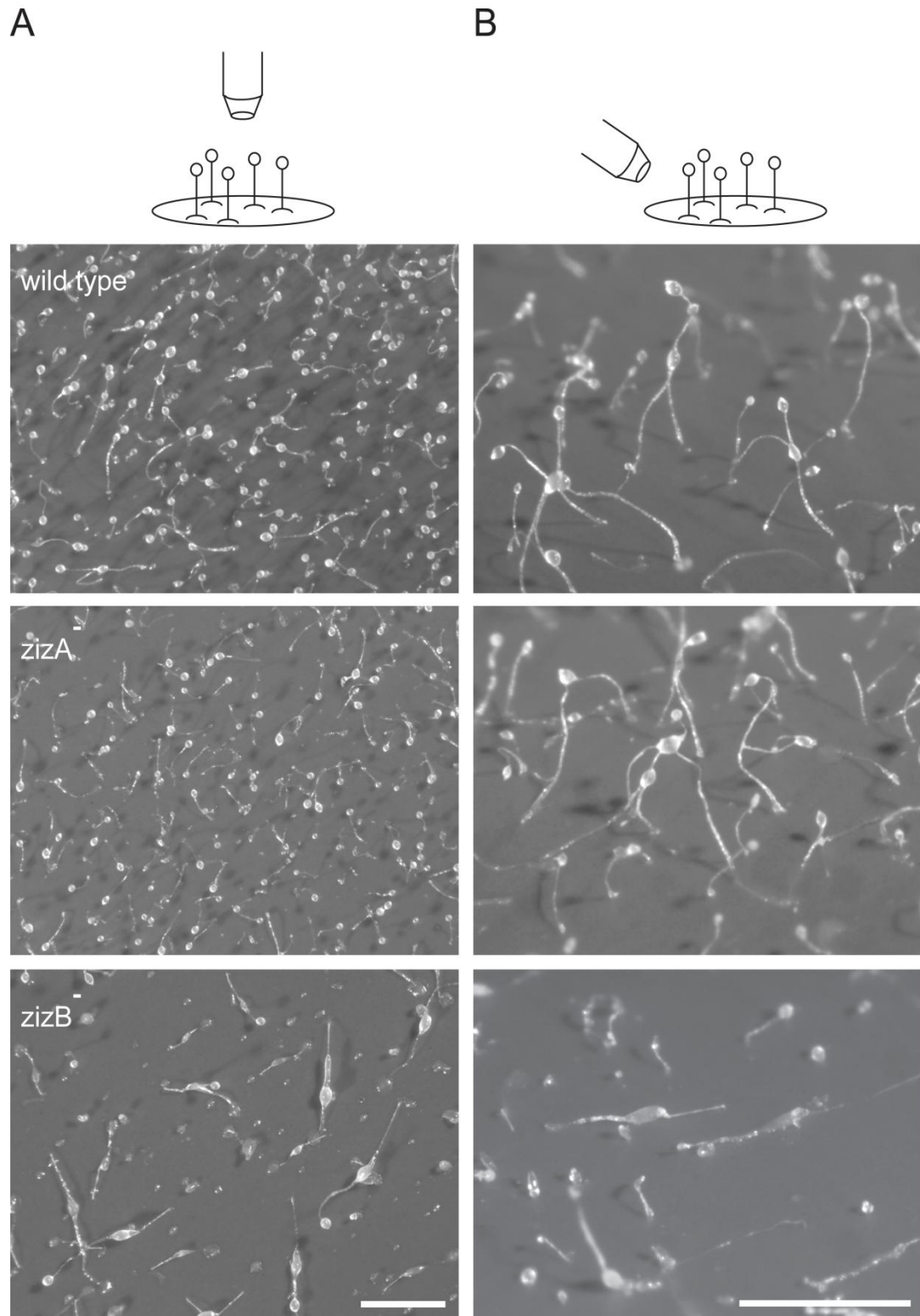


**Figure 4.7 Development of zizA<sup>-</sup> and zizB<sup>-</sup> cell lines.**

Cells were allowed to develop on a nitrocellulose filter over 24hr. Schematic images shows the angle of the camera used to record development from (A) aerial and (B) side angle view with wild type, zizA<sup>-</sup> and zizB<sup>-</sup> cell lines, with the representative image included. Size bar for A and B represents 0.5mm.

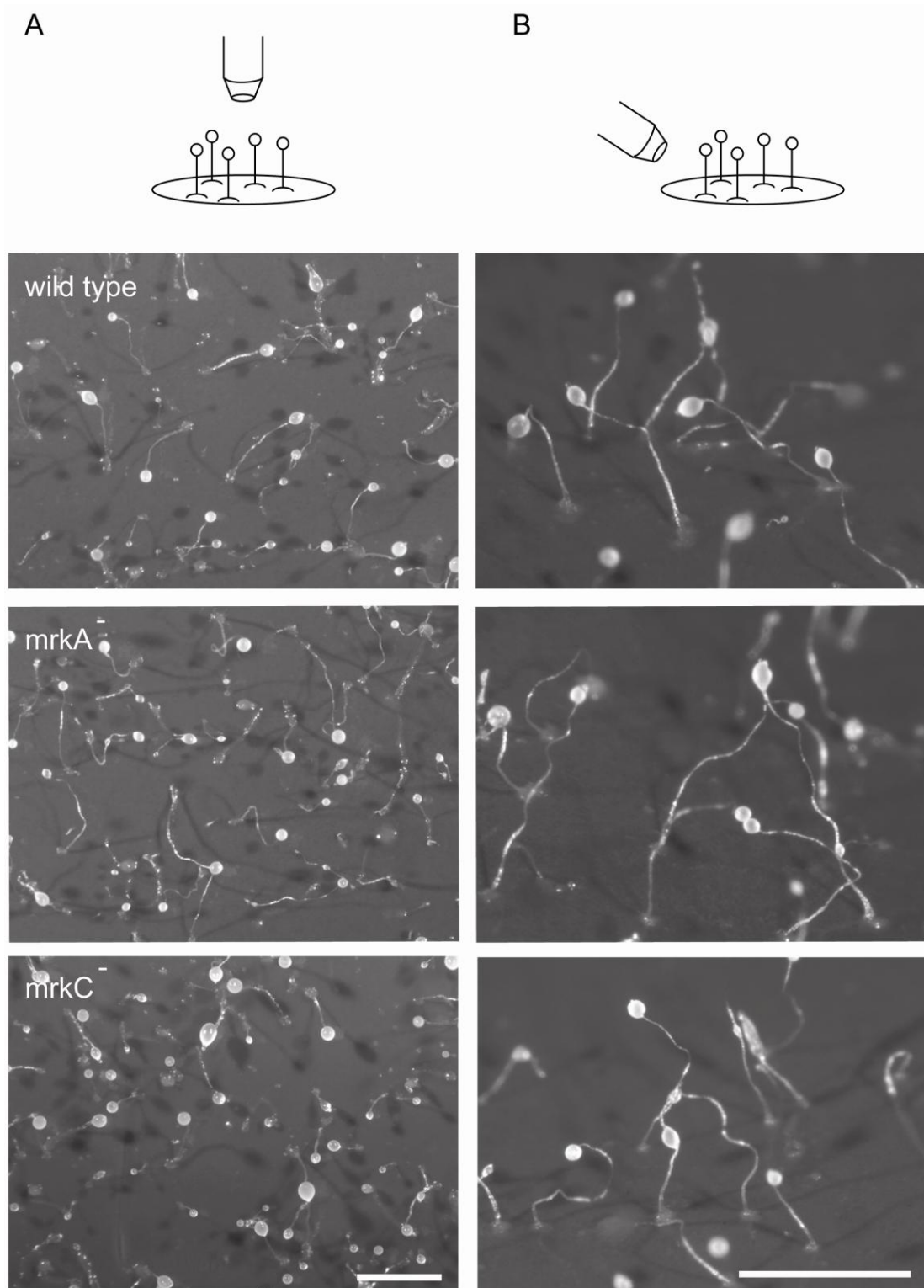


**Figure 4.8 Development of  $mrkA^-$  and  $mrkC^-$  cell lines.**

Cells were allowed to develop on a nitrocellulose filter over 24hr. Schematic images shows the angle of the camera used to record development from (A) aerial and (B) side angle view with wild type,  $mrkA^-$  and  $mrkC^-$  cell lines, with representative images included. Size bar for A and B represents 0.5mm.

Since the *zizB* null mutant exhibited a developmental phenotype and was unable to produce mature fruiting bodies, I assess whether this aberrant morphology was due to defects in the early stages of the development. Wild type, *zizA*<sup>-</sup> and *zizB*<sup>-</sup> cell lines were allowed to develop on a nitrocellulose filter and images were captured (from side angle view) at 8hr, 13hr and 24hr. These wild type (and *zizA*<sup>-</sup>) cells produced mounds at 8hr, developed to first-finger stage at 13hr and then into mature fruiting bodies at 24hr. In contrast, cells lacking the ZizB protein were slightly delayed in early development compared to wild type cells (still showing late streaming) at 8hr. These cells were also delayed in development at first finger stage (13hr), compared to the wild type cells, and showed sparse collapsed fruiting bodies with thickened stalks at 24hr (**Figure 4.9**).

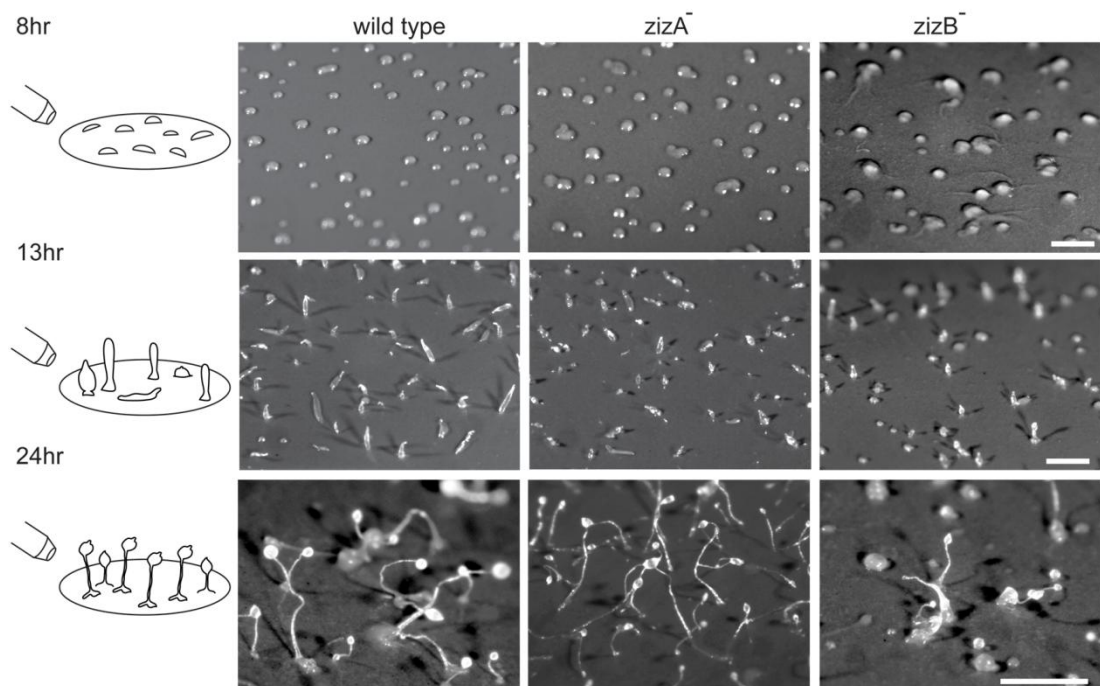


**Figure 4.9** Early stages of development for wild type, *zizA*<sup>-</sup> and *zizB*<sup>-</sup> cell lines.

Schematic images (seen on the left) show the angle of the camera (side angle view) and the 'typical' wild type structures (8hr mounds, 13hr first fingers and 24hr fruiting body) recorded at that stage of development. Cells were developed on a nitrocellulose filter and images were captured at 8hr, 13hr and 24hr for wild type, *zizA*<sup>-</sup> and *zizB*<sup>-</sup> cell lines. All size bars represent 0.5mm.



## 4.4 Discussion

### 4.4.1 Creating knockout cell lines

To investigate the role of the Zizimin and MARK family proteins, cell lines were created lacking the *zizA* or *zizB* genes or the *mrkA* or *mrkC* genes. These knockout cell lines were produced by homologous integration of a knockout cassette causing a deletion of a region from the centre of each target gene. In the case of ZizA and ZizB proteins, these deleted regions contained DHR1 and DHR2 domains. The DHR1 domain has been implicated in PIP3 binding and hence localisation (Cote et al., 2005; Kobayashi et al., 2001), whereas the DHR2 domain is responsible for GTPase binding and subsequent GEF activity of these proteins (Brugnera et al., 2002; Cote and Vuori, 2002; Cote and Vuori, 2006; Meller et al., 2002). In the case of MrkA and MrkC, the ser/thr kinase domain as well as the kinase associated domain was deleted from the knockout cassettes. The ser/thr kinase domain is located in the N-terminus of the MARK protein and carries out the main catalytic activity of these proteins (Drewes et al., 1997; Elbert et al., 2005). The *Dictyostelium* MARK protein also contains a kinase associated domain located in the C-terminus. Although, its exact function is unclear, it has been suggested to have an inhibitory effect on the catalytic domain. This domain was also deleted from the knockout cassette. Deletion of all (or the majority) of these domains within the knockout cassette ensured any potential partial protein still transcribed would not show functional activity.

This approach employed gene deletion to avoid revertants and transcription of partial gene products. This method deletes a large portion of the endogenous gene as opposed to the transposon technology method which inserts a resistance marker without deleting any regions of the target gene (Abe et al., 2003; Adley et al., 2006). Furthermore, the blasticidin resistance cassette was orientated within the pLPBLP expression vector such that transcription occurs in the opposite direction to that of the gene fragments, to avoid potential read through into the 3' region of the target gene.

Colony plating and selection of transformants enabled isolation of multiple independent colonies from a single electroporation. All these genes showed high transformation efficiency and rate of homologous integration. Although



PCR confirmation on both sides of the cassette (followed by loss of transcription) provides proof of gene ablation, this approach could potentially give rise to additional integration events. However, multiple independent knockout cell lines were isolated from a single colony for each mutant, that enabled each of these independently clones to be analysed in parallel to each other. If multiple integration events had occurred, these colonies would behave in a dissimilar manner during development.

#### 4.4.2 Effect of gene ablation on development

During unfavourable (starvation) conditions *Dictyostelium* cells undergo a change in morphology, developing from a single cell into a multi-cellular organism containing spores to ensure survival. During this process, surrounding cells migrate towards a cAMP signal, undergoing a number of morphological and physiological changes resulting in the formation of these multi-cellular fruiting bodies (containing spores) (Iranfar et al., 2003; van et al., 2002). Many proteins required for morphogenesis are cytoskeletal proteins, since development involves constant reorganisation of the cytoskeleton (Chisholm and Firtel, 2004; Dumontier et al., 2000; Palmieri et al., 2000; Park et al., 2004). For example, disruption of the myosin light chain gene causes aberrant development, where 50% of the aggregates did not progress past mound stage and the remaining 50% produced aberrant fruiting bodies with short thickened stalks (Chen et al., 1995). Zizimin and MARK proteins have been shown to be involved in regulating actin/microtubule dynamics of the cell, a function that is essential for cellular movement and thus development (Chen et al., 1995; Chisholm and Firtel, 2004; Rivero et al., 1999b). It was therefore tested, whether ablation of the *zizA* or *zizB* genes and the *mrkA* or *mrkC* genes gave rise to developmental defects.

Since ablation of the *zizA* gene did not give rise to any major morphological changes in development, a non-crucial role for this protein in multi-cellular aggregation and differentiation is suggested. However, functional redundancy has been shown in many other actin regulating and small GTPase related signalling families (Chisholm and Firtel, 2004; Para et al., 2009; Park et al., 2004; Rivero et al., 1996a; Rivero et al., 1996b; Witke et al., 1992). The

*Dictyostelium* Dock180 related proteins (Doc A-D) have been shown to have compensatory mechanisms. In this study, it was shown that the cell movement (a process required for development) defects of the single knockout cell lines of DocA and DocD were significantly enhanced in the double knockout mutant (Para *et al.*, 2009). Furthermore, the actin cross linking proteins,  $\alpha$ -actinin and gelation factor, also showed functional redundancy, where no apparent phenotype was seen in the single mutants, however, the double mutants had aberrant development, producing short squat fruiting bodies, compared to wild type cells (Rivero *et al.*, 1996b; Rivero *et al.*, 1999b). Another study showed that disruption of the actin binding proteins, profiling I and II, had defects in developmental morphology in the double knockout mutant, a phenotype that again, was not seen in the single knockout mutants (Haugwitz *et al.*, 1994). Further to these studies, RacB and RacGEF1 (Park *et al.*, 2004) and Trix RacGEF (Strehle *et al.*, 2006) also demonstrated functional redundancy. These studies indicate that the potential cellular role of ZizA may be (at least partially) compensated for by the other Zizimin proteins. This theory, however, would need to be further validated through the production of double knockout mutants.

In contrast, ablation of the *zizB* gene did cause developmental defects resulting in aberrant fruiting body morphology, where the majority of cells were unable to produce mature fruiting bodies. The aggregates that could progress further in development, had aberrant morphology with thickened stalks and collapsed fruiting bodies. Analysis of the early stages of development showed that there was a delay at both 8hr and 13hr in the *zizB* null mutants. This suggests a critical role for the ZizB protein (in development), which cannot be replaced by other related proteins.

A number of other GEF knockout mutants have also been shown to have specific key roles in development. The RacGEF GxcDD null mutant displayed a defect in the streaming behaviour during early development and a delay in developmental timing (Mondal *et al.*, 2007). Also, ablation of a gene encoding Aimless, a RasGEF protein, produced cells that were unable to undergo development, even after several days of starvation (Insall *et al.*, 1996). Cells lacking the small GTPase RacB and its specific GEF, RacGEF1 both exhibited strong morphogenesis defects. The RacB null cells showed a delay in early development, only reaching the mound stage after 10hr whereas wild type cells

reached the mound stage after 7hr (Park *et al.*, 2004). The RacGEF1 null showed a slight delay in development where the cells reached mound stage after 7hr, however, a greater proportion of cells had not entered the aggregate (still showing late streaming) (Park *et al.*, 2004). This study also demonstrated a range of other mutants with defective RacGEF1 (overexpression, and truncated RacGEF1 mutants) which showed more severe phenotypes. The overexpressor was unable to develop past mound stage and the N-terminal null mutant showed extreme delay in forming large streams that produced multi-tipped finger like structures from the centre of these streams (Park *et al.*, 2004). Constitutive activation, or dominant negative mutants of Rac1 in *Dictyostelium*, led to early and late developmental defects, where the constitutively active mutant had an extreme delay as these cells required 96hr post-starvation, to develop a sparse number of fruiting bodies (Dumontier *et al.*, 2000; Palmieri *et al.*, 2000). Actin regulation is key to cell movement and, hence, development. Therefore, a number of actin regulating proteins have shown to have critical roles in development (as shown in the above examples). This supports the aberrant developmental morphology seen in the *zizB* null mutant, since Zizimins are known to regulate actin dynamics (Meller *et al.*, 2002).

The *Dictyostelium* MARK protein (MrkA and MrkC) knockout cell lines did not show any developmental changes compared to wild type cells, thus, produced mature fruiting bodies. These proteins have not previously been studied in *Dictyostelium*, however, have shown to be part of the CAMK subgroup of the kinome (Goldberg *et al.*, 2006). MARK proteins have been studied in other systems, and have been shown to be important regulators of microtubule dynamics, through phosphorylation of MAP proteins. This phosphorylation causes the detachment of the MAPs from the microtubules increasing microtubule dynamics (Drewes *et al.*, 1995; Drewes *et al.*, 1997). Overexpression of human MARK1 and MARK2 proteins in Chinese Hamster Ovary (CHO) cells caused the microtubule network to almost entirely disappear; which they showed was due to the phosphorylation rather than overexpression. Since MARKs phosphorylate MAPs causing detachment from the microtubules, the over phosphorylation caused the destruction of this microtubule network (Drewes *et al.*, 1997). The *D.melanogaster* and *C.elegans* homologue of the MARK proteins, Par-1, and *S.cerevisiae* homologue, Kin1 and 2 have been

shown to regulate cell polarity (Drewes et al., 1997; Elbert et al., 2005; Hurov and Piwnica-Worms, 2007; Kempfues, 2000; Matenia and Mandelkow, 2009; Trinczek et al., 2004).

Cell polarity is an important aspect of *Dictyostelium* development, as, during early development, aggregation of the individual cells occurs through chemotaxis, which requires each cell to polarise by rapid reorganisation of its cytoskeleton to migrate towards a source of cAMP (Rubino et al., 1984; Williams and Harwood, 2003). As with the *zizA* null mutant, there were no morphological defects associated with the *mrkA* or *mrkC* null mutants, which may also be due to compensatory effects of the other Mrk proteins in *Dictyostelium*. The *S.cerevisiae* Kin1 and Kin2 have been shown to have functional redundancy (Elbert *et al.*, 2005). It is suggested that the role of *mrkA* and *mrkC* genes in *Dictyostelium* development is not crucial, since the absence of these genes did not cause a change in developmental phenotype. However, their potential function could be compensated for by the other related proteins. This theory would need to be confirmed through double knockout mutants.

## 4.5 Summary

In this chapter, gene knockout mutants were created by homologous integration in multiple independent clones, with ablation confirmed by loss of gene expression. No gross phenotypic changes were seen following ablation of *zizA*, *mrkA* or *mrkC*. In contrast, the loss of *zizB* caused altered development, leading to thickened, often collapsed stalks, and reduced spore heads. This indicated a key role of ZizB in development, which initiated the investigation of the role of the Zizimin proteins in other cellular processes and cell signalling events such as cell migration, cytokinesis, growth and stress.

## **5 Zizimin cellular function**

## 5.1 Introduction

The construction of the Zizimin (*zizA* and *zizB*) and MARK (*mrkA* and *mrkC*) knockout cassettes enabled the ablation of each gene in *Dictyostelium*. Independent isogenic cells lines lacking these proteins were produced, and initially examined for altered development. From these studies only the ZizB null mutant had a developmental defect, where it was unable to develop mature fruiting bodies over 24hr and showed a delay in early development (8hr and 13hr). In contrast, cells lacking the *zizA*, *mrkA* or *mrkC* genes did not show altered development compared to wild type cells.

Since the ZizB null mutant demonstrated defects in development, the Zizimin protein family was chosen for further analysis. In mammalian systems, Zizimin proteins regulate the Rho family of small GTPases (Rho, Rac and Cdc42) which function as molecular switches regulating processes that involve the reorganisation of the cytoskeleton including cell migration, development and cytokinesis (Chung et al., 2000; Dumontier et al., 2000; Han et al., 2006; Larochelle et al., 1996; Palazzo et al., 2001). Of the eight *Dictyostelium* Dock family proteins, two have been characterised (Dock180-related proteins, DocA and D), where double and single knockout mutants for each gene exhibited defects in cell migration (Para et al., 2009). I therefore investigated the possible involvement of the *Dictyostelium* Zizimin-related proteins in actin regulated cellular processes.

In this chapter, the cellular function of ZizA and ZizB were investigated. Here, I analysed different behavioural and morphological processes that involve reorganisation of the cytoskeleton including development (of cells overexpressing ZizA or ZizB), cell migration, localisation, cytokinesis, growth and stress response.

## 5.2 Expression profile of *Dictyostelium* Zizimin proteins

There are four Zizimin proteins in *Dictyostelium* (ZizA-D) and the relative importance for each of these proteins in cell function remains unclear. As an initial step in analysis, wild type cells were allowed to develop over 24hr and RNA was extracted from cells at 4hr time intervals. RNA was converted to cDNA using reverse transcriptase PCR, and the expression of each gene analysed for each time point. Quantification of expression levels was performed using the Quantity One 1-D analysis software and expression levels for each time point were normalised using the constitutively expressed *Ig7* control (Williams *et al.*, 2002).

Since *zizA* and *zizB* were chosen for further analysis, *zizC* and *zizD* were included in the expression profile as a comparison, where these genes showed lower expression levels to *zizA* and *zizB*. All four Zizimin genes were constantly expressed throughout the 24hr developmental cycle however the relative levels of expression varied. The *zizB* gene had the highest expression of the four *Dictyostelium* Zizimin genes followed by a stepwise reduction in the expression levels of *zizA*, *zizD* and *zizC*, respectively (**Figure 5.1**). Although the methodology employed here gives a semi-quantitative readout for gene expression, the results obtained are in agreement with the RNA-Seq database (<http://dictyexpress.biolab.si>) which shows a more quantitative expression profile, where *zizB* has the highest expression levels that peak at 8hr followed by *zizA* (which was constantly expressed throughout development). Furthermore the RNA-Seq data showed that *zizB* falls within the top 5% of genes expressed in *Dictyostelium*, peaking at 1500 copies at 8hr development (<http://dictybase.org>) (Rot *et al.*, 2009).

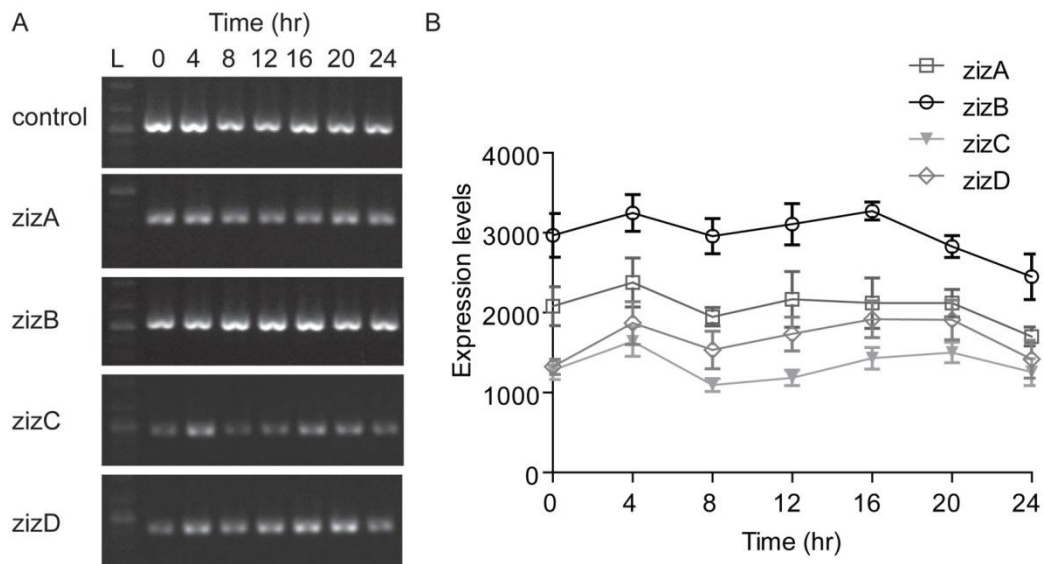


**Figure 5.1** *Dictyostelium* Zizimin gene expression throughout 24 hr development.

RNA samples were prepared from *Dictyostelium* cells during growth (0hr) or at 4hr intervals during development, with derived cDNA used to amplify specific *ziz* genes. (A) Agarose gel electrophoresis of *zizA–D* cDNA-derived PCR products throughout *Dictyostelium* development. *Ig7* was used as an expression control. (B) Quantification of the expression levels of *zizA–D* over 24hr development from three independent samples. L – Illustrates the 1kb ladder used as a molecular weight marker.

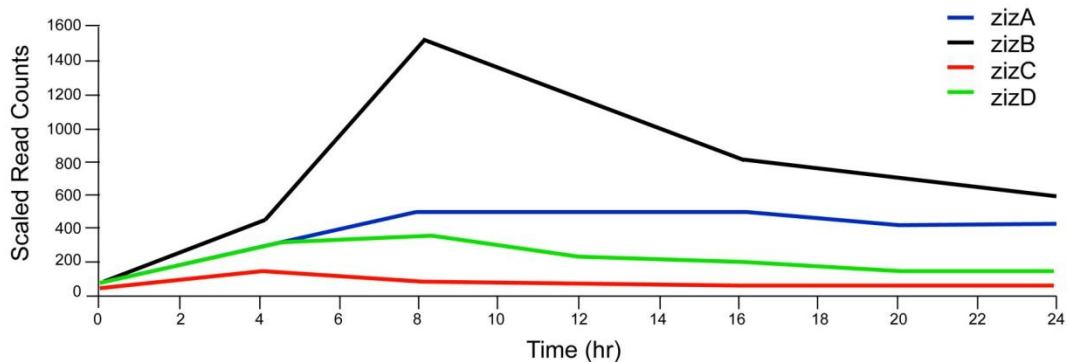


**Figure 5.2** RNA-Seq data for Zizimin A-D from DictyExpress.

The RNA-Seq database was used to illustrate the expression profile of the *Dictyostelium* Zizimin proteins (*zizA–D*) (<http://dictybase.org>). RNA-Seq data were collected from *Dictyostelium* at 4hr time intervals during development for each gene *zizA* (blue), *zizB* (black), *zizC* (red) and *zizD* (green).



### 5.3 Rescuing the developmental defects of *zizB* ablation

To assess whether the aberrant development of the *zizB*<sup>-</sup> cell line (shown in chapter 4) was due to defects caused by the ablation of the *zizB* gene, I reintroduced the full length *zizB* gene into the *zizB*<sup>-</sup> cell line. The full length open reading frames for *zizA* and *zizB* were tagged with C-terminal GFP (under the control of Actin 6 promoter) that were kindly provided by Douwe Veltman (Beatson Institute, Glasgow). In these experiments the ZizB-GFP construct was transformed into both wild type and *zizB*<sup>-</sup> cell lines producing *zizB*<sup>+</sup> and *zizB*<sup>-/+</sup> cell lines, respectively, and the ZizA-GFP construct was transformed only into wild type cells (producing *zizA*<sup>+</sup> cell line).

Developmental analysis of the Zizimin overexpression employed wild type, *zizA*<sup>+</sup>, *zizB*<sup>-</sup> (as shown in chapter 4), *zizB*<sup>+</sup> and *zizB*<sup>-/+</sup> cell lines which were starved on nitrocellulose membranes with the morphology recorded at 8hr, 13hr and 24hr. Cells overexpressing ZizA-GFP or ZizB-GFP did not show altered development, since these cell lines were able to produce mounds at 8hr, develop to a first-finger stage at 13hr and produced mature fruiting bodies at 24hr, similar to that in wild type cells. Furthermore, overexpression of ZizB-GFP was able to rescue the aberrant *zizB*<sup>-</sup> developmental morphology since the *zizB*<sup>-/+</sup> cell line was able to produce mounds, first fingers and mature fruiting bodies similar to wild type cells (**Figure 5.3**). These results confirm that the aberrant developmental morphology shown in the ZizB null cell line was caused by ablation of the *zizB* gene.

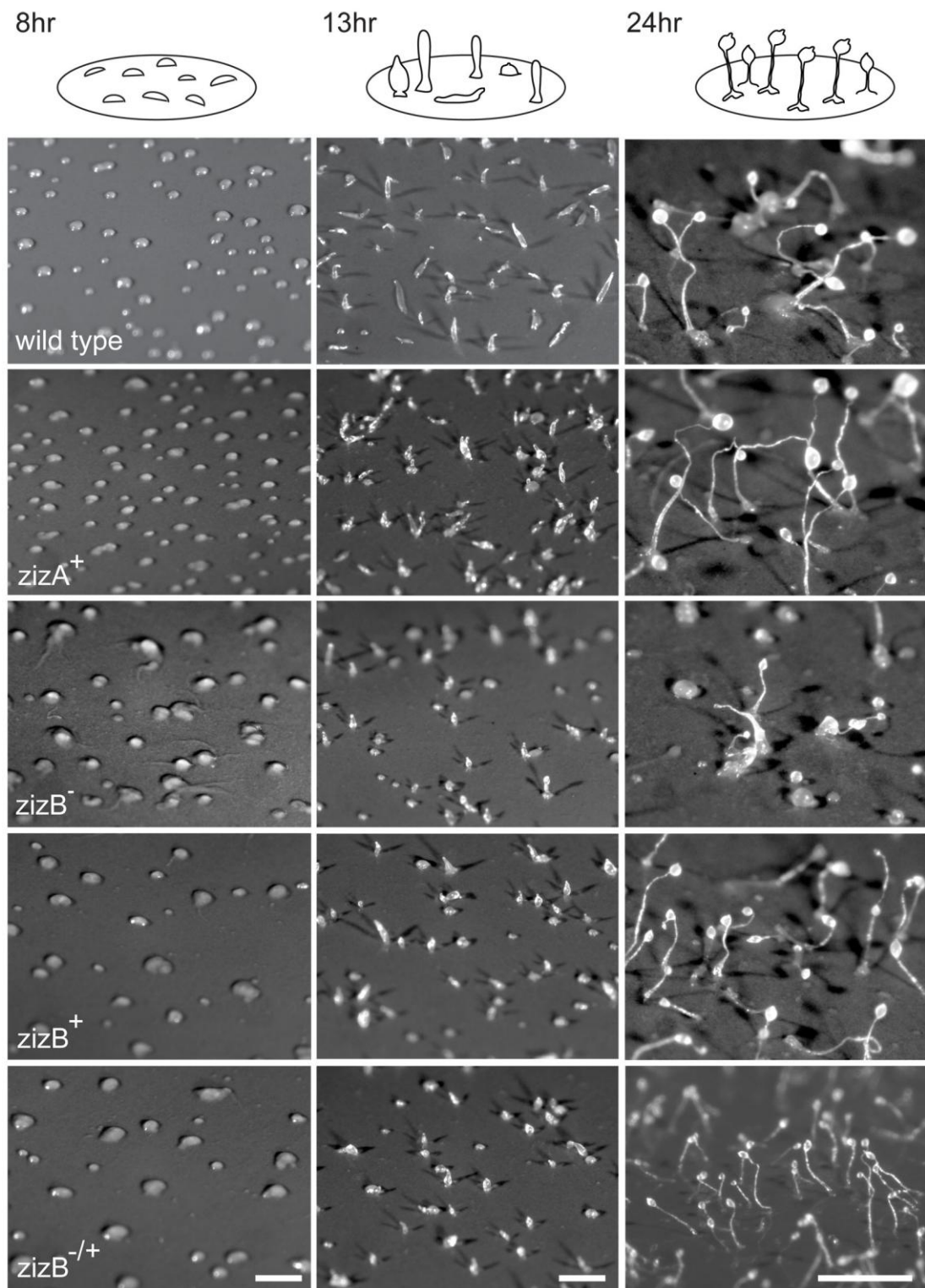


**Figure 5.3 Development of *zizA*<sup>+</sup> and *zizB*<sup>+</sup> cell lines.**

Schematic shows the developmental morphology of wild type cells at 8hr, 13hr and 24hr development. Wild type, *zizA*<sup>+</sup>, *zizB*<sup>-</sup> (as shown in chapter 4), *zizB*<sup>+</sup> and *zizB*<sup>-/+</sup> cell lines for were developed on a nitrocellulose membranes and visualised at 8hr, 13hr and 24hr development. Size bar represents 1mm.

## 5.4 Chemotaxis

During early development, cells release a chemoattractant (cAMP) to which surrounding cells migrate, leading to cell aggregation and initiation of the formation of multi-cellular fruiting bodies (Schaap and Wang, 1986). Since the *zizB*<sup>-</sup> cell line exhibited aberrant early development, I assessed whether these defects were caused by chemotaxis. In these experiments, the ability of the *zizA*<sup>-</sup> and *zizA*<sup>+</sup> cells and the *zizB*<sup>-</sup> and *zizB*<sup>+</sup> cells to chemotax along a cAMP gradient was investigated.

A cAMP gradient was applied to aggregation competent cells using a Dunn chamber. Image Pro6.3 software analysed individual cell movement, including directionality (illustrated by X-Y coordinate plots), velocity ( $\mu\text{m/s}$ ) and aspect (roundness). In these experiments, aspect refers to the ratio between the X and Y axes of a cell, whereby, a perfectly round cell will have an aspect of 1 and a more elongated polarized cell will have a number greater than 1. Cells lacking or overexpressing ZizA did not show altered chemotaxis compared to wild type Ax2 cells (**Figure 5.4, Table 5.1**). In contrast, cells lacking ZizB showed a significant loss in directionality, velocity and aspect (**Figure 5.5, Table 5.1**). The defect seen by *zizB* ablation was confirmed to be due to the loss of ZizB, since expression of the ZizB-GFP in the *zizB*<sup>-</sup> cell line (*zizB*<sup>-/+</sup>) was able to rescue this chemotactic defect (**Figure 5.5, Table 5.1**). Furthermore, the overexpression of ZizB did not show a significant defect in chemotaxis in wild type cell lines. A summary of the velocity and aspect results is shown for *zizA*<sup>-</sup>, *zizA*<sup>+</sup>, *zizB*<sup>-</sup>, *zizB*<sup>+</sup> and *zizB*<sup>-/+</sup> cells (**Table 5.1**).

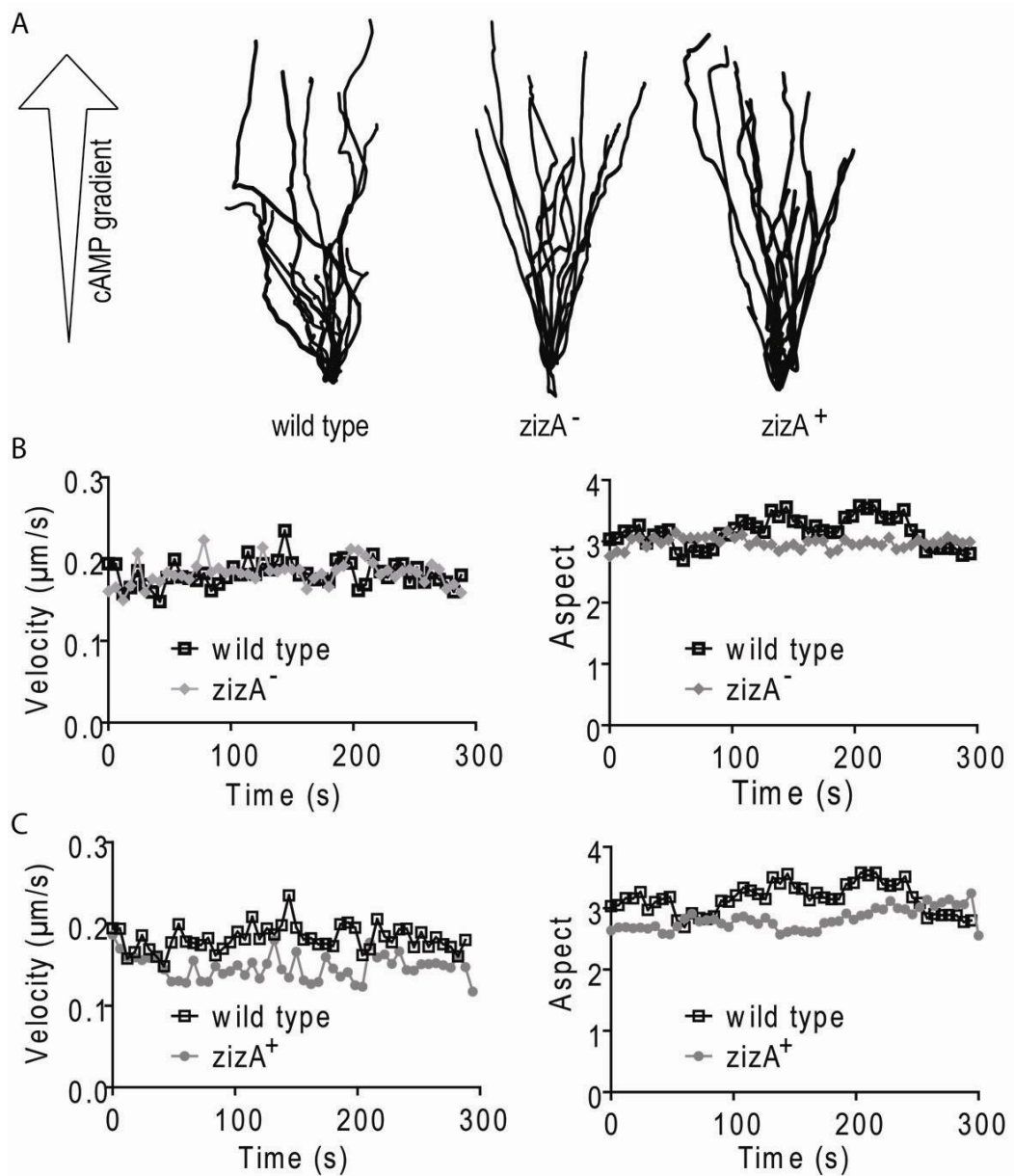


**Figure 5.4 Chemotactic effects of *zizA* ablation and overexpression.**

Aggregation competent *ZizA* null cells and cells overexpressing *ZizA*-GFP recorded using time lapse imaging over a 5min period (at 6 second intervals) in a Dunn Chamber towards cAMP (5μM). Computer-generated cell outlines using Image Pro6.3 software enabled recording of cell movement over this period. (A) X-Y coordinate plots (directionality) of the *zizA*<sup>-</sup> and *zizA*<sup>+</sup> cells compared to wild type Ax2 cells. (B - D) Analysis of the velocity (μm/s) and aspect (roundness) of the wild type Ax2 cells (black), *zizA*<sup>-</sup> and *zizA*<sup>+</sup> cells (grey), respectively. Statistical analysis was performed using a two-tailed unpaired student t-test (pre-test, Kolmogorov-Smirnoff, shows all data fits normal distribution). All experiments were performed at least in triplicate with an average of 25 cells analysed per experiment.

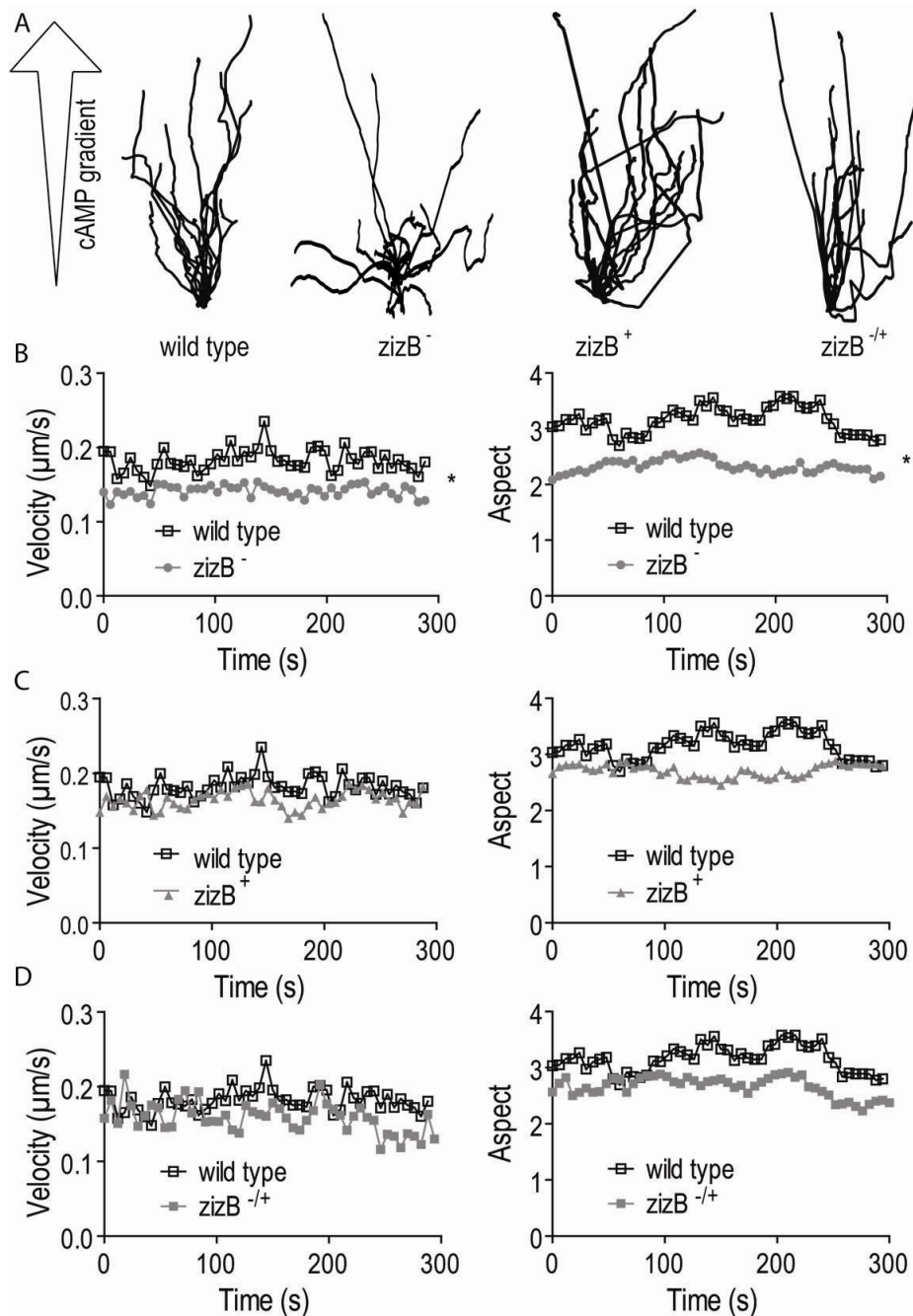


**Figure 5.5 Chemotactic effects of *zizB* ablation and overexpression.**

Aggregation competent *ZizB* null cells and cells overexpressing *ZizB*-GFP recorded using time lapse imaging over a 5 min period (at 6 second intervals) in a Dunn Chamber towards cAMP (5 μM). Computer-generated cell outlines using Image Pro6.3 software enabled recording of cell movement over this period. (A) X-Y coordinate plots (directionality) of the *zizB*<sup>-</sup> and *zizB*<sup>+</sup> cells compared to wild type Ax2 cells. (B - D) Analysis of the velocity (μm/s) and aspect (roundness) of the wild type Ax2 cells (black), *zizB*<sup>-</sup> and *zizB*<sup>+</sup> cells (grey), respectively. Statistical analysis was performed using a two-tailed unpaired student t-test (pre-test, Kolmogorov-Smirnoff, shows all data fits normal distribution). All experiments were performed at least in triplicate with an average of 25 cells analysed per experiment. \* P<0.05.

**Table 5.1 Summary of chemotaxis analysis**

Cell line	Velocity ( $\mu\text{m}/\text{min}$ )	Aspect
wild type	$10.92 \pm 0.12$	$3.16 \pm 0.03$
<i>zizA</i> <sup>-</sup>	$10.98 \pm 0.12$	$2.98 \pm 0.012$
<i>zizA</i> <sup>+</sup>	$9.48 \pm 0.42$	$2.83 \pm 0.03$
<i>zizB</i> <sup>-</sup>	$8.46 \pm 0.42$ *	$2.32 \pm 0.012$ *
<i>zizB</i> <sup>+</sup>	$9.84 \pm 0.72$	$2.71 \pm 0.112$
<i>zizB</i> <sup>-/+</sup>	$9.54 \pm 0.18$	$2.66 \pm 0.025$

Average velocity and aspect for the wild type, *zizA*<sup>-</sup>, *zizA*<sup>+</sup>, *zizB*<sup>-</sup> and *zizB*<sup>+</sup> cell lines during chemotaxis. Statistical analysis was performed using an unpaired two-tailed student t-test. All experiments were performed at least in triplicate with an average of 25 cells analysed per experiment. \* P < 0.05.

## 5.5 Cellular localisation of ZizA and ZizB

To visualise the cellular localisation of ZizA and ZizB, cells expressing ZizA-GFP or ZizB-GFP (producing *zizA*<sup>+</sup> and *zizB*<sup>+</sup> cell lines) were analysed. Full length expression of ZizA-GFP (285kDa) and ZizB-GFP (268kDa) was confirmed, where protein lysates from the *zizA*<sup>+</sup> and *zizB*<sup>+</sup> cell lines were separated by SDS-PAGE electrophoresis and analysed by Western blot analysis, using an anti-GFP antibody (**Figure 5.6**).

Using this approach, the expressed genes were clearly shown to be full length and showed little degradation. This enabled further analysis of cellular localisation and function. Live cell fluorescence imaging of ZizA-GFP and ZizB-GFP was used to determine the cellular localisation of each protein. ZizA-GFP showed a cytosolic localisation with enrichment in a structure adjacent to the nucleus (which resembled the microtubule organizing centre – MTOC) whereas ZizB-GFP showed enrichment at the cortex (**Figure 5.7**). Furthermore, the *zizB*<sup>+</sup> cells showed a marked increase in the number of filopodia per cell. Quantification of filopodia in wild type, *zizA*<sup>+</sup> and *zizB*<sup>+</sup> cell lines showed a highly significant 2-fold increase in filopodia formation in the *zizB*<sup>+</sup> cells (**Figure 5.8**).

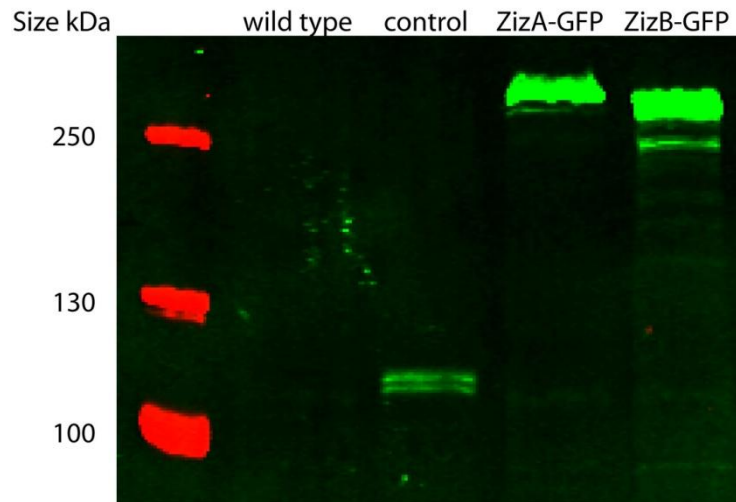


**Figure 5.6 Full length expressions of ZizA-GFP and ZizB-GFP.**

Full length protein expression was confirmed by Western blot analysis. The *zizA*<sup>+</sup> and *zizB*<sup>+</sup> cell lines, were lysed, separated on a SDS-PAGE gel and immunoblotted using an anti-GFP antibody, to identify full length expression of ZizA-GFP (~285kDa) and ZizB-GFP (~270kDa), respectively. Wild type and GFP control cell lysates (~120kDa) were used as controls.

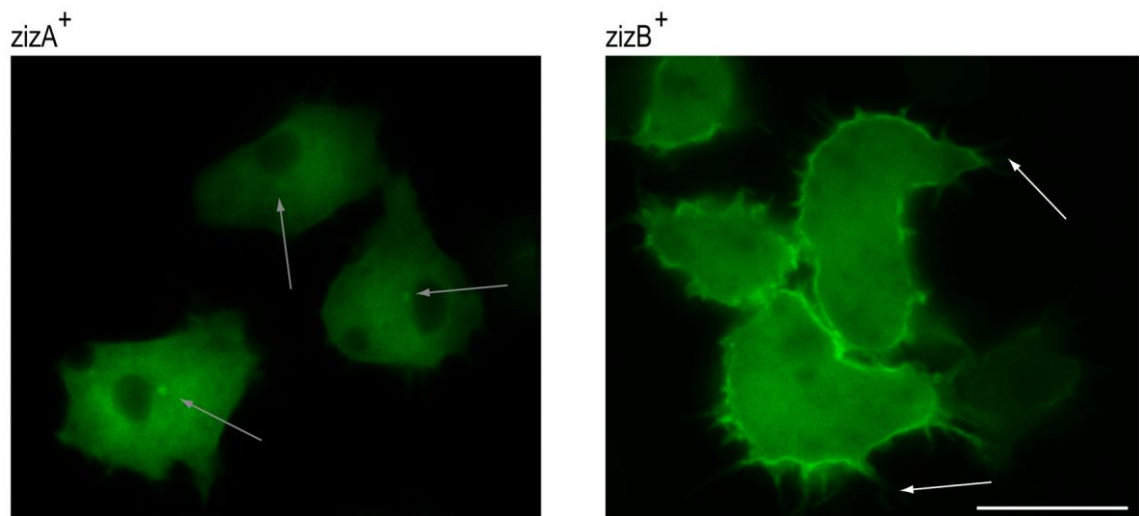


**Figure 5.7 Cellular localisation of ZizA-GFP and ZizB-GFP.**

Live cell imaging was used to visualise the cellular localisation of the ZizA-GFP and ZizB-GFP proteins in wild type cells overexpressing each gene (*zizA*<sup>+</sup> and *zizB*<sup>+</sup>, respectively). The ZizA-GFP protein shows cytosolic distribution with enrichment in a structure resembling the MTOC (indicated by the white arrows). The *zizB*-GFP show cytosolic distribution with enrichment at the cortex and gives rise to numerous filopodia (indicated by the white arrows). Size bar represents 10 $\mu$ m.



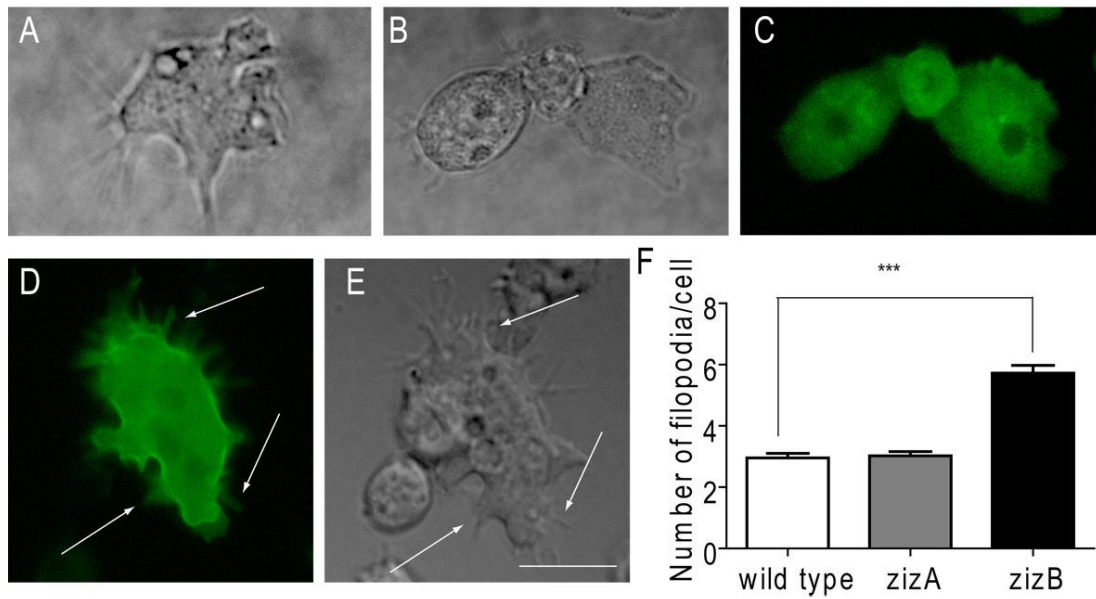


**Figure 5.8 Quantification of filopodia in *zizB*<sup>+</sup> cells.**

Live cell imaging was used to capture time lapse images of wild type, *zizA*<sup>+</sup> and *zizB*<sup>+</sup> cells, and the number of filopodia was counted at 3 time points over a 5 minute period. (A) Phase contrast image of wild type cells. (B & C) Images of *zizA*<sup>+</sup> cells in phase contrast and fluorescent views, respectively. (D & E) Images of *zizB*<sup>+</sup> cells in phase contrast and fluorescent views, respectively (arrows indicate the filopodia). (F) Illustrates the quantification of the number of filopodia for wild type, *zizA*<sup>+</sup> and *zizB*<sup>+</sup> cell lines. The average number of filopodia per cell (n=27) were analysed and compared using an unpaired, two tailed student t-test (\*\*\*)P <0.0001). Size bar represents 10µm.



## 5.6 Cytokinesis

Live cell imaging of the  $\text{zizB}^+$  cell lines showed a large number of cells which were undergoing cytokinesis. This cell behaviour was infrequently observed in wild type or  $\text{zizA}^+$  cells, suggesting a potential block in cytokinesis of the  $\text{zizB}^+$  cells. Furthermore, recording of these dividing cells often indicated aberrant formation of filopodia on the cleavage bridge (**Figure 5.9**). To investigate a role for Zizimin proteins in cell division, wild type,  $\text{zizA}^-$ ,  $\text{zizB}^-$ ,  $\text{zizA}^+$  and  $\text{zizB}^+$  cell lines were maintained in suspension culture for 3 days before being fixed with methanol and stained with 4',6-diamidino-2-phenylindole (DAPI), to count the number of nuclei per cell. From these experiments, ablation of each Zizimin protein ( $\text{zizA}^-$  and  $\text{zizB}^-$  cell lines) caused a significant increase in cells containing  $\geq 3$  nuclei compared to wild type cells (**Figure 5.10**). In contrast, overexpression of ZizA did not cause an increase in the number of nuclei per cell; however, overexpression of ZizB did cause a significant increase in cells with 2 and  $\geq 3$  nuclei and a significant decrease in cells with 1 nucleus (**Figure 5.11**).

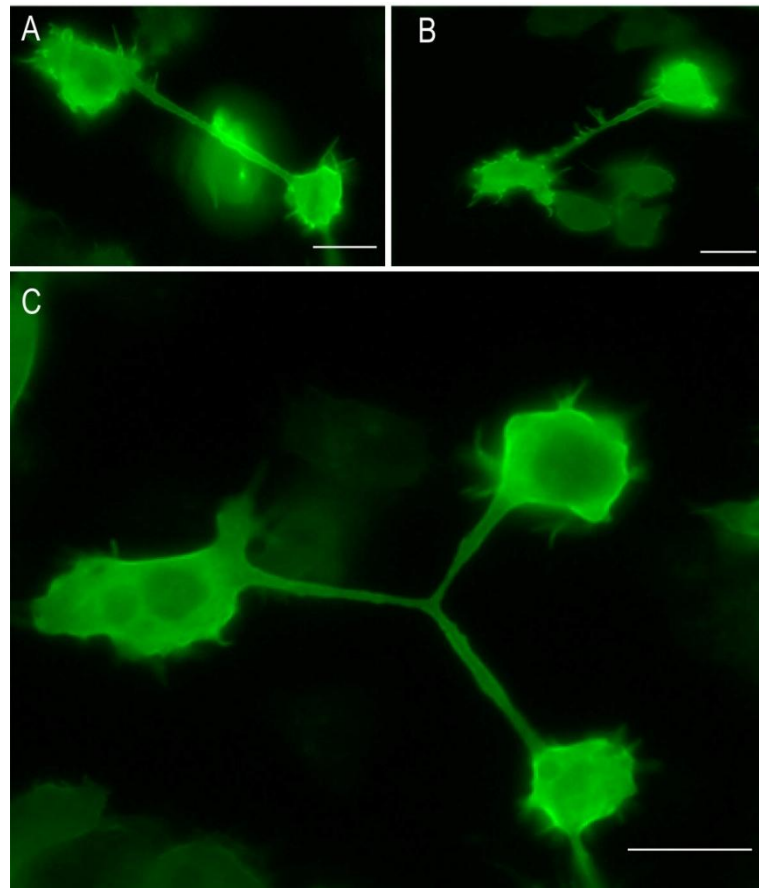


**Figure 5.9 Cytokinesis defect in cells overexpressing ZizB-GFP.**

Fluorescent images of live  $zizB^+$  cell line (expressing ZizB-GFP) during cytokinesis, suggesting a cytokinesis defect where (A & B) the cleavage furrow did not break or (C) where successive cell divisions did not lead to daughter cell separation. The presence of filopodia on the cleavage bridge is also shown in A and B. Size bars represents 10 $\mu$ m.

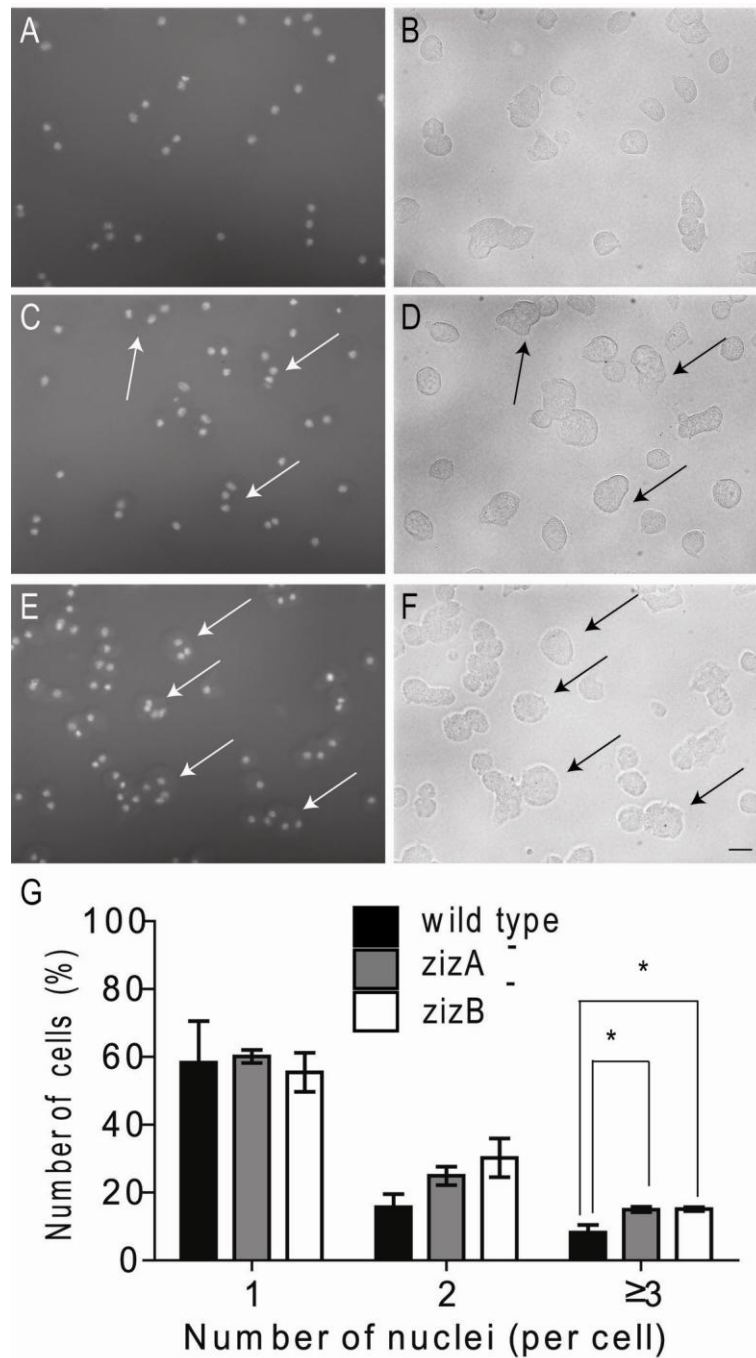


**Figure 5.10 Variation in nuclei number in cells lacking Zizimin activity.**

Wild type, zizA<sup>-</sup> and zizB<sup>-</sup> cell lines were grown in a shaking suspension for 3 days, fixed with methanol, stained with DAPI and nuclei per cell counted by fluorescent imaging (A, C, E) in comparison with cell number determined by phase contrast microscopy. (A & B) Wild type, (C & D) zizA<sup>-</sup> cells and (E & F) zizB<sup>-</sup> cells were analysed. (G) Quantification of cells with 1, 2 or ≥3 nuclei for wild type (black), zizA<sup>-</sup> (grey) and zizB<sup>-</sup> (white) cells. Experiments were performed at least in triplicate and averages of 400 cells were counted per experiment. \* P < 0.05. The size bar represents 10µm.

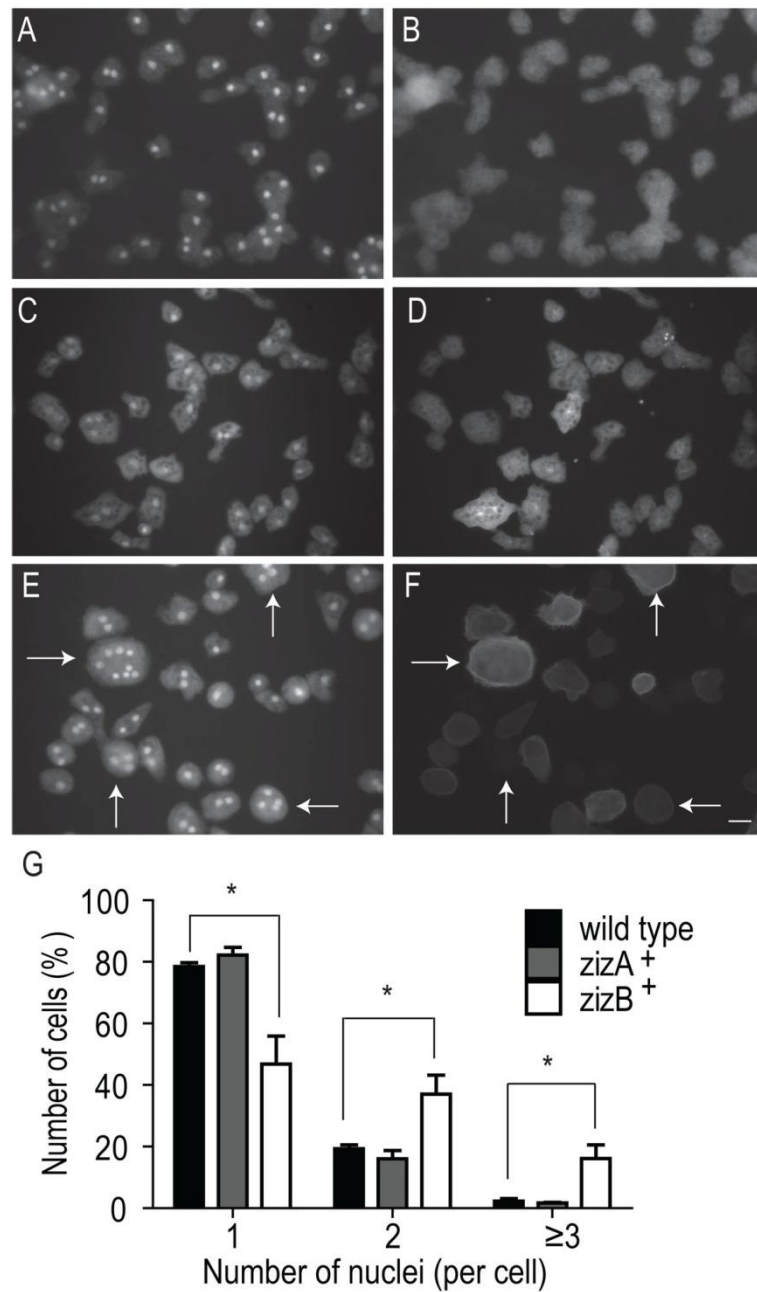


**Figure 5.11 Analysis of nuclei in Zizimin overexpressor cells.**

Wild type, *zizA*<sup>+</sup> and *zizB*<sup>+</sup> cell lines were grown in a shaking suspension for 3 days, fixed with methanol, stained with DAPI and nuclei per cell were counted by fluorescent imaging (A, C, E) in comparison with cell number determined by phase contrast microscopy. (A & B) Wild type, (C & D) *zizA*<sup>+</sup> cells and (E & F) *zizB*<sup>+</sup> cells were analysed. (G) Quantification of cells with 1, 2 or ≥3 nuclei for wild type (black), *zizA*<sup>+</sup> (grey) and *zizB*<sup>+</sup> (white) cells. Experiments were performed at least in triplicate and averages of 400 cells were counted per experiment. \* indicates P-value < 0.05. The size bar represents 10µm.

## 5.7 Growth

Since the  $zizA^-$ ,  $zizB^-$  and  $zizB^+$  cell lines showed a significant increase in the number of nuclei per cell, I analysed whether there was a decrease in the growth rate of these cells. Cells were inoculated in a shaking suspension (density of  $1 \times 10^5$  cells/ml) and counted at 24hr time intervals for 9 days. The  $zizA^-$  and  $zizA^+$  cell lines showed a significant decrease in growth rate at 168hr compared to wild type cells, whereby the doubling time increased to 18hr ( $zizA^-$ ) and 27hr ( $zizA^+$ ) compared to 12hr (wild type). Similarly, the  $zizB^-$  cell lines and the  $zizB^+$  cells showed a significant or highly significant decrease in growth rate at 168hr compared to wild type cells, where the doubling time increased to 16hr ( $zizB^-$ ) and 26hr ( $zizB^+$ ). Furthermore  $zizB^+$  cells had a lower saturation density ( $1.04 \times 10^7$  cells/ml) compared to wild type cells ( $1.56 \times 10^7$  cells/ml).

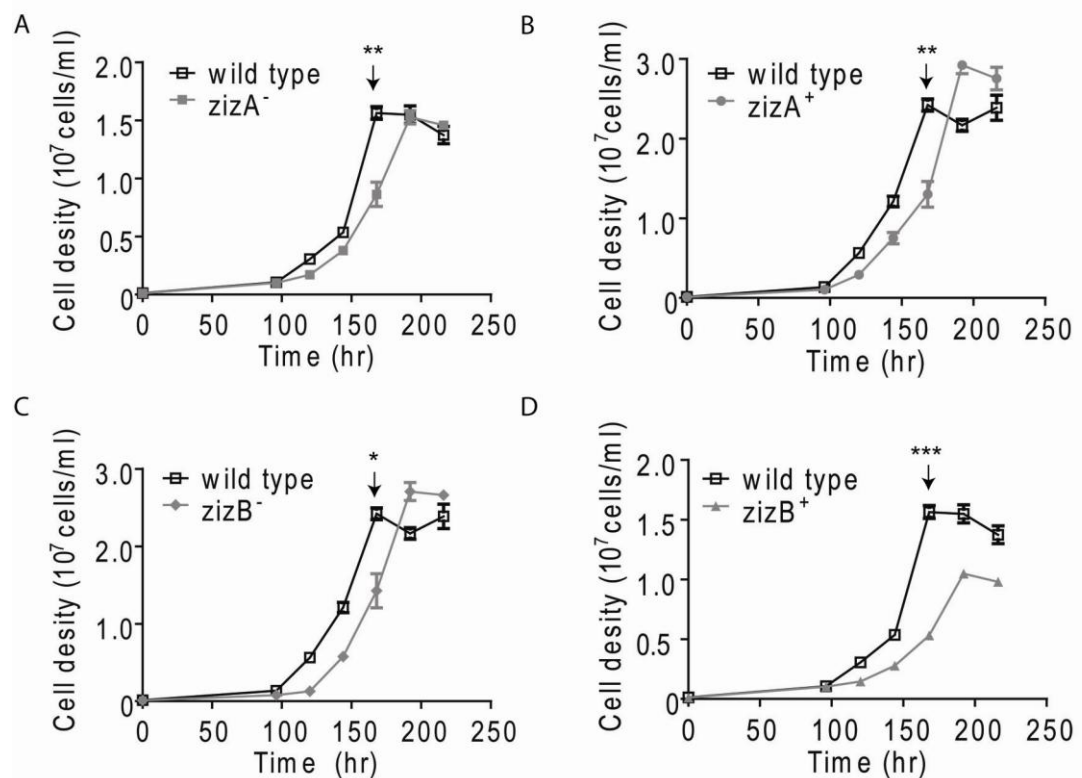


**Figure 5.12 Growth curve of cell lines lacking or overexpressing ZizA or ZizB.**

Wild type,  $zizA^-$ ,  $zizA^+$ ,  $zizB^-$  and  $zizB^+$  cell lines were grown in shaking suspension (from initial density of  $1 \times 10^5$  cells/ml) and counted at 24hr time intervals for 9 days. Cell density was statistically analysed for all experiments at 168hr compared to wild type. \*  $P < 0.05$ , \*\*  $P < 0.01$ , \*\*\*  $P < 0.001$ .

## 5.8 Stress

Hyperosmotic stress has been shown to involve actin cytoskeletal reorganisation through tyrosine phosphorylation of Signal Transduction and Activators of Transcription c (STATc) (Aizawa et al., 1999). In this process, both the signalling mechanism and the involved proteins remains unclear, thus, I examined a potential role for the Zizimin proteins in this response. In these studies, I first selected three genes previously shown to increase expression following cell exposure to stress: *yakA* (Pakes et al., 2011; Taminato et al., 2002), *gapA* and *rtoA* (Araki et al., 2003; Pakes et al., 2011). To confirm a stress-related increase in expression for these genes, wild type cells were pulsed with cAMP for 4hr and stressed for 30mins with either 200mM sorbitol (osmotic stress), 50 $\mu$ M dinitrophenol (DNP - oxidative stress) or at 33°C (heat stress). RNA was purified from osmotically stressed cells and analysed by reverse transcription PCR for changes in expression levels for each gene. In these experiments, RtoA showed a highly significant increase in expression and GapA and YakA showed a significant increase in expression compared to non-stressed control conditions (**Figure 5.13**). In comparison, treatment of cells with either heat or oxidative stress, gave rise to specific increases in gene transcription (**Figure 5.13**). Heat induced stress caused a 23% increase in RtoA transcription only, whereas treatment with DNP caused a 13% increase in YakA transcription only.

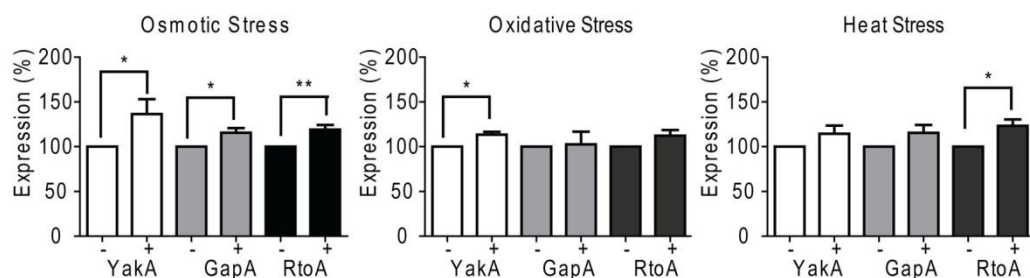


**Figure 5.13 Expression of *Dictyostelium* stress related genes following osmotic, oxidative and heat stress.**

Monitoring gene expression by reverse-transcriptase PCR for three stress-related genes; *yakA*, *gapA*, and *rtoA*, in presence (+) or absence (-) of the osmotic stress (200mM sorbitol), oxidative stress (50 $\mu$ M DNP) and heat stress (33°C) for 30mins. Results are shown as % expression compared to the control (100%) where  $n \geq 3$  independent experiments  $\pm$  SEM. \*  $P < 0.05$ , \*\*  $P < 0.01$ . Glycogen Synthase (*glcS*) was used as an expression control to normalise expression levels.

Since osmotic stress showed a significant increase in all three stress genes (Pakes et al., 2011) in wild type cells, the cell lines *zizA*<sup>-</sup>, *zizA*<sup>+</sup>, *zizB*<sup>-</sup> and *zizB*<sup>+</sup> were only analysed under these stress conditions. All cell lines were pulsed for 4hr and shaken in the presence (stress) or absence (non-stress control) of 200mM sorbitol for 30min. RNA was extracted and converted to cDNA using reverse transcriptase PCR. The cDNA was then analysed for changes in *yakA*, *gapA* and *rtoA* expression levels using PCR. The *zizA*<sup>+</sup> cell line only showed an increase in *GapA* expression levels compared to the control, thus, did not show the increase in expression levels of *yakA* and *rtoA* seen in osmotically stressed wild type cells. The *zizB*<sup>+</sup> cells showed a significant decrease in both *yakA* and *gapA* expression levels, compared to control, and did not show an increase in *rtoA* expression levels in response to osmotic stress. Thus, *ZizB* prevents the increase in *rtoA* expression levels seen in osmotically stressed wild type cells and significant reduction in *yakA* and *gapA* expression following exposure to osmotic stress. The *zizA*<sup>-</sup> and *zizB*<sup>-</sup> cell lines also did not show a significant increase in expression of any of the stress genes, clearly showing that *Zizimins* are required for osmotic stress gene induction.

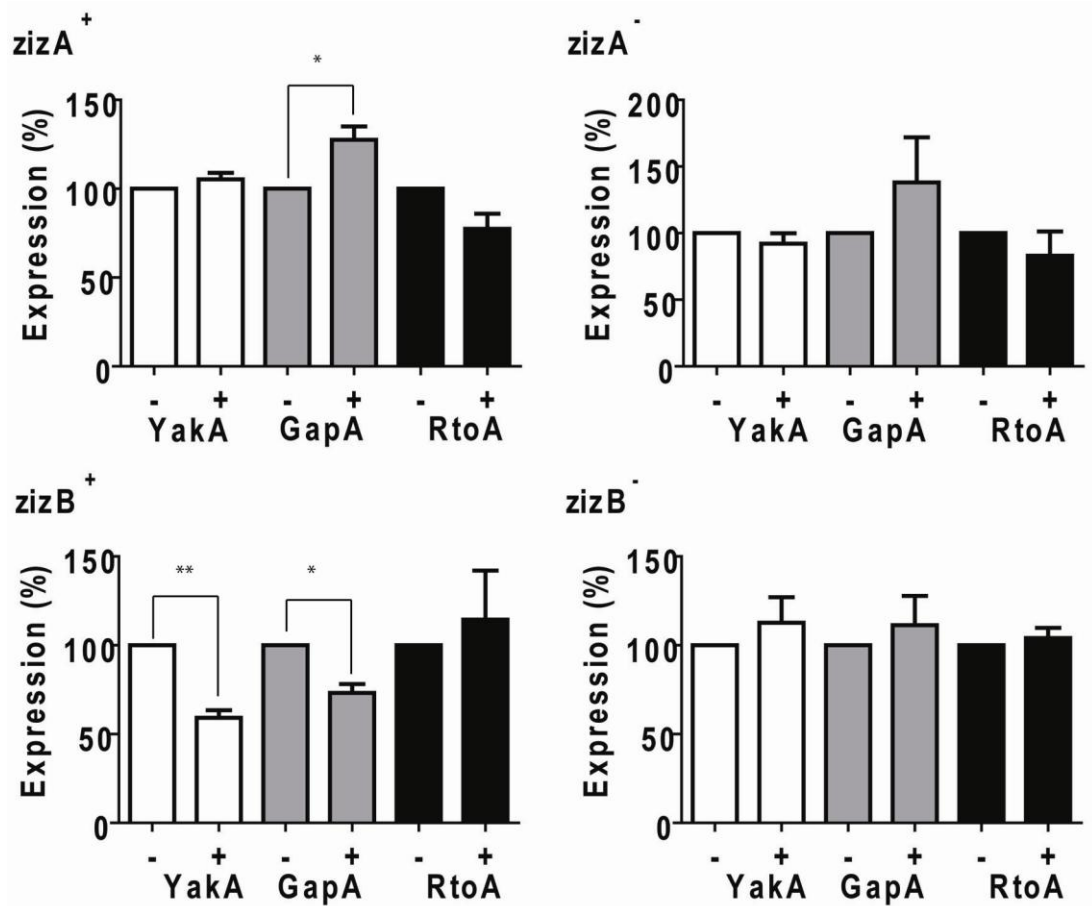


**Figure 5.14 Osmotic stress response of cells lacking or overexpressing ZizA or ZizB.**

Expression of *Dictyostelium zizA*<sup>+</sup>, *zizA*<sup>-</sup>, *zizB*<sup>+</sup> and *zizB*<sup>-</sup> cell lines were analysed in presence (+) or absence (-) of osmotic stress (200mM sorbitol) for 30mins. Gene expression was analysed by extracting RNA and converting it into cDNA by reverse-transcriptase PCR. The expression levels of three stress-related genes; *yakA*, *gapA*, and *rtoA*, were analysed by PCR, and quantified using Quantity One software. Results are shown as % expression compared to the control (100%) where  $n \geq 3$  independent experiments  $\pm$  SEM. \* indicates P-value < 0.05, \*\* indicate P-value < 0.01. Glycogen synthase (*glcS*) was used as an expression control to normalise expression levels.



## 5.9 Discussion

### 5.9.1 Expression levels

Since ZizB null cells showed a defect in development, I investigated the change in expression levels of the four Zizimin proteins (ZizA-D) over the 24hr developmental cycle. All the *Dictyostelium* Zizimin proteins showed expression throughout development; however, ZizB potentially had the highest expression levels. Reverse transcriptase PCR is a semi-quantitative analysis, thus, only indicates the overall trends of expression levels. The RNA-Seq database showed a slightly different expression profile where ZizA, ZizC and ZizD showed expression throughout development, however, ZizB showed increasing expression levels that peaked at 8hr. These discrepancies would need to be clarified by quantitative PCR, however, both these experiments show that ZizA and ZizB are expressed throughout development and ZizB could potentially be developmentally regulated.

Developmentally regulated gene expression has been shown in other *Dictyostelium* GEF proteins such as the putative RacGEF, GxcDD, which showed expression increasing throughout development, peaking at 9hr (Mondal *et al.*, 2007). GxcDD null cells also showed aberrant morphology in early development with defects in streaming and delays in development by 4hr (Mondal *et al.*, 2007; Shaulsky *et al.*, 1996). Trix is a RacGEF protein that bundles actin filaments and has also shown developmentally regulated gene expression, where the expression levels increase up to 9hr, however, there is a marked decrease in later development (Strehle *et al.*, 2006). PakA is another Rho GTPase regulator that has shown developmental up-regulation in the aggregate and multi-cellular stages (Chung and Firtel, 1999). Furthermore, mammalian Zizimin1 also shows developmental regulation and gradually increases in the rat brain (hippocampal neurons) (Kuramoto *et al.*, 2009). The developmental expression profile of these examples is similar to that seen with zizB, suggesting a specific role for zizB in early development and chemotaxis.

### 5.9.2 Development and chemotaxis

To confirm that the developmental defects caused by ZizB ablation were indeed through loss of this protein, a ZizB-GFP construct was expressed in

ZizB<sup>-</sup> cell lines. Complementation of ZizB-GFP in the zizB<sup>-</sup> cells was able to reverse the phenotype seen in development since no delay in early development (8hr and 13 hr) was seen and cells were able to produce mature fruiting bodies at 24hr. Therefore, ZizB was responsible for this aberrant morphogenesis and has an important role in early development. The ZizB protein did not catalyse a rate limiting step in development since expression of this protein in wild type cells had no effect on development. Similarly, wild type cells overexpressing ZizA (zizA<sup>+</sup> cells) did not show altered development. Since zizA<sup>-</sup> and zizA<sup>+</sup> cells did not show developmental defects, this suggests that they do not play a role in development, or have a role that can be compensated for by other similar GEF proteins (as explained in chapter 4).

Chemotaxis is an important process during early development. Therefore, to assess whether developmental defects were due to alterations in cell migration, I analysed chemotaxis in the ZizA and ZizB (null and overexpressing) cell lines. The zizA<sup>-</sup> and zizA<sup>+</sup> cells did not show any chemotactic defects, since there was no change in directionality, velocity or aspect compared to wild type cells. In contrast, the zizB<sup>-</sup> cells showed a significant decrease in velocity and aspect as well as displaying directionality defects (as indicated by the X-Y plots). As for development, the zizB<sup>+</sup> cells did not demonstrate significant chemotactic defects compared to wild type cells.

These data suggest that the effect of *zizB* ablation on *Dictyostelium* development may be caused by altered chemotaxis or regulation of critical signalling pathways necessary for both processes. A number of *Dictyostelium* GTPase signalling molecules have been shown to have morphological and cell migration defects as seen in ZizB deficient cells. Constitutively active Rac1b and RacGap1 null cells show inefficient directionality (inability to maintain linear direction) and defective chemotaxis including a 50% reduction in speed (Chung et al., 2000). It was shown that this reduction in speed was due to uncontrolled activation of F-actin assembly. Furthermore, dominant negative forms of Rac1b (and Rac1a and Rac1c) also caused major chemotactic defects, whereby cells failed to polarise and did not chemotax (Dumontier et al., 2000). RacGEF1 and RacB null cells show strong morphogenic and cell motility defects, also with a 50% reduction in chemotactic ability and F-actin polymerisation (Park *et al.*, 2004). RacG was found to promote F-actin polymerisation; therefore, cells

lacking RacG displayed reduced migration speed and directionality, where as cells expressing constitutively active RacG present severe motility defects (Somesh *et al.*, 2006).

A significant decrease in aspect suggests the ZizB null cells were not as elongated and polarised compared to wild type cells. Cellular polarisation in response to cAMP stimulation is important in chemotaxing cells as it initiates a series of signalling pathways which drive cell movement in the direction of the chemoattractant. This process involves dynamic reorganisation of the actin and microtubule cytoskeleton (Charest and Firtel, 2007; Fukata *et al.*, 2003; Watanabe *et al.*, 2004). F-actin polymerisation acts as the driving force behind cell movement, however, the interplay between actin and the microtubule network is important in stabilising the cell during migration due to the dynamic nature of the leading edge (Fukata *et al.*, 2003; Watanabe *et al.*, 2004).

From these studies it is clear that the actin cytoskeleton is important in defining cell shape and morphology as well as coordinating cellular behaviour such as cell movement. GTPase signalling is involved in regulating F-actin assembly thus initiating cell movement (Chung *et al.*, 2000). Since Zizimin proteins are known to regulate small GTPases in mammalian cells, it is possible that ZizB is regulating a Rac protein involved in development and chemotaxis. Zizimin GEFs function by catalysing the hydrolysis of GTPases, causing GDP to dissociate from the binding pocket, allowing GTP to bind. The absence of ZizB would therefore leave the target GTPase unable to rebind GTP and carry out its function. Hence, F-actin would not be polymerised by the target Rac and motility would be affected.

### 5.9.3 Localisation

To identify the cellular localisation of ZizA in *Dictyostelium*, ZizA-GFP was transformed into wild type cells and visualised using live cell fluorescence. ZizA-GFP showed cytosolic localisation with enrichment in a structure which resembled the MTOC; this was further confirmed by our collaborators through co-localisation with  $\alpha$ -tubulin (Pakes *et al.*, 2012). Microtubules are nucleated and organised by the MTOC, where the (-) end is anchored to the MTOC and new ( $\alpha$  and  $\beta$ ) tubulin monomers are added to the (+) end causing microtubule growth. In migrating cells, the MTOC reorganises its orientation towards the

leading edge through microtubule stabilisation, although, the exact mechanism remains unclear (Gundersen and Bulinski, 1988; Palazzo et al., 2001; Ueda et al., 1997).

A role for ZizA in the MTOC may be suggested through related studies in migrating fibroblasts. In these studies, the reorganisation of the MTOC has been shown to be stimulated through lysophosphatidic acid (LPA) serum, which also increased Cdc42-GTP levels (Palazzo *et al.*, 2001). Since Zizimins are known to regulate Rho small GTPases, it is possible that ZizA is involved in the subsequent regulation of the Rho GTPase responsible for MTOC reorganisation in *Dictyostelium*.

The cellular localisation of ZizB-GFP was cytosolic with enrichment at the cortex. This cortical association provides support for a role in actin regulation, since, this localisation is a feature of a number of Rac proteins such as RacB, RacF1, RacE, RacC, Rac1a and Rac1b, all of which have been shown to regulate the actin cytoskeleton (Dumontier et al., 2000; Larochelle et al., 1996; Palmieri et al., 2000; Park et al., 2004; Rivero et al., 1999a; Seastone et al., 1998). DGAP1 is an IQGAP related protein that localises to the cortex. GAP proteins have the opposite function of GEF proteins and inactivate GTPases by increasing the rate of GTP hydrolysis. DGAP1 null cells have an increase in F-actin and filopodia formation and have been shown to directly bind Rac1a. Since the absence of DGAP1 increases the activity of Rac1a in polymerising F-actin and filopodia formation, ZizB could be functioning as the Rac1a GEF since the overexpression has a similar profile to the DGAP1 null mutant.

Despite the absence of a characterised PH domain, the DHR1 domain has been shown to be involved in lipid binding and with increased specificity for PIP<sub>3</sub> (Cote et al., 2005; Kobayashi et al., 2001), however, the exact function of the domain remains unclear. PIP<sub>3</sub> accumulates at the leading edge of migrating cells and is degraded at the rear by Phosphatase and Tensin homologue (PTEN), creating a PIP<sub>3</sub> gradient. PIP<sub>3</sub> accumulation initiates the rapid translocation of PH domain proteins that are involved in actin reorganisation at the leading edge (Cote *et al.*, 2005). However, all Dock family proteins contain the characteristic DHR1 domain, although, not all these proteins have membrane association (as seen in *Dictyostelium* ZizA).

*Dictyostelium* Zizimins do not have a characterised PH domain, as present in the DH-PH GEF proteins and the mammalian Zizimins. PH domains are associated with membrane localisation (Baumeister et al., 2006; Falasca et al., 1998; Lemmon et al., 2002). A novel N-terminal PH domain has been identified in mammalian Zizimin-related DOCK proteins (Dock6-8) (Cote and Vuori, 2006), which were previously thought to not have a PH domain. In this study, Dock8 was characterised in non-stimulated porcine aortic endothelial cells expressing human PDGF  $\beta$ -receptor (PAE/PDGFR $\beta$ ) cells, where it localised in the cytosol with accumulation at the edges of lamellipodia protrusions (Ruusala and Aspenstrom, 2004). Here, the authors proposed a novel N-terminal PH domain. Therefore, it is possible that there is an uncharacterised PH domain present in the *Dictyostelium* Zizimins, since ZizB localises to the cortex.

Overexpression of ZizB (in zizB<sup>+</sup> cells) also showed a significant increase in the number of filopodia per cell compared to wild type cells as found in Rac overexpression and related proteins. Filopodia are finger-like actin driven protrusions from the surface of the cell that are involved in sensing the environment. These filopodia extend from the tip by actin assembly and are stabilised by parallel bundles of actin filaments (Faix and Rottner, 2006; Medalia et al., 2007). The increase in filopodia formation has been shown in a number of other *Dictyostelium* GTPase signalling molecules such as constitutively active Rac1 mutants (Dumontier et al., 2000; Medalia et al., 2007) and other actin assembly regulating molecules such as VASP. The VASP protein is thought to form a complex with WASP to stimulate actin assembly and filopodia formation (Han et al., 2002; Medalia et al., 2007). In mammalian systems Cdc42 signalling, which has been shown to be specifically regulated by Zizimin proteins, is involved in filopodia formation (Kozma et al., 1995; Meller et al., 2002; Nishikimi et al., 2005; Nobes and Hall, 1995). Expression of human Cdc42 in *Dictyostelium* induced numerous filopodia at the centre of the cell compared to wild type (Lee and Knecht, 2001). In fibroblasts, overexpression of the Cdc42 activating proteins, Zizimin1 (p220), showed increased filopodia formation (and microspike production) compared to wild type cells (Lin et al., 2006).

Overexpression of the *Dictyostelium* Dock-180 related proteins showed an increase in filopodia formation (Para et al., 2009). DocD elevated filopodia

similar to that of ZizB, and it was also shown to bind Rac1a, and accumulate at the leading edge of migrating cells (Para *et al.*, 2009). Altering the expression of molecules that regulate F-actin assembly, such as Rac1a, VASP and WASP, also increases filopodia production through an increase in F-actin polymerisation (Faix and Rottner, 2006; Lebrand *et al.*, 2004). Therefore, these data provided here are consistent with a role for ZizB in filopodia formation. Stimulation of Rac1a, if overexpressed, leads to an increase in F-actin polymerisation.

The cellular localisation of ZizA and ZizB, during chemotaxis and random cell movement, as well as global cAMP stimulation, has been investigated by our collaborators (Pakes *et al.*, 2012). Here we showed that ZizA localisation did not change during chemotaxis, random cell movement and global stimulation where it remains in the cytosol with enrichment in the MTOC. In contrast, ZizB localised to the front and sides of the cell and is excluded at the rear during chemotaxis and random cell movement. Furthermore, global stimulation with a single pulse of 1 $\mu$ M cAMP leads to transient removal of ZizB from the cortex to the cytosol and then returned back to the cortex 8 seconds after stimulation. This was unexpected, since the exact opposite behaviour is shown by both *Dictyostelium* Dock proteins (Para *et al.*, 2009) and other previously described RacGEF proteins such as DRG (Knetsch *et al.*, 2001) and RacGEF1 (Park *et al.*, 2004), in which there is rapid translocation to the cortex. A possible explanation for this movement would be a cortex-stabilising mechanism for ZizB, between cyclic periods of reorganisation caused by cAMP waves during chemotaxis. This is consistent with ZizB localisation at the front and side of the cell with exclusion from the trailing edge or retracting pseudopods, during both random cell movement and in chemotaxis. This localisation is distinct to proteins involved in initiating cell movement that are enriched at the leading edge (regulating and driving F-actin polymerisation) (Han *et al.*, 2006). Cortical localization may occur through DHR1 (phospholipid binding) activity, but domain-specific localization studies would be needed to confirm this.

#### **5.9.4 Cytokinesis and growth**

Live cell imaging showed zizB<sup>+</sup> cells were more commonly seen in cytokinesis, where multiple cells remained attached at the cleavage furrow and in some cases formed filopodia on the cleavage bridge. The potential block in

cell division was confirmed by examining the number of nuclei per cell, where  $\text{zizB}^+$  cells had a significant increase in multinucleate cells ( $\geq 3$  nuclei per cell) and a decrease in the number of cells with single or double nuclei compared to wild type cells. In contrast,  $\text{zizA}^+$  cell lines did not show a significant increase in the number of nuclei per cell compared to wild type. Examination of the number of nuclei in the  $\text{zizA}^-$  and  $\text{zizB}^-$  cell lines also showed a significant increase in multinucleate cells ( $\geq 3$  nuclei per cell). An empty vector transformed cell line should have been used as a control, since this may give rise to the observed phenotype. However, transformant expressing  $\text{zizA}^+$  cells did not show an increase in the number of nuclei, thus supporting the conclusion that  $\text{zizB}^+$ ,  $\text{zizA}^-$  and  $\text{zizB}^-$  cells had a significant increase in multinucleate cells.

Cell division is based on the coordinated activities of the microtubule and actin microfilament systems. This interaction between the microtubules and the actin cortex is important for actin to form the cleavage furrow in the correct place (Neujahr *et al.*, 1998). Cytokinesis occurs in the final stages of cell division where the cytoplasm is constricted and daughter cells separate and this is controlled via the regulation of the actin cytoskeleton. In mammalian cells, Rho small GTPases have a key role in cell division and cytokinesis (Kishi *et al.*, 1993; Mabuchi *et al.*, 1993). In HeLa cells constitutively active Cdc42 led to the formation of giant multinucleate cells (as well as cortical actin microspikes) (Dutartre *et al.*, 1996).

In *Dictyostelium*, RacE was the first Rho GTPase to show essential functions in cytokinesis, since ablation of RacE severely impaired cytokinesis (Gerald *et al.*, 1998; Larochelle *et al.*, 1996; Vithalani *et al.*, 1996). However, a number of other GTPases signalling molecules have defects in cell division and cytokinesis such as Rac1a/b/c constitutively active and dominant negative mutants (Dumontier *et al.*, 2000), as well as RacB and RacC (Rivero *et al.*, 2002) which all cause an increase in the number of multinucleate cells in a population. Among these, Rac1a plays a major role in cytokinesis since it regulates the rigidity of the cortical actin cytoskeleton through IQGAP and the actin-bundling protein, cortexillin (Faix, 2002).

A range of other proteins have been identified to cause a multinucleate phenotype on ablation, which provides clues to the pathways implicated in this

process. A similar cytokinesis defect was found in the dynamin A null strain which showed the cells unable to cleave the cytoplasmic bridge during the final stage of daughter cell separation (Gopaldass et al., 2012; Wienke et al., 1999). Ablation of both the *Dictyostelium* cortexillins (I and II) causes severe cytokinesis defects similar to that seen in the ZizB overexpressor and DynA knockout cell lines (Faix et al., 1996; Faix, 2002; Pakes et al., 2012; Wienke et al., 1999). Cortexillin is an actin bundling protein essential for cytokinesis (Faix et al., 1996; Faix, 2002). Cells lacking RhoGDI are multinucleate, have slow growth and interaction studies show RhoGDI binds to Rac1a, RacB, RacC and RacE, all of which have cytokinesis defects (Rivero et al., 2002). Rho GDP-dissociation inhibitor (RhoGDI) is a negative regulator of Rho small GTPases, inhibiting the dissociation of GDP, thus keeping the GTPases in the inactive state (Rivero et al., 2002). Since mammalian Zizimins regulate Cdc42, which has a role in cytokinesis, and regulators of the *Dictyostelium* small GTPases involved in cytokinesis (Rac1a, RacB, RacC, and RacE), have also shown defects in daughter cell separation and multinucleate cells, it is possible that ZizA and ZizB plays a role in cytokinesis through the regulation of one or more of these *Dictyostelium* Rac proteins, thus, regulating the actin/myosin dynamics essential in cell division.

To test whether the ZizA and ZizB proteins also showed growth defects, zizA<sup>+</sup>, zizA<sup>-</sup>, zizB<sup>+</sup> and zizB<sup>-</sup> cells were grown in a shaking culture for 9 days. The zizA<sup>+</sup>, zizA<sup>-</sup> and zizB<sup>-</sup> cells showed a significant delay in growth rate after 168hr, however, the zizB<sup>+</sup> cells had a highly significant decrease in growth and reached a lower saturation density compared to wild type cells. The zizA<sup>+</sup>, zizA<sup>-</sup> and zizB<sup>-</sup> cell lines all show an apparent delay in growth, however, they were all able to reach a saturation density common to wild type cells. Thus, more experiments would be necessary to define growth defects. In contrast, zizB<sup>+</sup> clearly shows a delay in growth and a decrease in saturation density compared to wild type cells.

RhoGDI knockout cell lines, which exhibit cytokinesis defects (as described above), were also shown to have a prolonged doubling time and a lower saturation density compared to wild type cells (Rivero et al., 2002). Rac1b constitutively active and dominant negative mutants show a 40-50% reduction



in growth rate (Palmieri *et al.*, 2000). Since the ZizA and ZizB null cells and ZizB overexpressor cells have a cytokinesis defect it is not surprising that they also show reduced growth rate. One potential mechanism for the role of ZizA and ZizB in growth (and cytokinesis) could be through Rac1 regulation, since Rac1b (and RhoGDI, a Rac1 regulating protein) showed both cytokinesis and growth defects. However, this does not preclude the possibility that ZizA or ZizB could have a role in both cytokinesis and growth via the regulation of another Rac which has shown cytokinesis defects (RacB, RacC and RacE), however, the growth rate in these mutants has yet to be explored.

### 5.9.5 Stress response

Hyperosmotic stress increases the expression of the previously reported stress-related genes, *yakA* (Pakes *et al.*, 2011; Taminato *et al.*, 2002), *gapA* and *rtoA* (Araki *et al.*, 2003; Pakes *et al.*, 2011) in wild type cells. However, oxidative and heat stress only caused an increase in gene expression, for *yakA* and *rtoA*, respectively. Since hyperosmotic stress caused an increase in transcription levels of all three stress-related genes, this stress condition was used to analyse stress-gene induction in cells lacking or overexpressing ZizA or ZizB. In these experiments, the *zizA*<sup>+</sup> cells still showed an increased *gapA* expression in response to osmotic stress, however, these cells showed a decrease in gene expression of *yakA* and *rtoA*. The *zizB*<sup>+</sup>, *zizA*<sup>-</sup> and *zizB*<sup>-</sup> cells all showed a decrease in expression of *yakA*, *gapA* and *rtoA* in response to osmotic stress. In the case of *zizB*<sup>+</sup> cells, there was a significant decrease in these expression levels for *yakA* and *gapA* compared to the non-stressed control cells.

*Dictyostelium* cells respond to hyperosmotic stress by reorganising the actin cytoskeleton, through tyrosine phosphorylation of STATc (Aizawa *et al.*, 1999). STATc rapidly translocates to the nucleus in response to osmotic stress, inducing an increase in *gapA* and *rtoA* transcription through JAK/STAT signalling (Araki *et al.*, 2003; Na *et al.*, 2007). The *gapA* and *rtoA* genes are regulated at two levels, since they display semi-constitutive activity during growth and development and are super-inducible, above this level, through hyperosmotic stress (Araki *et al.*, 2003). GapA is a RasGAP-related protein that is needed for normal cytokinesis through Rac1a and cortexillin interaction

(Mondal et al., 2010; Sakurai et al., 2001). RtoA catalyses the fusion of phospholipid vesicles and is involved in the cell cycle-phase-dependent mechanism that regulates initial cell type choice in developing *Dictyostelium* (Wood et al., 1996). The exact mechanism of how STATc induces *gapA* and *rtoA* increases in gene expression in response to osmotic shock is unclear. However, in mammalian vascular smooth muscle cells (SMC) Rac activity and subsequent generation of reactive oxygen species are necessary for activating tyrosine phosphorylation of JNK and STAT-dependent transcription (Pelletier et al., 2003). Expression of constitutively active Rac1 activated Jak2 and STAT-dependent transcription (Pelletier et al., 2003), suggesting that ZizA and ZizB proteins block the signalling of the STAT/JNK pathway through Rac1 regulation, thus, STATc can no longer increase *gapA* and *rtoA* expression. Dysregulation of Zizimin activity (through cells lacking and overexpressing ZizA and ZizB) would be expected to change Rac1 levels by increasing or decreasing the cycling of Rac1 between the active and inactive state. This model would need to be analysed to identify changes in the STATc phosphorylation in the ZizA and ZizB cell lines.

In *Dictyostelium*, YakA is a kinase essential for the transition from growth to development and mediates the response to starvation by inducing a growth arrest, decreasing vegetative mRNA expression and increasing *pkaC* expression, thus, increasing catalytic PKA activity (Souza et al., 1998; Souza et al., 1999; Taminato et al., 2002). Increasing the production of the PKA-C subunit induces the increase in expression of *acaA* (adenylate cyclase) and *carA* (cAMP receptor) (Schulkes and Schaap, 1995), which are all necessary to initiate early development. Moreover, YakA couples nutrient sensing to the initiation of development (Souza et al., 1998), which was proposed to be through RasG signalling, a small GTPase involved in controlling the growth to development transition (Khosla et al., 1996). *Dictyostelium* cells respond to stress through rapid reorganisation of the actin cytoskeleton, a process which is known to be regulated through Rac signalling. Therefore, it is possible that ZizA and ZizB could regulate the Rac small GTPase, which could in turn regulate YakA, since the absence of ZizA and ZizB causes a block in the increase of YakA under stress conditions. However, this relationship would need to be explored further.

## 5.10 Summary

In this chapter, the cellular roles of ZizA and ZizB were explored through assessing changes in a number of cellular functions following ablation or overexpression of ZizA and ZizB. ZizA was shown to be constantly expressed throughout development and did not exhibit any developmental or chemotactic defects. However, ZizA ablation caused cytokinesis and growth defects. ZizA-GFP localised to the cytosol with enrichment in the MTOC, suggesting a role in microtubule regulation. Analysis of hyperosmotic stress implicated ZizA stress-induced expression of *yakA*, *gapA* and *rtoA*. ZizB was found to have the highest expression levels of the four *Dictyostelium* Zizimin proteins and fell within the top 5% of all gene expression. ZizB null cells were also shown to have defects in early development and chemotaxis, which were subsequently rescued through ZizB complementation. Cortical localisation of ZizB-GFP suggests a role in regulation of actin through potential cortical stabilisation mechanism. Furthermore, ZizB shows cytokinesis and growth defects as well as stress-induced expression following hyperosmotic stress. These cellular functions outlined in this chapter suggest the Zizimins play a role in regulating the cytoskeleton where ZizA could potentially regulate microtubule dynamics and ZizB could potentially regulate and stabilise the actin filament network.

## **6 Zizimin binding partners**

## 6.1 Introduction

In the previous chapter I investigated the cellular role of the zizimin proteins. Cells either lacking or overexpressing ZizA or ZizB were analysed in a number of cellular functions including cell migration, development, cytokinesis, growth and stress. ZizA was shown to localise to the cytosol with enrichment in the MTOC, and be involved in cytokinesis, growth and stress. In contrast, ZizB localised to the cytosol with enrichment at the cortex and played a role in development, chemotaxis, cytokinesis, growth and stress. Furthermore, overexpression of ZizB showed a significant increase in filopodia formation. To understand the mechanisms of how ZizA and ZizB function within these cellular processes we investigated the potential binding partners of these proteins.

Zizimins are known to regulate Rho family small GTPases. In mammalian cells, zizimin 1-3 were shown to have specificity for Cdc42, however, in the absence of Cdc42, these proteins will bind and regulate Rac1 (Cote and Vuori, 2002; Gadea et al., 2008; Nishikimi et al., 2005). To date no homologues for Rho and Cdc42 have been identified in *Dictyostelium*, although 18 Rac proteins have been characterised, with a number showing functions that fulfil the roles of Rho and Cdc42. For example, Cdc42 is involved in filopodia formation (Allen et al., 1998; Lee and Knecht, 2001), however, in *Dictyostelium* the Rac1a protein regulates this process (Dumontier et al., 2000). Furthermore, expression of human Cdc42 in *Dictyostelium* cells induced filopodia like structures (Lee and Knecht, 2001). The RhoA GTPase has been shown to regulate myosin II dependent cell polarity at the back and sides of cells, a function that is controlled by PakA regulation (Charest and Firtel, 2007; Xu et al., 2003).

In this chapter, potential *Dictyostelium* binding partners are identified for the ZizA and ZizB proteins. Proteomic approaches were used to show protein-protein interactions using total cell lysates. Protein complexes were analysed by mass spectrometry. The specific Rac1a interaction was further confirmed with co-immunoprecipitation with Rac-GST proteins.

## 6.2 Proteomics

### 6.2.1 Intracellular protein-protein interaction

To identify potential binding partners of ZizA and ZizB, lysates from wild type, *zizA*<sup>+</sup> and *zizB*<sup>+</sup> cells lines (containing ZizA-GFP and ZizB-GFP, respectively) were immunoprecipitated using anti-GFP antibody agarose beads. In these experiments, protein binding partners, in the total lysate, attached to the ZizA-GFP or ZizB-GFP, are retained on the anti-GFP coated agarose beads, and the non-interacting proteins are released into the lysate. In preliminary experiments, the protein complex was separated on an SDS-PAGE gel and visualised by silver stain and Western blot analysis (**Figure 6.1**). Silver stain was used as it is more sensitive than Coomassie stain and therefore gives an indication of unique bands present in either the ZizA-GFP or ZizB-GFP complex. Western blot analysis identified degradation of the ZizA-GFP and ZizB-GFP indicated by a weak band at the predicted molecular weight (280kDa and 270kDa for ZizA and ZizB, respectively) and stronger bands at a reduced molecular weight. Each cell line was either stimulated with or without cAMP for 5hr (to initiate development) to see whether there was a change in degradation.

To inhibit degradation we doubled the recommended concentration of the protease inhibitor cocktail. The increase in concentration of the protease inhibitors did not block degradation of ZizA-GFP since a weak full length and a strong 30kDa band was still seen on the Western blot. In contrast, ZizB-GFP extracts contained a majority of the full length protein (~270KDa) although some smaller degradation fragments were still present (**Figure 6.2A**). Following the purification, all three fractions (pull down eluate, non-bound fraction and the total lysate) were separated on an SDS-PAGE gel and visualised with Coomassie stain (**Figure 6.2B**). The protein bands seen in the Coomassie stained gel for ZizA-GFP and ZizB-GFP lysates, which were absent in the control lysates, were excised (along with the corresponding region from the wild type control) and analysed by mass spectrometry to identify the interacting proteins (**Figure 6.3**). Eight unique bands were sent for analysis, along with the remaining gel, which was analysed for any unique bands that were not detected by the Coomassie stain.

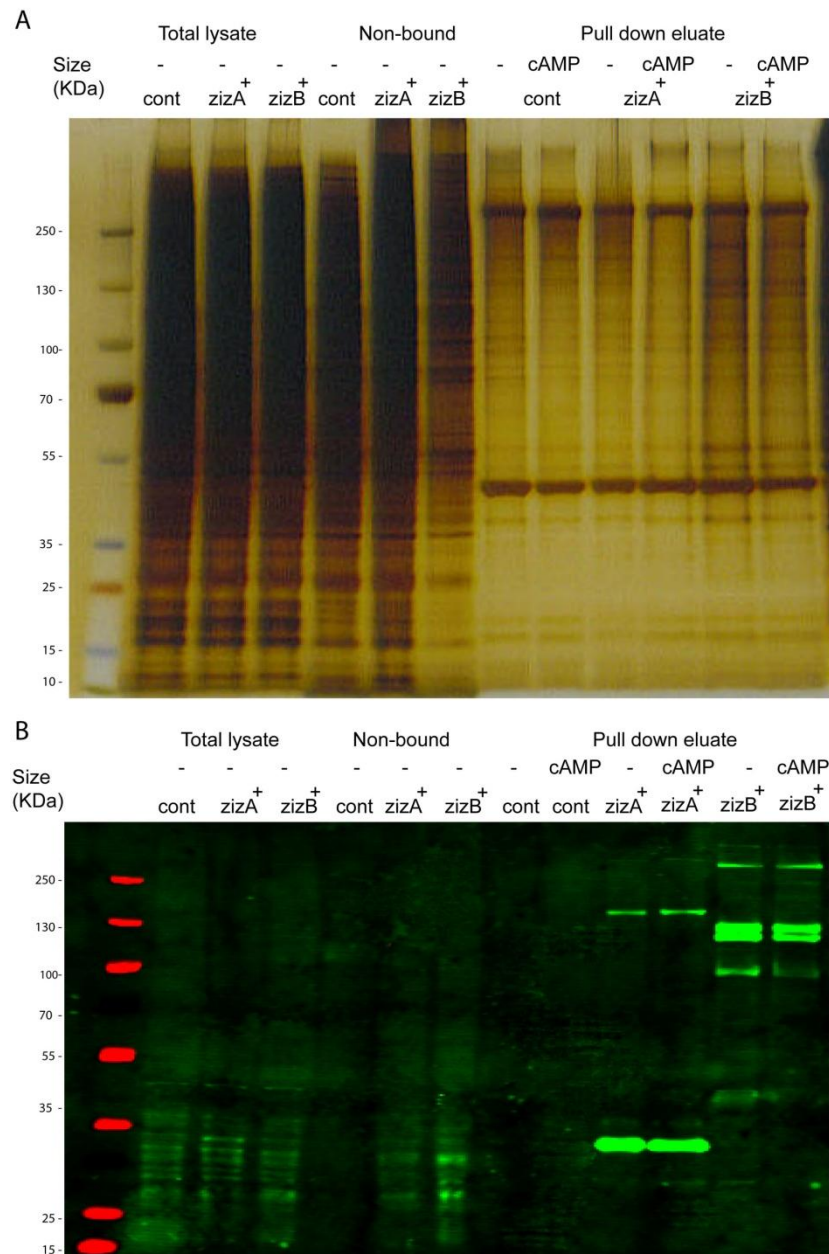


**Figure 6.1 Co-immunoprecipitation of ZizA and ZizB proteins – Silver stain.**

Zizimin A and B proteins were immunoprecipitated using anti-GFP coated beads. Extracts from wild type (cont), zizA<sup>+</sup> or zizB<sup>+</sup> cell lines (containing ZizA-GFP or ZizB-GFP) were used to identify protein bands specific to each ZizA or ZizB eluate (absent in wild type). (A) The fraction from each cell total lysate, non-bound eluate, and pull down eluate from growing (-) or 5hr cAMP pulsed (cAMP) cells were analysed. The purified complexes were separated on an SDS-PAGE gel and visualised with silver stain. (B) Western blot analysis was used to confirm full length protein in the lysates using anti-GFP antibody, showing the total lysate, non-bound eluates and pull down eluates for the wild type, zizA<sup>+</sup> and zizB<sup>+</sup> cells lines in growing (-) 5hr developed (cAMP) cell lysates.

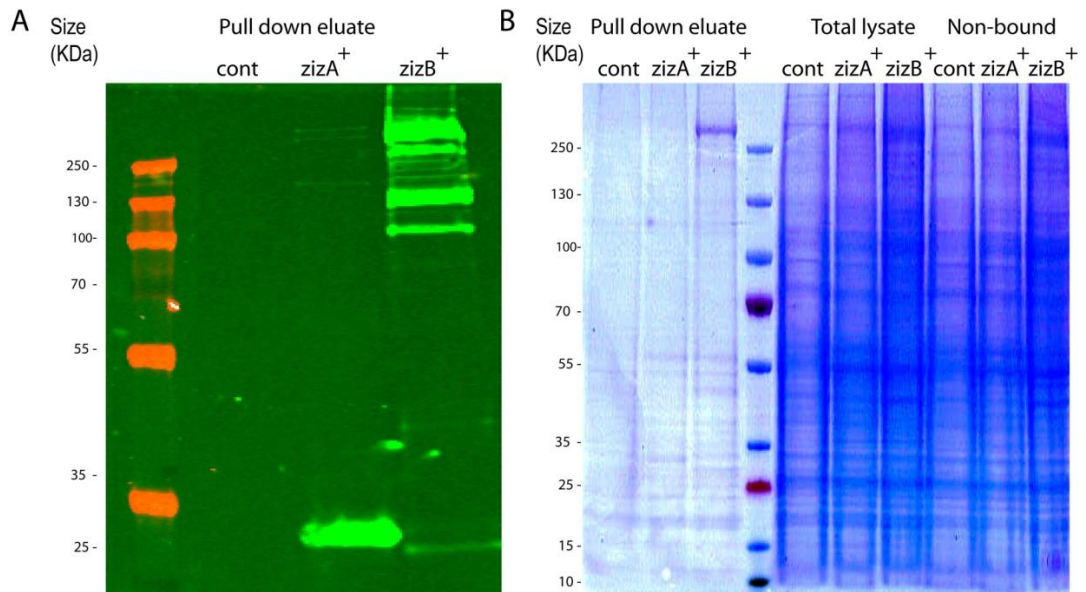


**Figure 6.2 Co-immunoprecipitation of ZizA and ZizB proteins – Coomassie stain.**

Zizimin A and B proteins were immunoprecipitated using anti-GFP coated beads. Extracts from wild type (cont), zizA<sup>+</sup> or zizB<sup>+</sup> cells (containing ZizA-GFP or ZizB-GFP) were used to identify specific binding partners. (A) Western blot analysis was used to confirm full length protein in the lysates using anti-GFP antibody. (B) The purified complex was separated on an SDS-PAGE gel and visualised with Coomassie stain.

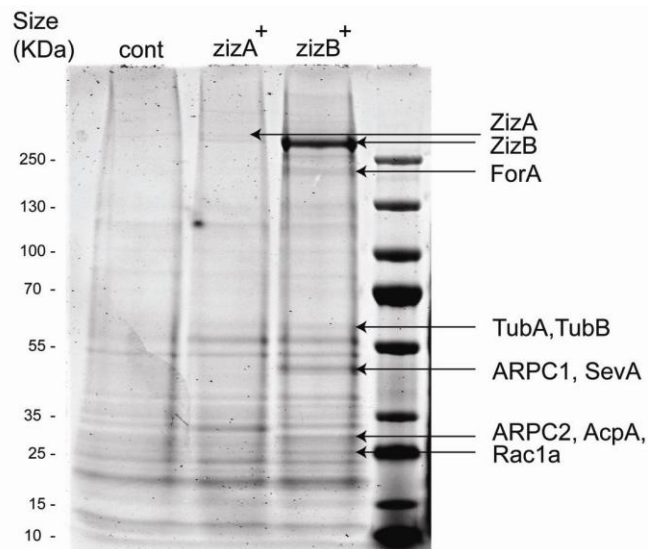


**Figure 6.3 Zizimin protein interaction analyses.**

Preparative protein gel electrophoresis was stained with Coomassie stain and the unique bands for ZizA and ZizB eluates were excised (along with the corresponding wild type region) and sent for mass spectrometry analysis to identify these specific binding partners. The remaining gel was also analysed for any unique peptides not detected by the Coomassie stain. Mass spectrometry analysis of these bands identified a range of potential interacting proteins (Table 6.1), including TubA and B, ForA, ARPC1 and C2, AcpA and B, SevA and Rac1a.



From the eight bands (and remaining gel) sent for mass spectrometry analysis, ~300 interactions were identified and carefully analysed to eliminate non-specific candidates (**Table 6.1**). The numbers in the list indicate the number of unique peptides. Initially, all proteins were identified using their Dictybase ID, to identify their known functions. Proteins that were found in both wild type and ZizA-GFP or ZizB-GFP were removed. The ribosomal and general housekeeping proteins were also eliminated since these are often identified using this approach. The remaining proteins are likely to have specific ZizA and ZizB interactions. These potential binding partners can be grouped according to cellular function, proteins with known GTPase function, actin associated proteins, actin and myosin associated proteins, myosin association only and other interactors that showed unique peptides but had variable cellular functions.

The outcome of this experimental approach was the identification of a range of actin and/or myosin associated binding partners. The specific ZizA binding partners were identified as  $\alpha$ - and  $\beta$ -tubulin subunits, TubA and TubB. ZizB showed a range of interacting proteins. Binding partners which were of particular interest were Rac1a, a small GTPase; formin A, a protein that functions as an actin filament nucleator; Cap32 and Cap34, which are capping protein subunits and the ArpC1 and ArpC2 proteins (coded for by *arcA* and *arcB* genes) which form part of the Arp2/3 complex. Since the amount of full length protein in the ZizA eluate was low, only a small number of specific binding partners were identified. The experiment was repeated several times however the degradation was unable to be resolved within the time frame.

**Table 6.1 List of potential ZizA and ZizB binding partners**

Groups	Name	Function Dictybase	AX2	ZizA	ZizB
GTPase	rab11A	GTPase - vesicular trafficking	2	0	8
	rab32A (rabE)	GTPase - vesicular trafficking	0	0	5
	rac1A	GTPase - actin cytoskeleton organisation	0	0	5
	ragA	GTPase - signalling pathways	0	0	4
	sarA	GTPase - GTP-binding protein Sar1A ARF/SAR superfamily protein - vesicular transport	0	0	4
	drg1	ortholog of human DRG1, which may be involved in cell proliferation, differentiation and death; highly conserved in eukaryotes; belongs to the GTP1/OBG family	0	0	6
Actin associated	forA	Actin binding protein	0	0	4
	acpA	Actin capping protein subunit	0	0	4
	acpB	Actin capping protein subunit	0	0	5
	sevA	Ca <sup>2+</sup> -dependent F-actin fragmenting protein	0	0	5
	comA	actin binding protein comitin mannose binding lectin B_lectin	0	0	6
	arcA	ARP complex SU1	0	0	4
	arcB	ARP complex SU2	0	0	7
Myosin and actin associated	cct3	subunit of the chaperonin CCT ring complex involved in the folding of actin and tubulin	0	0	9
	tcp1	subunit of the chaperonin CCT ring complex involved in the folding of actin and tubulin	0	0	9
	mlcR	component of actin-based molecular motor; myosin II (conventional myosin) component	0	0	6
Myosin associated	myoI	myosin	0	0	8
	mlkA	myosin light chain kinase	0	0	9
	tubB	tubulin binding	0	6	20
	tubA	tubulin binding	0	7	20
Other	abcF4	ATP-binding cassette	0	0	7
	<i>pks16</i>	<i>Fatty acid synthase</i>	0	0	23
	nxnA	Anexin calcium-regulated phospholipid- and membrane-binding protein	3	16	14
	cshA	catalyzes the condensation of acetyl-CoA and oxaloacetate to citrate	5	4	19
	smlA	cytosolic protein present in vegetative and developing cells	4	0	18

Mass spectrometry analysis was used to analyse unique bands from the ZizA or B pull down data. The MS/MS data was analysed using scaffold 3 software, here the analysis parameters were set to a minimum protein match of 95% and the minimum peptide threshold was set to 4 with a 90% match. This analysis indicated ~300 interactions which were carefully analysed to eliminate non-specific candidates. The remaining potential interaction proteins have been grouped according to cellular function, (blue) GTPases, (pink) actin associated proteins, (orange) actin and myosin association, (green) myosin association and (white) other interactors that were identified unique peptides but had variable cellular functions.

To confirm the ZizB interaction with Rac1a, ZizB-GFP was co-immunoprecipitated with a selection of Rac-GST proteins (Rac1a, RacA, RacC and RacG). These Rac-GST proteins were purified in bacteria and a preliminary test was run to estimate the loading of each Rac-GST (and GST alone) to the anti-GST coated agarose beads to ensure equal binding (**Figure 6.4A**). Binding of approximately equal amounts of each Rac protein to the GST beads and mixing the beads with extracts from wild type and zizB<sup>+</sup> cells enabled the direct binding of each Rac to ZizB to be identified. The protein complex was separated on an SDS-PAGE gel and visualised by Western blot analysis using anti-GFP and anti-GST antibodies (**Figure 6.4B**). This approach confirmed a direct binding of ZizB to Rac1a, and also showed an interaction with RacA, RacC and RacG.

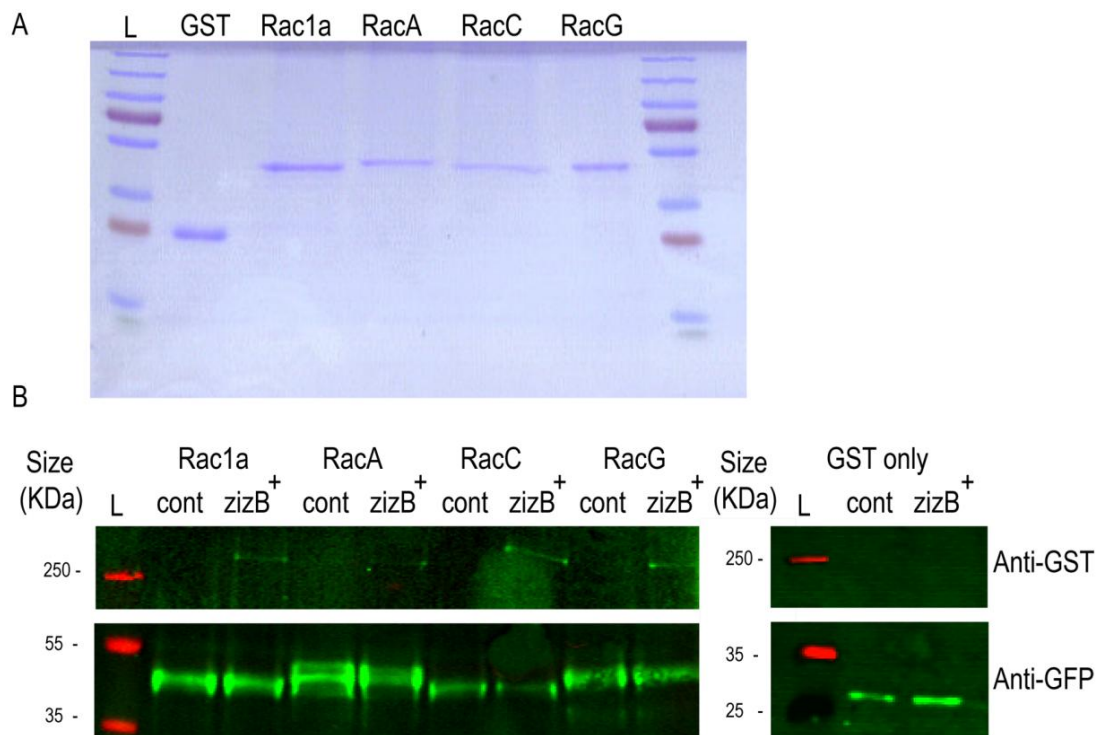


**Figure 6.4 Co-immunoprecipitation of ZizB with Rac-GST**

Assessment of direct Rac-GST/ZizB-GFP binding. (A) Preliminary test to estimate amount of specific Rac-GST binding to anti-GST beads. Eluate were separated on an SDS-PAGE gel and visualised with a Coomassie stain. (B) Rac1a-GST, RacA-GST, RacC-GST and RacG-GST were co-immunoprecipitated with extracts from wild type (cont) cells or cells overexpressing ZizB-GFP. The purified complex was separated on an SDS-PAGE gel and visualised by Western blot analysis to indicate Rac-proteins present in each immunoprecipitation (using an anti-GST antibody - lower panel), and the presence (or absence) of co-immunoprecipitated ZizB-GFP (using an anti-GFP antibody - upper panel). Cells expressing GST only were used as a control (analysis under identical conditions and run on a separate gel due to lane constraints). L indicates the molecular marker, and molecular masses are shown in KDa.

### 6.3 Discussion

To understand the cellular role of poorly characterised proteins, it is useful to identify direct binding partners. With regards to the *Dictyostelium* Zizimin proteins, the binding partners of ZizA and ZizB have yet to be established. Anti-GFP agarose beads were used to immobilise ZizA-GFP or ZizB-GFP along with any potential binding partners. The isolated protein complex was then separated on an SDS-PAGE gel and visualised with silver stain. I used silver staining in preliminary experiments as it is more sensitive compared to Coomassie stain and can detect proteins in the nanogram range (Chevallet *et al.*, 2006). However, silver stain cannot be used for the final analysis as mass spectrometry has a number of limitations in sample detection, preparation and protein modification and the silver staining procedure is known to modify the proteins, leading to low sequence coverage and interference (Chevallet *et al.*, 2006; Gharahdaghi *et al.*, 1999; Scheler *et al.*, 1998). Coomassie blue provides much better results in terms of linearity, homogeneity and interference with mass spectrometry (Neuhoff *et al.*, 1988; Richert *et al.*, 2004), thus, this method was used in the final experiments sent for analysis. Since Coomassie stain has a lower sensitivity than silver stain, a larger amount of protein had to be loaded in the gel to ensure the unique bands could be seen by the Coomassie staining and detected in the mass spectrometry analysis.

Western blot analysis showed the ZizA-GFP and ZizB-GFP proteins were degraded, leaving very little full length protein in the lysate. Since protein visualisation employed GFP binding, located at the C-terminal, loss of N-terminal protein was shown by the GFP binding to different smaller molecular weight fragments.

ZizA-GFP showed a faint band at the predicted full length molecular weight and one other strong band at a lower molecular weight (~30kDa). This would suggest that there is only one cleavage site which removes the GFP tag, since GFP has a molecular weight of 30kDa, and no other higher molecular weight bands were seen. Hence, the majority of the ZizA protein, along with specific binding partners, would not have been immobilised by the anti-GFP beads. This would potentially leave the small amount of proteins that did bind the anti-GFP

beads, below the detectable range. Since low protein levels have been shown to restrict the mass spectrometry analysis to identifying only the major protein interactions (Richert *et al.*, 2004), any weaker binding partners may not have been detected.

ZizB-GFP protein degradation occurred at multiple cleavage sites, leaving 3 distinct high molecular weight bands (~260kDa, 120kDa and 100kDa). Comparison of ZizB protein structure with the degradation fragment sizes suggest that all three products would lack regions of the N-terminus (and potentially some of the DHR1 domain) but would retain the C-terminal DHR2 domain. Furthermore, truncated versions of Dock proteins expressing only the DHR2 domain have been used to show the specific GTPase binding partners (Cote and Vuori, 2002; Cote and Vuori, 2006; Meller *et al.*, 2002). To identify binding partners for mammalian Zizimin1, a truncation of the full length protein, expressing only the DHR2 domain, was used to show binding to Cdc42 (Meller *et al.*, 2002). Another study showed COS7 cell lysates, expressing either Rac-Myc or Cdc42-Myc, were co-immunoprecipitated with GST fusion proteins of the DHR2 domains for the Dock180, Dock2, Dock3, Dock7 and Zizimin1 and showed specificity for either Rac or Cdc42 (Cote and Vuori, 2006). The DHR2 domain is associated with the GEF activity of this protein, therefore, would still be expected to bind target GTPases and hence be likely to still identify target interacting proteins.

During early development proteolytic activity is reduced (Fong and Rutherford, 1978), therefore, I investigated whether initiating development through pulsing the cells with cAMP for 5hr prior to cell lysis would decrease protein degradation. However, no change was seen in degradation between the growing and developed cell lysates. To overcome protease degradation, the protease cocktail inhibitor concentration in the lysis buffer was doubled from the recommended concentration. The ZizA-GFP degradation was not reduced by increasing the protease inhibitor concentration; however, ZizB-GFP degradation was largely inhibited. Coomassie staining revealed unique bands present in pull down eluate for the ZizA-GFP and ZizB-GFP that were not present in the wild type control. These unique bands along with their corresponding wild type control regions were analysed by mass spectrometry.

Immunoprecipitation experiments described here indicate ZizA interacted with two proteins, which mass spectrometry identified as TubA ( $\alpha$ -tubulin subunit) and TubB ( $\beta$ -tubulin subunit). *Dictyostelium* has two  $\alpha$ -tubulin subunits but only one  $\beta$ -tubulin subunit (and one  $\gamma$ -tubulin subunit) that form the main constituents of the microtubule cytoskeleton (Euteneuer et al., 1998; Trivinos-Lagos et al., 1993). Cell migration requires polarisation of the cell, a function that is controlled by the actin and microtubule cytoskeleton (Goode et al., 2000; Palazzo et al., 2001; Wittmann and Waterman-Storer, 2001). During cell migration, the MTOC and microtubules reorient towards the leading edge, where the microtubules exhibit net growth (Palazzo et al., 2001; Small and Kaverina, 2003; Wittmann and Waterman-Storer, 2001). Microtubules are thought to regulate Rho small GTPases, however, the mechanism of how this regulation occurs remains unclear (Waterman-Storer *et al.*, 1999). Some studies have shown the direct binding of Rac1 through co-immunoprecipitation (Best *et al.*, 1996), however, Rac1 does not co-localise with tubulin (Michaelson *et al.*, 2001). Therefore, it is thought that the main mechanism of this microtubule-dependent Rac1 regulation occurs through binding of microtubules to the corresponding GEF, which in turn regulates Rac1. Microtubule-dependent Rac activation through GEF binding provides one explanation for ZizA interaction with the TubA and TubB subunits.

The protein interaction approach employed here did not identify any Rac proteins as potential binding partners for ZizA. However, after reviewing the number of unique peptides (for TubA and TubB) identified in immunoprecipitation experimental analysis of ZizA (6), and comparing this to the number found in the ZizB experiment (20), showed ZizA to have around one third of the hits compared to ZizB. Applying the same ratio (6:20) (assuming the binding would occur in the same ratio) for the Rac protein interaction, where ZizB had 5 hits for Rac1a, would make the ZizA-Rac interaction approach  $\geq 1$ , and may thus fall under the detection threshold using mass spectrometry.

Immunoprecipitation indicated ZizB had a number of potential interactions with actin and myosin associated proteins. Two of these interactions were with ArpC1 and ArpC2, two *Dictyostelium* Arp2/3 subunits (Langridge and Kay, 2007). The Arp2/3 complex is an assembly of seven subunits that drives pseudopod formation and cell movement by catalysing nucleation of new

branched actin filaments (Insall and Machesky, 2009; Pollard, 2007). The Arp2/3 complex is activated by the WASP family proteins, Wiskott-Aldrich Syndrome Protein (WASP) and Suppressor of cyclic AMP receptor mutation and WASP and Verprolin homologous protein (SCAR/WAVE). These proteins act as scaffolds that integrate signals from small GTPases, such as Cdc42 (in mammalian systems) and Rac, to the initiation of actin branches by the Arp2/3 complex (Insall and Machesky, 2009). This complex represents one of many actin modifying enzymes that accumulate at the leading edge during chemotaxis, driving pseudopod formation and cell movement (Sasaki and Firtel, 2006).

The current model for the activation of the Arp2/3 – SCAR/WAVE complex involves binding of Rac1 to the SCAR/WAVE complex, comprising of Abl Interactor2 (Abi2), p53-Inducible mRNA (PIR121), Nck-associated protein1 (Nap1) and Haematopoietic Stem/Progenitor Cell protein 300 (HSPC300) (Dai and Pendergast, 1995; Pollitt et al., 2006; Pollitt and Insall, 2008; Qurashi et al., 2007). The activation of this complex triggers Arp2/3 dependent actin polymerisation. Although it has been shown that Rac1 binds SCAR/WAVE and PIR121, initiating Arp2/3 dependent F-actin polymerization, cells lacking SCAR or PIR121 retain the capacity to polymerise actin in response to cAMP stimulation. This suggests there is another mechanism for Arp2/3 activation in *Dictyostelium* (Blagg *et al.*, 2003). Thus, it is possible that Rac1 binds Arp2/3 directly, initiating F-actin polymerization, although this theory has yet to be investigated. This, therefore, suggests the interaction between ZizB and the Arp2/3 subunits ArpC1 and ArpC2 could be through secondary interaction with Rac1a or a direct physical interaction with ZizB, however, this remains to be shown.

Another ZizB binding partner identified in these experiments is the formin protein, ForA. These proteins function as actin filament nucleators by producing unbranched filaments for actin bundles (Insall and Machesky, 2009; Pollard, 2007; Wallar and Alberts, 2003). The *forA* knockout did not show any distinct phenotype in growth or development (Kitayama and Uyeda, 2003), however, another *Dictyostelium* formin ForH (dDia2), has been implicated in filopodia formation. This knockout mutant showed numerous defects in development, pseudopodia formation, filopodia formation as well as a decrease in cell motility



and chemotaxis (Schirenbeck et al., 2005a; Van Haastert and Bosgraaf, 2009). ForA could therefore be involved in filopodia formation by forming a complex with Rac1a and ZizB.

Cap32, Cap34 and SevA are actin binding proteins that were shown to interact with ZizB. Cap32 and Cap34 are subunits of the heterodimeric actin capping protein (Eddy *et al.*, 1997). Capping proteins block but do not sever (nor nucleate) actin filaments, thereby preventing the addition or loss of actin subunits at the barbed filament end (Hug et al., 1995). SevA is a severin protein that breaks the actin filament and remains bound to the barbed end (Eichinger *et al.*, 1991). Both Cap32/34 and SevA play key roles in the regulation of the actin cytoskeleton. Neither Cap32/34 nor SevA have been shown to interact directly with GTPases or their corresponding GEFs, therefore, this could potentially show a novel interaction in actin regulation.

ZizB was also shown to interact with myosin I and II (MyoI and mlcR) and a number of myosin associated proteins (Cct3, Tcp1 and MlkA). Conventional myosin (myosin II) plays a key role in the cytoskeletal reorganisation and is necessary for cytokinesis, migration, and filopodia formation (Moores *et al.*, 1996). Myosin II has two modes of function, stabilisation and ATP-powered contraction (Bosgraaf and Van Haastert, 2006). Myosin II is concentrated in the cleavage furrow during cytokinesis and in the posterior of migrating cells (Bosgraaf and Van Haastert, 2006; Moores et al., 1996; Zang et al., 1997). Myosin II null cells display reduced cortical tension since they are only able to divide during traction mediated cytokinesis (and not in suspension) (Egelhoff *et al.*, 1990), and have reduced chemotaxis with reduced speed and production of lateral pseudopods, due to reduced actin stabilisation by myosin (Heid *et al.*, 2004). Myosin II translocation to the cortex is regulated by the cGMP pathway of which P21 Activated Kinase A (PAKa) is an effector (Bosgraaf and Van Haastert, 2002). PAKa is also a downstream target of Rac1 (Chung and Firtel, 1999), thus ZizB could be involved in myosin regulation through Rac1 and PAKa.

Class-1 myosins (including MyoI) localise to cortical regions during cell migration and support the formation and maintenance of actin-rich structures (Rump *et al.*, 2011). This class of myosins play an important part in stabilising

the spindle fibres during cell division through microtubule binding. It is not clear whether the ZizB interaction is a direct physical interaction with myosin I or through a secondary interaction with tubulin, thus regulating and stabilising microtubules and spindle during cell division. The myosin associated proteins Chaperonin Containing TCP1 3 (CCT3) and Tailless-Complex Polypeptide 1 (TCP1) are Chaperonin protein subunits that form a CCT ring complex and are involved in the folding of actin and myosin. These potential interactions could be secondary interactions through the myosin interaction, however, little is known about these proteins.

ZizB was also shown to interact with Pks16, a poorly characterised fatty acid synthase protein. This interaction shows a novel interaction that could provide a novel function in fatty acid synthesis regulation. Pks16 forms part of the polyketide synthase subclass of fatty acid synthases (Eichinger et al., 2005; Ghosh et al., 2008; Zucko et al., 2007). Pks proteins are abundant in *Dictyostelium* with over 43 genes. This family of proteins catalyse the formation of long-chain fatty acids from acetyl-CoA, malonyl-CoA and NADPH. Fatty acid synthases are multifunctional proteins with several catalytic activities and an acyl carrier protein. The only known polyketide product is differentiation inducing factor (DIF) (Zucko et al., 2007), which induces a particular subset of stalk cells during development (Austin *et al.*, 2006). Although the mechanism for this interaction is unclear, it would be interesting to investigate further, potentially identifying a novel role for ZizB in regulating fatty acid synthase function.

To confirm direct binding of Rac1a and ZizB, co-immunoprecipitation was used with four Rac proteins, Rac1a, RacA, RacC and RacG. The Rac1a interaction was confirmed by showing a direct binding of ZizB to bacterially expressed Rac1a protein (**Figure 6.3**). This interaction is also conserved in the mammalian homologues (Dock7 and 8) (Pinheiro and Gertler, 2006; Ruusala and Aspenstrom, 2004). In mammalian systems, Rac1 controls filopodia formation and membrane ruffles (Ruusala and Aspenstrom, 2004; Watabe-Uchida et al., 2006a; Watabe-Uchida et al., 2006b).

The binding, *in vitro*, of other Rac proteins (RacA, RacC and RacG) in this approach will need to be confirmed *in vivo* through further studies. GEF proteins

or Rac regulators can have multiple substrates (Mondal et al., 2010; Park et al., 2004; Rivero et al., 2002). RacA belongs to the novel subfamily of RhoBTB proteins. It has been suggested to play a pivotal role as docking points for molecules participating in diverse signal transduction cascades and has been shown to bind GapA, PakA and PakC (Mondal et al., 2010; Park et al., 2004; Rivero and Somesh, 2002). RacC was shown to interact with WASP, in a yeast II hybrid screen. WASP plays a key role in RacC regulation at the leading edge of chemotaxing cells (Han *et al.*, 2006). RacG has a role in regulating a number of actin driven processes such as morphogenesis, cytokinesis and phagocytosis (Seastone et al., 1998; Somesh et al., 2006).

## 6.4 Summary

In this chapter, ZizA and ZizB binding partners were identified using protein binding studies. ZizA-GFP and ZizB-GFP and the interacting proteins were immobilised using anti-GFP agarose beads. The complexes were separated and analysed by mass spectrometry analysis. These experiments identified the tubulin subunits (TubA and TubB) as potential binding partners of ZizA. In contrast, the ZizB protein interacted with a range of actin and myosin associated proteins including Rac1a, TubA and TubB, ArpC1 and ArpC2, ForA, Cap32 and Cap34 and SevA. The Rac1a interaction was further confirmed through specific binding using GST fusion proteins. These potential binding partners provide evidence that the ZizA and ZizB proteins regulate the actin-myosin cytoskeleton dynamics.

## **7 Conclusion**

Dopamine receptor interacting proteins (DRIPs) are poorly characterised at the cellular level. In this project, I sort to examine the cellular roles for two potential DRIPs, using *Dictyostelium* as a model organism. Bioinformatic analysis identified these two proteins as Zizimin and MARK family proteins, respectively. Developmental analysis of the knockout cell lines showed only ZizB had a role in development, therefore, this protein family was chosen for further investigation.

Domain structure analysis of the human and *Dictyostelium* Dock family proteins identified the presence of 2 domains, which have previously been characterised as the DHR1 and DHR2 domains (Cote and Vuori, 2006; Cote and Vuori, 2007; Lin et al., 2006). Little is known about the mechanism of how the DHR1 domain functions, although, it has been shown to bind phospholipids and, thus, could be involved phospholipid dependent localisation (Cote et al., 2005; Kobayashi et al., 2001). The DHR2 domain, is the GEF domain, that binds Rho family small GTPases in their inactive state, facilitating the dissociation of GDP, allowing GTP to bind and activate the GTPase (Cote and Vuori, 2006; Lin et al., 2006; Meller et al., 2002; Nishikimi et al., 2005).

Phylogenetic analysis, sequence alignment and domain structure analysis shows evolutionary conservation of the *Dictyostelium* Zizimin proteins within the Zizimin/Zizimin-related subfamily. This suggests that the *Dictyostelium* Zizimin proteins are homologues of the mammalian Zizimin/Zizimin-related proteins; therefore, analysing the cellular function of these proteins in *Dictyostelium* will help elucidate potential cellular roles of the mammalian proteins.

### **7.1 The cellular function of ZizA in *Dictyostelium***

To understand the role of ZizA in the cell, I have knocked out and overexpressed this protein, and found no gross phenotypic changes in development or chemotaxis. However, GFP tagging of the protein showed it is localised to the cytosol with enrichment in the MTOC, thus implicating ZizA in the regulation of the microtubule network. This hypothesis was further supported by the protein interaction experiments which identified the ZizA

potential binding partners as TubA ( $\alpha$ -tubulin) and TubB ( $\beta$ -tubulin) subunits, which make up the microtubule cytoskeleton. Furthermore, experiments by our collaborator showed that ZizA co-localises with  $\alpha$ -tubulin in the MTOC (Pakes et al., 2012). The basic cellular function of the MTOC includes microtubule nucleation and spindle formation during cell division. During cell migration the MTOC reorients towards the leading edge, thus, initiating microtubule growth (Eng et al., 2007; Etienne-Manneville and Hall, 2001; Palazzo et al., 2001) and assists in cellular polarisation (Wittmann and Waterman-Storer, 2001). In mammalian systems, MTOC reorientation initiates increases active Cdc42 levels (Gundersen, 2002; Palazzo et al., 2001). This data is consistent with a role for Zizimins in regulating Cdc42 (as has been shown) to initiate MTOC function and this model is supported by our data for ZizA (**Figure 7.1**).

Despite a role for MTOC in cell polarisation and chemotaxis, ZizA null and overexpressor cell lines did not show any major defects in chemotaxis or development, which suggests it either does not play a major role in these cellular events or the loss of ZizA is compensated for by similar proteins. Another explanation could be that the driving force behind cell movement occurs via the actin cytoskeleton and not the microtubule network. In support of this, cells treated with the microtubule polymerisation inhibitor, nocodazole, are still able to undergo cell migration, however, the membrane ruffling and protrusions at the leading edge are reduced. Thus, microtubules are not essential for cell movement but do help stabilise and enhance this cellular function (Waterman-Storer et al., 1999; Wittmann and Waterman-Storer, 2001).

Cells lacking ZizA also showed defects in cytokinesis and a delay in growth. Since these processes are linked, and depend upon the microtubule cytoskeleton function, this data supports a role for ZizA in microtubule regulation. During cell division, interphase microtubules dissociate from the MTOC and are replaced with spindle building microtubules (Neujahr et al., 1997a; Neujahr et al., 1997b; Neujahr et al., 1998). Cell division is based on the coordinated activities of the microtubule and actin microfilament systems which is important for actin to form the cleavage furrow in the correct place (Neujahr et al., 1998). Myosin II is also involved in cytokinesis but is not essential, where it is thought to have a stabilising function. There are four Rac GTPases (RacE, RacB, RacC and Rac1) that have been shown to play a role in cytokinesis since

constitutively active mutants form multiple nucleate cells. RacE is essential during cytokinesis (Larochelle et al., 1996; Larochelle et al., 1997) where it has been shown to regulate 14-3-3, which interacts with microtubules and myosin II, facilitating myosin II cortical remodelling (Zhou *et al.*, 2010). Since Rac1 has been shown to regulate cortexillin, a protein which is involved in cytokinesis, another possible transduction mechanism could involve ZizA regulation of a Rac GTPase at the microtubule actin interface via cortexillin (**Figure 7.1**). This study attempted to isolate ZizA binding partners in co-immunoprecipitation experiments, but due to cleavage of the tagged protein, few interacting proteins (and no Rac proteins) were found.

Cells lacking ZizA were blocked in the hyperosmotic-induced stress response for multiple transcription targets. In contrast, ZizA overexpressing cell lines showed gene specific (*yakA* and *rtoA*) block in stress response, however, the *gapA* expression was still responsive. A rationale for the involvement of ZizA in the regulation of these stress-induced expression levels may be related to a role for this GEF through Rac regulation of the STAT/JNK pathway since STATc has been shown to increase *gapA* and *rtoA* expression following osmotic stress (Araki *et al.*, 2003). The mechanism of how ZizA regulates YakA is not clear, although, is possible since YakA regulation has been suggested to be controlled by RasG small GTPase signalling.

Thus, ZizA plays a role in a number of signal transduction pathways, based on the experiments in this work (**Figure 7.1**). Although the direct binding and Rac activation specificity still needs to be determined, the cellular function of ZizA is likely to involve the regulation of microtubule dynamics during cytokinesis and growth.

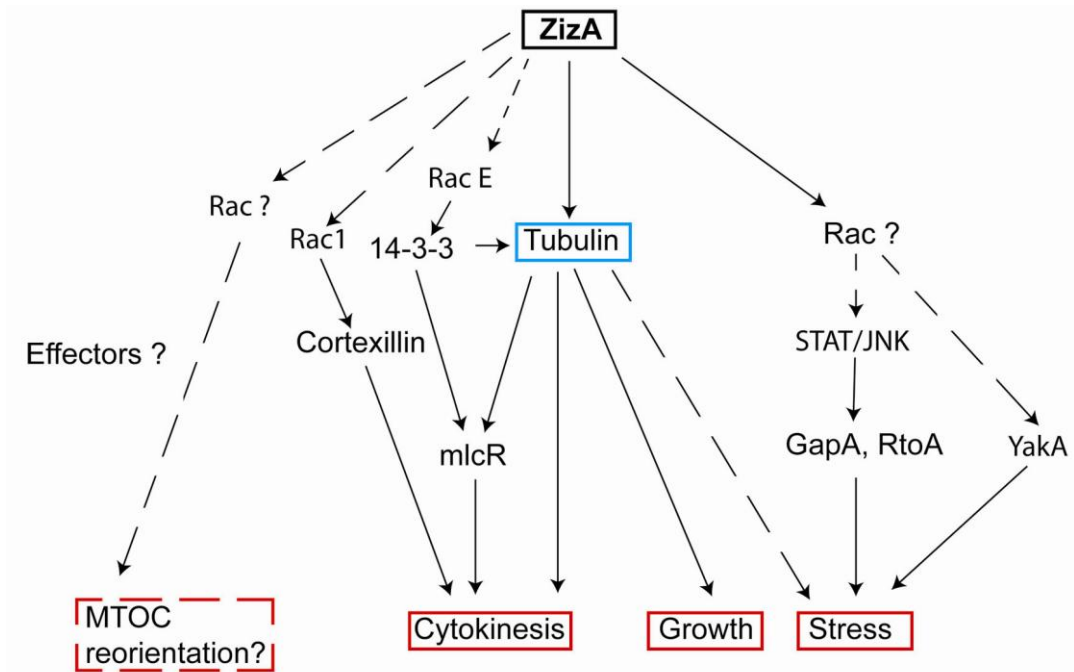


**Figure 7.1 Zizimin A transduction mechanisms**

Zizimin A signalling is implicated in cytokinesis, growth and stress (indicated in the red boxes). The interacting molecules as identified through mass spectrometry (indicated by the blue boxes) link ZizA to its function, where it was shown to interact with tubulin. The solid arrow shows pathways confirmed through literature and the dotted arrows indicate potential mechanisms that have not yet been investigated or fully characterised.

## 7.2 The cellular function of ZizB in *Dictyostelium*

To investigate a cellular role for ZizB, I knocked out and overexpressed this protein in wild type *Dictyostelium* cells. Ablation of ZizB caused defects in early development and aberrant morphology after 24hr, where sparse fruiting bodies were often collapsed with thickened stalks. Overexpression of ZizB did not cause a change in developmental morphology compared to wild type cells. Since chemotaxis is an essential part of early development, I analysed cells lacking or overexpressing ZizB during cell migration. The cells lacking ZizB showed a significant reduction in behaviour during chemotaxis (velocity, aspect and directionality). These coincidental phenotypes are often associated with alterations in cytoskeletal reorganisation, where F-actin polymerisation is necessary for this process. In agreement with this, the localisation of ZizB-GFP was cytosolic with enrichment in the cortex. Overexpression of ZizB also



caused an increase in filopodia formation, which is again consistent with a potential role for ZizB in actin regulation. Yet another role for actin regulation, the *zizB*<sup>+</sup> and *zizB*<sup>-</sup> cell lines showed defects cytokinesis where loss or overexpression of ZizB gave rise to multinucleate cells and a delayed generation time during growth in a suspension culture.

All of these phenotypes identified for the *zizB* mutant cells are in agreement with ZizB binding Rac1a (Chung et al., 2000; Dumontier et al., 2000; Palmieri et al., 2000). A number of GTPase regulating proteins have been identified for *Dictyostelium* Rac1 including GAPs (DGAP1 and GapA) (Faix et al., 1998; Mondal et al., 2010; Sakurai et al., 2001), GDI's (RhoGDI) (Rivero et al., 2002) and GEF's (MyoM, RacGEF1, RacGAP1, GxcDD) (Geissler et al., 2000; Mondal et al., 2007; Park et al., 2004), as well as some downstream effectors such as the SCAR/WAVE complex (Kobayashi et al., 1998) as well as PAKa and PAKc (Chung and Firtel, 1999) (**Figure 7.2**).

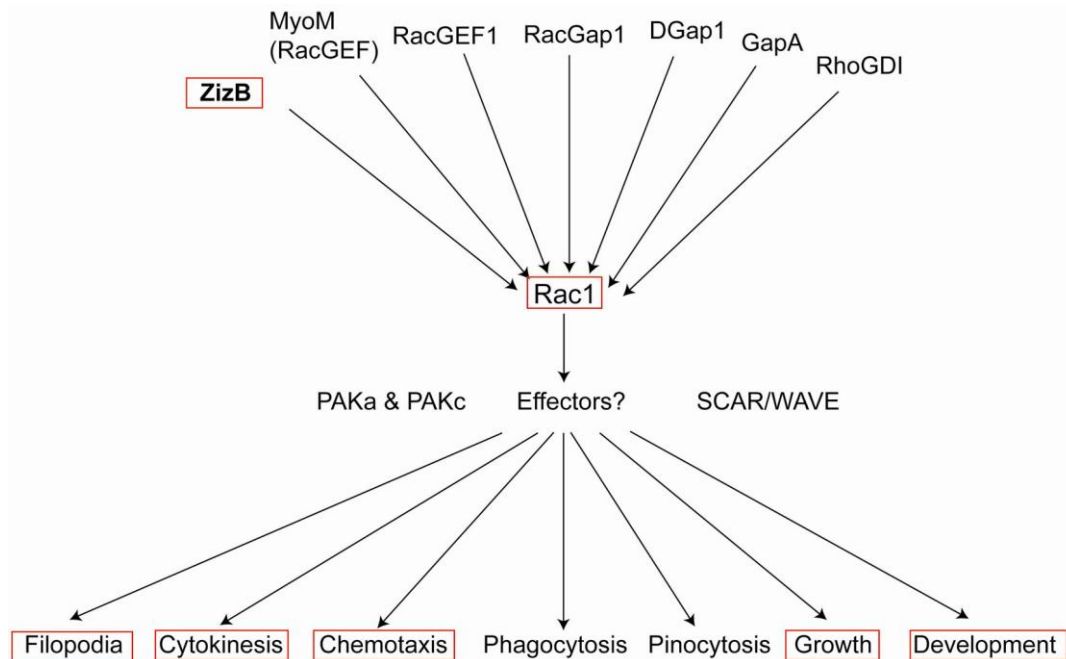


**Figure 7.2 Rac1 GTPase transduction mechanisms**

*Dictyostelium* Rac1 (a/b/c) has multiple functions within the cells, all of which require cytoskeletal reorganization including chemotaxis, development, cytokinesis, filopodia formation, endocytosis (phagocytosis and pinocytosis) and growth (Chung et al., 2000; Dumontier et al., 2000; Faix et al., 1998; Mondal et al., 2007; Palmieri et al., 2000). The red boxes highlight the ZizB cellular functions analysed in this work.

In *Dictyostelium*, Rac1a is one of the key GTPases involved in regulating F-actin polymerisation dependent processes, and is the most highly expressed Rac GTPase. Since ZizB was found to interact with Rac1a, data found in this work suggest a role for ZizB function in regulating Rac1a, thus, defects in either of these proteins would show similar cellular phenotypes. The Rac1a-ZizB interaction was confirmed through co-immunoprecipitation. Since, each interaction could either be through a direct binding to ZizB or an interaction via an intermediary binding partner. Independent of direct or indirect binding, these data indicate potential mechanisms for ZizB which were previously unknown.

A number of actin/cytoskeletal proteins were also found to bind ZizB. These studies have identified possible binding partners which suggest potential transduction pathways for the cellular role of ZizB (**Figure 7.3**); however, these binding partners would need to be further investigated to validate their interaction with ZizB. In these interaction studies, ForA was found to interact with ZizB. Formins nucleate unbranched actin filaments necessary for filopodia formation (Schirenbeck et al., 2005b; Wallar and Alberts, 2003). A related formin, ForH (dDia2) provides a mechanism by which Rac1 induces the formation of filopodia (Insall and Machesky, 2009; Pollard, 2007; Wallar and Alberts, 2003). A role for ZizB in ForA-dependent regulation of filopodia formation is therefore possible.

Another potential ZizB mechanism for filopodia formation (as well as chemotaxis and development) is through the Arp2/3 complex. In this study, ZizB was shown to interact with the Arp2/3 subunits, ARPC1 and ARPC2. The Arp2/3 complex polymerises branched F-actin, driving cell movement through Rac1-dependent activation of the SCAR/WAVE complex (King *et al.*, 2010). Although, Rac1 is also thought to bind Arp2/3 directly, since Arp2/3-dependent F-actin polymerisation still occurs in the absence of the SCAR/WAVE complex (Blagg *et al.*, 2003).

The rationale for the binding of ZizB to Cap32/34 and SevA is not clear. These proteins act as negative regulators of F-actin polymerisation by blocking actin filament growth (Eddy et al., 1996; Hug et al., 1995). Rho GTPases have not been implicated in capping or severin protein regulation, however, this interaction could provide evidence for a novel cellular function in the negative

regulation of the actin cytoskeleton through GTPase activation of Cap32/34 and SevA. However, these interactions remain to be investigated.

Immunoprecipitation studied here also identified a potential role for myosin I (MyoI) and myosin II (MlcR) interaction with ZizB. Therefore, another potential function for ZizB could be the regulation of the actin/myosin pathway. Myosin has key roles in cytoskeletal organisation and has been shown to have a stabilising function through an interaction with cortical actin and microtubules (Charest and Firtel, 2007; Zhou et al., 2010). These interactions are consistent with the potential stabilising role of ZizB since, global stimulation triggered the movement of ZizB from the cortex to the cytosol followed by the return to the cortex after 8sec. Further support for the stabilising role of ZizB is the localisation at the front and sides of the cells during migration, which is consistent with myosin II localisation during cell movement (Bosgraaf and Van Haastert, 2006).

Another phenotype for ZizB overexpression or deletion showed that cells lacking and overexpressing ZizB had cytokinesis defects and a delay in growth. Both of these cellular functions are reliant on the cytoskeleton and involve interactions between the actin/myosin II cytoskeleton and the microtubule network. Data in this study have shown that ZizB directly binds Rac1 and thus would be expected to regulate its activity. Overexpression of Rac1 has been shown to have defects in cell division and growth, where it is thought to function through DGap1 - cortexillin regulation (Faix, 2002). Thus, ZizB null cells are likely to show a diminished cytokinesis function through the Rac1 regulation in the cortexillin pathway. This pathway is distinct from the myosin II pathway, as it is responsible for the production of the contractile ring during cytokinesis, whereas myosin II is involved in the formation of the cleavage furrow through interactions between the microtubule network and the actin cytoskeleton (Bosgraaf and Van Haastert, 2006; Egelhoff et al., 1990; Faix, 2002).

Like other GTPase signalling molecules (including ZizA), overexpression or ablation of ZizB blocked osmotic stress-induced gene transcription of *yakA*, *gapA* and *rtoA*. Since Rac1 has been implicated in the regulation of the STAT/JNK pathway, the data in this study suggests that deregulation of Rac

activity blocks this stress pathway. Other pathways implicated in the stress response are the cAMP/DokA (Ott et al., 2000; Schuster et al., 1996) and the cGMP/myosin II heavy chain pathways (Oyama, 1996; Roelofs and Van Haastert, 2002). Although I have not assessed a role for altered cAMP signalling in ZizB, a role for myosin is likely. The mechanism how ZizB regulates the stress response requires more in depth investigation to gain a clear understanding.

Based on the experiments in this work, ZizB plays a role in regulating a number of actin-dependent cellular processes (**Figure 7.3**). The Shared phenotypes and the binding of ZizB to Rac1a suggest common signalling pathways for these two proteins in regulating actin dynamics during development, chemotaxis, filopodia formation, cytokinesis, growth and stress.

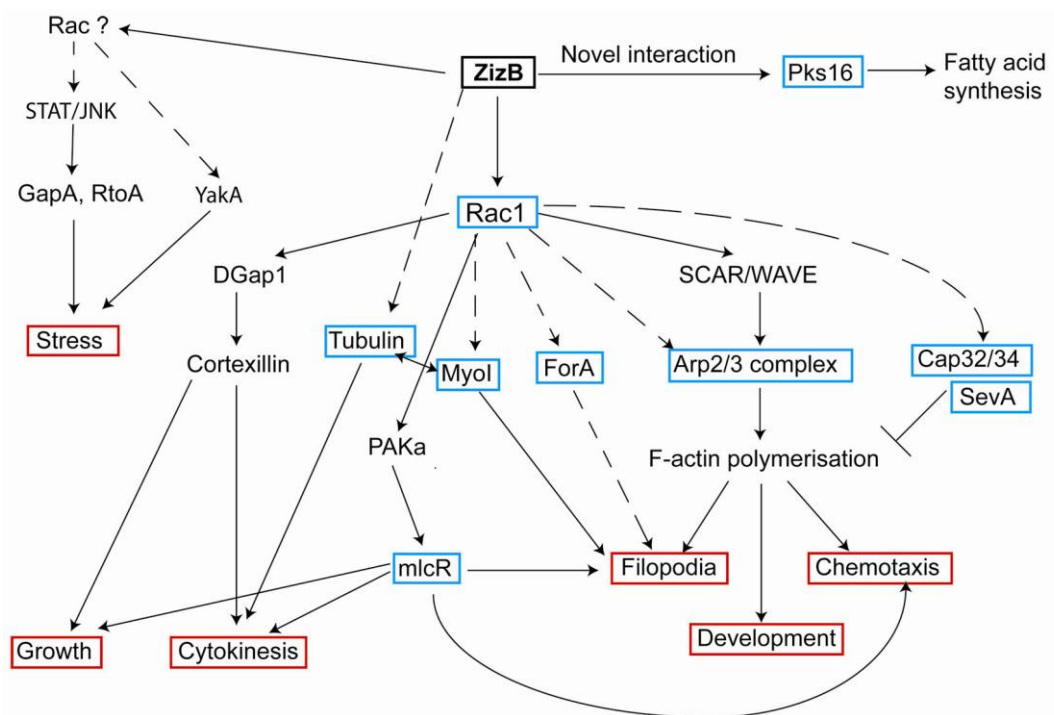


**Figure 7.3 Zizimin B transduction mechanisms**

Zizimin B signalling pathways show implications in filopodia formation, chemotaxis, development, cytokinesis, growth and stress (indicated in the red boxes). The interacting molecules as identified through mass spectrometry (indicated by the blue boxes) link ZizB to its function. The solid arrow shows pathways confirmed through literature and the dotted arrows indicate potential mechanisms that have not yet been investigated or fully characterised.

### 7.3 Summary

In the present study, I have shown that the *Dictyostelium* ZizA and ZizB have a range of cellular roles which involves the relation of the cytoskeleton. ZizA localises to the MTOC and functions to regulate cytokinesis, growth and stress through potential microtubule regulation. In contrast, ZizB localises to the cortex and is involved in development, chemotaxis, filopodia formation, cytokinesis, growth and stress. ZizB was also shown to interact with a number of actin/myosin associated proteins, and directly binds Rac1a, a GTPase that is involved in regulating F-actin polymerisation in multiple cellular processes. I propose that ZizB has a cortex-stabilising role between cyclic periods of reorganisation caused by cAMP waves during chemotaxis. This is supported by the behaviour of ZizB moving off the cortex upon global stimulation. These signalling mechanisms can be investigated in mammalian systems to provide further insight as to why these Zizimin proteins interact with the dopamine signalling pathway, and will help to explore a role for DRIP2 in cellular function.

## References

- Abe, T., Langenick, J. and Williams, J. G.** (2003). Rapid generation of gene disruption constructs by in vitro transposition and identification of a *Dictyostelium* protein kinase that regulates its rate of growth and development. *Nucleic Acids Res.* 31, e107.
- Adley, K. E., Keim, M. and Williams, R. S.** (2006). Pharmacogenetics: defining the genetic basis of drug action and inositol trisphosphate analysis. *Methods Mol. Biol.* 346, 517-534.
- Aizawa, H., Katadae, M., Maruya, M., Sameshima, M., Murakami-Murofushi, K. and Yahara, I.** (1999). Hyperosmotic stress-induced reorganization of actin bundles in *Dictyostelium* cells over-expressing cofilin. *Genes Cells* 4, 311-324.
- Allen, W. E., Zicha, D., Ridley, A. J. and Jones, G. E.** (1998). A role for Cdc42 in macrophage chemotaxis. *J. Cell Biol.* 141, 1147-1157.
- Araki, T., Tsujioka, M., Abe, T., Fukuzawa, M., Meima, M., Schaap, P., Morio, T., Urushihara, H., Katoh, M., Maeda, M. et al.** (2003). A STAT-regulated, stress-induced signalling pathway in *Dictyostelium*. *J. Cell Sci.* 116, 2907-2915.
- Austin, M. B., Saito, T., Bowman, M. E., Haydock, S., Kato, A., Moore, B. S., Kay, R. R. and Noel, J. P.** (2006). Biosynthesis of *Dictyostelium discoideum* differentiation-inducing factor by a hybrid type I fatty acid-type III polyketide synthase. *Nat. Chem. Biol.* 2, 494-502.
- Baumeister, M. A., Rossman, K. L., Sondek, J. and Lemmon, M. A.** (2006). The Dbs PH domain contributes independently to membrane targeting and regulation of guanine nucleotide-exchange activity. *Biochem. J.* 400, 563-572.
- Bergson, C., Levenson, R., Goldman-Rakic, P. S. and Lidow, M. S.** (2003). Dopamine receptor-interacting proteins: the Ca(2+) connection in dopamine signaling. *Trends Pharmacol. Sci.* 24, 486-492.
- Best, A., Ahmed, S., Kozma, R. and Lim, L.** (1996). The Ras-related GTPase Rac1 binds tubulin. *J. Biol. Chem.* 271, 3756-3762.
- Biou, V. and Cherfils, J.** (2004). Structural principles for the multispecificity of small GTP-binding proteins. *Biochemistry* 43, 6833-6840.
- Blagg, S. L., Stewart, M., Sambles, C. and Insall, R. H.** (2003). PIR121 regulates pseudopod dynamics and SCAR activity in *Dictyostelium*. *Curr. Biol.* 13, 1480-1487.
- Boeckeler, K., Adley, K., Xu, X., Jenkins, A., Jin, T. and Williams, R. S.** (2006). The neuroprotective agent, valproic acid, regulates the mitogen-activated protein kinase pathway through modulation of protein kinase A signalling in *Dictyostelium discoideum*. *Eur. J. Cell Biol.* 85, 1047-1057.

- Boguski, M. S. and McCormick, F.** (1993). Proteins regulating Ras and its relatives. *Nature* 366, 643-654.
- Bonci, A. and Hopf, F. W.** (2005). The dopamine D2 receptor: new surprises from an old friend. *Neuron* 47, 335-338.
- Bosgraaf, L. and Van Haastert, P. J.** (2002). A model for cGMP signal transduction in *Dictyostelium* in perspective of 25 years of cGMP research. *J. Muscle Res. Cell Motil.* 23, 781-791.
- Bosgraaf, L. and Van Haastert, P. J.** (2006). The regulation of myosin II in *Dictyostelium*. *Eur. J. Cell Biol.* 85, 969-979.
- Brugnera, E., Haney, L., Grimsley, C., Lu, M., Walk, S. F., Tosello-Tramont, A. C., Macara, I. G., Madhani, H., Fink, G. R. and Ravichandran, K. S.** (2002). Unconventional Rac-GEF activity is mediated through the Dock180-ELMO complex. *Nat. Cell Biol.* 4, 574-582.
- Cerione, R. A. and Zheng, Y.** (1996). The Dbl family of oncogenes. *Curr. Opin. Cell Biol.* 8, 216-222.
- Charest, P. G. and Firtel, R. A.** (2007). Big roles for small GTPases in the control of directed cell movement. *Biochem. J.* 401, 377-390.
- Charest, P. G., Shen, Z., Lakoduk, A., Sasaki, A. T., Briggs, S. P. and Firtel, R. A.** (2010). A Ras signaling complex controls the RasC-TORC2 pathway and directed cell migration. *Dev. Cell* 18, 737-749.
- Chen, L., Iijima, M., Tang, M., Landree, M. A., Huang, Y. E., Xiong, Y., Iglesias, P. A. and Devreotes, P. N.** (2007). PLA2 and PI3K/PTEN pathways act in parallel to mediate chemotaxis. *Dev. Cell* 12, 603-614.
- Chen, T. L., Kowalczyk, P. A., Ho, G. and Chisholm, R. L.** (1995). Targeted disruption of the *Dictyostelium* myosin essential light chain gene produces cells defective in cytokinesis and morphogenesis. *J. Cell Sci.* 108 ( Pt 10), 3207-3218.
- Chen, Y. M., Wang, Q. J., Hu, H. S., Yu, P. C., Zhu, J., Drewes, G., Piwnicka-Worms, H. and Luo, Z. G.** (2006). Microtubule affinity-regulating kinase 2 functions downstream of the PAR-3/PAR-6/atypical PKC complex in regulating hippocampal neuronal polarity. *Proc. Natl. Acad. Sci. U. S. A* 103, 8534-8539.
- Cheresh, D. A., Leng, J. and Klemke, R. L.** (1999). Regulation of cell contraction and membrane ruffling by distinct signals in migratory cells. *J. Cell Biol.* 146, 1107-1116.
- Cherfils, J. and Chardin, P.** (1999). GEFs: structural basis for their activation of small GTP-binding proteins. *Trends Biochem. Sci.* 24, 306-311.
- Chevallet, M., Lucche, S. and Rabilloud, T.** (2006). Silver staining of proteins in polyacrylamide gels. *Nat. Protoc.* 1, 1852-1858.
- Chisholm, R. L. and Firtel, R. A.** (2004). Insights into morphogenesis from a simple developmental system. *Nat. Rev. Mol. Cell Biol.* 5, 531-541.

- Chung, C. Y. and Firtel, R. A.** (1999). PAKa, a putative PAK family member, is required for cytokinesis and the regulation of the cytoskeleton in *Dictyostelium discoideum* cells during chemotaxis. *J. Cell Biol.* 147, 559-576.
- Chung, C. Y. and Firtel, R. A.** (2002). Signaling pathways at the leading edge of chemotaxing cells. *J. Muscle Res. Cell Motil.* 23, 773-779.
- Chung, C. Y., Lee, S., Briscoe, C., Ellsworth, C. and Firtel, R. A.** (2000). Role of Rac in controlling the actin cytoskeleton and chemotaxis in motile cells. *Proc. Natl. Acad. Sci. U. S. A* 97, 5225-5230.
- Citrome, L., Levine, J. and Allingham, B.** (2000). Changes in use of valproate and other mood stabilizers for patients with schizophrenia from 1994 to 1998. *Psychiatr. Serv.* 51, 634-638.
- Cote, J. F., Motoyama, A. B., Bush, J. A. and Vuori, K.** (2005). A novel and evolutionarily conserved PtdIns(3,4,5)P<sub>3</sub>-binding domain is necessary for DOCK180 signalling. *Nat. Cell Biol.* 7, 797-807.
- Cote, J. F. and Vuori, K.** (2002). Identification of an evolutionarily conserved superfamily of DOCK180-related proteins with guanine nucleotide exchange activity. *J. Cell Sci.* 115, 4901-4913.
- Cote, J. F. and Vuori, K.** (2006). In vitro guanine nucleotide exchange activity of DHR-2/DOCKER/CZH2 domains. *Methods Enzymol.* 406, 41-57.
- Cote, J. F. and Vuori, K.** (2007). GEF what? Dock180 and related proteins help Rac to polarize cells in new ways. *Trends Cell Biol.* 17, 383-393.
- Craddock, N. and Jones, I.** (2001). Molecular genetics of bipolar disorder. *Br. J. Psychiatry Suppl* 41, s128-s133.
- Craddock, N. and Sklar, P.** (2009). Genetics of bipolar disorder: successful start to a long journey. *Trends Genet.* 25, 99-105.
- Dai, Z. and Pendergast, A. M.** (1995). Abi-2, a novel SH3-containing protein interacts with the c-Abl tyrosine kinase and modulates c-Abl transforming activity. *Genes Dev.* 9, 2569-2582.
- De, L. A. and Spudich, J. A.** (1987). Disruption of the *Dictyostelium* myosin heavy chain gene by homologous recombination. *Science* 236, 1086-1091.
- Drechsel, D. N., Hyman, A. A., Cobb, M. H. and Kirschner, M. W.** (1992). Modulation of the dynamic instability of tubulin assembly by the microtubule-associated protein tau. *Mol. Biol. Cell* 3, 1141-1154.
- Drewes, G., Ebnet, A., Preuss, U., Mandelkow, E. M. and Mandelkow, E.** (1997). MARK, a novel family of protein kinases that phosphorylate microtubule-associated proteins and trigger microtubule disruption. *Cell* 89, 297-308.
- Drewes, G., Trinczek, B., Illenberger, S., Biernat, J., Schmitt-Ulms, G., Meyer, H. E., Mandelkow, E. M. and Mandelkow, E.** (1995). Microtubule-associated protein/microtubule affinity-regulating kinase (p110mark). A novel protein kinase that regulates tau-microtubule interactions and dynamic



instability by phosphorylation at the Alzheimer-specific site serine 262. *J. Biol. Chem.* 270, 7679-7688.

**Dumontier, M., Hocht, P., Mintert, U. and Faix, J.** (2000). Rac1 GTPases control filopodia formation, cell motility, endocytosis, cytokinesis and development in *Dictyostelium*. *J. Cell Sci.* 113 ( Pt 12), 2253-2265.

**Dutartre, H., Davoust, J., Gorvel, J. P. and Chavrier, P.** (1996). Cytokinesis arrest and redistribution of actin-cytoskeleton regulatory components in cells expressing the Rho GTPase CDC42Hs. *J. Cell Sci.* 109 ( Pt 2), 367-377.

**Ebneth, A., Drewes, G., Mandelkow, E. M. and Mandelkow, E.** (1999). Phosphorylation of MAP2c and MAP4 by MARK kinases leads to the destabilization of microtubules in cells. *Cell Motil. Cytoskeleton* 44, 209-224.

**Eddy, R. J., Han, J. and Condeelis, J. S.** (1997). Capping protein terminates but does not initiate chemoattractant-induced actin assembly in *Dictyostelium*. *J. Cell Biol.* 139, 1243-1253.

**Eddy, R. J., Han, J., Sauterer, R. A. and Condeelis, J. S.** (1996). A major agonist-regulated capping activity in *Dictyostelium* is due to the capping protein, cap32/34. *Biochim. Biophys. Acta* 1314, 247-259.

**Egelhoff, T. T., Manstein, D. J. and Spudich, J. A.** (1990). Complementation of myosin null mutants in *Dictyostelium discoideum* by direct functional selection. *Dev. Biol.* 137, 359-367.

**Eichinger, L., Noegel, A. A. and Schleicher, M.** (1991). Domain structure in actin-binding proteins: expression and functional characterization of truncated severin. *J. Cell Biol.* 112, 665-676.

**Eichinger, L., Pachebat, J. A., Glockner, G., Rajandream, M. A., Sucgang, R., Berriman, M., Song, J., Olsen, R., Szafranski, K., Xu, Q. et al.** (2005). The genome of the social amoeba *Dictyostelium discoideum*. *Nature* 435, 43-57.

**Elbert, M., Rossi, G. and Brenwald, P.** (2005). The yeast par-1 homologs kin1 and kin2 show genetic and physical interactions with components of the exocytic machinery. *Mol. Biol. Cell* 16, 532-549.

**Eng, E. W., Bettio, A., Ibrahim, J. and Harrison, R. E.** (2007). MTOC reorientation occurs during FcγR-mediated phagocytosis in macrophages. *Mol. Biol. Cell* 18, 2389-2399.

**Etienne-Manneville, S.** (2004). Cdc42--the centre of polarity. *J. Cell Sci.* 117, 1291-1300.

**Etienne-Manneville, S. and Hall, A.** (2001). Integrin-mediated activation of Cdc42 controls cell polarity in migrating astrocytes through PKCζ. *Cell* 106, 489-498.

**Etienne-Manneville, S. and Hall, A.** (2002). Rho GTPases in cell biology. *Nature* 420, 629-635.

- Euteneuer, U., Graf, R., Kube-Granderath, E. and Schliwa, M.** (1998). *Dictyostelium* gamma-tubulin: molecular characterization and ultrastructural localization. *J. Cell Sci.* 111 ( Pt 3), 405-412.
- Faix, J.** (2002). The actin-bundling protein cortexillin is the downstream target of a Rac1-signaling pathway required for cytokinesis. *J. Muscle Res. Cell Motil.* 23, 765-772.
- Faix, J., Clougherty, C., Konzok, A., Mintert, U., Murphy, J., Albrecht, R., Muhlbauer, B. and Kuhlmann, J.** (1998). The IQGAP-related protein DGAP1 interacts with Rac and is involved in the modulation of the F-actin cytoskeleton and control of cell motility. *J. Cell Sci.* 111 ( Pt 20), 3059-3071.
- Faix, J., Kreppel, L., Shaulsky, G., Schleicher, M. and Kimmel, A. R.** (2004). A rapid and efficient method to generate multiple gene disruptions in *Dictyostelium discoideum* using a single selectable marker and the Cre-loxP system. *Nucleic Acids Res.* 32, e143.
- Faix, J. and Rottner, K.** (2006). The making of filopodia. *Curr. Opin. Cell Biol.* 18, 18-25.
- Faix, J., Steinmetz, M., Boves, H., Kammerer, R. A., Lottspeich, F., Mintert, U., Murphy, J., Stock, A., Aebi, U. and Gerisch, G.** (1996). Cortexillins, major determinants of cell shape and size, are actin-bundling proteins with a parallel coiled-coil tail. *Cell* 86, 631-642.
- Falasca, M., Logan, S. K., Lehto, V. P., Baccante, G., Lemmon, M. A. and Schlessinger, J.** (1998). Activation of phospholipase C gamma by PI 3-kinase-induced PH domain-mediated membrane targeting. *EMBO J.* 17, 414-422.
- Fong, D. and Rutherford, C. L.** (1978). Protease activity during cell differentiation of the cellular slime mold *Dictyostelium discoideum*. *J. Bacteriol.* 134, 521-527.
- Fukata, M., Nakagawa, M. and Kaibuchi, K.** (2003). Roles of Rho-family GTPases in cell polarisation and directional migration. *Curr. Opin. Cell Biol.* 15, 590-597.
- Funamoto, S., Milan, K., Meili, R. and Firtel, R. A.** (2001). Role of phosphatidylinositol 3' kinase and a downstream pleckstrin homology domain-containing protein in controlling chemotaxis in *Dictyostelium*. *J. Cell Biol.* 153, 795-810.
- Gadea, G., Sanz-Moreno, V., Self, A., Godi, A. and Marshall, C. J.** (2008). DOCK10-mediated Cdc42 activation is necessary for amoeboid invasion of melanoma cells. *Curr. Biol.* 18, 1456-1465.
- Geissler, H., Ullmann, R. and Soldati, T.** (2000). The tail domain of myosin M catalyses nucleotide exchange on Rac1 GTPases and can induce actin-driven surface protrusions. *Traffic.* 1, 399-410.
- Gerald, N., Dai, J., Ting-Beall, H. P. and De, L. A.** (1998). A role for *Dictyostelium* racE in cortical tension and cleavage furrow progression. *J. Cell Biol.* 141, 483-492.

- Gharahdaghi, F., Weinberg, C. R., Meagher, D. A., Imai, B. S. and Mische, S. M.** (1999). Mass spectrometric identification of proteins from silver-stained polyacrylamide gel: a method for the removal of silver ions to enhance sensitivity. *Electrophoresis* 20, 601-605.
- Ghosh, R., Chhabra, A., Phatale, P. A., Samrat, S. K., Sharma, J., Gosain, A., Mohanty, D., Saran, S. and Gokhale, R. S.** (2008). Dissecting the functional role of polyketide synthases in *Dictyostelium discoideum*: biosynthesis of the differentiation regulating factor 4-methyl-5-pentylbenzene-1,3-diol. *J. Biol. Chem.* 283, 11348-11354.
- Glotzer, M.** (1997). Cytokinesis. *Curr. Biol.* 7, R274-R276.
- Goldberg, J. M., Manning, G., Liu, A., Fey, P., Pilcher, K. E., Xu, Y. and Smith, J. L.** (2006). The *Dictyostelium* kinome--analysis of the protein kinases from a simple model organism. *PLoS. Genet.* 2, e38.
- Goldstein, L. S.** (2001). Kinesin molecular motors: transport pathways, receptors, and human disease. *Proc. Natl. Acad. Sci. U. S. A* 98, 6999-7003.
- Goode, B. L., Drubin, D. G. and Barnes, G.** (2000). Functional cooperation between the microtubule and actin cytoskeletons. *Curr. Opin. Cell Biol.* 12, 63-71.
- Gopaldass, N., Patel, D., Kratzke, R., Dieckmann, R., Hausherr, S., Hagedorn, M., Monroy, R., Kruger, J., Neuhaus, E. M., Hoffmann, E. et al.** (2012). Dynamins A, Myosin IB and Abp1 Couple Phagosome Maturation to F-Actin Binding. *Traffic.* 13, 120-130.
- Gottesman, I. I. and Erlenmeyer-Kimling, L.** (2001). Family and twin strategies as a head start in defining prodromes and endophenotypes for hypothetical early-interventions in schizophrenia. *Schizophr. Res.* 51, 93-102.
- Gundersen, G. G.** (2002). Evolutionary conservation of microtubule-capture mechanisms. *Nat. Rev. Mol. Cell Biol.* 3, 296-304.
- Gundersen, G. G. and Bulinski, J. C.** (1988). Selective stabilization of microtubules oriented toward the direction of cell migration. *Proc. Natl. Acad. Sci. U. S. A* 85, 5946-5950.
- Han, J. W., Leeper, L., Rivero, F. and Chung, C. Y.** (2006). Role of RacC for the regulation of WASP and phosphatidylinositol 3-kinase during chemotaxis of *Dictyostelium*. *J. Biol. Chem.* 281, 35224-35234.
- Han, Y. H., Chung, C. Y., Wessels, D., Stephens, S., Titus, M. A., Soll, D. R. and Firtel, R. A.** (2002). Requirement of a vasodilator-stimulated phosphoprotein family member for cell adhesion, the formation of filopodia, and chemotaxis in *Dictyostelium*. *J. Biol. Chem.* 277, 49877-49887.
- Hasegawa, H., Kiyokawa, E., Tanaka, S., Nagashima, K., Gotoh, N., Shibuya, M., Kurata, T. and Matsuda, M.** (1996). DOCK180, a major CRK-binding protein, alters cell morphology upon translocation to the cell membrane. *Mol. Cell Biol.* 16, 1770-1776.

- Haugwitz, M., Noegel, A. A., Karakesisoglou, J. and Schleicher, M.** (1994). *Dictyostelium* amoebae that lack G-actin-sequestering profilins show defects in F-actin content, cytokinesis, and development. *Cell* 79, 303-314.
- Heid, P. J., Wessels, D., Daniels, K. J., Gibson, D. P., Zhang, H., Voss, E. and Soll, D. R.** (2004). The role of myosin heavy chain phosphorylation in *Dictyostelium* motility, chemotaxis and F-actin localization. *J. Cell Sci.* 117, 4819-4835.
- Huang, Y. E., Iijima, M., Parent, C. A., Funamoto, S., Firtel, R. A. and Devreotes, P.** (2003). Receptor-mediated regulation of PI3Ks confines PI(3,4,5)P3 to the leading edge of chemotaxing cells. *Mol. Biol. Cell* 14, 1913-1922.
- Hug, C., Jay, P. Y., Reddy, I., McNally, J. G., Bridgman, P. C., Elson, E. L. and Cooper, J. A.** (1995). Capping protein levels influence actin assembly and cell motility in *Dictyostelium*. *Cell* 81, 591-600.
- Hurov, J. and Piwnicka-Worms, H.** (2007). The Par-1/MARK family of protein kinases: from polarity to metabolism. *Cell Cycle* 6, 1966-1969.
- Illenberger, S., Drewes, G., Trinczek, B., Biernat, J., Meyer, H. E., Olmsted, J. B., Mandelkow, E. M. and Mandelkow, E.** (1996). Phosphorylation of microtubule-associated proteins MAP2 and MAP4 by the protein kinase p110mark. Phosphorylation sites and regulation of microtubule dynamics. *J. Biol. Chem.* 271, 10834-10843.
- Insall, R., Kuspa, A., Lilly, P. J., Shaulsky, G., Levin, L. R., Loomis, W. F. and Devreotes, P.** (1994). CRAC, a cytosolic protein containing a pleckstrin homology domain, is required for receptor and G protein-mediated activation of adenyl cyclase in *Dictyostelium*. *J. Cell Biol.* 126, 1537-1545.
- Insall, R. H., Borleis, J. and Devreotes, P. N.** (1996). The aimless RasGEF is required for processing of chemotactic signals through G-protein-coupled receptors in *Dictyostelium*. *Curr. Biol.* 6, 719-729.
- Insall, R. H. and Machesky, L. M.** (2009). Actin dynamics at the leading edge: from simple machinery to complex networks. *Dev. Cell* 17, 310-322.
- Iranfar, N., Fuller, D. and Loomis, W. F.** (2003). Genome-wide expression analyses of gene regulation during early development of *Dictyostelium discoideum*. *Eukaryot. Cell* 2, 664-670.
- Jaber, M., Jones, S., Giros, B. and Caron, M. G.** (1997). The dopamine transporter: a crucial component regulating dopamine transmission. *Mov Disord.* 12, 629-633.
- Jaffe, A. B. and Hall, A.** (2005). Rho GTPases: biochemistry and biology. *Annu. Rev. Cell Dev. Biol.* 21, 247-269.
- Kamimura, Y., Xiong, Y., Iglesias, P. A., Hoeller, O., Bolourani, P. and Devreotes, P. N.** (2008). PIP3-independent activation of TorC2 and PKB at the cell's leading edge mediates chemotaxis. *Curr. Biol.* 18, 1034-1043.

- Kay, R. R., Dhokia, B. and Jermyn, K. A.** (1983). Purification of stalk-cell-inducing morphogens from *Dictyostelium discoideum*. *Eur. J. Biochem.* 136, 51-56.
- Kay, R. R., Garrod, D. and Tilly, R.** (1978). Requirement for cell differentiation in *Dictyostelium discoideum*. *Nature* 271, 58-60.
- Kemphues, K.** (2000). PARsing embryonic polarity. *Cell* 101, 345-348.
- Khosla, M., Spiegelman, G. B. and Weeks, G.** (1996). Overexpression of an activated rasG gene during growth blocks the initiation of *Dictyostelium* development. *Mol. Cell Biol.* 16, 4156-4162.
- King, J. S. and Insall, R. H.** (2008). Chemotaxis: TorC before you Akt.. *Curr. Biol.* 18, R864-R866.
- King, J. S. and Insall, R. H.** (2009). Chemotaxis: finding the way forward with *Dictyostelium*. *Trends Cell Biol.* 19, 523-530.
- King, J. S., Veltman, D. M., Georgiou, M., Baum, B. and Insall, R. H.** (2010). SCAR/WAVE is activated at mitosis and drives myosin-independent cytokinesis. *J. Cell Sci.* 123, 2246-2255.
- Kishi, K., Sasaki, T., Kuroda, S., Itoh, T. and Takai, Y.** (1993). Regulation of cytoplasmic division of *Xenopus* embryo by rho p21 and its inhibitory GDP/GTP exchange protein (rho GDI). *J. Cell Biol.* 120, 1187-1195.
- Kitayama, C. and Uyeda, T. Q.** (2003). ForC, a novel type of formin family protein lacking an FH1 domain, is involved in multicellular development in *Dictyostelium discoideum*. *J. Cell Sci.* 116, 711-723.
- Kiyokawa, E., Hashimoto, Y., Kobayashi, S., Sugimura, H., Kurata, T. and Matsuda, M.** (1998a). Activation of Rac1 by a Crk SH3-binding protein, DOCK180. *Genes Dev.* 12, 3331-3336.
- Kiyokawa, E., Hashimoto, Y., Kurata, T., Sugimura, H. and Matsuda, M.** (1998b). Evidence that DOCK180 up-regulates signals from the CrkII-p130(Cas) complex. *J. Biol. Chem.* 273, 24479-24484.
- Klopfenstein, D. R., Holleran, E. A. and Vale, R. D.** (2002). Kinesin motors and microtubule-based organelle transport in *Dictyostelium discoideum*. *J. Muscle Res. Cell Motil.* 23, 631-638.
- Klopfenstein, D. R. and Vale, R. D.** (2004). The lipid binding pleckstrin homology domain in UNC-104 kinesin is necessary for synaptic vesicle transport in *Caenorhabditis elegans*. *Mol. Biol. Cell* 15, 3729-3739.
- Knecht, D. A. and Loomis, W. F.** (1987). Antisense RNA inactivation of myosin heavy chain gene expression in *Dictyostelium discoideum*. *Science* 236, 1081-1086.
- Knetsch, M. L., Schafers, N., Horstmann, H. and Manstein, D. J.** (2001). The *Dictyostelium* Bcr/Abr-related protein DRG regulates both Rac- and Rab-dependent pathways. *EMBO J.* 20, 1620-1629.

- Kobayashi, K., Kuroda, S., Fukata, M., Nakamura, T., Nagase, T., Nomura, N., Matsuura, Y., Yoshida-Kubomura, N., Iwamatsu, A. and Kaibuchi, K.** (1998). p140Sra-1 (specifically Rac1-associated protein) is a novel specific target for Rac1 small GTPase. *J. Biol. Chem.* 273, 291-295.
- Kobayashi, S., Shirai, T., Kiyokawa, E., Mochizuki, N., Matsuda, M. and Fukui, Y.** (2001). Membrane recruitment of DOCK180 by binding to PtdIns(3,4,5)P<sub>3</sub>. *Biochem. J.* 354, 73-78.
- Kozma, R., Ahmed, S., Best, A. and Lim, L.** (1995). The Ras-related protein Cdc42Hs and bradykinin promote formation of peripheral actin microspikes and filopodia in Swiss 3T3 fibroblasts. *Mol. Cell Biol.* 15, 1942-1952.
- Kuramoto, K., Negishi, M. and Katoh, H.** (2009). Regulation of dendrite growth by the Cdc42 activator Zizimin1/Dock9 in hippocampal neurons. *J. Neurosci. Res.* 87, 1794-1805.
- Langridge, P. D. and Kay, R. R.** (2007). Mutants in the *Dictyostelium* Arp2/3 complex and chemoattractant-induced actin polymerization. *Exp. Cell Res.* 313, 2563-2574.
- Larochelle, D. A., Vithalani, K. K. and De, L. A.** (1996). A novel member of the rho family of small GTP-binding proteins is specifically required for cytokinesis. *J. Cell Biol.* 133, 1321-1329.
- Larochelle, D. A., Vithalani, K. K. and De, L. A.** (1997). Role of *Dictyostelium* racE in cytokinesis: mutational analysis and localization studies by use of green fluorescent protein. *Mol. Biol. Cell* 8, 935-944.
- Lebrand, C., Dent, E. W., Strasser, G. A., Lanier, L. M., Krause, M., Svitkina, T. M., Borisy, G. G. and Gertler, F. B.** (2004). Critical role of Ena/VASP proteins for filopodia formation in neurons and in function downstream of netrin-1. *Neuron* 42, 37-49.
- Lee, E. and Knecht, D. A.** (2001). Cytoskeletal alterations in *Dictyostelium* induced by expression of human cdc42. *Eur. J. Cell Biol.* 80, 399-409.
- Lemmon, M. A., Ferguson, K. M. and Abrams, C. S.** (2002). Pleckstrin homology domains and the cytoskeleton. *FEBS Lett.* 513, 71-76.
- Lewis, D. A. and Lieberman, J. A.** (2000). Catching up on schizophrenia: natural history and neurobiology. *Neuron* 28, 325-334.
- Lilly, P., Wu, L., Welker, D. L. and Devreotes, P. N.** (1993). A G-protein beta-subunit is essential for *Dictyostelium* development. *Genes Dev.* 7, 986-995.
- Lilly, P. J. and Devreotes, P. N.** (1995). Chemoattractant and GTP gamma S-mediated stimulation of adenylyl cyclase in *Dictyostelium* requires translocation of CRAC to membranes. *J. Cell Biol.* 129, 1659-1665.
- Lin, Q., Yang, W., Baird, D., Feng, Q. and Cerione, R. A.** (2006). Identification of a DOCK180-related guanine nucleotide exchange factor that is capable of mediating a positive feedback activation of Cdc42. *J. Biol. Chem.* 281, 35253-35262.

- Mabuchi, I., Hamaguchi, Y., Fujimoto, H., Morii, N., Mishima, M. and Narumiya, S.** (1993). A rho-like protein is involved in the organisation of the contractile ring in dividing sand dollar eggs. *Zygote*. 1, 325-331.
- Matenia, D. and Mandelkow, E. M.** (2009). The tau of MARK: a polarized view of the cytoskeleton. *Trends Biochem. Sci.* 34, 332-342.
- Mattei, S., Klein, G., Satre, M. and Aubry, L.** (2006). Trafficking and developmental signaling: Alix at the crossroads. *Eur. J. Cell Biol.* 85, 925-936.
- Mattei, S., Ryves, W. J., Blot, B., Sadoul, R., Harwood, A. J., Satre, M., Klein, G. and Aubry, L.** (2005). Dd-Alix, a conserved endosome-associated protein, controls *Dictyostelium* development. *Dev. Biol.* 279, 99-113.
- Medalia, O., Beck, M., Ecke, M., Weber, I., Neujahr, R., Baumeister, W. and Gerisch, G.** (2007). Organization of actin networks in intact filopodia. *Curr. Biol.* 17, 79-84.
- Meili, R., Ellsworth, C., Lee, S., Reddy, T. B., Ma, H. and Firtel, R. A.** (1999). Chemoattractant-mediated transient activation and membrane localization of Akt/PKB is required for efficient chemotaxis to cAMP in *Dictyostelium*. *EMBO J.* 18, 2092-2105.
- Meller, N., Irani-Tehrani, M., Kiosses, W. B., Del Pozo, M. A. and Schwartz, M. A.** (2002). Zizimin1, a novel Cdc42 activator, reveals a new GEF domain for Rho proteins. *Nat. Cell Biol.* 4, 639-647.
- Meller, N., Merlot, S. and Guda, C.** (2005). CZH proteins: a new family of Rho-GEFs. *J. Cell Sci.* 118, 4937-4946.
- Michaelson, D., Silletti, J., Murphy, G., D'Eustachio, P., Rush, M. and Philips, M. R.** (2001). Differential localization of Rho GTPases in live cells: regulation by hypervariable regions and RhoGDI binding. *J. Cell Biol.* 152, 111-126.
- Missale, C., Nash, S. R., Robinson, S. W., Jaber, M. and Caron, M. G.** (1998). Dopamine receptors: from structure to function. *Physiol Rev.* 78, 189-225.
- Mondal, S., Burgute, B., Rieger, D., Muller, R., Rivero, F., Faix, J., Schleicher, M. and Noegel, A. A.** (2010). Regulation of the actin cytoskeleton by an interaction of IQGAP related protein GAPA with filamin and cortexillin I. *PLoS. One.* 5, e15440.
- Mondal, S., Neelamegan, D., Rivero, F. and Noegel, A. A.** (2007). GxcDD, a putative RacGEF, is involved in *Dictyostelium* development. *BMC. Cell Biol.* 8, 23.
- Montezinho, L. P., Mork, A., Duarte, C. B., Penschuck, S., Geraldles, C. F. and Castro, M. M.** (2007). Effects of mood stabilizers on the inhibition of adenylate cyclase via dopamine D(2)-like receptors. *Bipolar. Disord.* 9, 290-297.
- Moores, S. L., Sabry, J. H. and Spudich, J. A.** (1996). Myosin dynamics in live *Dictyostelium* cells. *Proc. Natl. Acad. Sci. U. S. A* 93, 443-446.

- Morita, E., Sandrin, V., Chung, H. Y., Morham, S. G., Gygi, S. P., Rodesch, C. K. and Sundquist, W. I.** (2007). Human ESCRT and ALIX proteins interact with proteins of the midbody and function in cytokinesis. *EMBO J.* 26, 4215-4227.
- Muinonen-Martin, A. J., Veltman, D. M., Kalna, G. and Insall, R. H.** (2010). An improved chamber for direct visualisation of chemotaxis. *PLoS. One.* 5, e15309.
- Muller-Oerlinghausen, B., Berghofer, A. and Bauer, M.** (2002). Bipolar disorder. *Lancet* 359, 241-247.
- Na, J., Tunggal, B. and Eichinger, L.** (2007). STATc is a key regulator of the transcriptional response to hyperosmotic shock. *BMC. Genomics* 8, 123.
- Neuhoff, V., Arold, N., Taube, D. and Ehrhardt, W.** (1988). Improved staining of proteins in polyacrylamide gels including isoelectric focusing gels with clear background at nanogram sensitivity using Coomassie Brilliant Blue G-250 and R-250. *Electrophoresis* 9, 255-262.
- Neujahr, R., Albrecht, R., Kohler, J., Matzner, M., Schwartz, J. M., Westphal, M. and Gerisch, G.** (1998). Microtubule-mediated centrosome motility and the positioning of cleavage furrows in multinucleate myosin II-null cells. *J. Cell Sci.* 111 ( Pt 9), 1227-1240.
- Neujahr, R., Heizer, C., Albrecht, R., Ecke, M., Schwartz, J. M., Weber, I. and Gerisch, G.** (1997a). Three-dimensional patterns and redistribution of myosin II and actin in mitotic *Dictyostelium* cells. *J. Cell Biol.* 139, 1793-1804.
- Neujahr, R., Heizer, C. and Gerisch, G.** (1997b). Myosin II-independent processes in mitotic cells of *Dictyostelium discoideum*: redistribution of the nuclei, re-arrangement of the actin system and formation of the cleavage furrow. *J. Cell Sci.* 110 ( Pt 2), 123-137.
- Newberg, A. R., Catapano, L. A., Zarate, C. A. and Manji, H. K.** (2008). Neurobiology of bipolar disorder. *Expert. Rev. Neurother.* 8, 93-110.
- Nishikimi, A., Meller, N., Uekawa, N., Isobe, K., Schwartz, M. A. and Maruyama, M.** (2005). Zizimin2: a novel, DOCK180-related Cdc42 guanine nucleotide exchange factor expressed predominantly in lymphocytes. *FEBS Lett.* 579, 1039-1046.
- Nobes, C. D. and Hall, A.** (1995). Rho, rac, and cdc42 GTPases regulate the assembly of multimolecular focal complexes associated with actin stress fibers, lamellipodia, and filopodia. *Cell* 81, 53-62.
- Odorizzi, G., Katzmann, D. J., Babst, M., Audhya, A. and Emr, S. D.** (2003). Bro1 is an endosome-associated protein that functions in the MVB pathway in *Saccharomyces cerevisiae*. *J. Cell Sci.* 116, 1893-1903.
- Ohkouchi, S., El-Halawany, M. S., Aruga, F., Shibata, H., Hitomi, K. and Maki, M.** (2004). DdAlix, an Alix/AIP1 homolog in *Dictyostelium discoideum*, is required for multicellular development under low Ca<sup>2+</sup> conditions. *Gene* 337, 131-139.



- Ohkouchi, S., Saito, H., Aruga, F., Maeda, T., Shibata, H. and Maki, M.** (2005). *Dictyostelium discoideum* requires an Alix/AIP1 homolog, DdAlix, for morphogenesis in alkaline environments. *FEBS Lett.* 579, 1745-1750.
- Ott, A., Oehme, F., Keller, H. and Schuster, S. C.** (2000). Osmotic stress response in *Dictyostelium* is mediated by cAMP. *EMBO J.* 19, 5782-5792.
- Oyama, M.** (1996). cGMP accumulation induced by hypertonic stress in *Dictyostelium discoideum*. *J. Biol. Chem.* 271, 5574-5579.
- Oyama, M. and Blumberg, D. D.** (1986). Changes during differentiation in requirements for cAMP for expression of cell-type-specific mRNAs in the cellular slime mold, *Dictyostelium discoideum*. *Dev. Biol.* 117, 550-556.
- Pakes, N. K., Jayasinghe, S. N. and Williams, R. S.** (2011). Bio-electrospraying and aerodynamically assisted bio-jetting the model eukaryotic *Dictyostelium discoideum*: assessing stress and developmental competency post treatment. *J. R. Soc. Interface* 8, 1185-1191.
- Pakes, N. K., Veltman, D. M., Rivero, F., Nasir, J., Insall, R. and Williams, R. S.** (2012). ZizB, a novel RacGEF regulates development, cell motility and cytokinesis in *Dictyostelium*. *J. Cell Sci.*
- Palazzo, A. F., Joseph, H. L., Chen, Y. J., Dujardin, D. L., Alberts, A. S., Pfister, K. K., Vallee, R. B. and Gundersen, G. G.** (2001). Cdc42, dynein, and dynactin regulate MTOC reorientation independent of Rho-regulated microtubule stabilization. *Curr. Biol.* 11, 1536-1541.
- Palmieri, S. J., Nebl, T., Pope, R. K., Seastone, D. J., Lee, E., Hinchcliffe, E. H., Sluder, G., Knecht, D., Cardelli, J. and Luna, E. J.** (2000). Mutant Rac1B expression in *Dictyostelium*: effects on morphology, growth, endocytosis, development, and the actin cytoskeleton. *Cell Motil. Cytoskeleton* 46, 285-304.
- Para, A., Krischke, M., Merlot, S., Shen, Z., Oberholzer, M., Lee, S., Briggs, S. and Firtel, R. A.** (2009). *Dictyostelium* Dock180-related RacGEFs regulate the actin cytoskeleton during cell motility. *Mol. Biol. Cell* 20, 699-707.
- Park, K. C., Rivero, F., Meili, R., Lee, S., Apone, F. and Firtel, R. A.** (2004). Rac regulation of chemotaxis and morphogenesis in *Dictyostelium*. *EMBO J.* 23, 4177-4189.
- Pelletier, S., Duhamel, F., Coulombe, P., Popoff, M. R. and Meloche, S.** (2003). Rho family GTPases are required for activation of Jak/STAT signaling by G protein-coupled receptors. *Mol. Cell Biol.* 23, 1316-1333.
- Peracino, B., Borleis, J., Jin, T., Westphal, M., Schwartz, J. M., Wu, L., Bracco, E., Gerisch, G., Devreotes, P. and Bozzaro, S.** (1998). G protein beta subunit-null mutants are impaired in phagocytosis and chemotaxis due to inappropriate regulation of the actin cytoskeleton. *J. Cell Biol.* 141, 1529-1537.
- Pinheiro, E. M. and Gertler, F. B.** (2006). Nervous Rac: DOCK7 regulation of axon formation. *Neuron* 51, 674-676.

- Pollard, T. D.** (2007). Regulation of actin filament assembly by Arp2/3 complex and formins. *Annu. Rev. Biophys. Biomol. Struct.* 36, 451-477.
- Pollitt, A. Y., Blagg, S. L., Ibarra, N. and Insall, R. H.** (2006). Cell motility and SCAR localisation in axenically growing *Dictyostelium* cells. *Eur. J. Cell Biol.* 85, 1091-1098.
- Pollitt, A. Y. and Insall, R. H.** (2008). Abi mutants in *Dictyostelium* reveal specific roles for the SCAR/WAVE complex in cytokinesis. *Curr. Biol.* 18, 203-210.
- Pollock, N., de Hostos, E. L., Turck, C. W. and Vale, R. D.** (1999). Reconstitution of membrane transport powered by a novel dimeric kinesin motor of the Unc104/KIF1A family purified from *Dictyostelium*. *J. Cell Biol.* 147, 493-506.
- Qurashi, A., Sahin, H. B., Carrera, P., Gautreau, A., Schenck, A. and Giangrande, A.** (2007). HSPC300 and its role in neuronal connectivity. *Neural Dev.* 2, 18.
- Raftopoulou, M. and Hall, A.** (2004). Cell migration: Rho GTPases lead the way. *Dev. Biol.* 265, 23-32.
- Richert, S., Luche, S., Chevallet, M., van, D. A., Leize-Wagner, E. and Rabilloud, T.** (2004). About the mechanism of interference of silver staining with peptide mass spectrometry. *Proteomics.* 4, 909-916.
- Ridley, A. J.** (2001). Rho family proteins: coordinating cell responses. *Trends Cell Biol.* 11, 471-477.
- Ridley, A. J. and Hall, A.** (1992). The small GTP-binding protein rho regulates the assembly of focal adhesions and actin stress fibers in response to growth factors. *Cell* 70, 389-399.
- Ridley, A. J., Paterson, H. F., Johnston, C. L., Diekmann, D. and Hall, A.** (1992). The small GTP-binding protein rac regulates growth factor-induced membrane ruffling. *Cell* 70, 401-410.
- Rivero, F., Albrecht, R., Dislich, H., Bracco, E., Graciotti, L., Bozzaro, S. and Noegel, A. A.** (1999a). RacF1, a novel member of the Rho protein family in *Dictyostelium discoideum*, associates transiently with cell contact areas, macropinosomes, and phagosomes. *Mol. Biol. Cell* 10, 1205-1219.
- Rivero, F., Dislich, H., Glockner, G. and Noegel, A. A.** (2001). The *Dictyostelium discoideum* family of Rho-related proteins. *Nucleic Acids Res.* 29, 1068-1079.
- Rivero, F., Furukawa, R., Fechheimer, M. and Noegel, A. A.** (1999b). Three actin cross-linking proteins, the 34 kDa actin-bundling protein, alpha-actinin and gelation factor (ABP-120), have both unique and redundant roles in the growth and development of *Dictyostelium*. *J. Cell Sci.* 112 ( Pt 16), 2737-2751.
- Rivero, F., Furukawa, R., Noegel, A. A. and Fechheimer, M.** (1996a). *Dictyostelium discoideum* cells lacking the 34,000-dalton actin-binding protein

can grow, locomote, and develop, but exhibit defects in regulation of cell structure and movement: a case of partial redundancy. *J. Cell Biol.* 135, 965-980.

**Rivero, F., Illenberger, D., Somesh, B. P., Dislich, H., Adam, N. and Meyer, A. K.** (2002). Defects in cytokinesis, actin reorganization and the contractile vacuole in cells deficient in RhoGDI. *EMBO J.* 21, 4539-4549.

**Rivero, F., Koppel, B., Peracino, B., Bozzaro, S., Siegert, F., Weijer, C. J., Schleicher, M., Albrecht, R. and Noegel, A. A.** (1996b). The role of the cortical cytoskeleton: F-actin crosslinking proteins protect against osmotic stress, ensure cell size, cell shape and motility, and contribute to phagocytosis and development. *J. Cell Sci.* 109 ( Pt 11), 2679-2691.

**Rivero, F. and Somesh, B. P.** (2002). Signal transduction pathways regulated by Rho GTPases in *Dictyostelium*. *J. Muscle Res. Cell Motil.* 23, 737-749.

**Roelofs, J. and Van Haastert, P. J.** (2002). Characterization of two unusual guanylyl cyclases from *Dictyostelium*. *J. Biol. Chem.* 277, 9167-9174.

**Rot, G., Parikh, A., Curk, T., Kuspa, A., Shaulsky, G. and Zupan, B.** (2009). dictyExpress: a *Dictyostelium discoideum* gene expression database with an explorative data analysis web-based interface. *BMC. Bioinformatics.* 10, 265.

**Rubino, S., Fighetti, M., Unger, E. and Cappuccinelli, P.** (1984). Location of actin, myosin, and microtubular structures during directed locomotion of *Dictyostelium* amebae. *J. Cell Biol.* 98, 382-390.

**Rump, A., Scholz, T., Thiel, C., Hartmann, F. K., Uta, P., Hinrichs, M. H., Taft, M. H. and Tsiavalariis, G.** (2011). Myosin-1C associates with microtubules and stabilizes the mitotic spindle during cell division. *J. Cell Sci.* 124, 2521-2528.

**Ruusala, A. and Aspenstrom, P.** (2004). Isolation and characterisation of DOCK8, a member of the DOCK180-related regulators of cell morphology. *FEBS Lett.* 572, 159-166.

**Sakurai, M., Adachi, H. and Sutoh, K.** (2001). Mutational analyses of *Dictyostelium* IQGAP-related protein GAp: possible interaction with small GTPases in cytokinesis. *Biosci. Biotechnol. Biochem.* 65, 1912-1916.

**Sasaki, A. T. and Firtel, R. A.** (2006). Regulation of chemotaxis by the orchestrated activation of Ras, PI3K, and TOR. *Eur. J. Cell Biol.* 85, 873-895.

**Schaap, P., Van Lookeren Campagne, M. M., Van, D. R., Spek, W., Van Haastert, P. J. and Pinas, J.** (1986). Postaggregative differentiation induction by cyclic AMP in *Dictyostelium*: intracellular transduction pathway and requirement for additional stimuli. *Dev. Biol.* 118, 52-63.

**Schaap, P. and Wang, M.** (1986). Interactions between adenosine and oscillatory cAMP signaling regulate size and pattern in *Dictyostelium*. *Cell* 45, 137-144.

- Schaar, B. T., Kinoshita, K. and McConnell, S. K.** (2004). Doublecortin microtubule affinity is regulated by a balance of kinase and phosphatase activity at the leading edge of migrating neurons. *Neuron* 41, 203-213.
- Scheler, C., Lamer, S., Pan, Z., Li, X. P., Salnikow, J. and Jungblut, P.** (1998). Peptide mass fingerprint sequence coverage from differently stained proteins on two-dimensional electrophoresis patterns by matrix assisted laser desorption/ionization-mass spectrometry (MALDI-MS). *Electrophoresis* 19, 918-927.
- Schirenbeck, A., Arasada, R., Bretschneider, T., Schleicher, M. and Faix, J.** (2005a). Formins and VASPs may co-operate in the formation of filopodia. *Biochem. Soc. Trans.* 33, 1256-1259.
- Schirenbeck, A., Bretschneider, T., Arasada, R., Schleicher, M. and Faix, J.** (2005b). The Diaphanous-related formin dDia2 is required for the formation and maintenance of filopodia. *Nat. Cell Biol.* 7, 619-625.
- Schulkes, C. and Schaap, P.** (1995). cAMP-dependent protein kinase activity is essential for preaggregative gene expression in *Dictyostelium*. *FEBS Lett.* 368, 381-384.
- Schuster, S. C., Noegel, A. A., Oehme, F., Gerisch, G. and Simon, M. I.** (1996). The hybrid histidine kinase DokA is part of the osmotic response system of *Dictyostelium*. *EMBO J.* 15, 3880-3889.
- Seastone, D. J., Lee, E., Bush, J., Knecht, D. and Cardelli, J.** (1998). Overexpression of a novel rho family GTPase, RacC, induces unusual actin-based structures and positively affects phagocytosis in *Dictyostelium discoideum*. *Mol. Biol. Cell* 9, 2891-2904.
- Seeman, P.** (1987). Dopamine receptors and the dopamine hypothesis of schizophrenia. *Synapse* 1, 133-152.
- Seeman, P. and Kapur, S.** (2000). Schizophrenia: more dopamine, more D2 receptors. *Proc. Natl. Acad. Sci. U. S. A* 97, 7673-7675.
- Seeman, P., Schwarz, J., Chen, J. F., Szechtman, H., Perreault, M., McKnight, G. S., Roder, J. C., Quirion, R., Boksa, P., Srivastava, L. K. et al.** (2006). Psychosis pathways converge via D2high dopamine receptors. *Synapse* 60, 319-346.
- Shaulsky, G., Escalante, R. and Loomis, W. F.** (1996). Developmental signal transduction pathways uncovered by genetic suppressors. *Proc. Natl. Acad. Sci. U. S. A* 93, 15260-15265.
- Siderovski, D. P. and Willard, F. S.** (2005). The GAPs, GEFs, and GDIs of heterotrimeric G-protein alpha subunits. *Int. J. Biol. Sci.* 1, 51-66.
- Sinha, S. and Yang, W.** (2008). Cellular signaling for activation of Rho GTPase Cdc42. *Cell Signal.* 20, 1927-1934.
- Small, J. V. and Kaverina, I.** (2003). Microtubules meet substrate adhesions to arrange cell polarity. *Curr. Opin. Cell Biol.* 15, 40-47.

- Smith, F. D., Oxford, G. S. and Milgram, S. L.** (1999). Association of the D2 dopamine receptor third cytoplasmic loop with spinophilin, a protein phosphatase-1-interacting protein. *J. Biol. Chem.* 274, 19894-19900.
- Somesh, B. P., Vlahou, G., Iijima, M., Insall, R. H., Devreotes, P. and Rivero, F.** (2006). RacG regulates morphology, phagocytosis, and chemotaxis. *Eukaryot. Cell* 5, 1648-1663.
- Souza, G. M., da Silva, A. M. and Kuspa, A.** (1999). Starvation promotes *Dictyostelium* development by relieving PufA inhibition of PKA translation through the YakA kinase pathway. *Development* 126, 3263-3274.
- Souza, G. M., Lu, S. and Kuspa, A.** (1998). YakA, a protein kinase required for the transition from growth to development in *Dictyostelium*. *Development* 125, 2291-2302.
- Strange, P. G.** (2001). Antipsychotic drugs: importance of dopamine receptors for mechanisms of therapeutic actions and side effects. *Pharmacol. Rev.* 53, 119-133.
- Strehle, A., Schleicher, M. and Faix, J.** (2006). Trix, a novel Rac guanine-nucleotide exchange factor from *Dictyostelium discoideum* is an actin-binding protein and accumulates at endosomes. *Eur. J. Cell Biol.* 85, 1035-1045.
- Sun, T. Q., Lu, B., Feng, J. J., Reinhard, C., Jan, Y. N., Fantl, W. J. and Williams, L. T.** (2001). PAR-1 is a Dishevelled-associated kinase and a positive regulator of Wnt signalling. *Nat. Cell Biol.* 3, 628-636.
- Sunahara, R. K., Guan, H. C., O'Dowd, B. F., Seeman, P., Laurier, L. G., Ng, G., George, S. R., Torchia, J., Van Tol, H. H. and Niznik, H. B.** (1991). Cloning of the gene for a human dopamine D5 receptor with higher affinity for dopamine than D1. *Nature* 350, 614-619.
- Taminato, A., Bagattini, R., Gorjao, R., Chen, G., Kuspa, A. and Souza, G. M.** (2002). Role for YakA, cAMP, and protein kinase A in regulation of stress responses of *Dictyostelium discoideum* cells. *Mol. Biol. Cell* 13, 2266-2275.
- Tamura, K., Dudley, J., Nei, M. and Kumar, S.** (2007). MEGA4: Molecular Evolutionary Genetics Analysis (MEGA) software version 4.0. *Mol. Biol. Evol.* 24, 1596-1599.
- Timm, T., Li, X. Y., Biernat, J., Jiao, J., Mandelkow, E., Vandekerckhove, J. and Mandelkow, E. M.** (2003). MARKK, a Ste20-like kinase, activates the polarity-inducing kinase MARK/PAR-1. *EMBO J.* 22, 5090-5101.
- Trinczek, B., Brajenovic, M., Ebner, A. and Drewes, G.** (2004). MARK4 is a novel microtubule-associated proteins/microtubule affinity-regulating kinase that binds to the cellular microtubule network and to centrosomes. *J. Biol. Chem.* 279, 5915-5923.
- Trivinos-Lagos, L., Ohmachi, T., Albrightson, C., Burns, R. G., Ennis, H. L. and Chisholm, R. L.** (1993). The highly divergent alpha- and beta-tubulins from *Dictyostelium discoideum* are encoded by single genes. *J. Cell Sci.* 105 ( Pt 4), 903-911.

- Tsuang, M.** (2000). Schizophrenia: genes and environment. *Biol. Psychiatry* 47, 210-220.
- Ueda, M., Graf, R., MacWilliams, H. K., Schliwa, M. and Euteneuer, U.** (1997). Centrosome positioning and directionality of cell movements. *Proc. Natl. Acad. Sci. U. S. A* 94, 9674-9678.
- Vallone, D., Picetti, R. and Borrelli, E.** (2000). Structure and function of dopamine receptors. *Neurosci. Biobehav. Rev.* 24, 125-132.
- Van Haastert, P. J. and Bosgraaf, L.** (2009). The local cell curvature guides pseudopodia towards chemoattractants. *HFSP. J.* 3, 282-286.
- Van Haastert, P. J., Keizer-Gunnink, I. and Kortholt, A.** (2007). Essential role of PI3-kinase and phospholipase A2 in *Dictyostelium discoideum* chemotaxis. *J. Cell Biol.* 177, 809-816.
- Van Tol, H. H., Wu, C. M., Guan, H. C., Ohara, K., Bunzow, J. R., Civelli, O., Kennedy, J., Seeman, P., Niznik, H. B. and Jovanovic, V.** (1992). Multiple dopamine D4 receptor variants in the human population. *Nature* 358, 149-152.
- van, D. N., Shaw, C., Katoh, M., Morio, T., Sucgang, R., Ibarra, M., Kuwayama, H., Saito, T., Urushihara, H., Maeda, M. et al.** (2002). A transcriptional profile of multicellular development in *Dictyostelium discoideum*. *Development* 129, 1543-1552.
- Veltman, D. M., Keizer-Gunnink, I. and Haastert, P. J.** (2009). An extrachromosomal, inducible expression system for *Dictyostelium discoideum*. *Plasmid* 61, 119-125.
- Vithalani, K. K., Shoffner, J. D. and De, L. A.** (1996). Isolation and characterization of a novel cytokinesis-deficient mutant in *Dictyostelium discoideum*. *J. Cell Biochem.* 62, 290-301.
- Vito, P., Pellegrini, L., Guiet, C. and D'Adamio, L.** (1999). Cloning of AIP1, a novel protein that associates with the apoptosis-linked gene ALG-2 in a Ca<sup>2+</sup>-dependent reaction. *J. Biol. Chem.* 274, 1533-1540.
- Vlahou, G. and Rivero, F.** (2006). Rho GTPase signaling in *Dictyostelium discoideum*: insights from the genome. *Eur. J. Cell Biol.* 85, 947-959.
- Wallar, B. J. and Alberts, A. S.** (2003). The formins: active scaffolds that remodel the cytoskeleton. *Trends Cell Biol.* 13, 435-446.
- Watabe-Uchida, M., Govek, E. E. and Van, A. L.** (2006a). Regulators of Rho GTPases in neuronal development. *J. Neurosci.* 26, 10633-10635.
- Watabe-Uchida, M., John, K. A., Janas, J. A., Newey, S. E. and Van, A. L.** (2006b). The Rac activator DOCK7 regulates neuronal polarity through local phosphorylation of stathmin/Op18. *Neuron* 51, 727-739.
- Watanabe, T., Wang, S., Noritake, J., Sato, K., Fukata, M., Takefuji, M., Nakagawa, M., Izumi, N., Akiyama, T. and Kaibuchi, K.** (2004). Interaction

with IQGAP1 links APC to Rac1, Cdc42, and actin filaments during cell polarization and migration. *Dev. Cell* 7, 871-883.

**Waterman-Storer, C. M., Worthylake, R. A., Liu, B. P., Burridge, K. and Salmon, E. D.** (1999). Microtubule growth activates Rac1 to promote lamellipodial protrusion in fibroblasts. *Nat. Cell Biol.* 1, 45-50.

**Wennerberg, K., Rossman, K. L. and Der, C. J.** (2005). The Ras superfamily at a glance. *J. Cell Sci.* 118, 843-846.

**White, E.** (2003). The pims and outs of survival signaling: role for the Pim-2 protein kinase in the suppression of apoptosis by cytokines. *Genes Dev.* 17, 1813-1816.

**Wienke, D. C., Knetsch, M. L., Neuhaus, E. M., Reedy, M. C. and Manstein, D. J.** (1999). Disruption of a dynamin homologue affects endocytosis, organelle morphology, and cytokinesis in *Dictyostelium discoideum*. *Mol. Biol. Cell* 10, 225-243.

**Wilkins, A. and Insall, R. H.** (2001). Small GTPases in *Dictyostelium*: lessons from a social amoeba. *Trends Genet.* 17, 41-48.

**Williams, H. P. and Harwood, A. J.** (2003). Cell polarity and *Dictyostelium* development. *Curr. Opin. Microbiol.* 6, 621-627.

**Williams, R. S., Boeckeler, K., Graf, R., Muller-Taubenberger, A., Li, Z., Isberg, R. R., Wessels, D., Soll, D. R., Alexander, H. and Alexander, S.** (2006). Towards a molecular understanding of human diseases using *Dictyostelium discoideum*. *Trends Mol. Med.* 12, 415-424.

**Williams, R. S., Cheng, L., Mudge, A. W. and Harwood, A. J.** (2002). A common mechanism of action for three mood-stabilizing drugs. *Nature* 417, 292-295.

**Williamson, B. D., Favis, R., Brickey, D. A. and Rutherford, C. L.** (1996). Isolation and characterization of glycogen synthase in *Dictyostelium discoideum*. *Dev. Genet.* 19, 350-364.

**Witke, W., Schleicher, M. and Noegel, A. A.** (1992). Redundancy in the microfilament system: abnormal development of *Dictyostelium* cells lacking two F-actin cross-linking proteins. *Cell* 68, 53-62.

**Wittmann, T. and Waterman-Storer, C. M.** (2001). Cell motility: can Rho GTPases and microtubules point the way? *J. Cell Sci.* 114, 3795-3803.

**Wood, S. A., Ammann, R. R., Brock, D. A., Li, L., Spann, T. and Gomer, R. H.** (1996). RtoA links initial cell type choice to the cell cycle in *Dictyostelium*. *Development* 122, 3677-3685.

**Wu, L., Valkema, R., Van Haastert, P. J. and Devreotes, P. N.** (1995). The G protein beta subunit is essential for multiple responses to chemoattractants in *Dictyostelium*. *J. Cell Biol.* 129, 1667-1675.

- Xu, J., Wang, F., Van, K. A., Herzmark, P., Straight, A., Kelly, K., Takuwa, Y., Sugimoto, N., Mitchison, T. and Bourne, H. R.** (2003). Divergent signals and cytoskeletal assemblies regulate self-organizing polarity in neutrophils. *Cell* 114, 201-214.
- Yelo, E., Bernardo, M. V., Gimeno, L., Caraz-Garcia, M. J., Majado, M. J. and Parrado, A.** (2008). Dock10, a novel CZH protein selectively induced by interleukin-4 in human B lymphocytes. *Mol. Immunol.* 45, 3411-3418.
- Zang, J. H., Cavet, G., Sabry, J. H., Wagner, P., Moores, S. L. and Spudich, J. A.** (1997). On the role of myosin-II in cytokinesis: division of *Dictyostelium* cells under adhesive and nonadhesive conditions. *Mol. Biol. Cell* 8, 2617-2629.
- Zhan, L., Kerr, J. R., Lafuente, M. J., Maclean, A., Chibalina, M. V., Liu, B., Burke, B., Bevan, S. and Nasir, J.** (2010a). Altered expression and coregulation of dopamine signalling genes in schizophrenia and bipolar disorder: (Altered expression of dopamine signalling genes). *Neuropathol. Appl. Neurobiol.*
- Zhan, L., Kerr, J. R., Lafuente, M. J., Maclean, A., Chibalina, M. V., Liu, B., Burke, B., Bevan, S. and Nasir, J.** (2010b). Altered expression and coregulation of dopamine signalling genes in schizophrenia and bipolar disorder: (Altered expression of dopamine signalling genes. ...). *Neuropathol. Appl. Neurobiol.*
- Zhan, L., Liu, B., Jose-Lafuente, M., Chibalina, M. V., Grierson, A., Maclean, A. and Nasir, J.** (2008). ALG-2 interacting protein AIP1: a novel link between D1 and D3 signalling. *Eur. J. Neurosci.* 27, 1626-1633.
- Zheng, Y., Zangrilli, D., Cerione, R. A. and Eva, A.** (1996). The pleckstrin homology domain mediates transformation by oncogenic db1 through specific intracellular targeting. *J. Biol. Chem.* 271, 19017-19020.
- Zhou, H. M., Brust-Mascher, I. and Scholey, J. M.** (2001). Direct visualization of the movement of the monomeric axonal transport motor UNC-104 along neuronal processes in living *Caenorhabditis elegans*. *J. Neurosci.* 21, 3749-3755.
- Zhou, Q., Kee, Y. S., Poirier, C. C., Jelinek, C., Osborne, J., Divi, S., Surcel, A., Will, M. E., Eggert, U. S., Muller-Taubenberger, A. et al.** (2010). 14-3-3 coordinates microtubules, Rac, and myosin II to control cell mechanics and cytokinesis. *Curr. Biol.* 20, 1881-1889.
- Zucko, J., Skunca, N., Curk, T., Zupan, B., Long, P. F., Cullum, J., Kessin, R. H. and Hranueli, D.** (2007). Polyketide synthase genes and the natural products potential of *Dictyostelium discoideum*. *Bioinformatics.* 23, 2543-2549.



## Appendix

### Publications

#### Journal of Cell Science (2012)

#### **ZizB, a novel RacGEF regulates development, cell motility and cytokinesis in *Dictyostelium*.**

**Nicholl K. Pakes**, Douwe M. Veltman, Francisco Rivero, Jamal Nasir, Robert Insall, and Robin S.B. Williams

#### Summary

Dock (Dedicator of Cytokinesis) proteins represent a family of Guanine nucleotide Exchange Factors (GEFs) that include the well studied Dock180 family and the poorly characterised zizimin family. Our current understanding of Dock180 function is to regulate Rho small GTPases, playing a role in a number of cell processes including cell migration, development and division. Here, we have employed a tractable model for cell motility research, *Dictyostelium discoideum*, to help elucidate the role of the related zizimin proteins. We show that gene ablation of zizA causes no change in development whereas ablation of zizB gives rise to an aberrant developmental morphology and a reduction in cell directionality and velocity, and altered cell shape. Fluorescently labeled ZizA protein associates with the microtubule organizing centre (MTOC), whereas the ZizB protein exhibits cortical enrichment. Overexpression of ZizB also causes an increase in the number filopodia and a partial inhibition of cytokinesis. Analysis of ZizB protein binding partners indicates interacts with Rac1a and a range of actin-interacting proteins. In conclusion our work provides the first insight into the molecular and cellular functions of zizimin GEF proteins playing a role in cell movement, filopodia formation and cytokinesis.

**Journal of the Royal Society Interface (2011)****Bio-electrospraying and aerodynamically assisted bio-jetting the model eukaryotic *Dictyostelium discoideum*: assessing stress and developmental competency post treatment**

**Nicholl K. Pakes**, Suwan N. Jayasinghe, and Robin S. B. Williams

**Summary**

Bio-electrospraying (BES) and aerodynamically assisted bio-jetting (AABJ) have recently been established as important novel biospray technologies for directly manipulating living cells. To elucidate their potential in medical and clinical sciences, these bio-aerosol techniques have been subjected to increasingly rigorous investigations. In parallel to these studies, we wish to introduce these unique biotechnologies for use in the basic biological sciences, for handling a wide range of cell types and systems, thus increasing the range and the scope of these techniques for modern research. Here, the authors present the analysis of the new use of these biospray techniques for the direct handling of the simple eukaryotic biomedical model organism *Dictyostelium discoideum*. These cells are widely used as a model for immune cell chemotaxis and as a simple model for development. We demonstrate that AABJ of these cells did not cause cell stress, as defined by the stress-gene induction, nor affect cell development. Furthermore, although BES induced the increased expression of one stress-related gene (*gapA*), this was not a generalized stress response nor did it affect cell development. These data suggest that these biospray techniques can be used to directly manipulate single cells of this biomedical model without inducing a generalized stress response or perturbing later development.